

1974

Contributions To The Study Of Erosion Along The North Shore Of Lake Erie

Pierre J. Gelinias

Follow this and additional works at: <https://ir.lib.uwo.ca/digitizedtheses>

Recommended Citation

Gelinias, Pierre J., "Contributions To The Study Of Erosion Along The North Shore Of Lake Erie" (1974). *Digitized Theses*. 752.
<https://ir.lib.uwo.ca/digitizedtheses/752>

This Dissertation is brought to you for free and open access by the Digitized Special Collections at Scholarship@Western. It has been accepted for inclusion in Digitized Theses by an authorized administrator of Scholarship@Western. For more information, please contact tadam@uwo.ca, wlsadmin@uwo.ca.

ABSTRACT

Severe erosion occurs on the bluffs along the north shore of Lake Erie, between Rondeau to the west and Long Point to the east. The long-term rates of erosion are estimated by comparisons of early surveys of the shoreline (1800-1820) with recent air photographs of the same areas (1963-1964). Erosion rates are on the average 1.30 meters per year with variation of 0.25 m/yr near the western boundary to 3.0 m/yr east of Port Stanley and east of Port Burwell. Wind-generated waves are recognized as the main factor causing erosion; using a five-year record of winds and a modified Sverdrup-Munk-Bretschneider forecasting technique, the total wave energy at breaking is estimated at six locations along the shoreline. A good correlation is found between the calculated wave energy and the observed erosion rates. Discrepancies occur in several areas suggesting a local geological control. The effects of storm setups and fluctuating lake levels are also analysed, but their influence is felt more readily in the short term.

The glacial materials forming the bluffs control locally the rates of erosion through their resistance to erosion, resistance to failure, and their texture. Studies on erosion mechanisms show that cycles of drying and wetting will have a very detrimental effect on the stability of the clay-silt tills because they induce

CONTRIBUTIONS TO THE STUDY OF EROSION
ALONG THE NORTH SHORE OF LAKE ERIE

by

PIERRE J. GELINAS

Department of Civil Engineering

Submitted in partial fulfillment
of the requirements for the degree of

Doctor of Philosophy

Faculty of Graduate Studies
The University of Western Ontario
London, Canada

March 1974

© Pierre J. Gelinas 1974

ABSTRACT

Severe erosion occurs on the bluffs along the north shore of Lake Erie, between Rondeau to the west and Long Point to the east. The long-term rates of erosion are estimated by comparisons of early surveys of the shoreline (1800-1820) with recent air photographs of the same areas (1963-1964). Erosion rates are on the average 1.30 meters per year with variation of 0.25 m/yr near the western boundary to 3.0 m/yr east of Fort Stanley and east of Fort Burwell. Wind-generated waves are recognized as the main factor causing erosion; using a five-year record of winds and a modified Sverdrup-Munk-Bretschneider forecasting technique, the total wave energy at breaking is estimated at six locations along the shoreline. A good correlation is found between the calculated wave energy and the observed erosion rates. Discrepancies occur in several areas suggesting a local geological control. The effects of storm setups and fluctuating lake levels are also analysed, but their influence is felt more readily in the short term.

The glacial materials forming the bluffs control locally the rates of erosion through their resistance to erosion, resistance to failure, and their texture. Studies on erosion mechanisms show that cycles of drying and wetting will have a very detrimental effect on the stability of the clay-silt tills because they induce

slaking and swelling of the material. Resistance to mechanical erosion is very low for cohesionless materials (sands and silts) and increase very much for saturated clays or clayey silt tills.

The equilibrium between inertial forces and the forces of erosion is reached either slowly by flattening of slopes and surface weathering, or suddenly when slides occur. Several shallow landslides were observed in the areas where the bluffs are higher, and where water-bearing sands occupy the top of the sequence. Field borings and instrumentation were done at four sites and the properties of the materials were measured in the laboratory. A model of slope stability is presented in which the effects of erosion and weathering control the factors of safety at any time.

ACKNOWLEDGEMENTS

This investigation was conducted under the guidance of Dr. R.M. Quigley, Professor of Civil Engineering and Geology. The writer wishes to express his special and sincere appreciation to Dr. Quigley for his advice and comments on the work.

The interest and suggestions of Dr. Lo, Professor of Soil Mechanics and Dr. Dreimanis, Professor of Geology are sincerely appreciated.

Special thanks are also given to Mr. Gary Lusk, who helped with the field and laboratory work and to fellow graduate students for their comments and criticisms.

Finally, I would like to express my sincere gratitude and thanks to my wife for her help and comprehension throughout those years.

This project was financed partly by a N.R.C. scholarship which is gratefully acknowledged.

TABLE OF CONTENTS

	page
CERTIFICATE OF EXAMINATION	ii
ABSTRACT	iii
ACKNOWLEDGEMENTS	v
TABLE OF CONTENTS	vi
LIST OF FIGURES	x
LIST OF TABLES	xiv
CHAPTER 1. INTRODUCTION	1
1.1 Statement of the Problem	1
1.2 Scope of the Problem	3
1.3 Previous Work on Lake Erie	5
CHAPTER 2. EROSION RATES	8
2.1 Introduction	8
2.2 Method of estimating Erosion Rates	8
2.3 Sources of Error in Estimating Erosion Rates.....	9
2.4 Results.....	13
2.5 Discussion	13
CHAPTER 3. THE CAUSES OF EROSION	30
3.1 Wind Field	30
3.1.1 Choice of a Weather Station	30
3.1.2 Type of Data Available	31
3.1.3 Processing of the Wind Data	32
3.1.4 Results of the Wind Analysis	33
3.1.5 Vertical Profiles of Wind Velocity	41

	page
4.1	Bedrock Geology, Southwestern Ontario 120
4.2	Bedrock Contours, North Shore of Lake Erie ... 123
4.3	Index Map for the Geological Sections 191
4.4	Geological Sections (1-7) 132
4.5	Geological Sections (8-14) 132
4.6	Geological Sections (15-21) 133
4.7	Geological Sections (22-28) 133
4.8	Geological Sections (29-34) 134
4.9	Pebble Lithology on the Beach at Port Burwell . 138
4.10	Distribution of Lake Erie Bottom Sediments ... 140
4.11	Stages of Shrinkage Drying 144
4.12	Shrinkage Curves for Fort Stanley Till 147
4.13	Water Sorption on Dry Soil Aggregate 152
4.14	Aggregate Size Reduction Upon Drying and Wetting Cycles 154
4.15	Changes in Atterberg Limits with Dry-wet Cycles 156
4.16	Erosion Tests on Fort Stanley Till 159
4.17	Probability of Rainfall Intensity, Port Stanley 164
4.18	Rainfall Intensity-Duration-Frequency, Great Lakes Region 167
5.1	Shallow Mudslide, Port Bruce 178
5.2	Shallow Slides on Stabilized Slopes, Port Burwell 179
5.3	Location of Exploratory Boreholes 184
5.4	Geology and Groundwater Conditions at Port Burwell 186
5.5	Geology and Groundwater Conditions at the Geography Station, Port Bruce 187
5.6	Geology and Groundwater Conditions at Iona 188
5.7	Geology and Groundwater Conditions at Tyrconnell (Wallacetown) 189

	page
4.4 Physical weathering of Tills	141
4.4.1 Drying and shrinkage	142
4.4.2 Drying and shrinkage of Till	143
4.4.3 Structural Changes During Shrinkage	146
4.5 Swelling and Slaking of Clay-Silt Tills	148
4.5.1 Swelling and Slaking Mechanisms	149
4.5.2 Sorption of water by Soil Aggregates	151
4.5.3 Size Reduction Due to Dry-wet Cycles	153
4.5.4 Erosion Tests	155
4.6 Field Measurements	160
4.6.1 Joints and Fissures	161
4.6.2 Wetting and Slaking	163
CHAPTER 5. MASS MOVEMENTS AND STABILITY ANALYSIS	169
5.1 Description of Lake Erie North Shore	169
5.1.1 General Topography	169
5.1.2 Morphology of the Slopes	171
5.1.3 Mass Movements	173
5.2 Field Investigations	182
5.2.1 Exploratory Borings	183
5.2.2 Groundwater Investigations	185
5.2.3 Groundwater Fluctuations	191
5.2.4 Hydraulic Conductivity	192
5.2.5 Discussion of the Results	201
5.3 Laboratory Investigations	203
5.3.1 Natural Water Content	204
5.3.2 Atterberg Limits	204
5.3.3 Specific Gravity	205

	page
5.3.4 Grain Size Analysis	205
5.3.5 Mineralogy	207
5.3.6 Summary of Identification Tests	212
5.3.7 Shear Strength	214
5.4 Stability of Lake Erie Bluffs	220
5.4.1 Preliminary Considerations	221
5.4.2 Softening and Progressive Failure ...	221
5.4.3 Methods of Stability Analysis	223
5.4.4 Results of Stability Analyses	227
5.4.5 Discussion	236
CHAPTER 6. SUMMARY AND CONCLUSIONS.....	238
6.1 Summary	238
6.2 Conclusions	239
6.3 Suggestions for Future work	243
BIBLIOGRAPHY	244
APPENDICES	254
Appendix 1 water waves Theories	254
Appendix 2 Geological Sections	257

LIST OF FIGURES

	<u>Page</u>
1.1 Lake Erie Region. Location of the Study area ..	2
2.1 Erosion Rates, Howard Twp	16
2.2 Erosion Rates, Orford Twp	17
2.3 Erosion Rates, Aldborough Twp	18
2.4 Erosion Rates, Dunwich Twp	19
2.5 Erosion Rates, Southwold Twp	20
2.6 Erosion Rates, Yarmouth Twp	21
2.7 Erosion Rates, Malahide Twp	22
2.8 Erosion Rates, Bayham Twp	23
2.9 Erosion Rates, Houghton Twp	24
2.10 General Map of Erosion Rates	25
2.11 Frequency Distribution of Erosion Rates	26
3.1 Wind Velocity Frequency Diagram	36
3.2 Wind Velocity Histogram, Clear Creek, Ont.....	37
3.3 Frequency of Strong Winds	38
3.4 Frequency of Strong Winds in Each Direction ...	40
3.5 Vertical Wind Profile, Clear Creek	44
3.6 Prediction of U_{10} from Wind Profiles	45
3.7 Computation of Effective Fetch	48
3.8 Wave Forecasting Stations	50
3.9 Relationship between wave Period, Wave Length and Depth of Water4.....	52
3.10 Bathymetric Chart of Lake Erie	53
3.11 Wave Period as a Function of Depth of Water ...	55
3.12 Significant Wave Height in Terms of Wind Velocity, Fetch, and Depth of Water	55

	Page
3.13	Wave Forecasting Chart 57
3.14	Wave Height and Depth of water at breaking 62
3.15	Wave Refraction Diagram 64
3.16	Wave Refraction on Slopes with Straight Parallel Contours 66
3.17	Wave Energy Components 67
3.18	Wave Height Histogram, all Directions 69
3.19	Seasonal Distribution of wave heights 71
3.20	Wave Energy Distribution Along the Shoreline ... 74
3.21	Wave Energy Distribution in all Directions 75
3.22	Seasonal Variation of wave energy 77
3.23	Physical Model of wind Setup 80
3.24	Numerical Model for wind Setup Calculation 83
3.25	Storm Setup Contours for S wind (U = 40 mph) ... 86
3.26	Storm Setup Contours for S wind (U = 50 mph) ... 87
3.27	Storm Setup Contours for SW Wind (U = 40 mph) .. 88
3.28	Storm Setup Contours for SW wind (U = 50 mph) .. 89
3.29	Storm Setup Contours for W winds (U = 40 mph) .. 90
3.30	Storm Setup Contours for W winds (U = 50 mph) .. 91
3.31	Frequency of Strong Winds, S, SW, and W 92
3.32	Lake Erie Levels Since Last Glacial Stage 97
3.33	Hydrograph of Lake Erie, 1860-1971, 100
3.34	Annual Hydrograph of Lake Erie 102
3.35	Models for Long-Term Fluctuations in Lake Levels 108
3.36	Probability Model for Lake Levels 110
3.37	Influence of Lake Levels on the Location of the Breakers Zone 112
3.38	Relationship Between Wave Energy and Erosion Rate 116

	page
4.1 Bedrock Geology, Southwestern Ontario	120
4.2 Bedrock Contours, North Shore of Lake Erie ...	123
4.3 Index Map for the Geological Sections	191
4.4 Geological Sections (1-7)	132
4.5 Geological Sections (8-14)	132
4.6 Geological Sections (15-21)	133
4.7 Geological Sections (22-28)	133
4.8 Geological Sections (29-34)	134
4.9 Pebble Lithology on the Beach at Port Burwell .	138
4.10 Distribution of Lake Erie Bottom Sediments ...	140
4.11 Stages of Shrinkage Drying	144
4.12 Shrinkage Curves for Fort Stanley Till	147
4.13 Water Sorption on Dry Soil Aggregate	152
4.14 Aggregate Size Reduction Upon Drying and Wetting Cycles	154
4.15 Changes in Atterberg Limits with Dry-Wet Cycles	156
4.16 Erosion Tests on Fort Stanley Till	159
4.17 Probability of Rainfall Intensity, Port Stanley	164
4.18 Rainfall Intensity-Duration-Frequency, Great Lakes Region	167
5.1 Shallow Mudslide, Port Bruce	178
5.2 Shallow Slides on Stabilized Slopes, Port Burwell	179
5.3 Location of Exploratory Boreholes	184
5.4 Geology and Groundwater Conditions at Port Burwell	186
5.5 Geology and Groundwater Conditions at the Geography Station, Port Bruce	187
5.6 Geology and Groundwater Conditions at Iona	188
5.7 Geology and Groundwater Conditions at Tyrconnell (Wallacetown)	189

	page
5.8	Piezometer Installation 193
5.9	Type Curves to Determine Transmissibility ... 199
5.10	Injection Test in Piezometer GS-1, Port Bruce. 200
5.11	Groundwater Flow Model, Port Bruce Vicinity .. 202
5.12	Plasticity and Activity of Glacial Sediments . 206
5.13	Typical Grain Size Curves For Glacial Sediments 208
5.14	Granulometry of Glacial Materials 209
5.15	X-Ray Trace, Fort Stanley Drift (-2 microns) . 211
5.16	Typical Stress-Strain Curves, Fort Stanley Drift 217
5.17	Shear Strength Parameters, Glacial Materials . 218
5.18	Forces in the Slice Method` 225
5.19	Stability conditions at Tyrconnell (Wallacetown) 228
5.20	Stability Conditions at Iona 230
5.21	Stability Conditions at the Geography Station at Low Lake Level 232
5.22	Stability Conditions at the Geography Station at High Lake Level 233
5.23	Stability Conditions at Port Burwell 235

LIST OF TABLES

		page
2.1	Early Surveys and Maps of Lake Erie	10
2.2	Erosion Rates at 1-km Intervals	14-15
3.1	Frequency of Winds at Clear Creek (1956-1960).	34
3.2	Mean Velocity of Winds at Clear Creek	35
3.3	Effective Fetch	49
3.4	Wave Energy Parameters	60
3.5	Wave Breaking Parameters	63
3.6	Distribution of Energy at Breaking	72
3.7	Normal and Longshore Energy Distribution	73
3.8	Maximum Monthly Lake Setup Observed at Port Stanley (1965-1969)	94
3.9	Extreme Lake Levels Recorded at Port Stanley..	99
3.10	Parameters Used for Harmonic Analysis	105
3.11	Coefficients a_j and b_j from Harmonic Analysis.	106
3.12	Variance Explained by the Harmonic Model	107
3.13	Lake Bottom Profiles	113
4.1	Time- and Rock-Stratigraphic Names of the Wisconsin Stage in the Erie Basin	126
4.2	Index Properties of Glacial Tillis	145
4.3	Influence of Water Content on Soil Erosion ...	158
4.4	Mean Rainfall Intensity and Duration for 2-, 5-10-, and 25-Year Return Period, Great Lakes...	166
5.1	Dimensions of Spreading slides in Sand	176
5.2	Piezometers and Observation Wells	194-95
5.3	Index Soil Properties	213
5.4	Drained Shear Strength Parameters	219

The author of this thesis has granted The University of Western Ontario a non-exclusive license to reproduce and distribute copies of this thesis to users of Western Libraries. Copyright remains with the author.

Electronic theses and dissertations available in The University of Western Ontario's institutional repository (Scholarship@Western) are solely for the purpose of private study and research. They may not be copied or reproduced, except as permitted by copyright laws, without written authority of the copyright owner. Any commercial use or publication is strictly prohibited.

The original copyright license attesting to these terms and signed by the author of this thesis may be found in the original print version of the thesis, held by Western Libraries.

The thesis approval page signed by the examining committee may also be found in the original print version of the thesis held in Western Libraries.

Please contact Western Libraries for further information:

E-mail: libadmin@uwo.ca

Telephone: (519) 661-2111 Ext. 84796

Web site: <http://www.lib.uwo.ca/>

CHAPTER 1
INTRODUCTION

1.1 Statement of the problem.

Evidence of very active erosion of the shoreline along the north shore of Lake Erie is clear even to a casual observer: huge scars are seen in several places on the edge of the bluffs with accumulation of debris at the base of the slope; large blocks of till severed from the cliff are being washed away by waves; water in the nearshore area is muddy and turbid; beaches behind jetties and groins grow longer year after year due to accretion of sand; the Department of Highways had to relocate roads west of Port Bruce and Port Stanley because of erosion of part of the road; farmers complain regularly to governments that they are losing large tracts of rich land to the lake; finally cottage owners along the shoreline see their property endangered or destroyed by encroachment of the lake.

The magnitude of erosive forces has been investigated along a 120-kilometer shoreline between two sand spits, Pointe-aux-Pins to the west and Long Point to the east. The bulk of the study concerns a length of about 50 kilometers between Port Stanley and Port Burwell, area where maximum rates of erosion are observed (Figure 1.1). This area was chosen because it is there that the processes of erosion are the most active due to the favorable exposure of the

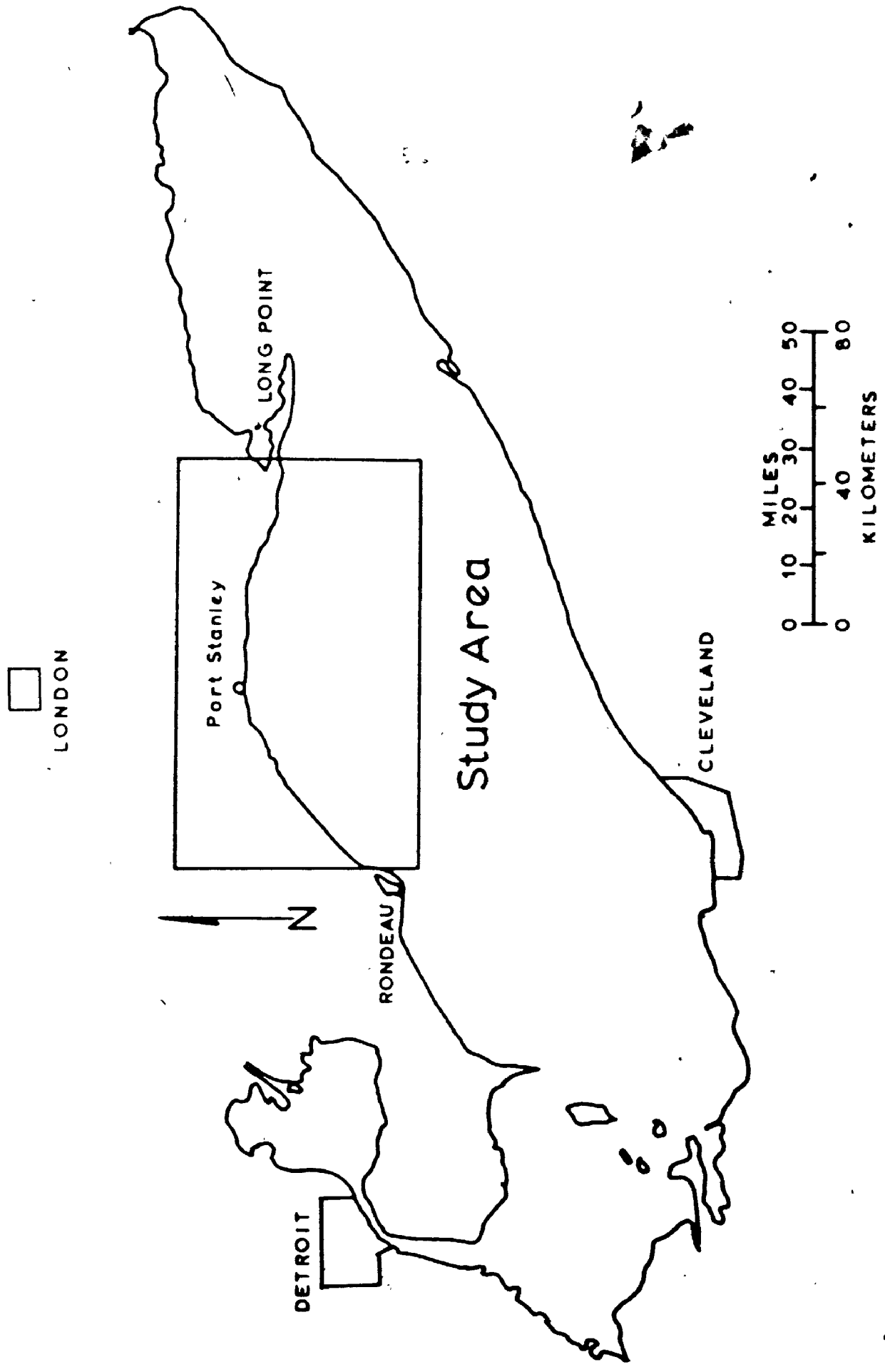


Fig. 1.1 Lake Erie Region. Location of the Study Area.

shore to southwest dominant winds and storms, the great thickness of unconsolidated glacial and lacustrine soils subjected to erosion (up to 40 meters), and also because of the regularity of the shoreline. The coast in the western basin has a lower relief and does not experience the same storm intensity; the area east of Long Point is protected by the sand spit and the shore is more resistant to erosion.

The purpose of this study is to estimate erosion rates in the chosen area, to look for causes and mechanisms of erosion, to investigate the factors contributing to the resistance to erosion, and finally to study the effects of these processes on the stability of the bluffs.

1.2 Scope of the problem.

The analysis of natural erosion processes is complex in the sense that it involves several variables that are interdependent and that are generally difficult to define; long-term rates of erosion also reflect heterogeneity and randomness of natural materials and processes; variations in topography, properties of materials, geometry of slopes, distribution of rainfall and storms, lake levels, wave action and so on. The most significant factors that are involved in this study are briefly introduced.

Erosion rates are conditioned by active and passive factors. The efficient cause of erosion is due to the action

of a mass of water wasting its energy at its boundaries; wave action at the surface of Lake Erie is then seen as the most important contribution to erosion. A chapter on wind-generated waves and their energy contribution will be complemented by a study of the influence of storm setups and lake level fluctuations, factors that control the level of application of wave energy on the shore profile. Other hydraulic effects due to runoff and seepage are also important in the process of erosion by causing the formation of gullies and controlling the moisture content and groundwater potential in the materials subjected to erosion.

The passive factors of erosion are mainly of geological nature; the materials will be described in terms of the general geology of the area and its physiography and topography. The general composition of the sediments eroded and their stratigraphy along the bluffs is the key in explaining anomalously high erosion rates in certain localities.

Geological processes of weathering cause the degradation of glacial sediments through cycles of drying and wetting, thereby reducing the resistance to erosion of these soils. Chemical weathering seems to play a minor role in the desintegration of soil structure because of the rapidity of erosion and exposure of fresh material. The resistance of different soil groups to erosion is also discussed in a special section.

The geometry of the bluffs and the occurrence of

landslides are the response of a coastline subjected to erosion. The equilibrium between the dynamic forces of erosion and the inertial forces of cohesion and internal friction of the soils is continuously shifting and mass movements are steps meant to restore that equilibrium. Hence the geometry of the slopes and the type of slides occurring in the bluffs represent states of equilibrium at any one time.

A section will describe the slope in terms of its morphology and also study the mechanical properties of the materials participating in slides. Slope stability calculations will be made to assess the safety of different profiles where toe erosion is important since this problem has to be resolved before any protective measure is planned.

The four parts of this thesis are then to acknowledge the magnitude of erosion rates (chapter 2), to study the influence of active factors such as waves and lake levels on erosion (chapter 3), to assess the importance of geology and weathering as factors of resistance to erosion (chapter 4), and to see the response of the bluffs to those effects by studying their stability (chapter 5).

1.3 Previous work on Lake Erie.

Numerous people have studied different aspects of the natural environment of Lake Erie. These studies concern for instance geology, sedimentology, hydrology, hydrogeology, physiography, erosion, wave action, meteorology, limnology, engineering problems, and so on.

townships, second one in the measurement of distances from air photographs and finally errors that stem from the fitting process. Analysis of the causes of error leads to the maximum accuracy that can be expected from the method.

Instruments used in the early nineteenth century for surveying were essentially the chain measuring 66 feet and composed of 100 links, and a circumferentor which is a tripod-mounted compass with an alidad (Thompson, 1966). Measurements of angles was taken from the magnetic north and it was not the practice of doing backsight.

The accuracy in chaining is usually taken as 1 in 500; most reference points used for erosion estimates are the intersection of a township line with the first concession road normal to it; the distance of that point from the shoreline is usually between 1 and 2 kilometers. The standard error in locating the shoreline on old maps will be plus or minus 3 meters.

Errors due to angular measurements can be important but it is assumed that these errors cancel out over a long distance.

A more serious cause of error can be assigned to negligence. Usually it is not specified in original notebooks whether the survey of the township line ended on the top of the bluffs or near the shoreline; that omission introduces an uncertainty which is taken as half of the bluff height at that point, assuming a slope angle of 45° , steep enough to prevent chaining downslope. For an average bluff height of 30 meters, the average error will be plus or minus

15 meters in locating the shoreline.

The horizontal scale for air photographs used for comparison is 1:15840 or 4 inches to the mile. Due to fluctuations in ground elevation and distortion, the accuracy of horizontal distance measurements is not better than 1 in 200 or 5 meters per kilometer. These limits were checked on topographic maps of the same area by measuring distances between points appearing both on maps and photographs.

The fitting of the two sets of maps by superposition also introduces important sources of error. The matching points are chosen at the junction of a township line and a concession road since these lines only were actually surveyed; this error of matching is in the order of plus or minus 10 meters due to paper expansion, thickness of lines, etc. Finally measuring the distance between the position of the two shorelines can be done with an accuracy of plus or minus 5 meters.

The total maximum error is found by adding the individual errors and by dividing this figure by the time interval between the surveys. For a total possible error of plus or minus 38 meters, the average accuracy for annual erosion rates is plus or minus 0,25 meter per year if the average time interval is taken as 150 years. This kind of accuracy would be too large over a short period of time or if the erosion rates were very small; fortunately, for the range of erosion rates considered in this study, the accuracy is 20% on the average rate of erosion (1,3 meter per year) and is better than 10% in areas subjected to strong erosion.

CHAPTER 2

EROSION RATES

2.1 Introduction.

The first step in this study is to evaluate with enough accuracy the rates of erosion along different sections of the shoreline. Since many factors vary with time, such as lake levels, precipitation, storm occurrences, etc., it is advisable to chose a large time interval over which mean annual rates of erosion can be calculated. In doing so, the average rates may become meaningless if applied to a short time interval for design purposes; but over several decades which is the normal life of engineering works, the average erosion rates indicate the response of the shoreline to changes in natural conditions (lake levels, wave action, etc.) and also discriminate between soils having a high or low resistance to erosion.

2.2 Method for estimating erosion rates.

The method adopted here is to compare the position of the shoreline when the area was first surveyed in the beginning of the nineteenth century with its actual position as determined from recent air photographs covering the same area (Wood, 1951). The survey of the townships bordering Lake Erie was done between 1797 and 1816, when settlement of the area began under Colonel Thomas Talbot (Miller, 1967).

Maps giving the plans of the townships were issued from 1803 to 1824 after all concession lines and boundaries were surveyed (Table 2.1). Original field notes and plans of these surveys are not published but are available on microfilm, after the original kept by the Ontario Department on Lands and Forests. Townships maps and plans exist in many copies and several are kept at the University of Western Ontario Map Library. The original scale of those maps is half a mile to the inch (1:31680).

The present shoreline configuration has been taken from air photographs dating from 1963 and 1964. The Department of Public Works (DPM 1969) used these photographs to draw maps of the shoreline at a scale of 1320 feet to the inch (1:15840) and the maps were reduced to a scale of half a mile to the inch in another version of the same report. This last set of recent maps was used for comparison since the scale is the same as the original plans.

The total erosion loss between the two surveys is estimated by superposition of the two sets of maps and by measuring the distance between the former shoreline and the present one. This technique however has many shortcomings and the accuracy of the estimates has to be assessed.

2.3 Sources of error in estimating erosion rates.

The accuracy of the determination of erosion rates is limited in many ways; a first source of error is present in the methods used to carry the early surveys of the

Table 2.1
Early Surveys and Maps

<u>Township</u>	<u>Year surveyed (map)</u>	<u>Time interval to 1964 (years)</u>
Aldbrough	1803	161
Bayham	1809	155
Bunwich	1803	161
Doughton	(1819)	145
Howard	(1821)	143
Malahide	1810	154
Orford	(1816)	148
Southwold	1809	155
Yarmouth	1809	155

Source: Ontario Department of Lands and Forests, Unpublished "Reports and Field Notes", Microfilm Series. Regional History Room, U.W.O. Weldon Library.

townships, second one in the measurement of distances from air photographs and finally errors that stem from the fitting process. Analysis of the causes of error leads to the maximum accuracy that can be expected from the method.

Instruments used in the early nineteenth century for surveying were essentially the chain measuring 66 feet and composed of 100 links, and a circumferentor which is a tripod-mounted compass with an alidad (Thompson, 1966). Measurements of angles was taken from the magnetic north and it was not the practice of doing backsight.

The accuracy in chaining is usually taken as 1 in 500; most reference points used for erosion estimates are the intersection of a township line with the first concession road normal to it; the distance of that point from the shoreline is usually between 1 and 2 kilometers. The standard error in locating the shoreline on old maps will be plus or minus 3 meters.

Errors due to angular measurements can be important but it is assumed that these errors cancel out over a long distance.

A more serious cause of error can be assigned to negligence. Usually it is not specified in original notebooks whether the survey of the township line ended on the top of the bluffs or near the shoreline; that omission introduces an uncertainty which is taken as half of the bluff height at that point, assuming a slope angle of 45° , steep enough to prevent chaining downslope. For an average bluff height of 30 meters, the average error will be plus or minus

15 meters in locating the shoreline.

The horizontal scale for air photographs used for comparison is 1:15840 or 4 inches to the mile. Due to fluctuations in ground elevation and distortion, the accuracy of horizontal distance measurements is not better than 1 in 200 or 5 meters per kilometer. These limits were checked on topographic maps of the same area by measuring distances between points appearing both on maps and photographs.

The fitting of the two sets of maps by superposition also introduces important sources of error. The matching points are chosen at the junction of a township line and a concession road since these lines only were actually surveyed; this error of matching is in the order of plus or minus 10 meters due to paper expansion, thickness of lines, etc. Finally measuring the distance between the position of the two shorelines can be done with an accuracy of plus or minus 5 meters.

The total maximum error is found by adding the individual errors and by dividing this figure by the time interval between the surveys. For a total possible error of plus or minus 38 meters, the average accuracy for annual erosion rates is plus or minus 0.25 meter per year if the average time interval is taken as 150 years. This kind of accuracy would be too large over a short period of time or if the erosion rates were very small; fortunately, for the range of erosion rates considered in this study, the accuracy is 20% on the average rate of erosion (1.3 meter per year) and is better than 10% in areas subjected to strong erosion.

2.4 Results.

In order to measure rates of erosion, the shoreline was divided in segments of one kilometer, and the area between the two shorelines was measured and divided by the time interval between the two surveys; the values are expressed in meters per year. The data is tabulated in Table 2.2 taking as the origin the western boundary of Howard Township and going towards the east. Figures 2.1 to 2.9 show graphically the same results for each township. In plotting the results, the rate of erosion at any point is the average value over a three-kilometer section centered on that point; the reason for this smoothing of the results is to remove much of the variability caused by local irregularities such as slides, gullies or the presence of protective measures such as groins. Figure 2.10 is an erosion summary for the area.

A histogram, Figure 2.11, shows the distribution of erosion rates along the shoreline and permits the computation of a mean erosion rate for the whole study area; the mean rate is 1,30 meter per year and the standard deviation is 0,73 meter per year. Assuming that the bluffs are vertical and that the average height is 25 meters, this rate of erosion means that 4 million cubic meters of soil are washed away by waves and currents into Lake Erie every year.

2.5 Discussion.

The principal feature of the erosion maps is that

Table 2.2

Erosion Rates at 1-km intervals

Distance (km)	Erosion (m/yr)		Distance (km)	Erosion (m/yr)	
1	0,00	Howard Twp.	31	1,01	
2	0,00		32	0,97	
3	0,00		33	0,67	
4	0,05		34	0,42	
5	0,12		35	0,38	
6	0,22		36	0,53	
7	0,26		37	0,39	
8	0,27		38	0,10	
9	0,28		39	0,28	Dunwich Twp.
10	0,32		40	0,41	
11	0,40		41	0,58	
12	0,46	Orford Twp.	42	0,71	
13	0,42		43	0,94	
14	0,56		44	1,10	
15	0,17		45	1,19	
16	0,22		46	1,33	
17	0,62		47	1,27	
18	0,87		48	1,28	
19	0,82		49	1,48	
20	0,85		50	1,72	
21	0,89		51	1,72	
22	0,69	Aldborough Twp.	52	1,17	
23	0,32		53	0,82	
24	0,38		54	0,85	
25	0,72		55	1,33	
26	0,80		56	1,45	
27	0,92		57	0,97	Southwold
28	1,30		58	1,01	Twp.
29	1,59		59	1,13	
30	1,17		60	1,28	

Table 2.2 (continued)

Distance (km)	Erosion (m/yr)		Distance (km)	Erosion (m/yr)	
61	1,30		91	1,35	
62	0,80		92	1,18	
63	1,27		93	1,22	
64	2,05		94	1,56	
65	2,25		95	1,70	
66	1,07	Yarmouth Twp.	96	1,48	
67	-0,34	Port Stanley	97	1,49	Bayham Twp.
68	1,17		98	1,60	
69	2,67		99	1,07	
70	3,17*		100	-1,80	
71	2,75		101	-5,40	Fort Burwell
72	2,58		* 102	0,77	
73	2,43		103	2,02	
74	2,20		104	2,30	
75	2,81		105	2,90	
76	2,73		106	3,02*	
77	1,97		107	2,83	
78	1,78		108	2,82	
79	1,52		109	2,68	Houghton Twp.
80	1,62		110	2,80	
81	1,76		111	2,70	
82	2,00		112	2,32	
83	0,98	Malahide Twp.	113	2,24	
* 84	0,47	Port Bruce	114	2,17	
85	1,10		115	2,06	
86	1,77		116	2,02	
87	1,82		117	1,91	
88	1,92		118	1,75	
89	2,06		119	2,02	
90	1,80		120	2,01	
			121	1,89	
			122	1,67	
			123	1,55	
			124	1,90	East Bdry.

* maximum rates

Negative values = accretion

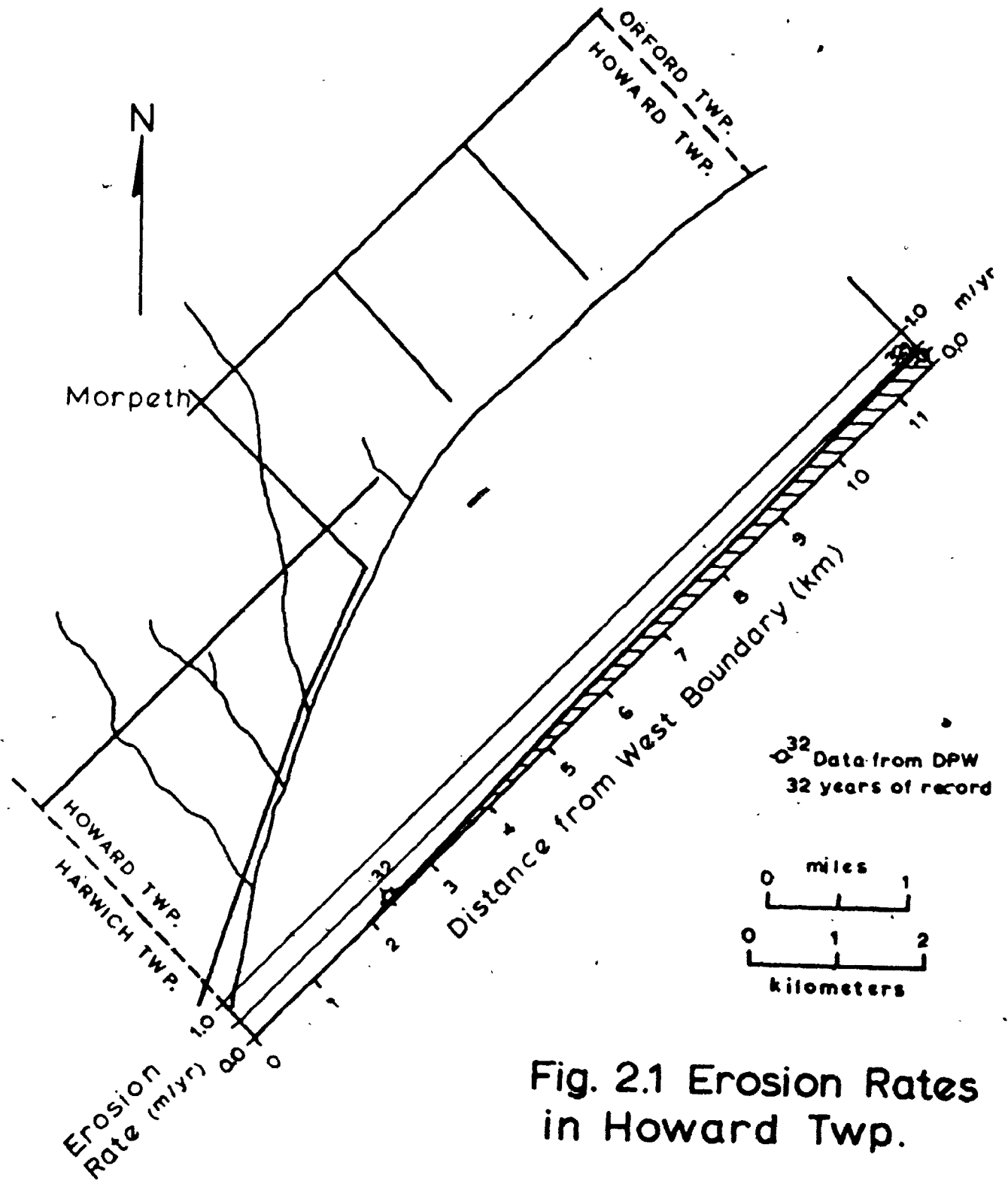


Fig. 2.1 Erosion Rates in Howard Twp.

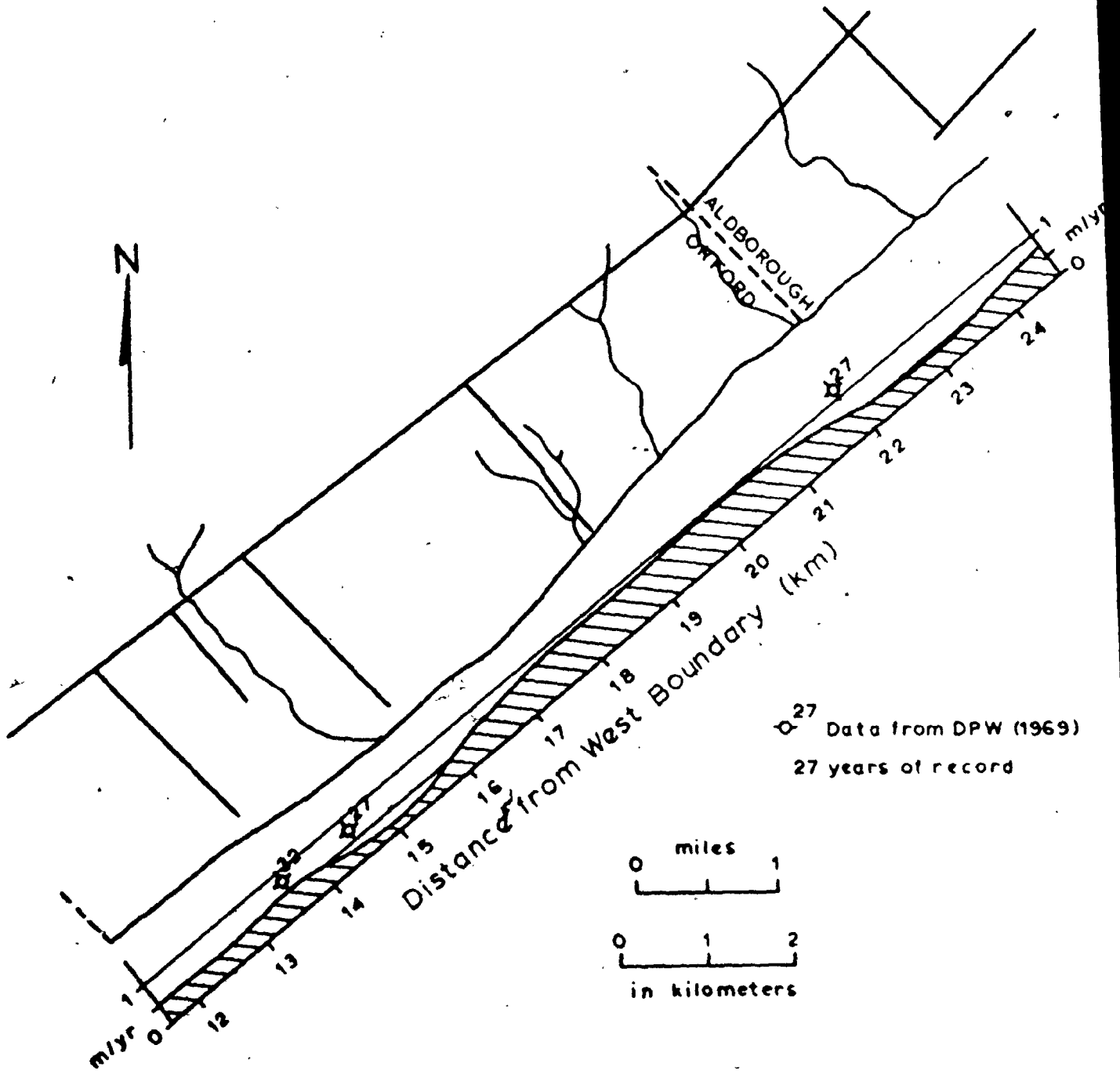


Fig. 2.2 Erosion Rates, Orford Twp.

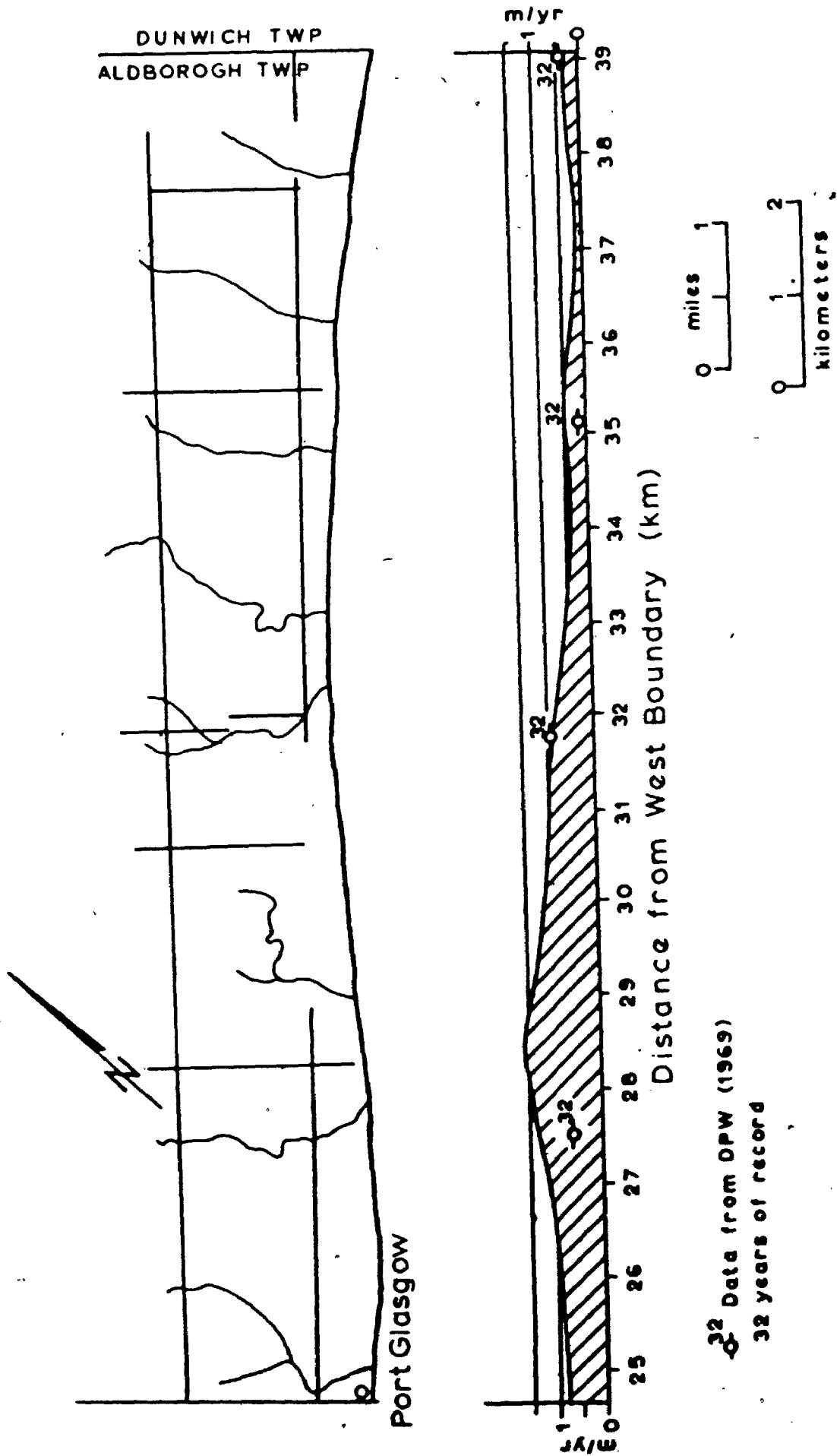


Fig. 2.3 Erosion Rates,
Aldborough Twp.

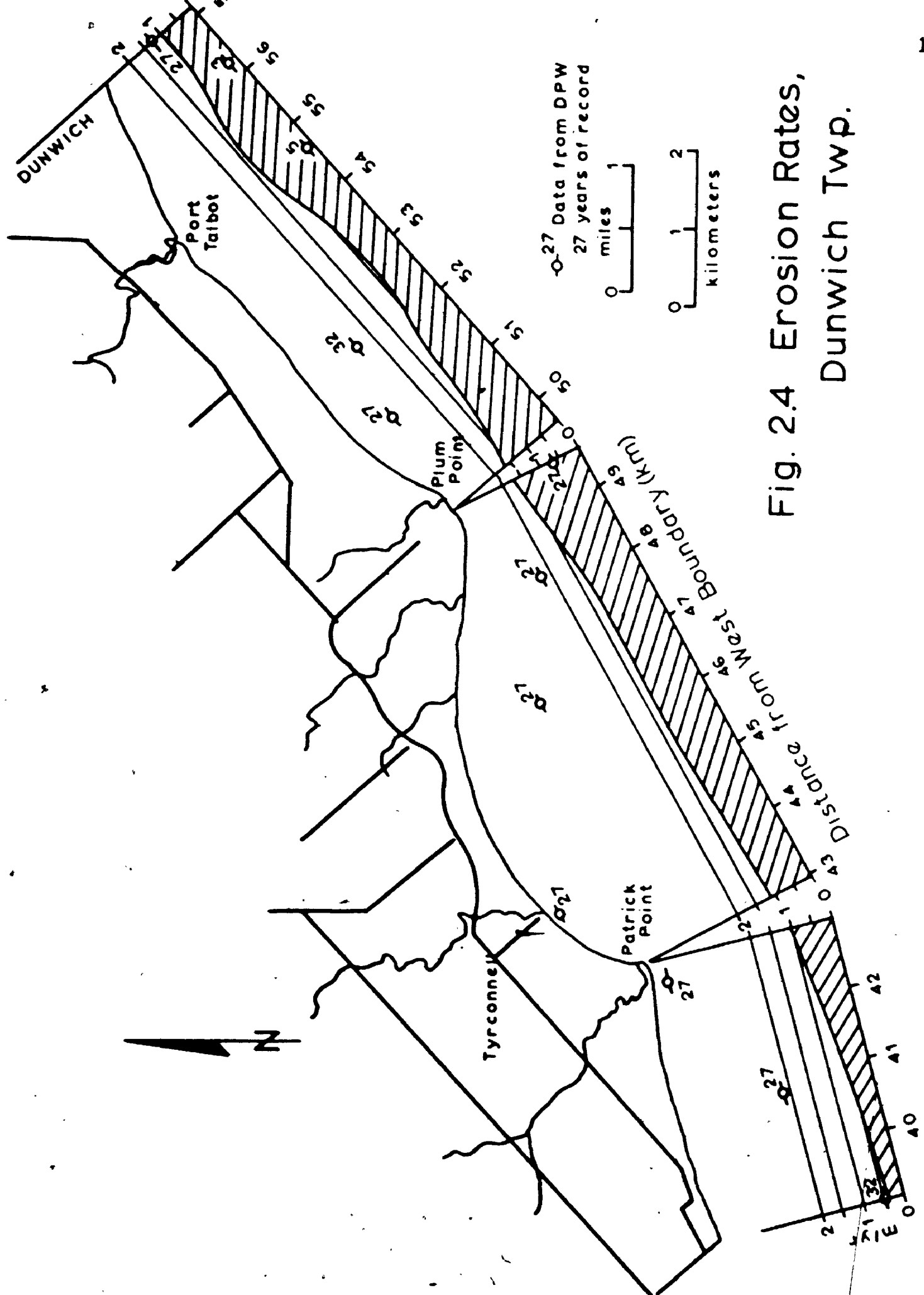
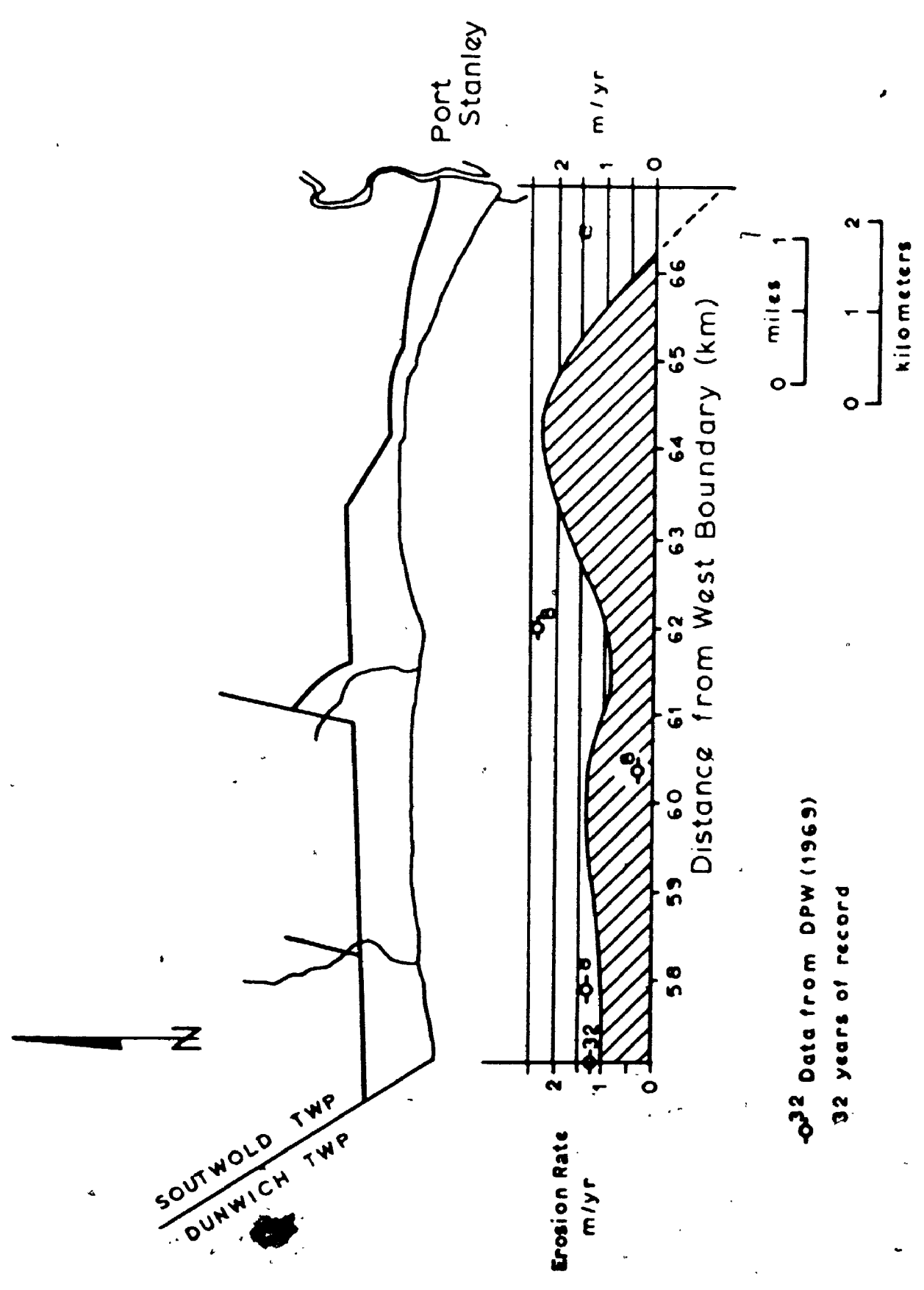


Fig. 2.4 Erosion Rates,
Dunwich Twp.



0.32 Data from DPW (1969)
 0.8 32 years of record

Fig. 2.5 Erosion Rates, Southwold Twp.

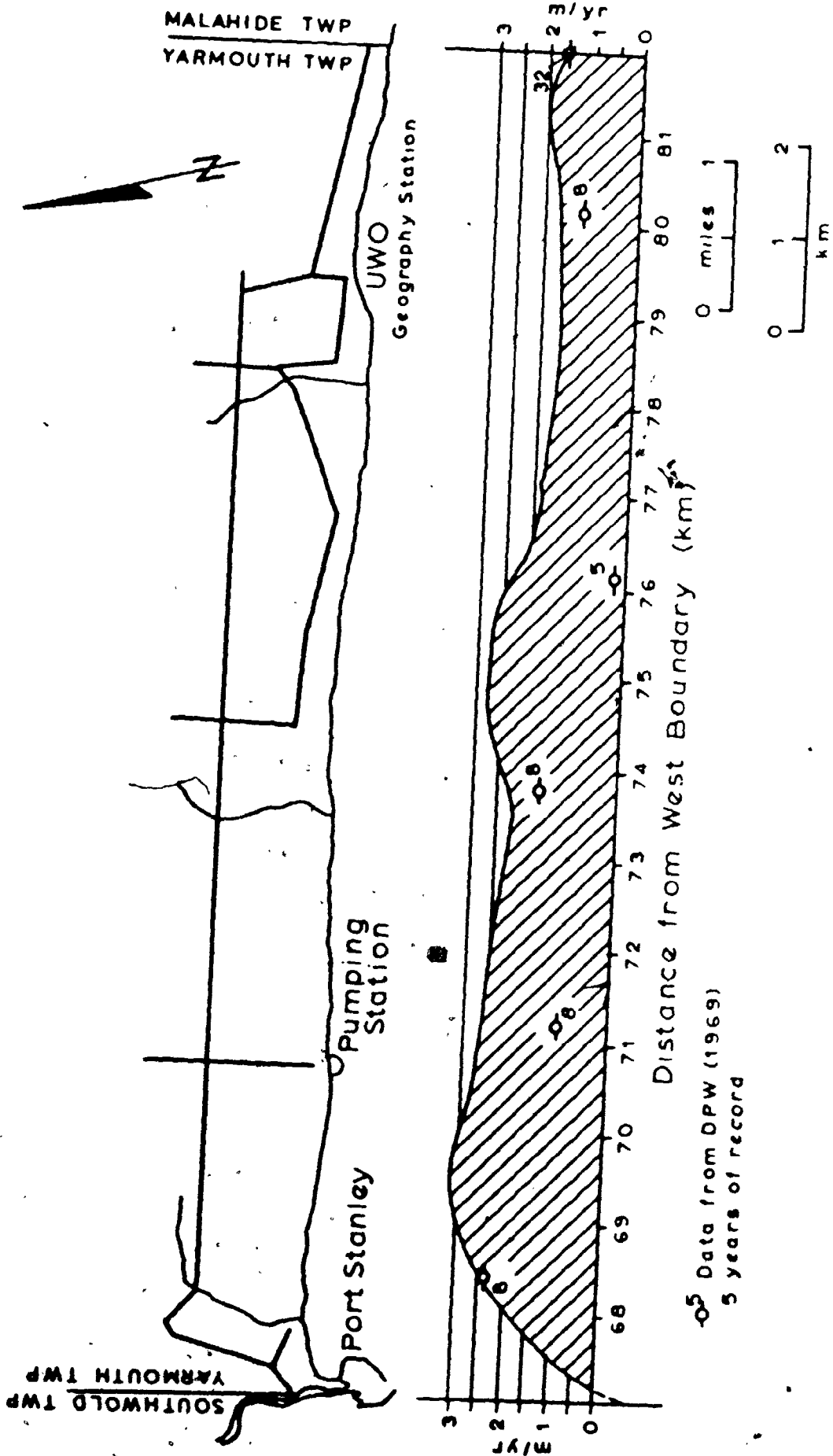


Fig. 2.6 Erosion Rates, Yarmouth Twp.

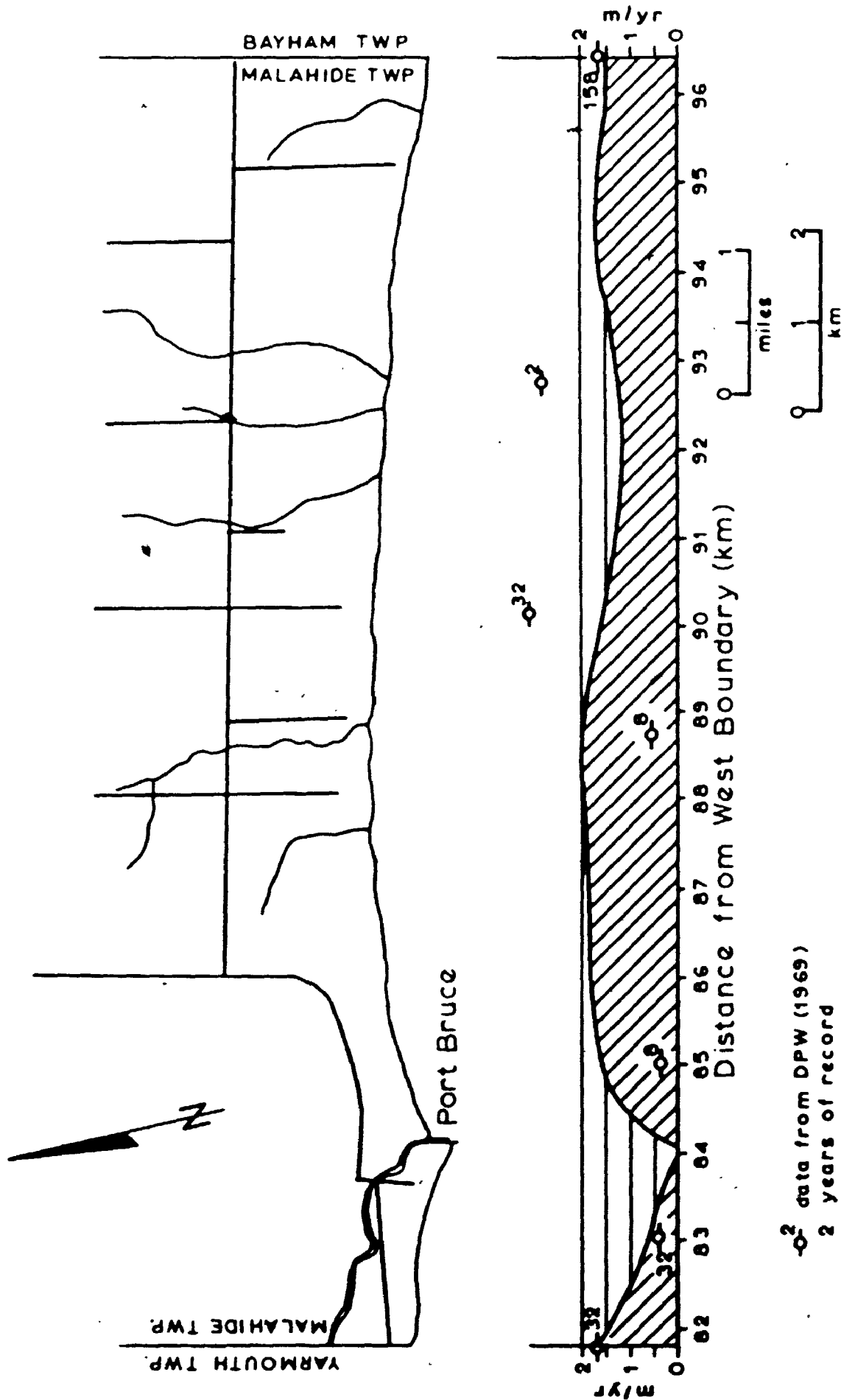


Fig. 2.7 Erosion Rates, Malahide Twp.

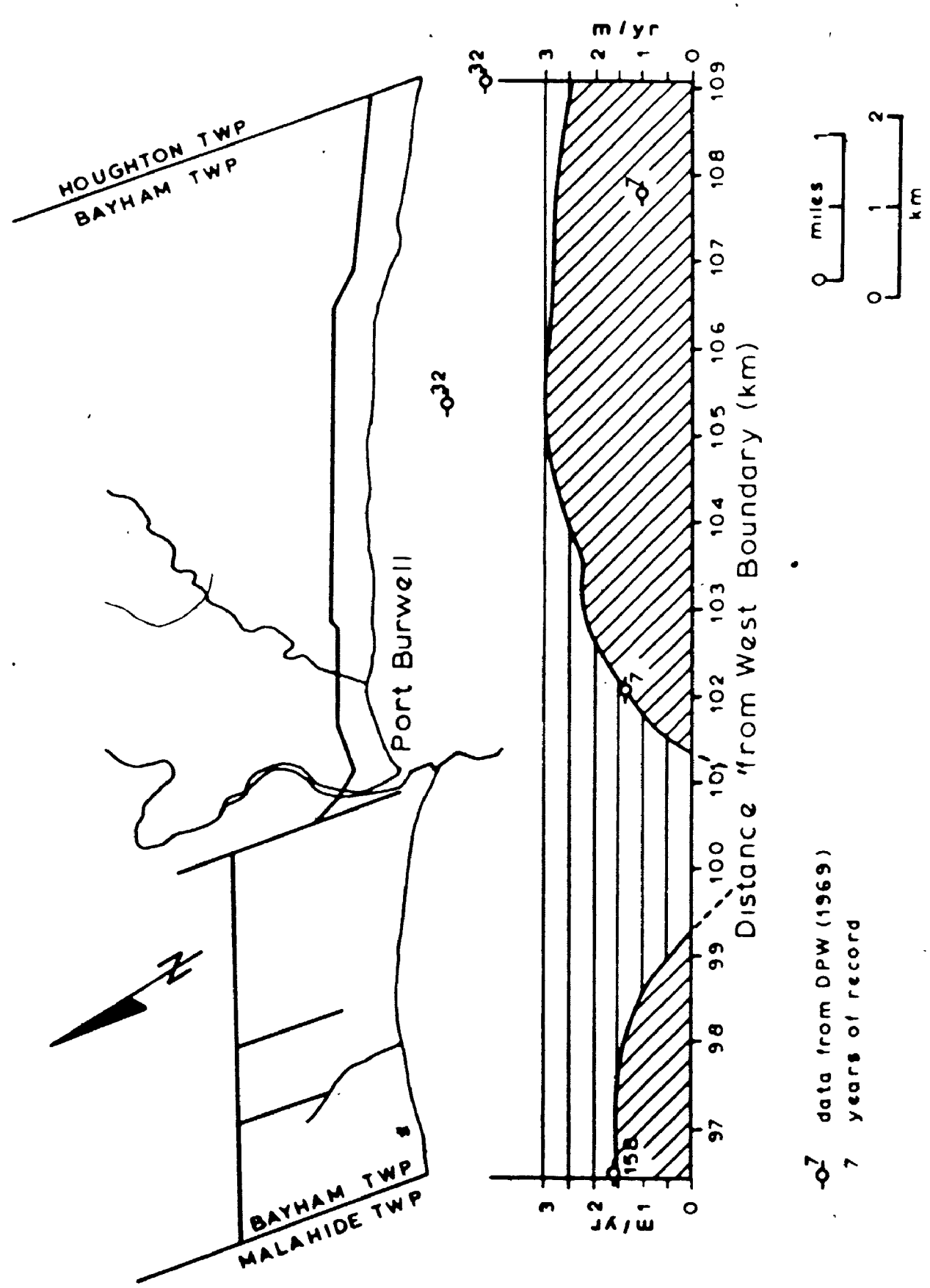


Fig. 2.8 Erosion Rates, Bayham Twp.

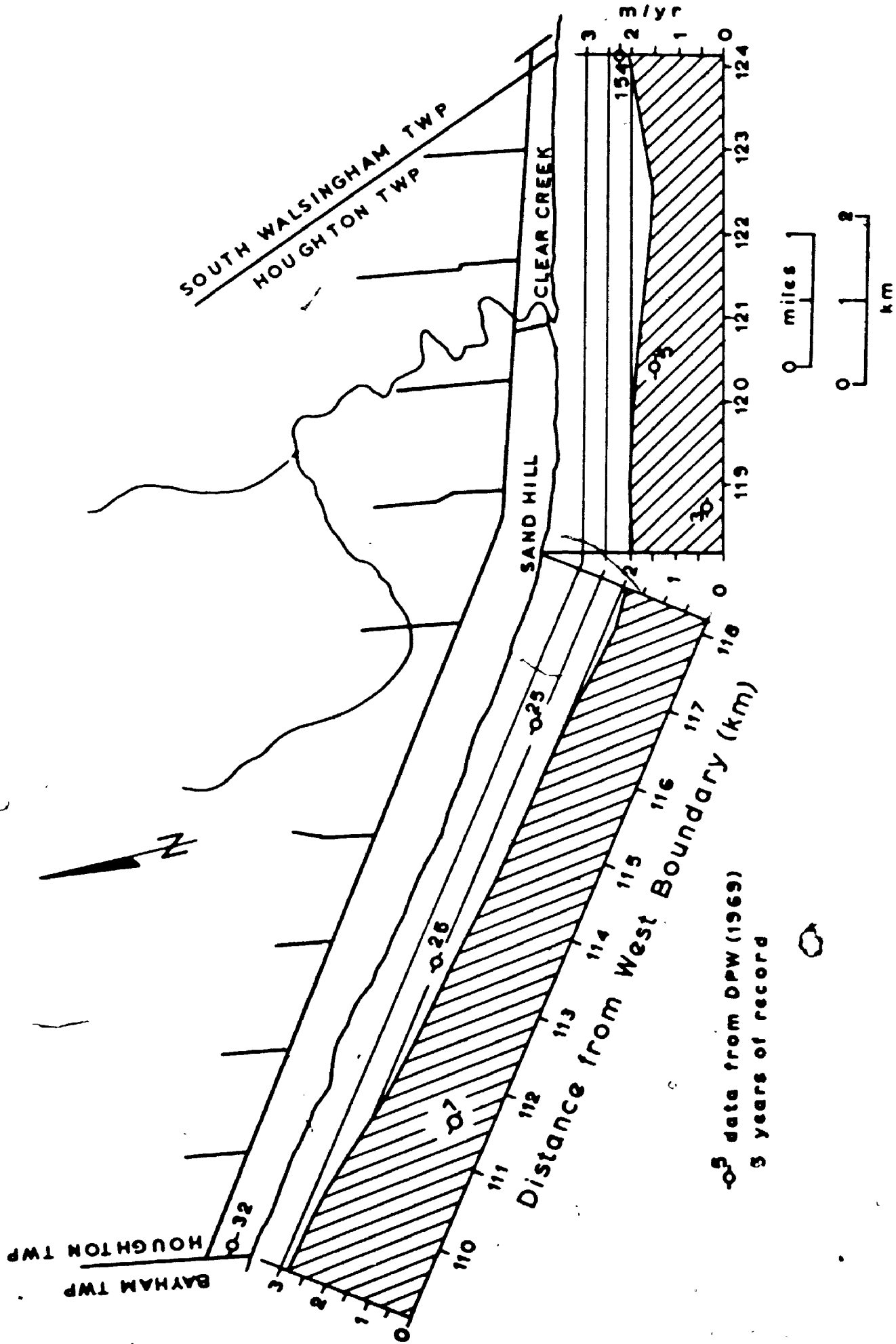


Fig. 2.9 Erosion Rates, Houghton Twp.

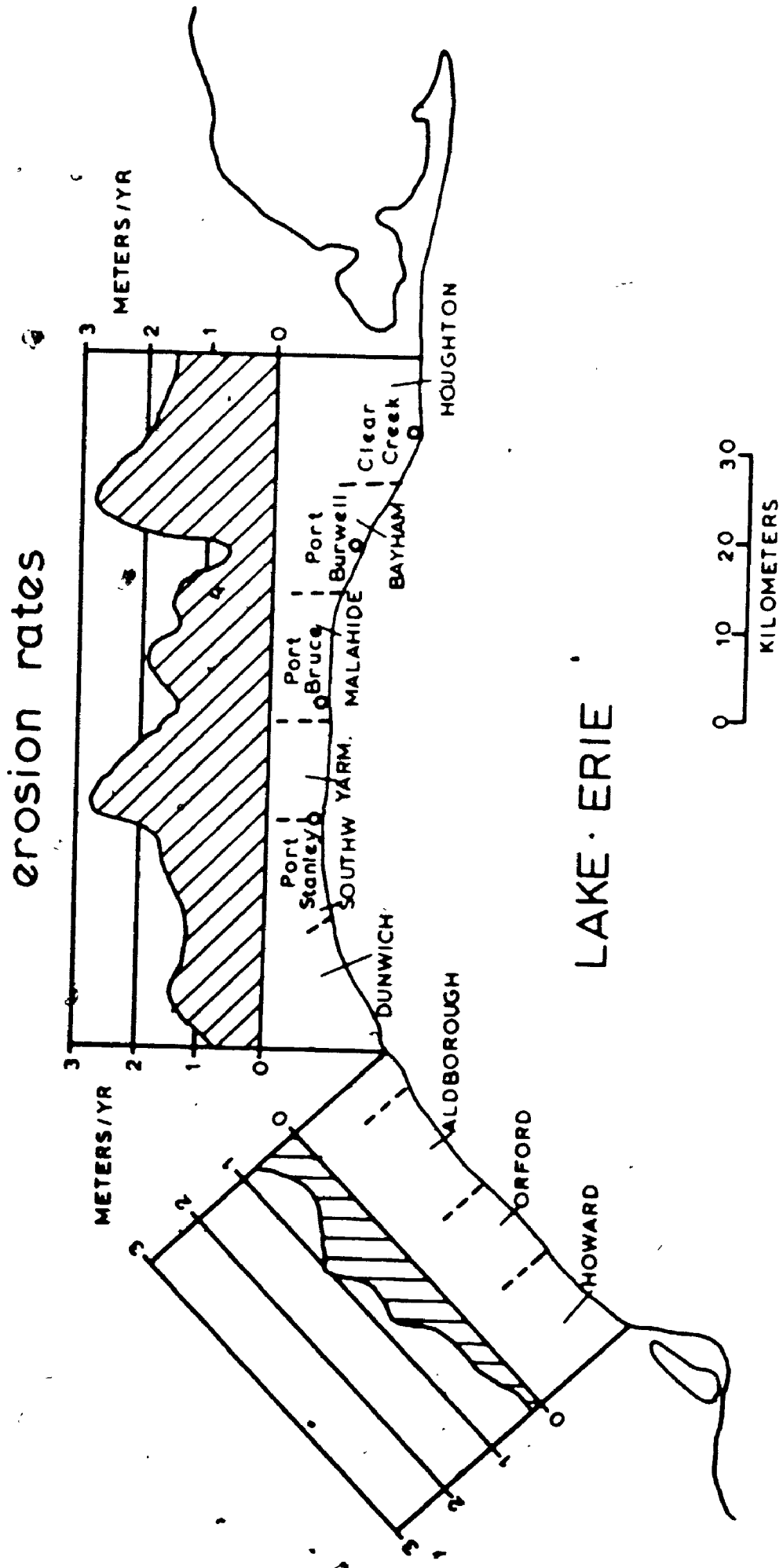


Fig. 2.10 Summary of Erosion Rates, Central Lake Erie.

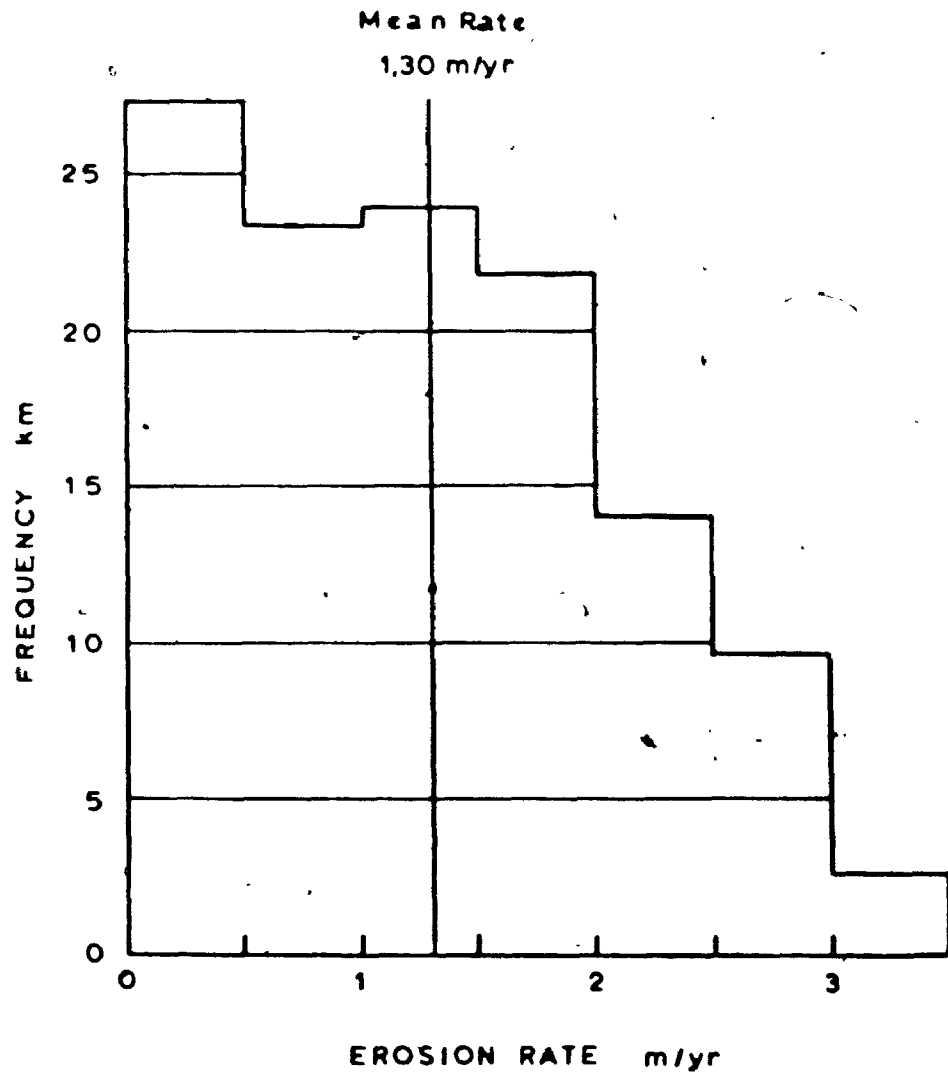


Fig. 2.11 Frequency Distribution
of Erosion Rates

erosion rates increase from the western end of the study area towards Port Stanley where there is a maximum and also the high rates in the region east of Port Burwell. Another feature is the negative or zero erosion rates observed in the vicinity of Port Stanley, Port Bruce and Port Burwell; these villages are in fact protected by jetties and have a harbor. The negative rates correspond to areas of accretion of sand on beaches at a rate greater than erosion rates; the fact that they occur on the western side of the jetties is an indication of the general current directions along the north shore of Lake Erie.

Other natural zones of sand accretion are the spits at Pointe-aux-Pins and Long Point; the occurrence of low erosion rates in the western part of the study area can in part be explained by the presence of Pointe-aux-Pins which acts as a natural barrier to storms and currents from the west and southwest.

The principal problem to be discussed here is the relevance or meaning of long-term erosion rates as compared with actual rates. Erosion of the bluffs occurs usually during very short periods of time, during storms for instance, followed by long intervals where erosion is active only offshore in the breaker zone. Short-term effects such as fluctuation in lake levels, storms setups, storm waves and landslides will cause very high erosion rates over a few days or a few weeks and almost no erosion for the rest of the year.* Point measurements were made at the extremity of the beach, west of Port Stanley, in November 1971; during

a ten-day period between November 1 and November 11, the toe of the bluffs receded by 0,40 meter, which would represent an annual rate of 14,6 meters as compared with the long-term rate of 2,2 meters per year. November is usually the month when storms are more frequent than in any other time of the year.

The interest of long-term measurements is that most lake effects average out over many years; for instance cycles of high and low water levels may extend over several decades and major storms are rare in occurrence, usually less than five per year (Platzman 1963). Long-term rates represent then the influence of the geological conditions at any particular point and illustrate the response of other factors such as stratigraphy, grain size, mechanical properties of the materials, gravity and weathering to the active forces of erosion derived from wave action.

Comparison of long-term rates was attempted with the short-term rates as determined by point measurements by the Department of Public Works (DPW 1969). Due to a different method of measuring erosion rates, comparisons are difficult. DPW data is given as a series of punctual erosion rates (45 in the study area) with time intervals of 2 to 32 years except for two points on the boundaries of townships where the time intervals are 154 years (east of Houghton Twp.) and 158 years (east of Malahide Twp.). The last two points are in close agreement with the rates determined by the superposition method; the other points vary widely about the long-term rates and reasons for that are numerous. First, the

time interval between surveys is important; for intervals of less than 12 years, the rates represent erosion with lake levels declining continuously; for intervals of more than 25 years, erosion rates represent the effects of one cycle of high and low water (high in 1952 and low in 1964). Since the length of these cycles varies widely as will be seen later, a mean erosion rate should encompass several such cycles. Secondly, punctual measurements of erosion rates are influenced by local irregularities of the shoreline: width of beaches, slope angle, presence of gullies, landslides, defence works, etc., which can influence the local rates in a positive or negative way. The point measurements of LPW are indicated for comparison on Figures 2.1 to 2.9.

Comparison of results of this study agrees very well with the figures given by Wood (1951) since the method is similar but the time interval longer by about 25 years.

Subsequent chapters will attempt to explain these observed rates of erosion by looking at some of the factors that seem to control it. Next section will deal with hydrodynamic effects of waves, setup and lake levels which are the driving force of erosion. The inertial forces of resistance are due to the materials composing the bluffs; their nature, origin and distribution will be studied together with the degradation of these materials by the processes of weathering, a preliminary step before erosion occurs. Finally slope stability will be analysed in relation to active erosion along the bluffs since landslides are seen as a direct consequence of toe erosion.

CHAPTER 3

THE CAUSES OF EROSION

This chapter is an attempt to analyse the process of erosion from the dynamic effects of Lake Erie. Consisting of several parts, this chapter will discuss in turn the wind field over Lake Erie in the proximity of the study area, wind-generated waves, the distribution of wave energy in the nearshore area, storm setups and lake levels as they affect erosion rates.

3.1 Wind field.

There are two ways of studying the wind field over an area to obtain the parameters needed for wave forecasting. The most common method is to use synoptic weather charts and to determine the gradient or geostrophic winds by measuring the spacing and curvature of isobars; this method is ideal for wide open seas or oceans. However, for inland waters, gradient winds are modified near the ground by friction over land and no accurate value can be obtained for the fetch area being considered: This is why it is suggested (U.S.Army 1966) that actual measurements of wind velocity and direction be obtained at a station close to the area of forecasting (Cole 1967).

3.1.1 Choice of a weather station.

In the study area there are three stations that

report wind data. The Fort Stanley weather station is well located in the center of the study area but it reports winds only four times daily. At Long Point, the anemometer is situated at the tip of the spit and hourly readings are taken for nine months every year. The data used in the thesis was taken at the Clear Creek radio station in the eastern part of the study area (Figure 1.1). This station has been reporting hourly winds for aviation purposes between 1940 and 1961. The anemometer is at 25.9 meters above lake level and within 800 meters of the shoreline. It is assumed that the data from this station is representative of the wind field over Lake Erie in the central basin. This assumption is supported by the fact that a good correlation has been established between the wind velocity recorded at Clear Creek and storm setup on Lake Erie measured between Toledo, Ohio and Buffalo (Platzman 1963).

3.1.2 Type of data available.

The data from Clear Creek was obtained from the Meteorological Branch of the Department of Transport on microfilm and shows the wind direction and velocity for every hour between January 1956 and December 1960. This length of time is thought sufficient to include typical storms on Lake Erie; a previous study (Platzman 1963) reports an average of four such storms per year over the lake.

The wind velocity is reported in miles per hour

and the direction as one of the sixteen points of the compass (N, NNE, NE, ENE, ...). Wind velocity and direction is measured by taking the mean value of a one-minute sample every hour; during intervals of strong winds, the gust speed is also noted. Two bias were observed in this data: odd numbers for velocity readings occur six times less than even numbers; the other bias is in recording direction: the secondary points NNE, ENE, ESE, ... occur systematically less often than the main directions N, NE, E, ... These two observations will be considered in the statistical handling of the data.

3.1.3 Processing of the wind data.

The hourly wind readings were tabulated from the microfilms and were grouped around eight principal directions (N, NE, E, ...); this last step was done to remove a bias found in the data and also for a practical reason: in forecasting waves, it is assumed that the wind blowing in a given direction generates waves in all directions within 45° on either side of the wind direction; this results in longer duration for the wind blowing in a given direction and also allows for inherent variability in the wind field.

Every time the wind shifts to a new direction, the duration of the interval is recorded and the average velocity is computed for that period. The data in this form is ready to be fed into the wave forecasting charts to be described in the next section.

Other statistical work performed on the data includes computation of wind frequency and average velocity by direction and by month, and also the velocity distribution in each direction.

3.1.4 Results of wind analysis.

The velocity-frequency diagram, Figure 3.1, shows a predominance of westerly and southwesterly winds over Lake Erie and also pictures a large proportion of strong winds (greater than 10 meters per second) in these directions. Table 3.1 gives a monthly percentage frequency distribution of winds in each direction and Table 3.2 the mean velocity observed in each direction. Westerly winds are predominant most of the time except in late summer. Strong winds are occurring in the W and SW directions from November to February. Maximum velocities are recorded in November both for W and SW directions.

Also important in this study is the distribution of strong winds. A histogram, Figure 3.2, illustrates the frequency of winds in class intervals of 4 miles per hour (1.8 meter per second); the interest of that distribution lies in the frequency of occurrence of winds stronger than 10 meters per second which are responsible for storm conditions on Lake Erie.

Using the five-year record from 1956 to 1961, a probability model is derived using a logarithmic law (Figure 3.3). For winds with a velocity superior to 10 meters per

Table 3.1

Frequency of winds at Clear Creek
(1956-1960)

in %

Month	N	NE	E	SE	S	SW	W	NW	C
J	12.2	12.7	6.6	1.6	5.4	12.9	29.6	17.3	1.6
F	6.5	13.0	9.1	2.4	5.6	12.3	31.2	16.4	3.5
M	10.2	19.8	12.6	2.6	4.3	10.7	22.8	12.6	4.2
A	5.5	12.9	13.1	5.3	6.6	18.2	25.4	10.1	2.9
M	6.7	12.8	11.8	7.2	9.4	20.0	19.0	10.3	2.7
J	5.4	7.9	8.0	6.4	9.9	22.9	23.6	13.5	2.7
J	7.6	8.6	8.4	4.2	9.6	22.5	24.2	10.4	4.5
A	11.5	14.0	5.1	3.8	7.8	25.6	17.7	10.8	4.3
S	12.9	14.0	5.7	5.0	11.9	20.3	12.0	15.3	3.0
O	12.3	14.4	9.4	3.5	11.4	14.3	14.6	18.5	1.5
N	4.1	10.0	4.7	2.6	9.5	20.0	29.7	17.4	1.9
D	8.8	12.4	5.4	1.6	5.5	20.7	28.9	14.9	1.7
Total	8.6	12.8	8.3	4.0	8.0	18.2	23.9	14.0	2.6

Table 3.2
 Mean Velocity of Winds at Clear Creek
 (1956-1960)

Month	In meters per second							
	N	NE	E	SE	S	SW	W	NW
J	4.1	5.0	4.9	3.8	6.0	7.5	7.5	5.3
F	4.3	5.5	5.3	3.4	4.1	6.5	7.3	5.8
M	4.9	6.0	5.1	3.6	4.4	6.5	6.2	4.9
A	3.9	5.3	5.8	3.8	4.1	5.6	6.2	4.7
M	4.5	5.3	4.8	3.6	4.1	5.0	5.2	4.8
J	3.2	3.6	4.3	3.2	3.4	4.5	4.9	4.4
J	3.1	4.0	4.0	3.2	3.4	4.2	4.4	3.5
A	3.2	3.6	3.8	3.6	3.3	4.6	4.4	3.4
S	3.3	4.0	3.9	3.2	4.4	5.6	5.4	4.0
O	3.6	4.5	4.5	4.2	5.5	6.3	6.6	4.7
N	3.6	4.7	4.1	4.5	6.0	8.3	9.2	5.8
D	4.4	5.3	5.0	5.0	6.7	7.9	8.0	5.3
Total	3.8	4.8	4.7	3.6	4.6	5.9	6.5	4.8

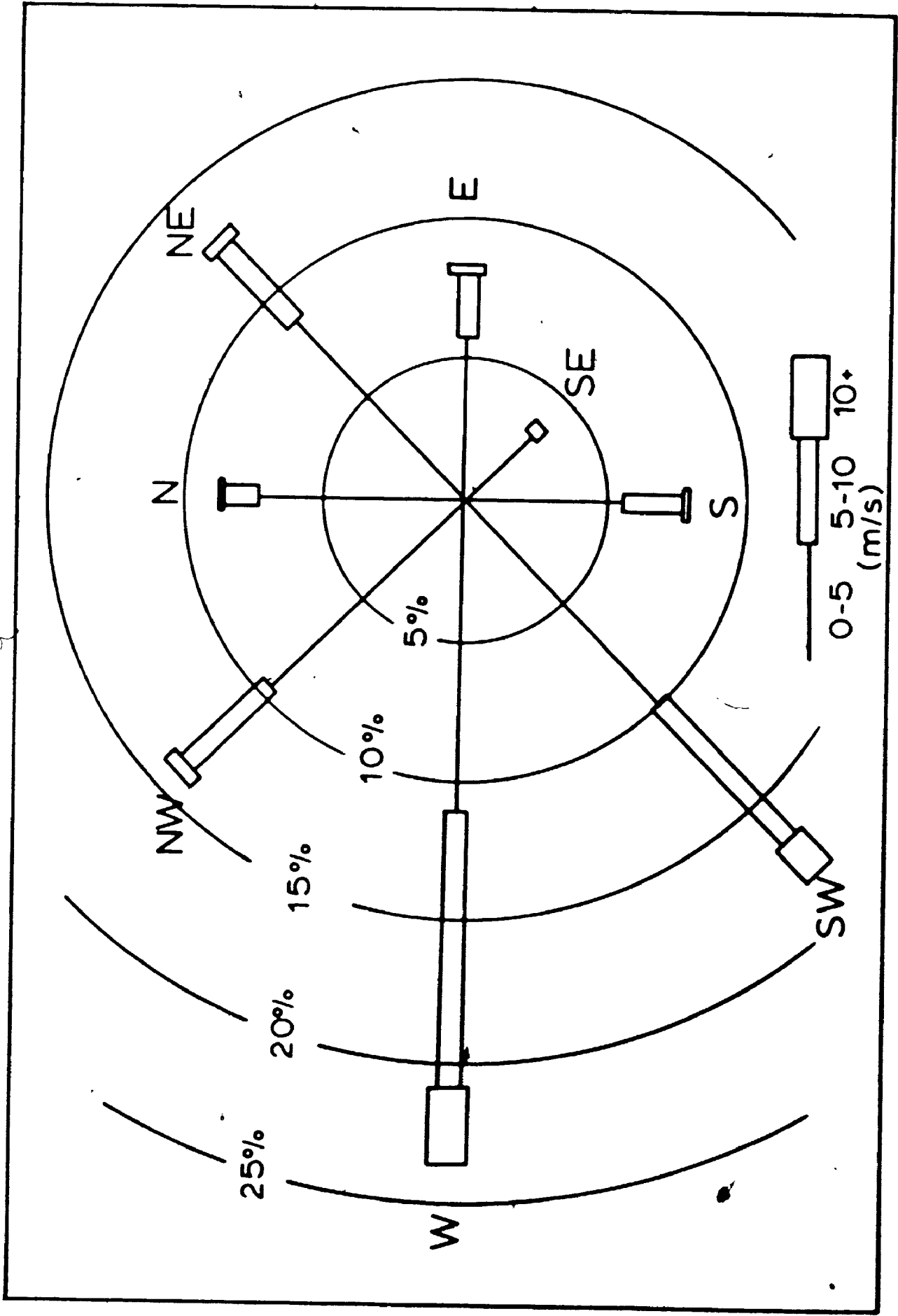


Fig. 3.1 Wind Velocity-Frequency Diagram

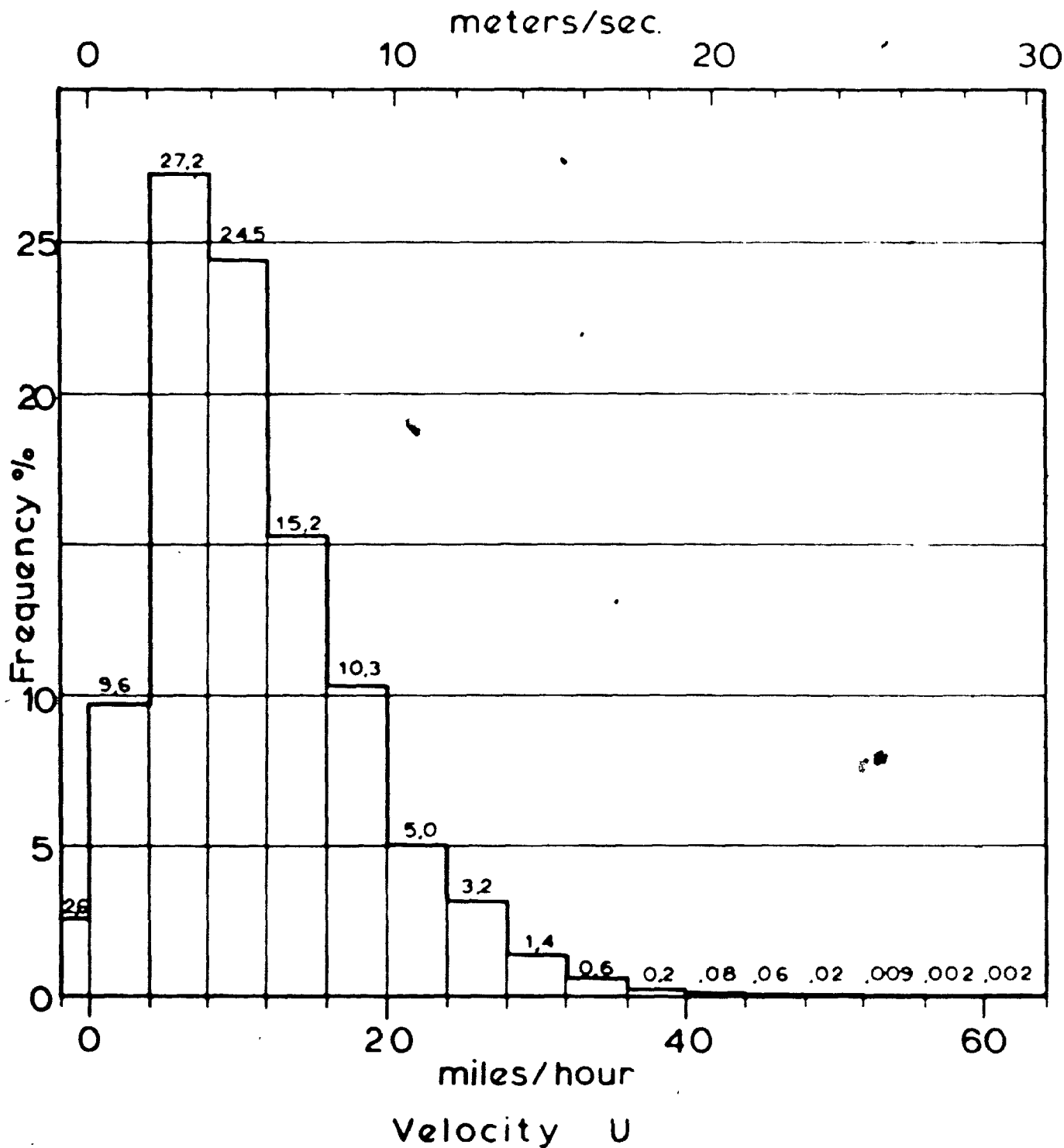


Fig. 32 Wind Velocity Histogram, Clear Creek, Ontario.

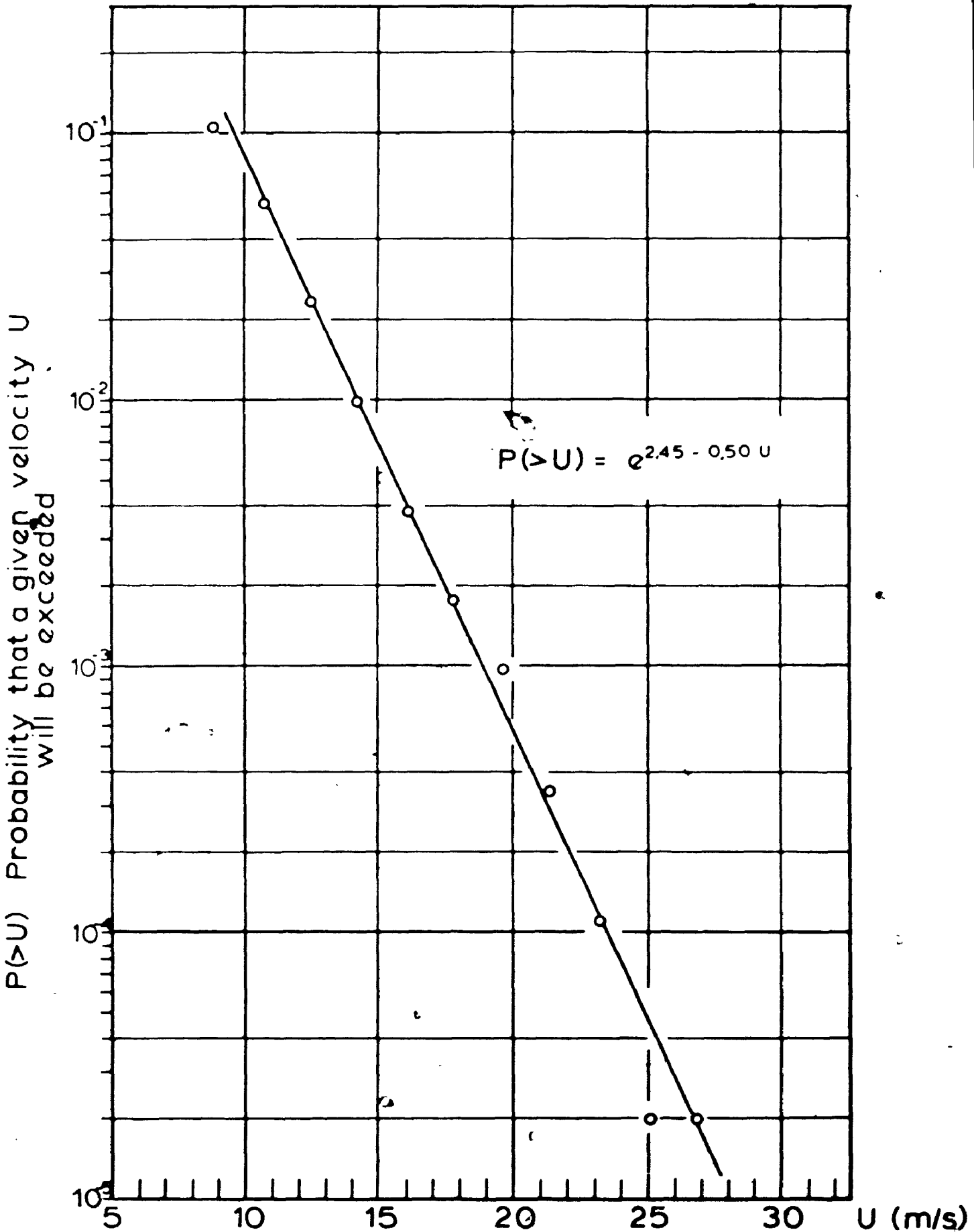


Fig. 3.3 Frequency of Strong Winds.

second, the probability, $F(>U)$ that the velocity at any time is equal or greater than a specified velocity U is given by the following equation:

$$\ln F(>U) = a + bU$$

where a and b are constants to be determined. By making the substitution

$$Y = \ln F(>U)$$

the first equation is reduced to the familiar equation of the straight line:

$$Y = a + bU$$

By least squares method, the parameter a equals 2.45 and b is equal to -0.50. The solution is then

$$Y = 2.45 - 0.50 U$$

and the regression line becomes after substitution

$$\ln F(>U) = 2.45 - 0.5 U$$

which can be expressed as an exponential permitting easy evaluation of the probability $F(>U)$

$$F(>U) = \exp(2.45 - 0.50 U) \quad \text{for } U \geq 10 \text{ m/s}$$

This model may be used for design only for winds with a velocity greater than 10 meters per second (22mph).

From observed frequencies over the same period, a graph, Figure 3.4, was prepared to show the probability in each direction of a certain velocity being observed or exceeded over a certain interval of time. Lines of equal probability are drawn for 1%, 0.1%, 0.01% and 0.001% corresponding roughly to annual occurrences of 90 hours, 9 hours, 1 hour and 0.1 hour respectively. Again it is visually clear that strong winds are more likely to blow in the

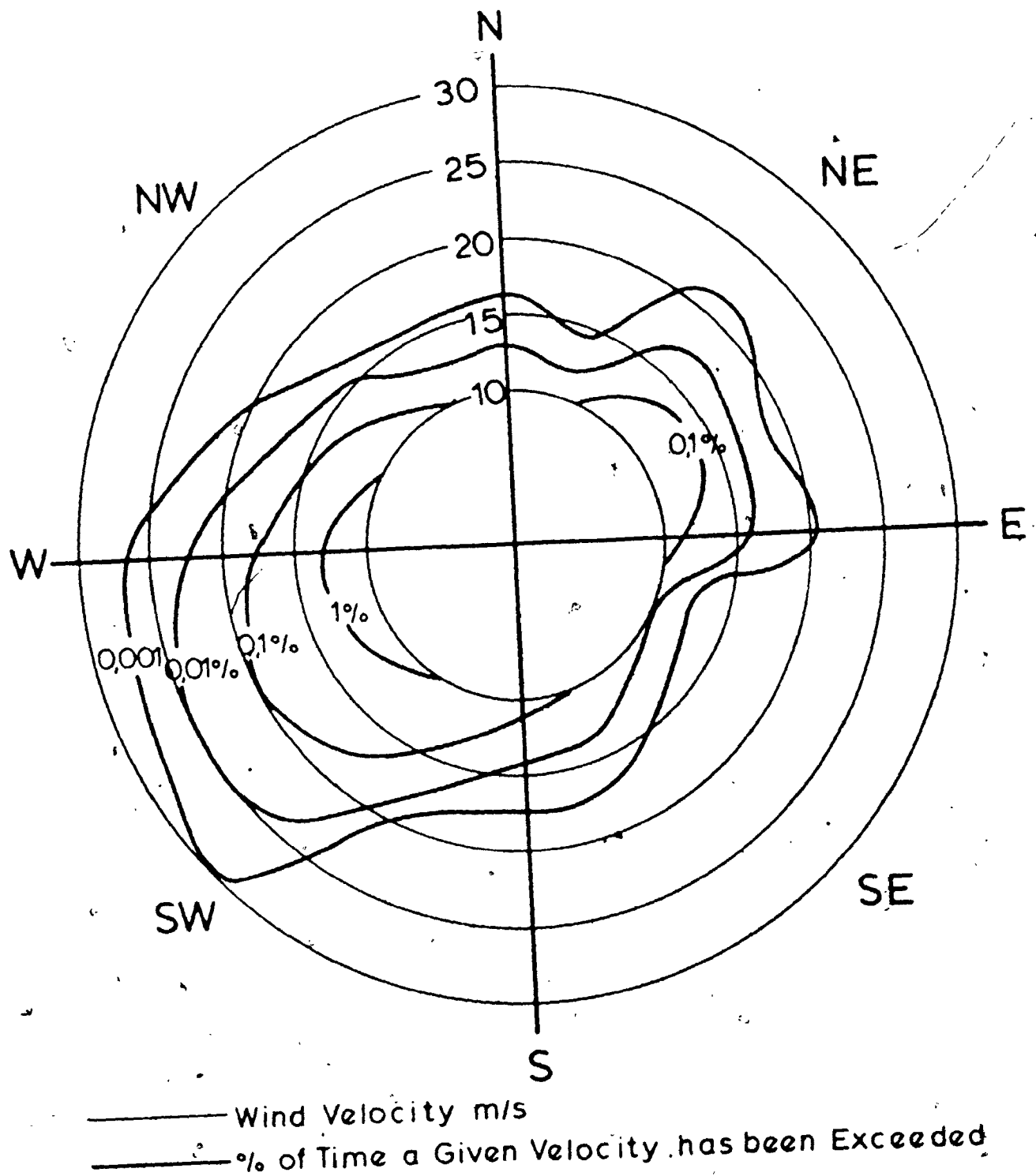


Fig. 3.4 Frequency of Strong Winds in each Direction.

SW and W directions.

Bearing in mind that the energy generated by waves on Lake Erie is a function of wind velocity, duration and fetch, it is clear that southwesterly winds will be more important in the erosion process due to their frequency, velocity and critical orientation with respect to the long axis of the lake (WSW-ENE) and the shoreline in the central and eastern portions of the study area. The action of westerly winds will be somewhat subdued because the winds run nearly parallel to the shoreline in the central section.

3.1.5 Vertical profiles of wind velocity.

Wave forecasting and storm setup calculations are dependant on wind velocity and a relationship exists between the vertical velocity profile and the wind stress responsible for wave generation. The wind velocity measured from an anemometer is function of the height of the instrument above ground. Several models describe the vertical wind distribution.

The most commonly used model is known as the "Prandtl-von Karman universal velocity distribution law" (Bretschneider 1967) which reads:

$$U_z/U_f = 1/k \ln(Z/Z_0) \quad (1)$$

where U_z is the wind velocity at an elevation Z above surface U_f is the friction velocity defined as $(\tau/\rho)^{1/2}$ in which τ is the shear stress at the surface of water and ρ the density of air, Z_0 is the friction length defined below and $k=0,4$

the von Karman constant.

In practice all measurements are referred to the standard anemometer level of 10 meters above the free surface. Then for an elevation of 10 meters, Equation (1) becomes:

$$U_{10}/U_f = 1/k \ln(10/Z_0) \quad (2)$$

Dividing Equation (1) by Equation (2)

$$U_z/U_{10} = \ln(Z/Z_0)/\ln(10/Z_0) \quad (3)$$

Equation (3) allows the calculation of standard wind velocity U_{10} provided the wind velocity at any elevation and the coefficient Z_0 are known. The friction length Z_0 is determined from the following equation (Bretshneider 1967)

$$Z_0 = Z \exp(-k/C^2) \quad (4)$$

where Z is the anemometer elevation in meters, k is the von Karman constant, and C a dimensionless drag coefficient determined experimentally; for Lake Erie, $C = 0.0025$ (Keulegan 1953). Z_0 is then for $Z = 25.9$ meters (at Clear Creek) equal to 0.009 meter.

An other model used by structural engineers (ASCE Task Committee on Wind Forces 1961) is referred to as the one-seventh power law:

$$U_z/U_{10} = (Z/10)^{1/7} \quad (5)$$

These two models give essentially the same profile and were designed without reference to water and air temperature differences which may be important over lakes.

A recent study on Lake Ontario (Weiler 1969) defines a more general model

$$U_z/U_{10} = (Z/10)^p \quad (6)$$

where the coefficient "p" is a variable which is function

of the nature of the surface and the temperature difference ($T_a - T_w$) between the air (T_a) and the water (T_w). For a wide range of the ratio $(T_a - T_w)/T_a$, between -1,0 and -0,1, the value of "p" is 0,05 and for the range between 0 and 0,1 this value of "p" varies between 0,1 and 0,2, based on experiments on a tower 2 kilometers offshore.

The vertical wind profiles for dimensionless ratios U_z/U_{10} are shown on Figure 3.5 and the difference in the two models for winds blowing at 10 meters per second is shown in Figure 3.6. As can be seen from this last figure the standard anemometer velocity at 10 meters elevation does not vary by more than 5% depending on the model chosen, and the reduction in velocity measured on the anemometer at Clear Creek ($Z = 25,9$ m) is less than 12%. This standard wind velocity will be used for wave forecasting and storm setup calculations.

3.2 Wind-generated waves.

In this study only waves created by wind stress will be investigated; the generation of waves being a complex problem, many variables will affect or limit the growth of waves; the more important factors are discussed below.

3.2.1 Factors limiting the growth of waves.

Four factors have to be considered in the prediction of wave height, length and period; these are wind.

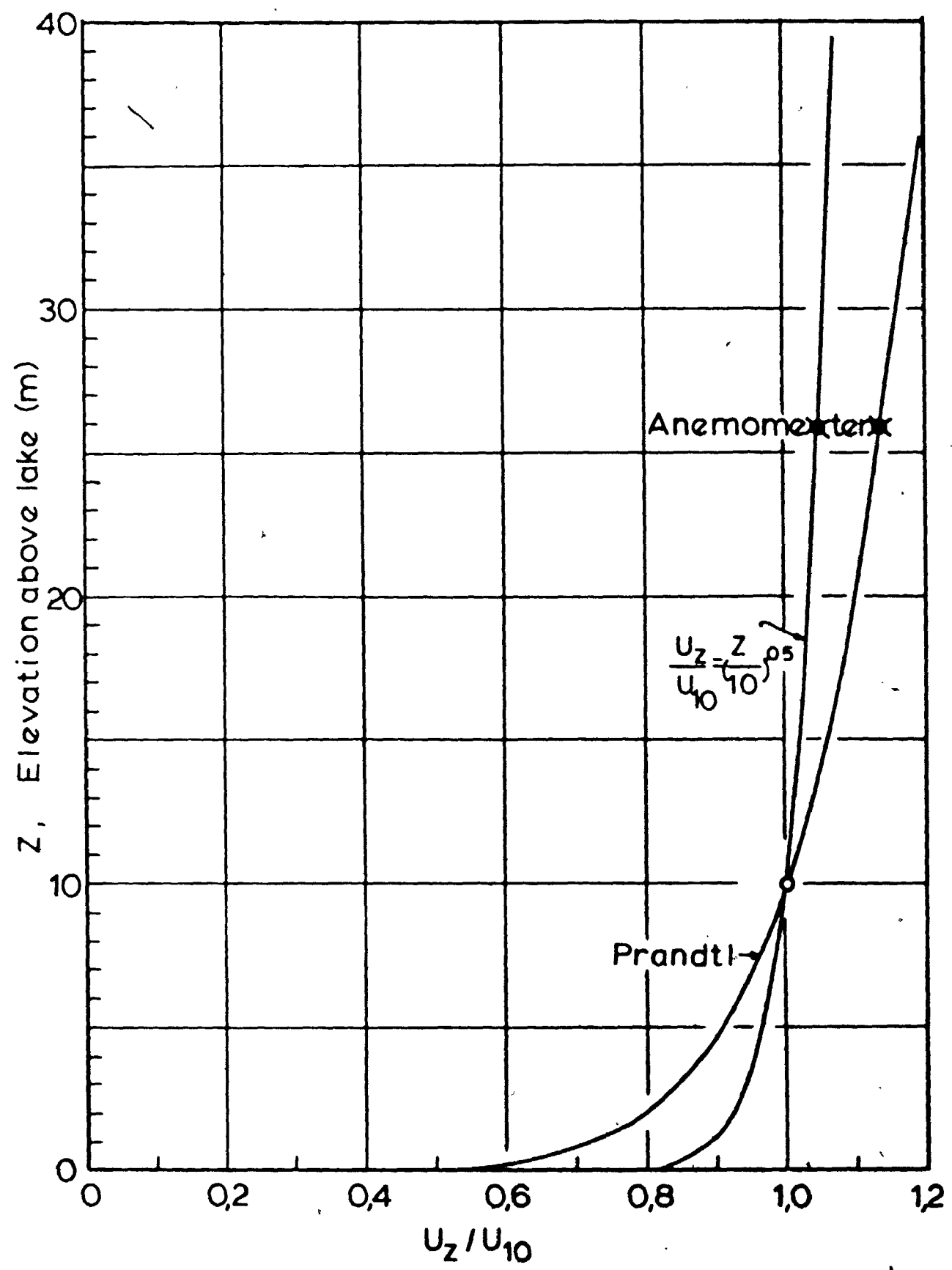


Fig. 3.5 Vertical Wind Profile, Clear Creek.

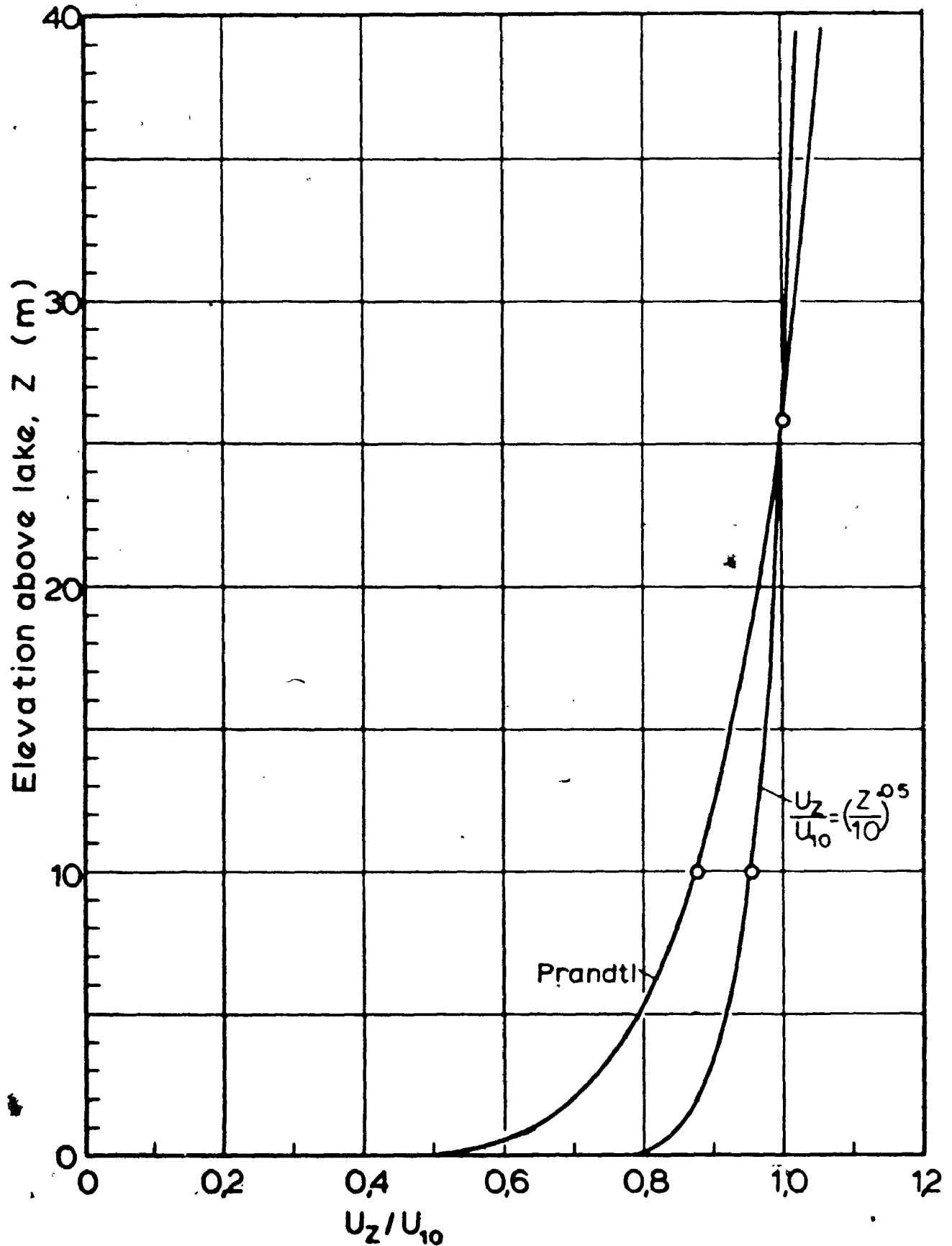


Fig. 3.6 Prediction of U_{10} from Wind Profile

velocity, wind duration, fetch and depth of water.

Wind velocity is the driving force in generating waves and it will be assumed that the average velocity of the wind blowing in a given direction for a certain interval of time (the duration) is representative of the wind velocity at any time within that interval. It is also assumed that the velocity measured at Clear Creek and reduced to the standard velocity at 10 meters (section 3.1.5) is representative of the wind field over the whole area under study as discussed previously.

Wind duration is an other factor limiting wave growth. The duration used in the forecasting technique is taken as the length of time in hours that the wind was blowing in the same 45° sector whose apex is centered on any of the eight major points of the compass (N, NE, E, ...). This procedure is justified since wind creates waves in all directions at plus or minus 45° with the direction of the blowing wind (U.S.Army 1966).

The fetch or the distance on the water surface subjected to wind stresses is also important in restraining wave growth. For oceans and seas the fetch is determined mainly from the size of cyclones and anticyclones as reported on synoptic weather charts. For inland waters with irregular shorelines a modified fetch length is required; the method used here is based on the following assumptions (U.S. Army 1962): 1) the wind blowing in a given direction transfers energy in the direction of the wind and in all directions within 45° on either side of that direction; 2) the

wind transfers a unit amount of energy to the water in the direction of the wind and along any other direction an amount modified by the cosine of the angle between that direction and the direction of the wind. The method of calculating the effective fetch consists in constructing fifteen radials originating at any point along the shoreline and extending to the opposite shoreline; these radials are at 6° intervals on either side of the wind direction; the length X_i of each radial is measured and multiplied by the cosine of the angle "i" it makes with the wind direction. The effective fetch is the quotient of the sum of all ($X_i \cos i$) by the sum of all ($\cos i$) as illustrated on figure 3.7. The effective fetch for all wind directions has been computed for six locations along the north shore of Lake Erie, Figure 3.8, and the results are summarized in Table 3.3, where the effective fetch is in kilometers.

This technique yields shorter fetch length in general but it also takes into account the effect of wind blowing almost parallel to the shoreline, wind that also produces waves and currents.

Depth of water is an other limiting factor since it affect wave height, period and length especially in shallow water where bottom friction is important. In the classical theory of oscillatory waves (see Appendix 1) wave length, L , wave period, T , wave velocity, C , and depth of water, d , are related by the following equations:

$$L = CT$$

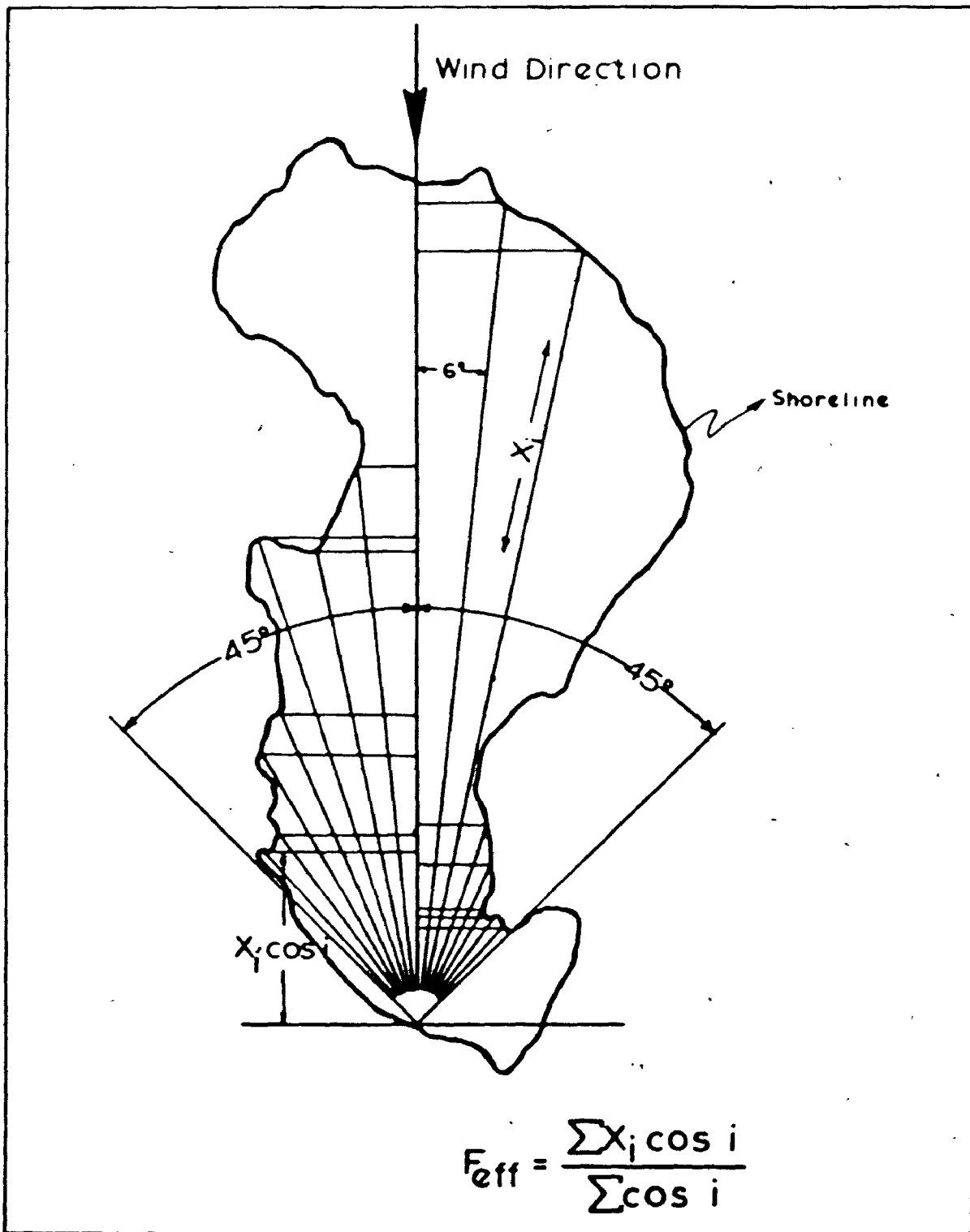


Fig. 3.7 Computation of Effective Fetch.

Table 3.3
 Effective Fetch
 in kilometers

Station	NE	E	SE	S	SW	W	North
1	--	31	65	79	136	83	--
2	--	15	54	97	133	71	6
3	--	37	82	114	119	41	--
4	--	53	100	123	94	12	--
5	--	75	117	113	62	--	--
6	37	106	110	86	32	--	--

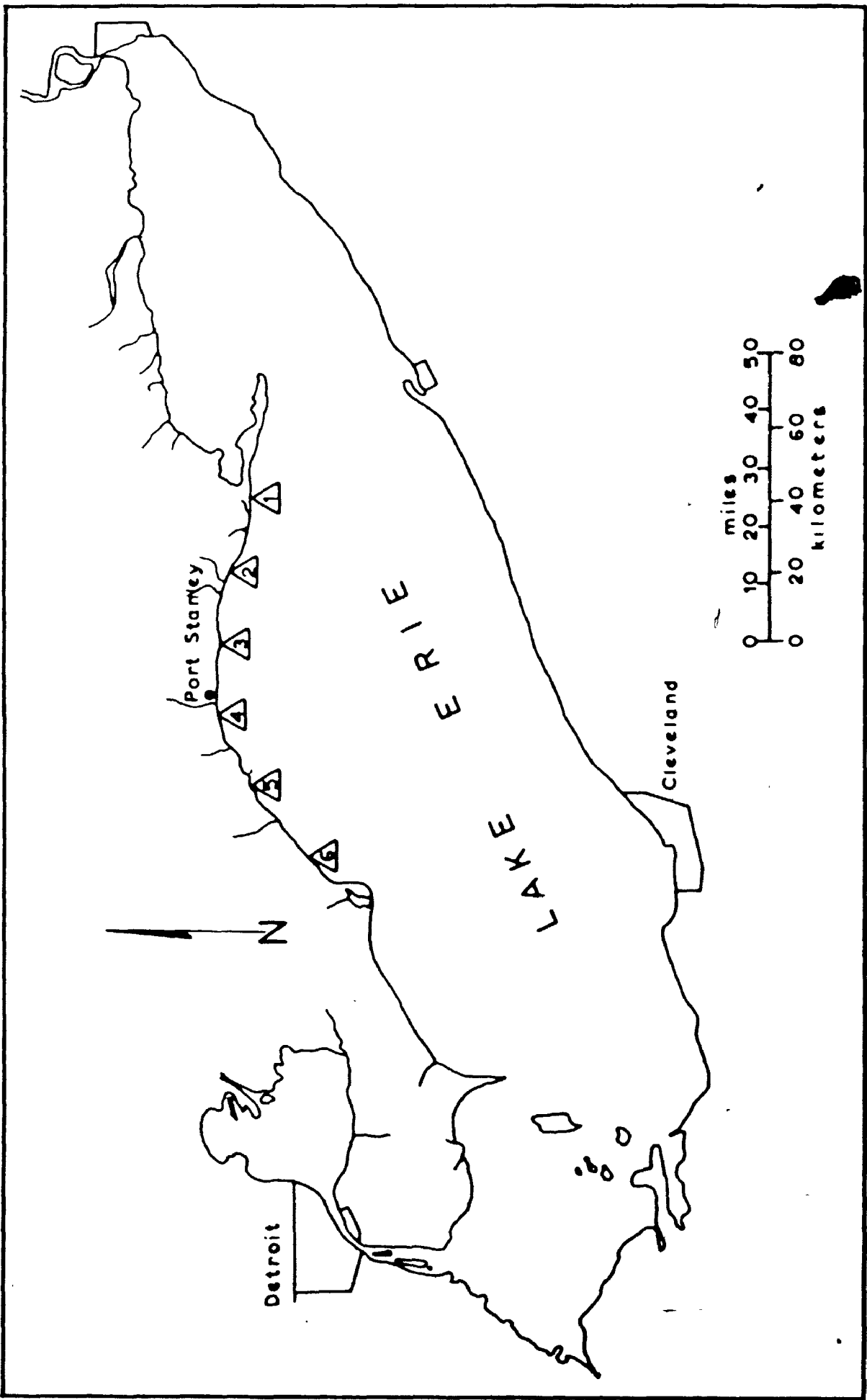


Fig. 3.8 Wave Forecasting Stations

and

$$C^2 = (gL/2\pi) \tanh(2\pi d/L)$$

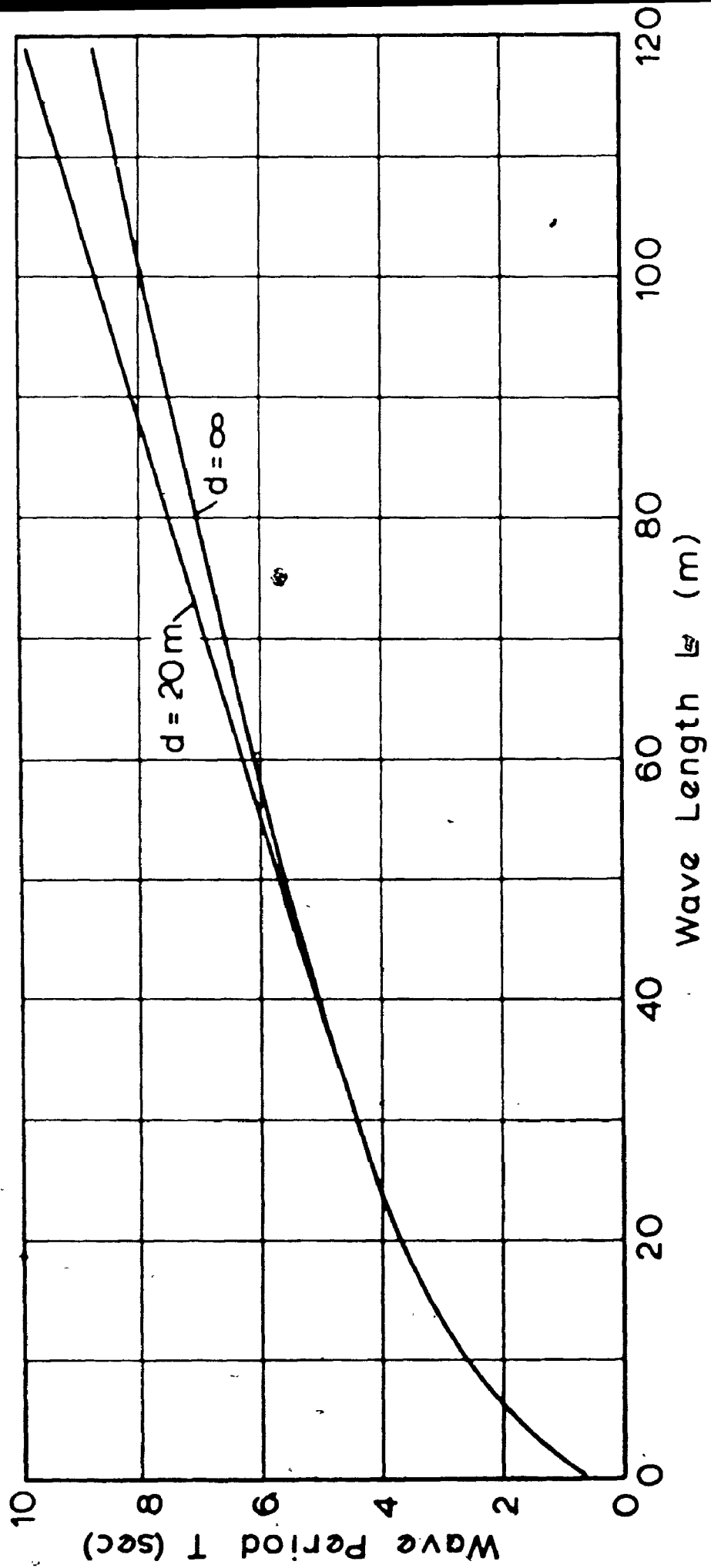
wave lengths in deep water are compared with the wave lengths in water 20-meter deep in Figure 3.9. The average depth of Lake Erie in the central basin has been taken as 20 meters on the basis of depth contours from a map prepared by the International Joint Commission on the Great Lakes (Figure 3.10). The effect of depth of water on wave height and period will be discussed in the next section.

3.2.2 wave forecasting techniques.

Methods of wave forecasting using meteorological data are numerous but only three have had wide application; the first one, the Sverdrup-Munk-Bretschneider method (SMB) (Bretschneider 1958) will be discussed in more detail later; the spectral method of Pierson, Neumann and James (Neumann 1953) gives a solution in terms of total wave energy and is based on the assumption of a fully developed sea; finally Larbyshire (1957) derived curves for limited fetches in deep water; this latter method was used (Brebner and Kennedy 1962) to study the wave characteristics of Lake Ontario but no comparison can be made with Lake Erie which is very shallow compared to Lake Ontario.

For shallow lakes or seas, only the SMB method is well documented and widely used in North America (Cole 1967). It gives a solution in terms of significant wave parameters. The significant wave height, H_s , and wave period,

Fig. 3.9 Relationship between Wave Period, Length, and Depth of Water



from International Joint Commission, 1969

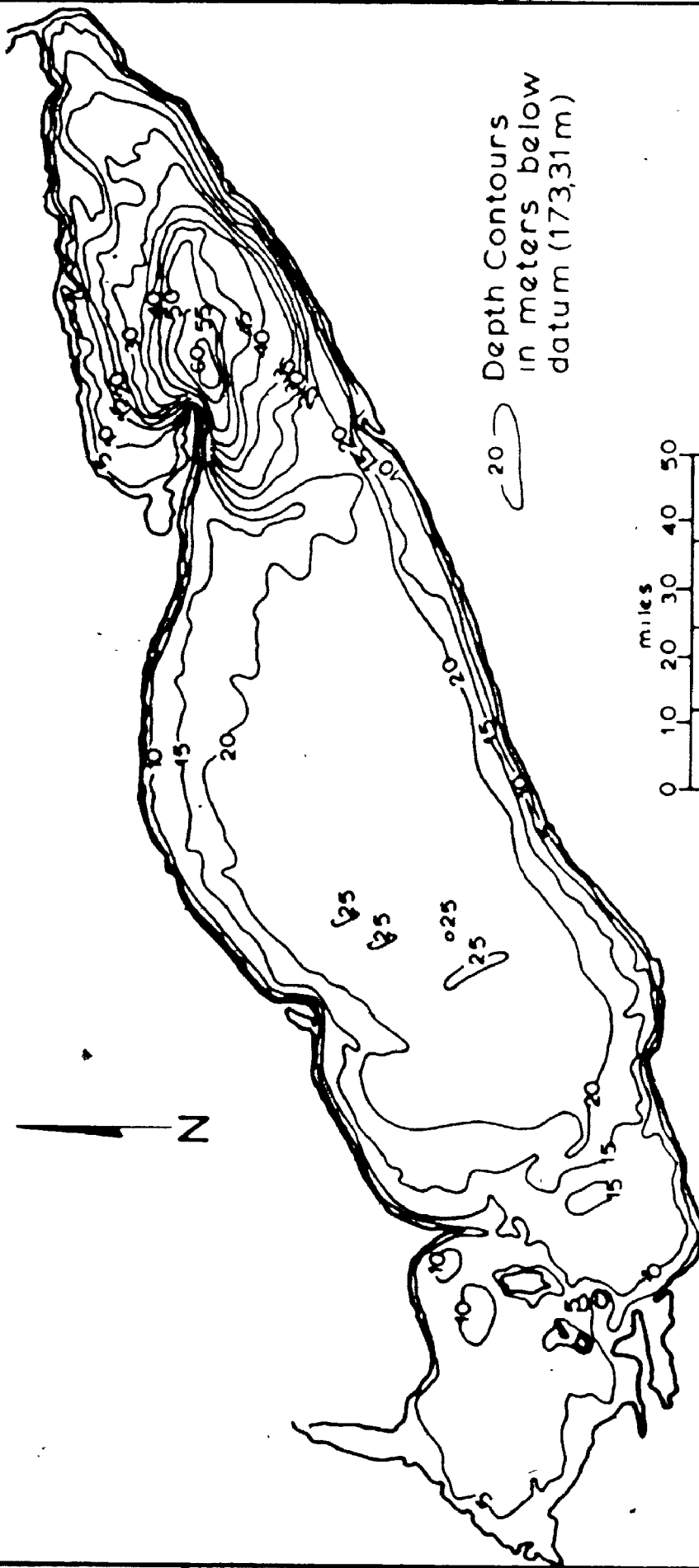


Fig. 310 Bathymetric Chart of Lake Erie.

T_s , are defined as the mean value of the one-third highest wave heights and wave periods observed over an interval of time (Bretschneider 1966). Different statistical models exist (Putz 1952, Longuet-Higgins 1952, Bretschneider 1959) that make possible the computation of means, maxima and frequency distribution of wave heights and periods from the significant height, H_s , and significant period, T_s . Throughout this study, all calculations involving T and H will be in terms of H_s and T_s .

A graphical solution to the problem of wave forecasting is available (U.S. Army 1966) but it is valid only for deep-water conditions, which is in water where the ratio of the depth of water, d , to wave length, L , is equal or greater than one half. For Lake Erie, this graph has to be modified for longer waves because bottom friction affects the height of the waves.

A correction for wave period was suggested by Sibul (1955) based on laboratory experiments simulating the change in wave period with depth of water. A plot (Figure 3.11) of the results in terms of T_o/T and d/L_o is presented in which the subscript "o" refers to deep water conditions. It can be seen that the period T will be affected for very small values of depth d or for very large values of wave length, L_o . For Lake Erie, with an average depth of 20 meters in the study area (Figure 3.10) only very unusual storms will generate such wave lengths and this type of conditions has not been met during the five years of record. Therefore in the construction of the forecasting chart, this correction has been neglected and the deep-water wave

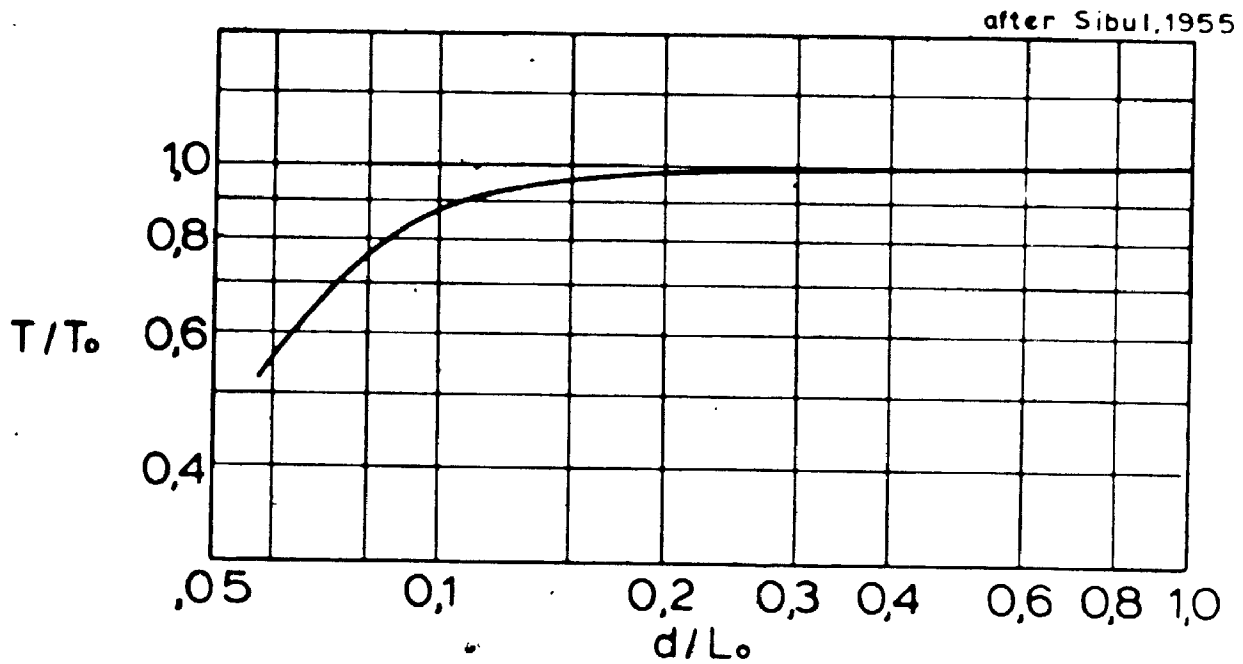


Fig. 3.11 Wave Period as a Function of Depth.

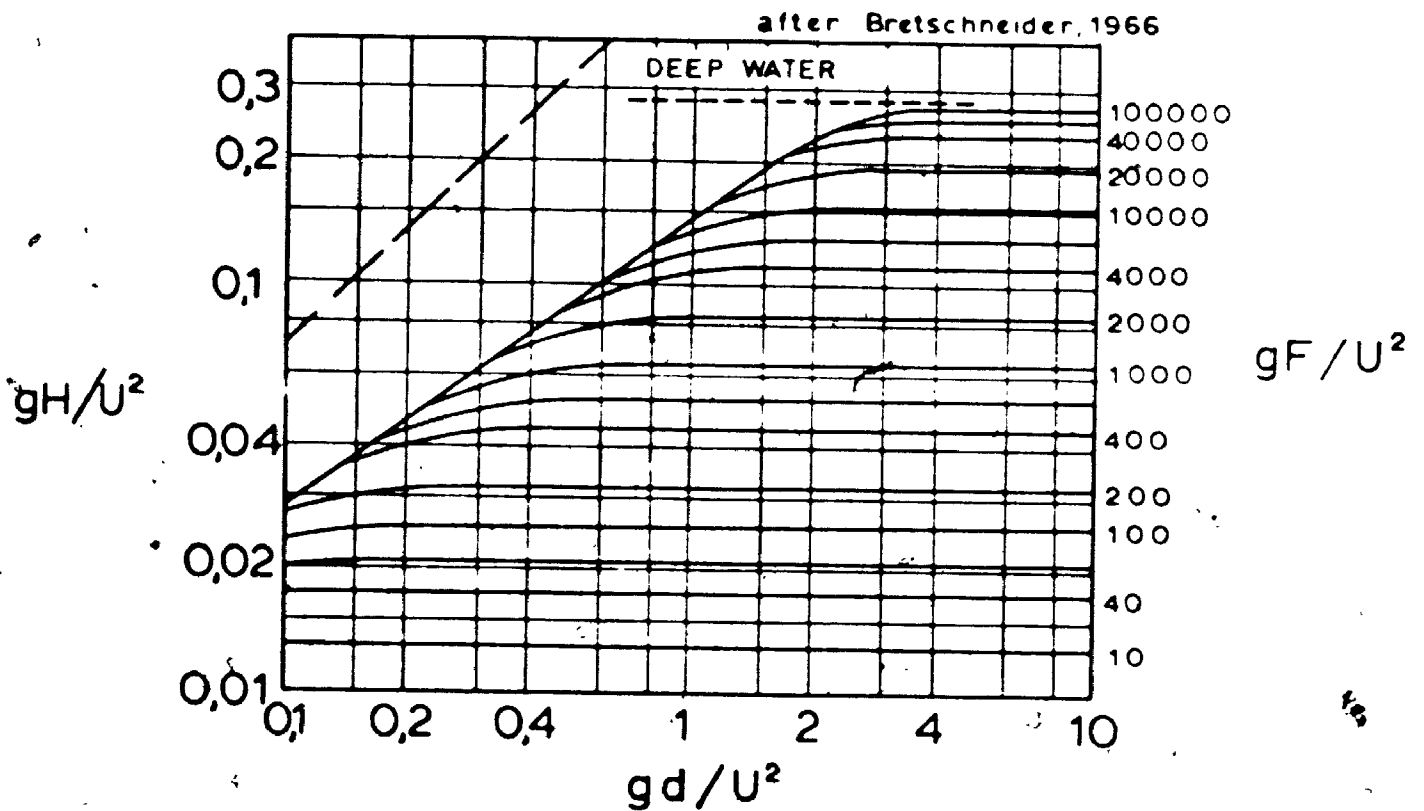


Fig. 3.12 Significant Wave Height (H) in terms of Wind Velocity (U), Fetch (F), and Depth (D).

period has been adopted.

The correction for wave height is more important in shallow water. Following studies on wave generation in shallow water (lakes and bays) Bretschneider and Reid (1953) concluded that deep-water relationships remain valid but must be corrected for bottom friction and percolation. Further studies (Bretschneider 1954, 1956, 1958) taking into consideration bottom friction loss (Futnam and Johnson 1949) have resulted in the formulation of wave parameters relationships in terms of dimensionless coefficients (Bretschneider 1963). Figure 3.12 gives those results for a lake of constant depth with the following variables: wind velocity, U , water depth, d , fetch, F , and wave height, H . This graph was used to compute wave height, H_s , under various combinations of wind velocity and fetch for a constant depth of 20 meters.

Taking these corrections into consideration, a modified forecasting chart has been drawn (Figure 3.13). The independent variables are the wind velocity, U , in miles per hour or meters per second, the effective fetch length, F , in kilometers and the duration of the wind, L , in hours; the dependent variables are the significant wave height, H_s , in meters, and the wave period, T_s , in seconds. The solution is obtained by entering the wind velocity on the left hand side of the chart and by drawing a horizontal line until it reaches the curve for the specified duration or the limiting fetch, whichever comes first; the coordinates of that point are the significant wave height and significant

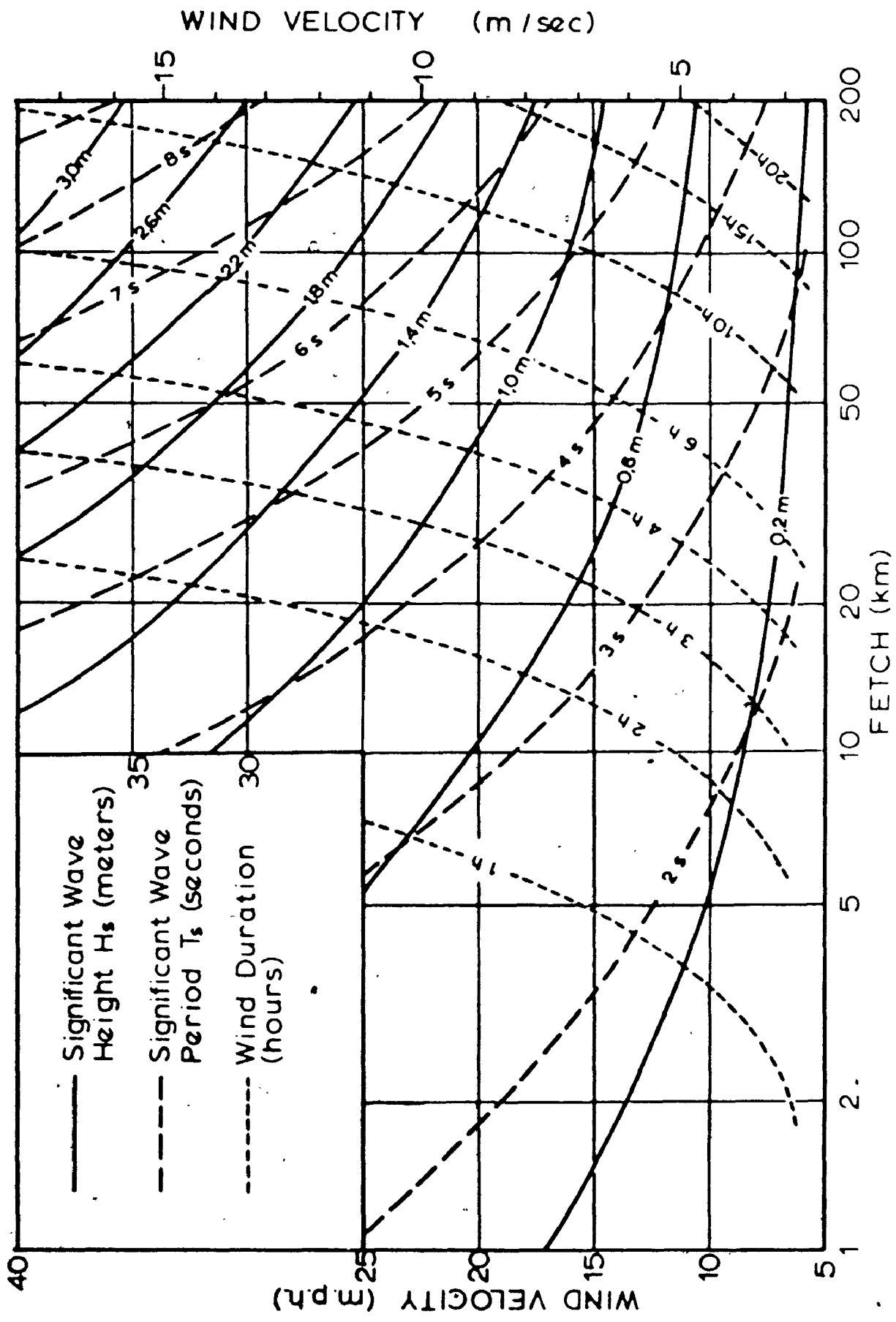


Fig. 3.13 Wave Forecasting Chart.

wave period for a given set of conditions.

This procedure was used to analyse the entire wind data over five years and was repeated for six locations along the shoreline (Figure 3.8). wave parameters (H_s and T_s) were grouped in classes of one second for the periods and 0.4 meter for the heights. These classes and their energy contribution are summarized in Table 3.4. The data for each station was tabulated by wind direction and month of the year.

3.2.3 energy computations.

The total energy of a single oscillatory wave is given by the following equation (Appendix 1):

$$E_t = \rho g (H_s^2 L / 8)$$

where

E_t is the total energy of a single wave offshore in Joules per unit length of wave crest;

H_s is the significant wave height in meters;

L is the significant wave length in meters at the prevailing depth of 20 meters for a specified wave period, T_s as given in Figure 3.9;

ρ is the density of water in kilograms per cubic meter ;

g is the acceleration of gravity in meters per second squared.

Since E_t is given for a single wave, the amount of energy per unit of time is calculated by dividing E_t by the significant period, T_s . This last figure is in Watts.

Since wave energy in deep water is composed equally of potential and kinetic energy, the amount of energy moving forward with the wave is only half of E_t in deep water and an increasing amount in shallow water. The coefficient 'n' (Appendix 1)

$$n = \frac{1}{2} (1 + (4\pi d/L) / (\sinh(4\pi d/L)))$$

is used to calculate the forward wave energy for any ratio d/L and is widely tabulated (U.S. Army 1966). Therefore the energy forward is given by

$$E_f = nE_t$$

The energy forward, E_f , in watts is tabulated for different wave conditions in Table 3.4.

3.2.4 Shoaling, refraction and breaking of waves.

The quantity of forward energy is modified in more than one way when waves enter shallow water. As the depth, d , decreases, the waves start feeling the bottom and the orbital movement of water particles changes from circular to elliptical. When the horizontal component of the orbital velocity u becomes equal or greater than the wave velocity, C , the waves break (Appendix 1). The height of the wave at breaking, H_b , and the depth of water at breaking, d_b , can be calculated by tracing the curves for the horizontal orbital velocity, u , versus d/L_0 and C versus d/L_0 and finding the intersection of the two curves; one may also use a graphical solution (U.S. Army 1966) where the depth at breaking, d_b , and height at breaking, H_b , are related to the

Table 3.4
Wave Energy Parameters

Period T_s (sec)	Height H_s (m)	Total Energy E_t (Joules x 1000)	Forward Energy $E_f = nE_t/T_s$ (kw)
0-2	0,0-0,2	0,02	0,010
0-2	0,2-0,6	0,09	0,045
2-3	0,0-0,4	0,12	0,024
2-3	0,2-0,6	1,96	0,40
3-4	0,0-0,2	0,97	0,14
3-4	0,2-0,6	3,89	0,55
3-4	0,6-1,0	15,2	2,18
3-4	1,0-1,4	26,4	3,76
4-5	0,2-0,6	9,8	1,09
4-5	0,6-1,0	25,2	2,83
4-5	1,0-1,4	56,5	6,32
4-5	1,4-1,8	82,0	9,20
5-6	0,6-1,0	51,4	4,87
5-6	1,0-1,4	89,0	8,44
5-6	1,4-1,8	145	13,7
5-6	1,8-2,2	194	18,3
6-7	1,4-1,8	221	18,7
6-7	1,8-2,2	304	25,7
6-7	2,2-2,6	400	33,8
7-8	1,8-2,2	467	35,6
7-8	2,2-2,6	559	42,7
7-8	2,6-3,0	761	58,2
8-9	2,6-3,0	973	67,5
8-9	3,0-3,4	1185	82,5
8-9	3,4-3,8	1500	104,5

period and height in deep water (Figure 3.14). Table 3.5 gives these parameters for the different wave groups. For example, a wave having a height, H_0 , of 1.8 meters in deep water and a period of 7 seconds will have a height at breaking, H_b , of 2.1 meters in water 2.6-meter deep (d_b).

An other important change in wave characteristics occurs by refraction of waves approaching the shoreline obliquely; by this process the direction of a wave moving in shallow water oblique to the contours is changed; that portion of the wave entering shallow water is slowed down with respect to the other end moving in deeper water, causing the crest to bend towards alignment with underwater contours.

The phenomenon of refraction can be analyzed using Snell's law of refraction employed in optics; it is expressed in the form:

$$\frac{\sin a_1}{\sin a_2} = \frac{C_2}{C_1}$$

where a_1 and a_2 are the the angle that the wave crest makes with the first and second underwater contour line respectively and C_1 and C_2 the wave velocity, ($C=L/T$), at the depth of the first and second contour (Figure 3.15). Orthogonals, which are lines perpendicular to the wave crests at any point, can be drawn showing the direction of wave motion from deep to shallow water. The profile of wave crests can therefore be calculated by successive application of the refraction law, knowing the initial angle of approach of waves in deep water and the location of underwater contours.

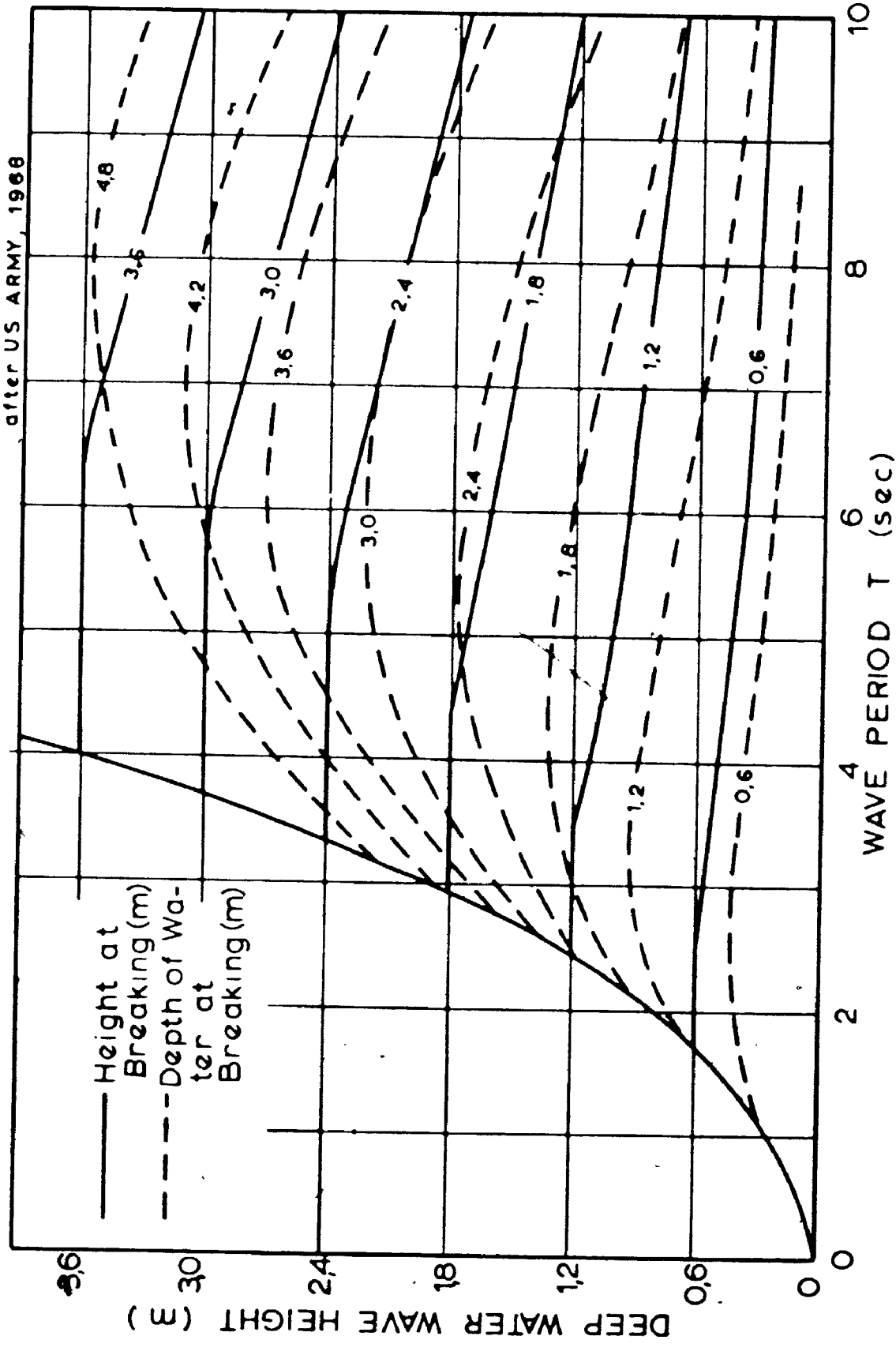


Fig. 3.14 Wave Height and Depth of Water at Breaking.

Table 3.5

Wave breaking Parameters

Period T_s (sec)	Deep Water Wave Height H_0 (m)	Height at Breaking H_b (m)	Depth of water at breaking d_b (m)	Depth to wavelength (d_b/L_0) ratio
0-2	0,0-0,2	0,1	0,1	0,04
0-2	0,2-0,6	0,4	0,6	0,16
2-3	0,0-0,2	0,1	0,2	0,02
2-3	0,2-0,6	0,4	0,6	0,06
3-4	0,0-0,2	0,2	0,2	0,01
3-4	0,2-0,6	0,5	0,6	0,03
3-4	0,6-1,0	0,9	1,1	0,05
3-4	1,0-1,4	1,2	1,7	0,09
4-5	0,2-0,6	0,5	0,7	0,02
4-5	0,6-1,0	0,9	1,2	0,04
4-5	1,0-1,4	1,2	1,6	0,05
4-5	1,4-1,8	1,6	2,2	0,07
5-6	0,6-1,0	1,0	1,2	0,03
5-6	1,0-1,4	1,3	1,7	0,04
5-6	1,4-1,8	1,7	2,2	0,05
5-6	1,8-2,2	2,1	2,7	0,06
6-7	1,4-1,8	1,8	2,3	0,04
6-7	1,8-2,2	2,2	2,8	0,04
6-7	2,2-2,6	2,6	3,2	0,05
7-8	1,8-2,2	2,3	2,9	0,04
7-8	2,2-2,6	2,7	3,4	0,04
7-8	2,6-3,0	3,0	3,8	0,05
8-9	2,6-3,0	3,1	4,0	0,04
8-9	3,0-3,4	3,6	4,4	0,05
8-9	3,4-3,8	3,9	4,9	0,05

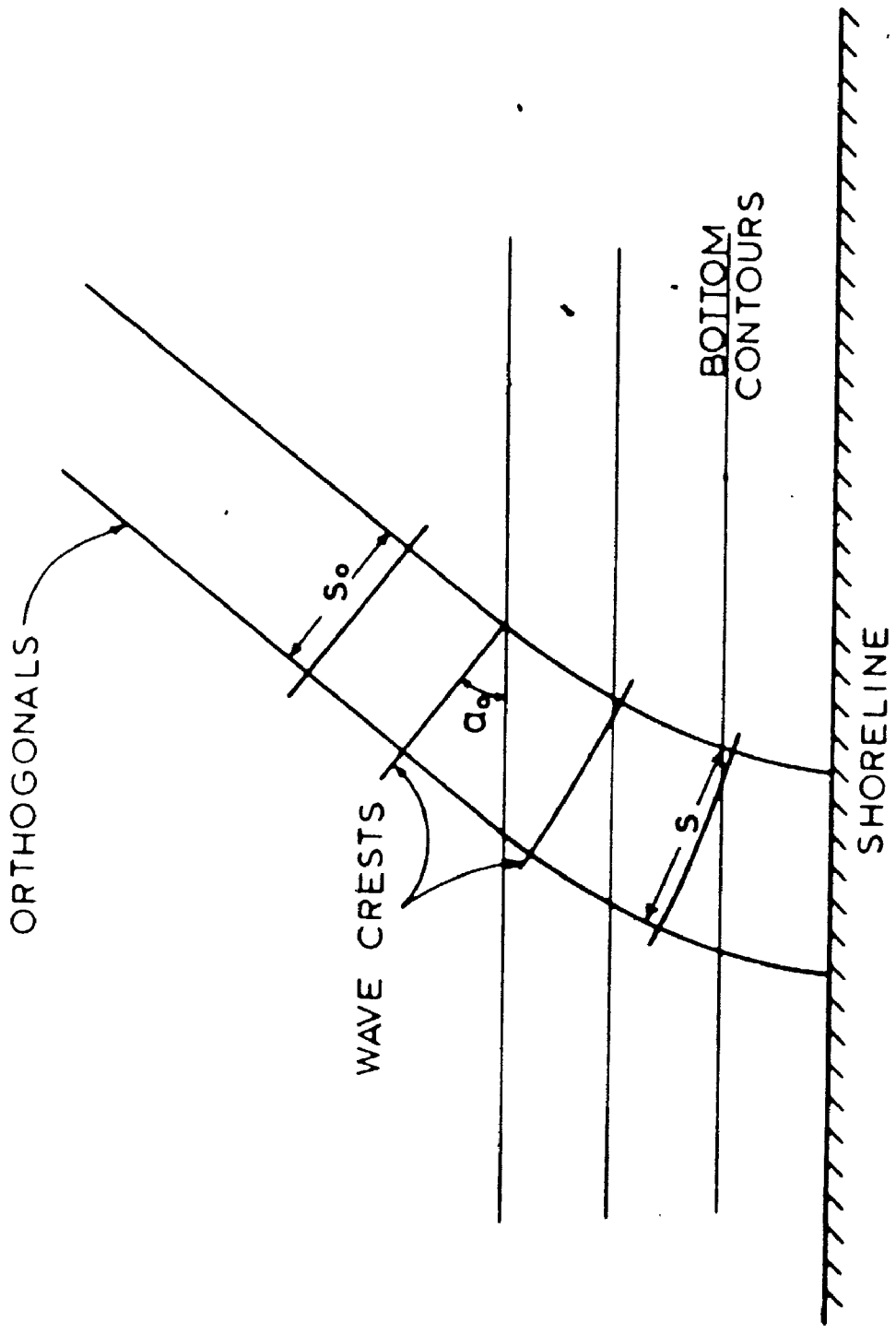


Fig. 3.15 Wave Refraction Diagram.

v

A refraction coefficient, K_r , is defined by taking the square root of the ratio of the spacing between adjacent orthogonals in deep water, s_0 , and in shallow water, s , at breaking point. Since the contours in the study area are nearly straight and parallel to the shoreline (Figure 3.10) because the lake bottom is a wavecut terrace (Lewis 1966), a graphical solution exists provided that underwater contours are straight and parallel to the shoreline (Johnson, O'Brien and Isaacs 1949). Figure 3.16 relates the incident angle, a_0 , of the wave crest with the refracted angle, a , the value of K_r and the ratio of depth to wave length.

These parameters (K_r , the coefficient of refraction and the angle $b = 90^\circ - a$ between the shoreline and the wave front) were tabulated at each station for the different wave classes and are used to calculate the net forward energy of the refracted wave at the point of breaking, E_{fb} .

$$E_{fb} = E_f \cdot K_r^2$$

Since $K_r^2 = s_0/s$, it merely indicates that a unit length of the wave crest is s_0 in deep water but increases to s after the wave has been refracted (Fig. 3.15). The limiting values of K_r are then one when a is 0° and zero when a is 90° which is when the waves are parallel or normal to the shore.

The wave energy at breaking, E_{fb} , can be broken down in two components, longshore energy, E_l , and energy normal to the shoreline, E_n , (Figure 3.17) where b is the angle of incidence of the wave on the shore and $1/\sin b$ is the length of shoreline along which a unit width of wave crest applies its energy. Therefore,

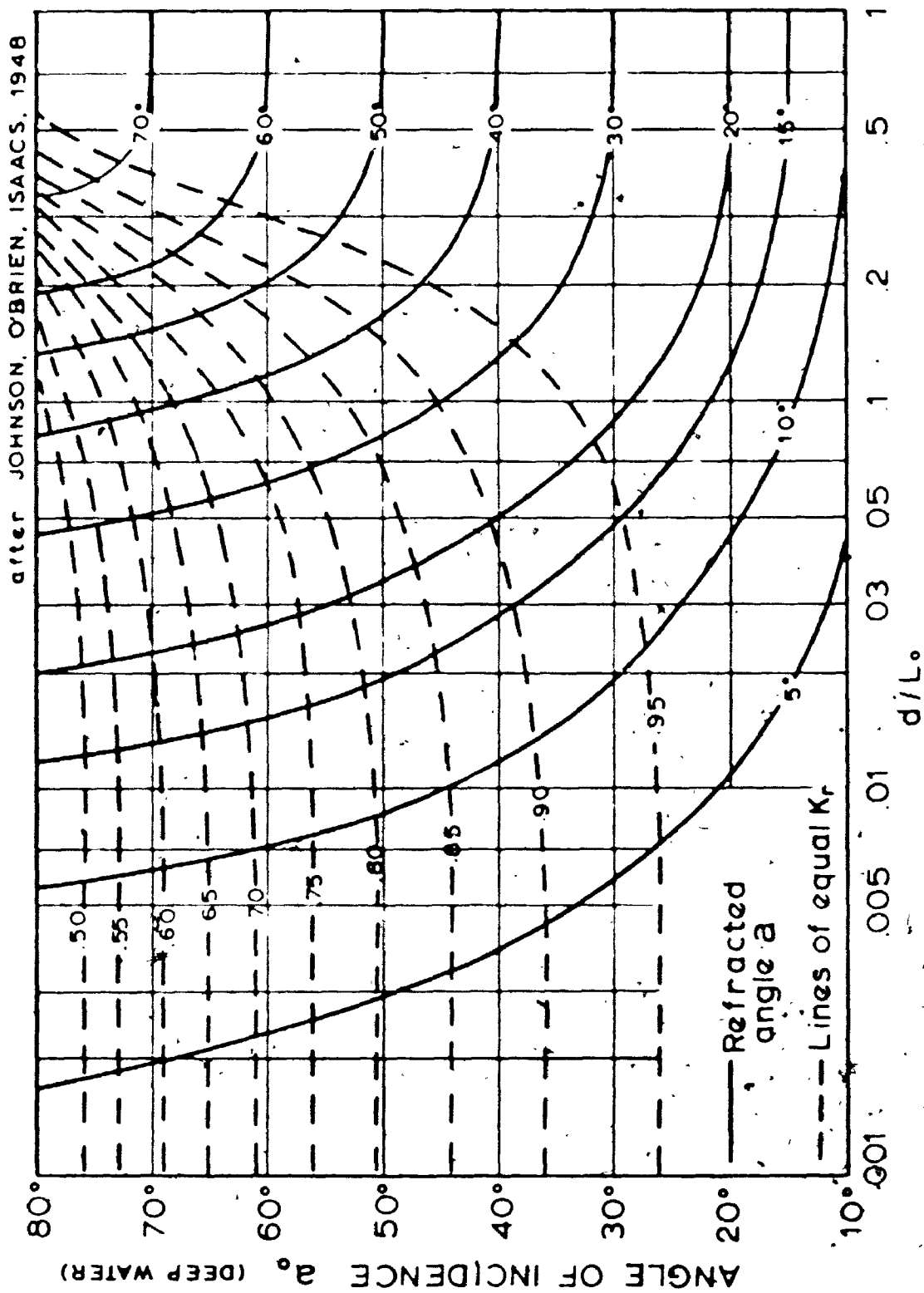


Fig. 3.16 Wave Refraction on Slopes with Straight, Parallel Contours.

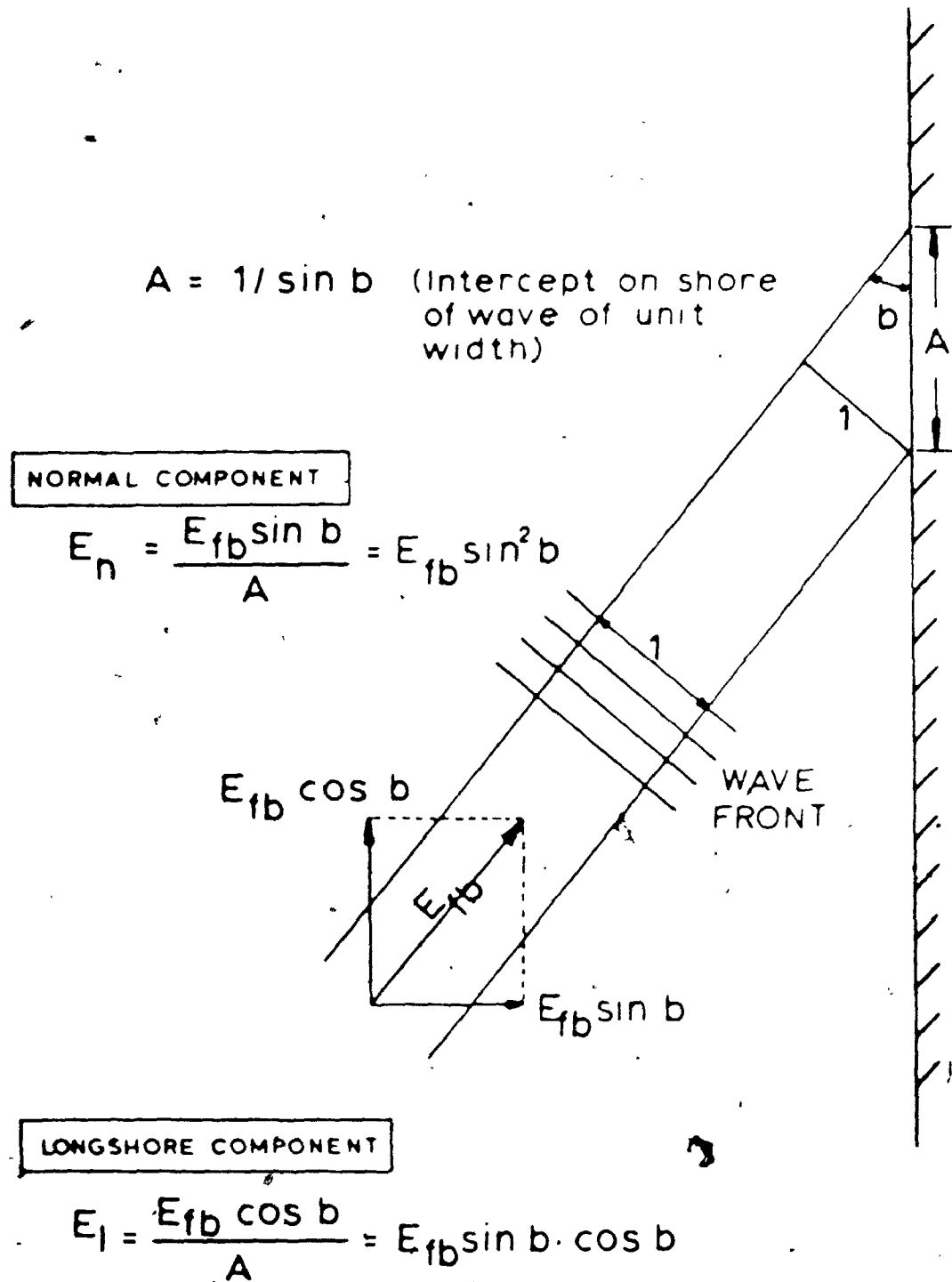


Fig. 3.17. Wave Energy Components.

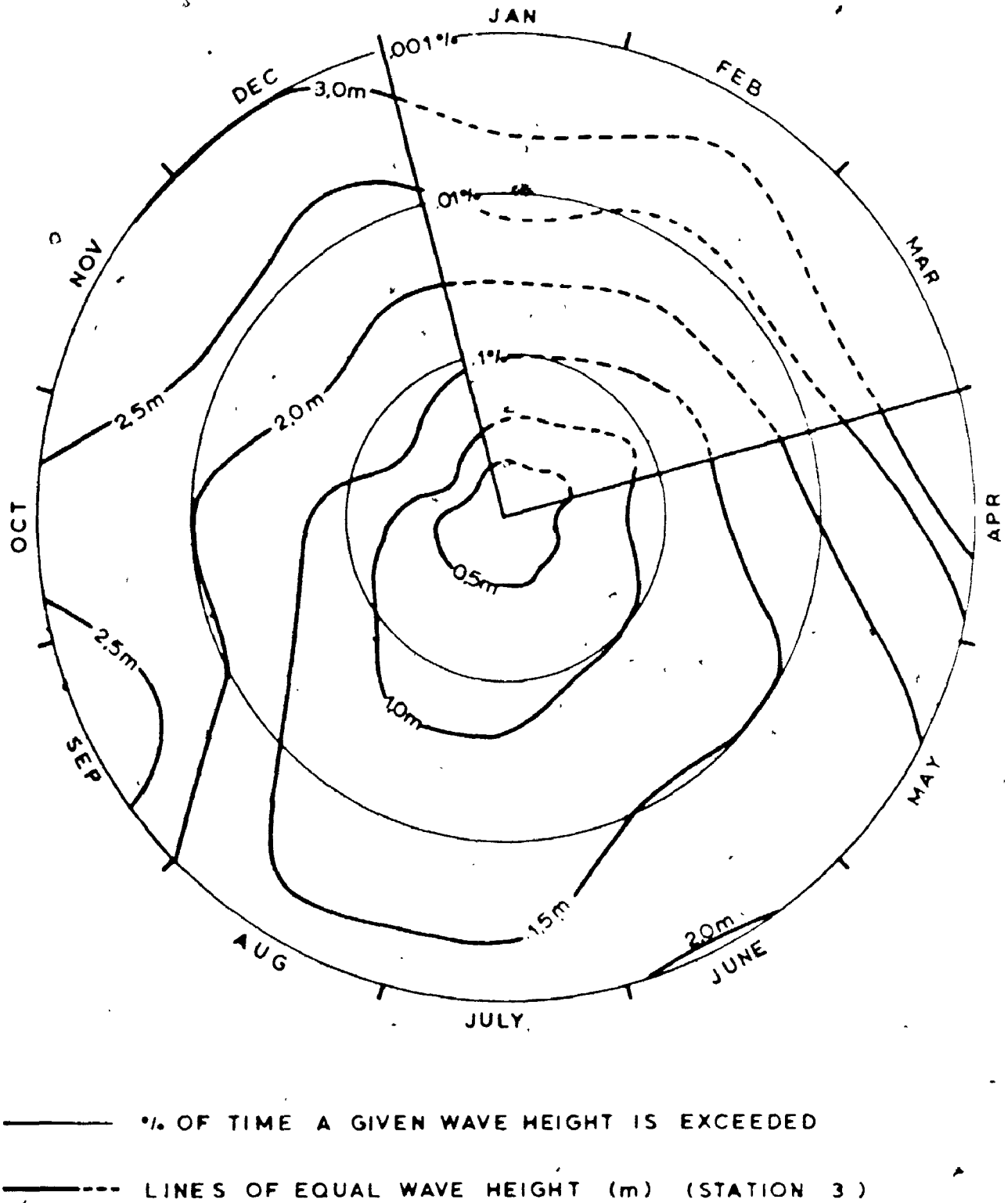


Fig. 3.19 Seasonal Distribution of Wave Heights.

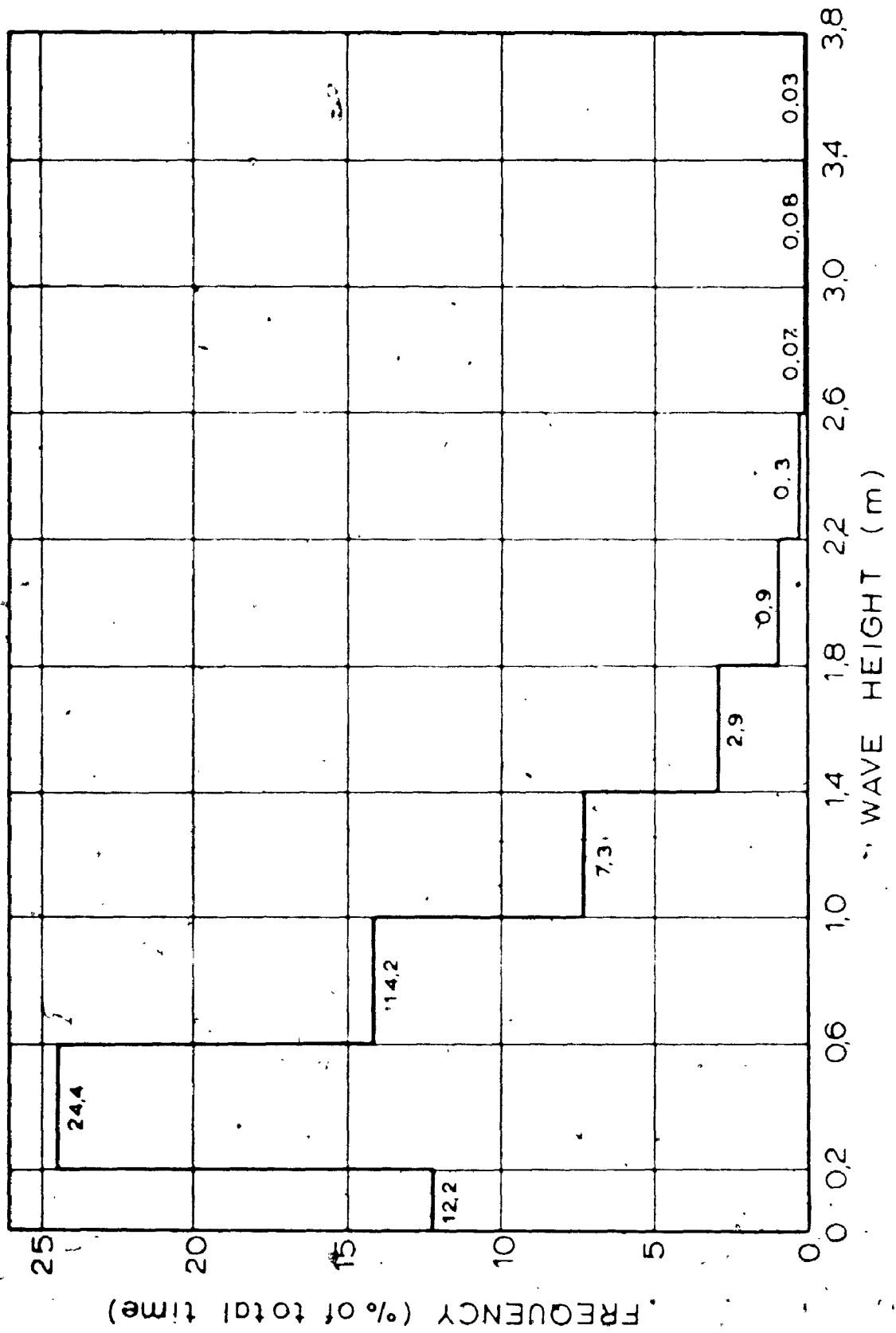
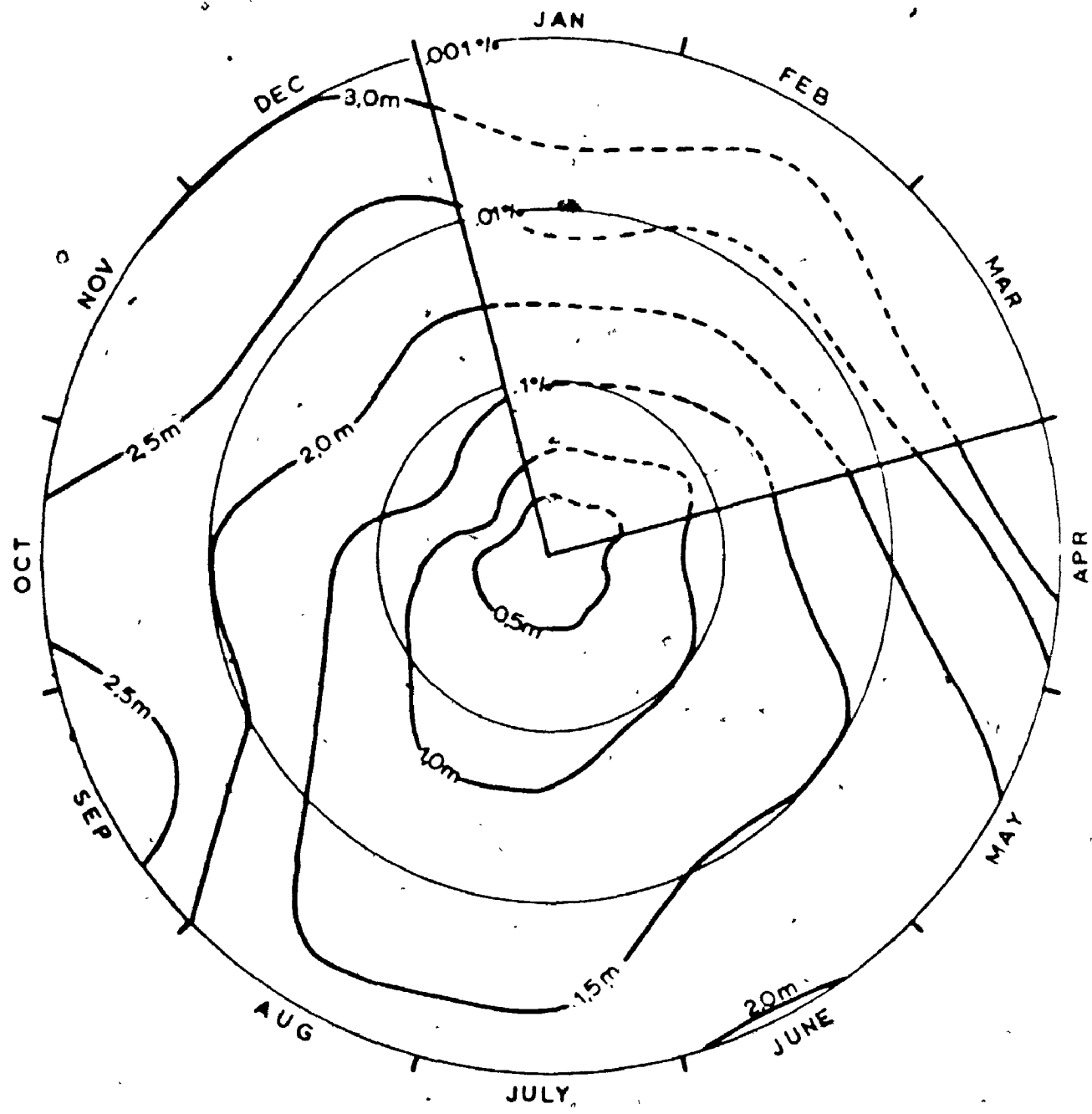


Fig. 3.18 Wave Height Histogram, all Directions (1956-60).

Figure 3.19, illustrates the percentage of time during each month that a given wave height, H_s , is exceeded; high waves are more likely to occur in November, December and April since Lake Erie is usually frozen between January and March (Phillips and McCulloch 1972).

wave energy at breaking has been computed for each of the six stations taking into account shoaling and refraction of wave crests. Table 3.6 gives the values of total energy forwards at breaking, E_{Tb} , in watts and Table 3.7 gives the component of that energy normal to the shoreline, E_n , which is responsible for erosion, and the component of energy parallel to the shoreline, E_l , responsible for littoral drift; the resultant of longshore energy is in the eastern direction except probably at the tip of the sand spit near Erieau. Figure 3.20 shows the distribution of wave energy along the shoreline at different localities; a maximum occurs near the township line between Bayham and Houghton Townships, 12 kilometers east of Port Burwell; minimum energy occurs on the eastern shore of the Rondeau spit.

Figure 3.21 shows the distribution of energy from different directions at each of the stations; as expected, from the geometry of the area and the dominant winds over Lake Erie, the most important contribution is from the southwest. It is worth mentioning the very little amount of energy coming from the south east; this anomaly may be due to the length of the record analysed but five years seems sufficient since other studies on Lake Erie (Saville 1953) use three years of records, and two years of records were used



— % OF TIME A GIVEN WAVE HEIGHT IS EXCEEDED
- - - LINES OF EQUAL WAVE HEIGHT (m) (STATION 3)

Fig. 3.19 Seasonal Distribution of Wave Heights.

Table 3.6

Distribution of
energy at breaking

$$E_{fb} = E_f \cdot K_r^2$$

(watts)

Station

	1	2	3	4	5	6
KE	---	---	---	---	---	27
E	35	9	39	47	91	111
EB	20	14	20	21	25	26
B	126	120	141	146	133	115
n	645	1100	825	678	484	240
n	451	690	286	102	---	---
na	---	8	---	---	---	---
TOTAL	1507	1941	1311	994	733	519

Table 3.7

Normal and Longshore Energy Distribution

Normal energy component, E_n

(watts)

per meter of shoreline

	1	2	3	4	5	6
NE	---	---	---	---	---	20
E	27	7	31	37	74	91
SE	18	11	17	10	24	25
S	126	114	141	146	130	108
SW	720	1064	715	587	420	199
W	375	575	225	51	---	---
NW	---	6	---	---	---	---
TOTAL	1266	1777	1129	760	640	443

Longshore Energy Component, E_l

(watts)

per meter of shoreline

	1	2	3	4	5	6
NE	---	---	---	---	---	12 n
E	14 n	4 n	16 n	20 n	35 n	43 n
SE	6 n	5 n	7 n	7 n	6 n	4 n
S	4 n	26 n	---	---	22 E	28 E
SW	299 E	197 E	281 E	231 E	165 E	91 E
W	199 E	256 E	117 E	42 E	---	---
NW	---	3 E	---	---	---	---
RESULTANT	474 E	421 E	375 E	246 E	146 E	60 E

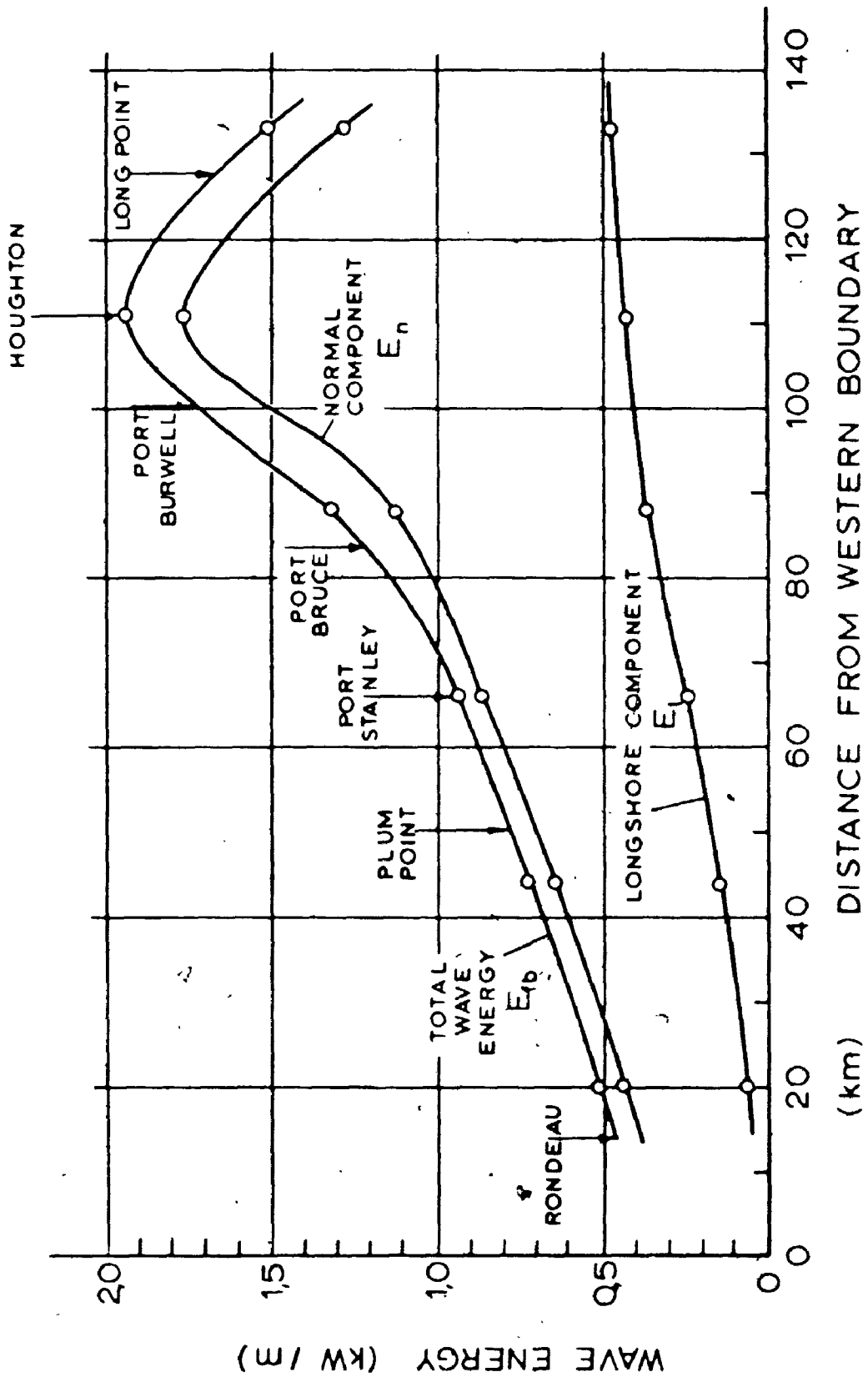


Fig. 3.20 Wave Energy Distribution along the Shoreline.

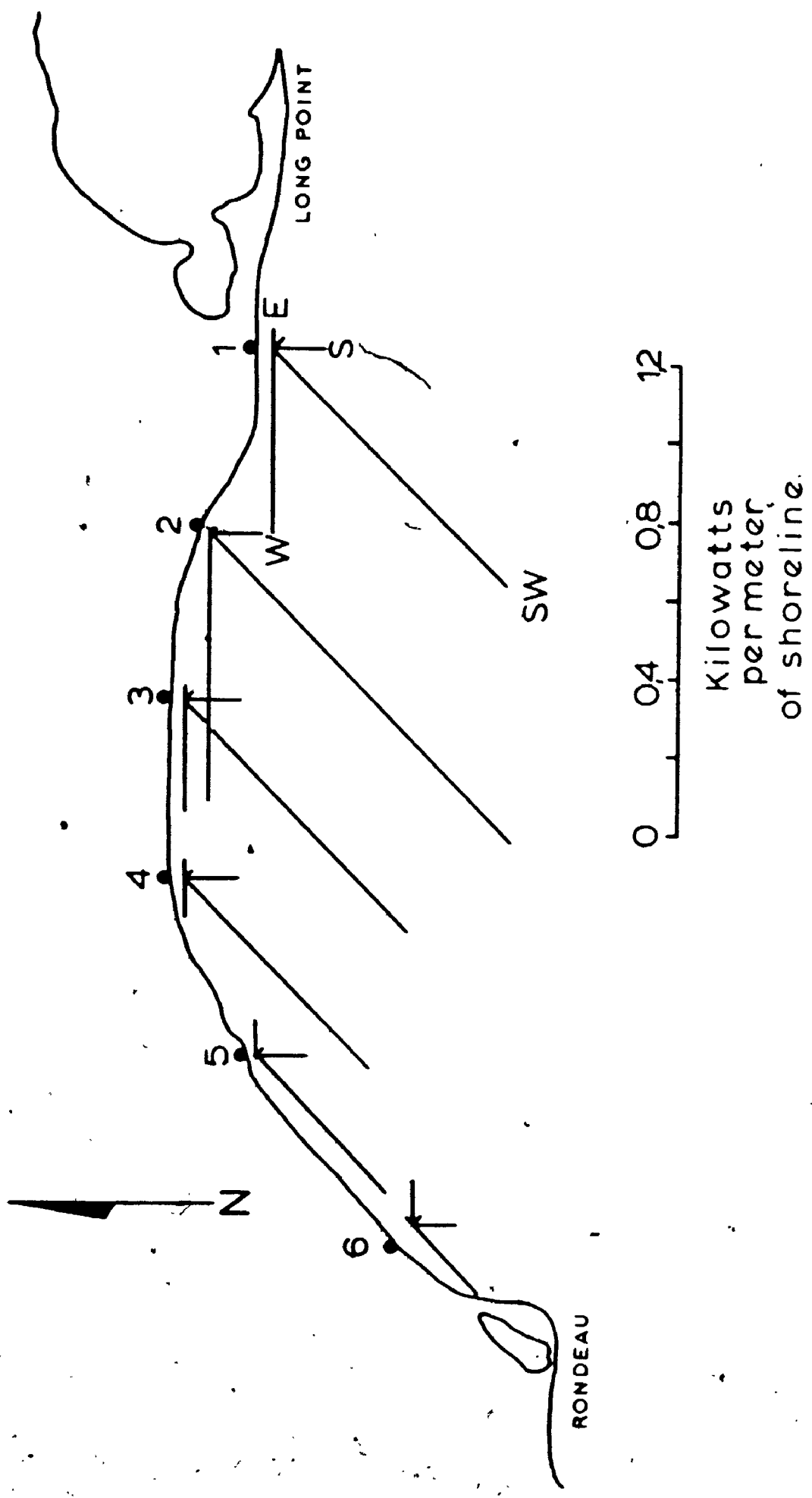


Fig. 3.21 Wave Energy E_{fb} Distribution in All Directions.

to analyse surface winds at Douglas Point, on Lake Huron, for similar purposes (Richards 1964).

Using station 3 again, the seasonal distribution of wave energy, E_{fb} , has been analysed, Figure 3.22. During ice-free periods, from April to December, the energy wasted in the nearshore area is about 70% of the yearly total; November and December alone account for 37% of the total; if the winter period is excluded, 53% of the wave energy is concentrated in those two months.

The relationship between rates of erosion and wave energy will be studied later after considering the effects of storm setup and lake levels on erosion.

3.3 Wind setup.

The purpose of this section is to study the hydrodynamic effects of storms on lake levels. The terms 'wind tide', 'wind setup' and 'storm surge' have all been applied indifferently to describe the phenomenon although 'wind setup' has often been used more specifically for inland waters. The wind setup is that displacement of the water level from the initial undisturbed state due only to wind action (Keulegan 1953). During storms one end of the lake experiences a seiche or drop in water level and a surge occurs at the opposite end.

Wind setups on Lake Erie have been recognized very early by meteorologists (Blunt 1897, Henry 1902, Garriott 1903, Hayford 1922) and a hydrodynamic approach to the

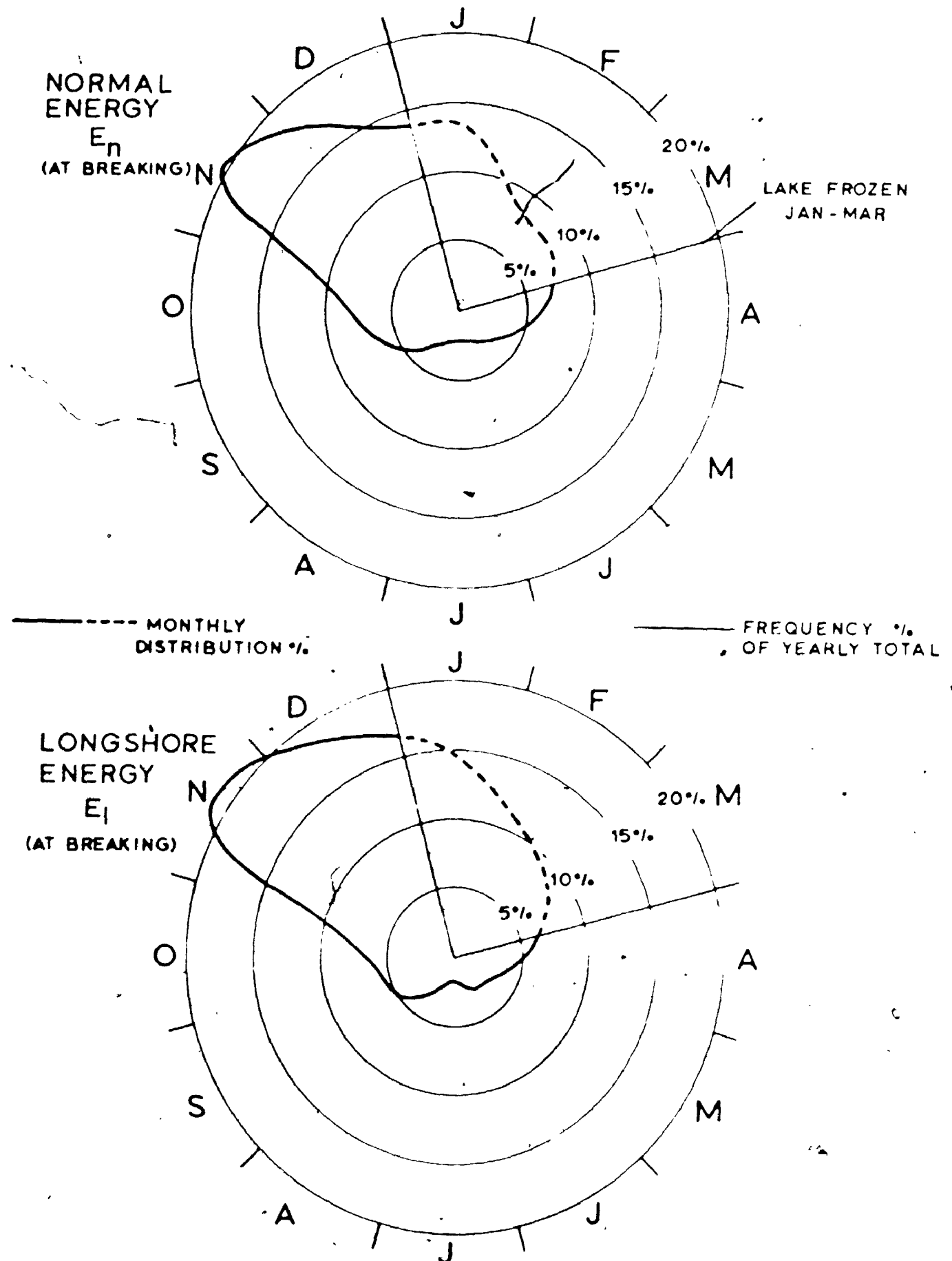


Fig. 3.22 Seasonal Variation of Wave Energy.

problem was attempted more recently by Hellstrom (1941), Keulegan (1953), Hunt (1958), Flatzman (1963) and Bretschneider (1967) develops a model permitting the evaluation of wind setup at any point on the lake surface. Most models are designed to predict the total setup between the two extremities of the lake. In this section, a close look will be given at the influence of wind setup in the central basin of the lake where erosion is highest.

3.3.1 wind stress.

A model for vertical distribution of wind velocity was developed earlier in section 3.1.5, and the standard wind velocity at 10 meters above water surface (U_{10}) was used for wave forecasting. The same value U_{10} will be used to estimate wind stress.

Energy from the wind is transferred in the boundary layer to the free surface of water by means of friction forces. That force, the wind stress τ_s , is defined by Keulegan (1953) as:

$$\tau_s = C_B \rho U_{10}^2 \quad \text{Eq. 3.3.1}$$

where C_B is the wind stress coefficient, ρ is the density of air in kilograms per meter cube and U_{10} the standard wind velocity 10 meters above lake surface, in meters per second. By back calculation on observed wind setups on Lake Erie (Keulegan 1953, Flatzman 1963) and in Florida (Bretschneider 1967), the coefficient C_B has been evaluated to be $3 \cdot 10^{-6}$.

3.3.2 Model of Wind Setup.

To obtain a solution to the setup problem, it is necessary to know the shoreline profile of the lake, its depth at any point, and to use a suitable model describing wind setup.

The derivation of the differential equation describing the slope of a lake surface subjected to wind stresses was done by Keulegan (1953) by assuming the X-axis along the greatest dimension of the lake. At any point 'x', the wind setup is 'h', that is the elevation of the raised water surface above (or below) the level of undisturbed water. The width of the lake is taken as 'b', the cross-sectional area is 'A' and the mean depth is 'H' (Figure 3.23). It follows that:

$$A = b(H+h) \quad \text{Eq. 3.3.2}$$

Two sections Δx apart are chosen, the first at a distance 'x' and the other at (x + Δx). Let 'F' be the total pressure force on the section x; at (x + Δx), that pressure becomes

$$F + A\rho g (dh/dx)\Delta x \quad \text{Eq. 3.3.3}$$

The difference of pressure between the two sections is then

$$A\rho g (dh/dx)\Delta x \quad \text{Eq. 3.3.4}$$

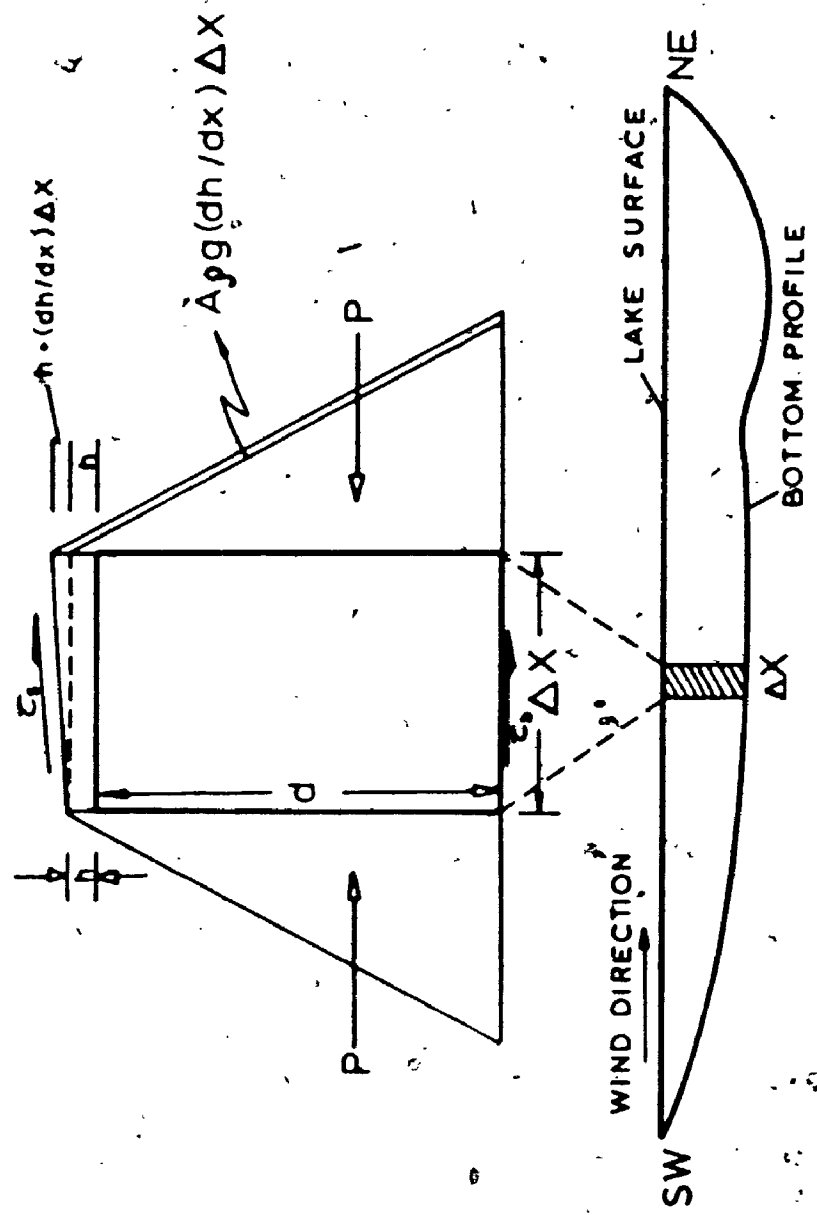


Fig. 3.23 Physical Model of Wind Setup.

In order to maintain equilibrium resisting forces are provided by frictional forces: τ_s , the wind stress at the surface and τ_b , the stress at lake bottom induced by the gravity flow current. These forces are then equal to

$$B (\tau_s + \tau_b) \Delta x \quad \text{Eq. 3.3.6}$$

Equating the last two equations, with $A = B(h+h)$, and dividing by Δx , one gets

$$\frac{dh}{dx} = \frac{\tau_s + \tau_b}{\rho g(h+h)} \quad \text{Eq. 3.3.7}$$

which is the equation for the setup on a lake of arbitrary shape. The condition of continuity states that

$$\int_{x=0}^{x=L} B h dx = 0, \quad L = \text{length of the lake.}$$

which means that the volume of water lowered below quiet lake level must be equal to the volume of water raised above the undisturbed level.

The ratio (τ_b / τ_s) is known empirically by the study of historical wind setups in different localities (Keulegan 1953, Bretschneider 1967) and is very close to 0.1. Then

$$(\tau_b + \tau_s) = 1.1 \tau_s$$

The wind setup equation can be reduced to the form:

$$\frac{dh}{dx} = \frac{k \cdot \tau_s^2}{g(h+h)} \quad \text{Eq. 3.3.8}$$

with $k = 3.3 \cdot 10^{-6}$ after Eq. 3.3.1. This last equation is general but cannot be applied directly except in cases where the geometry of the lake and its bottom configuration can be

2

OF/DE

3



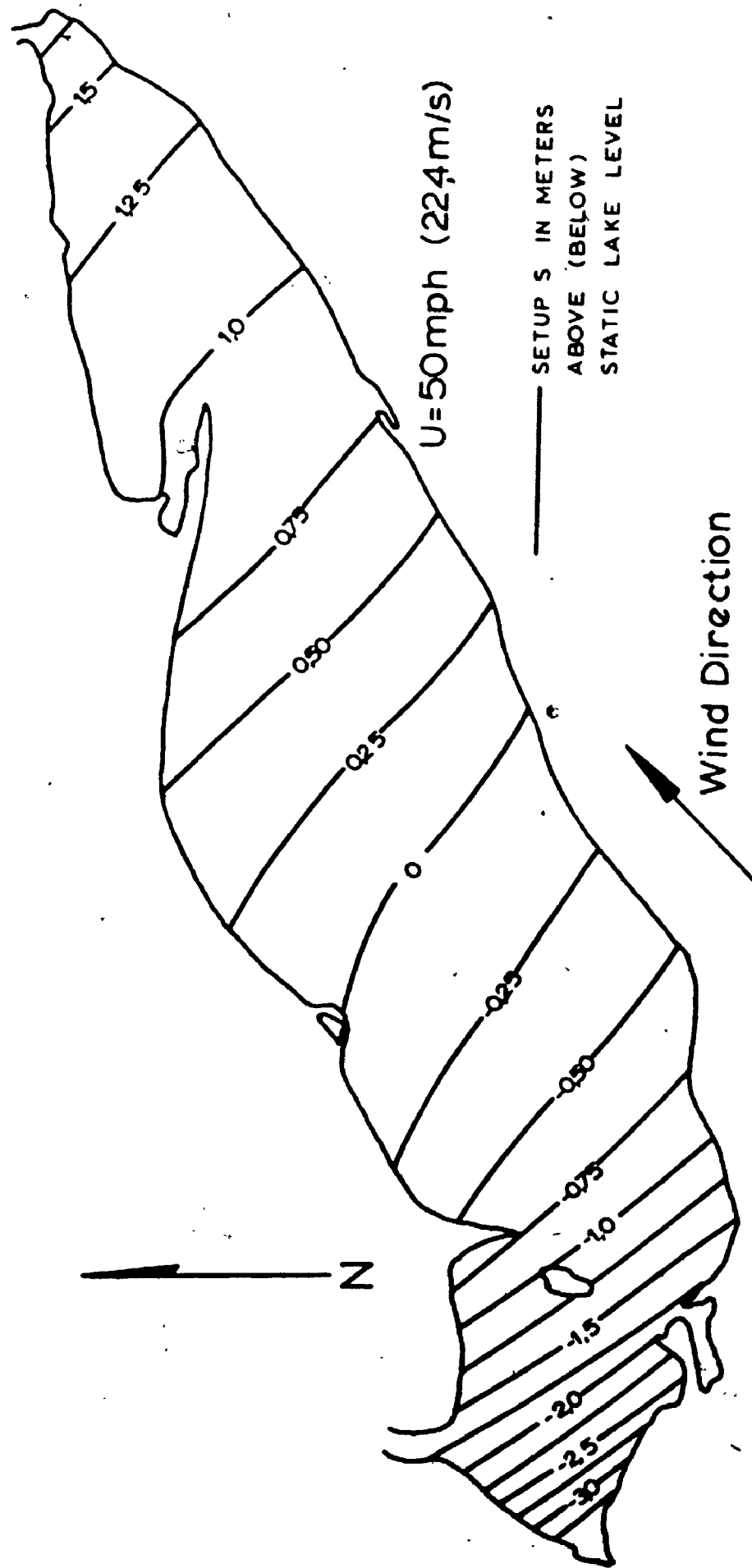


Fig. 328 Storm Setup Contours for SW Wind, U=50 mph (22.4m/s)

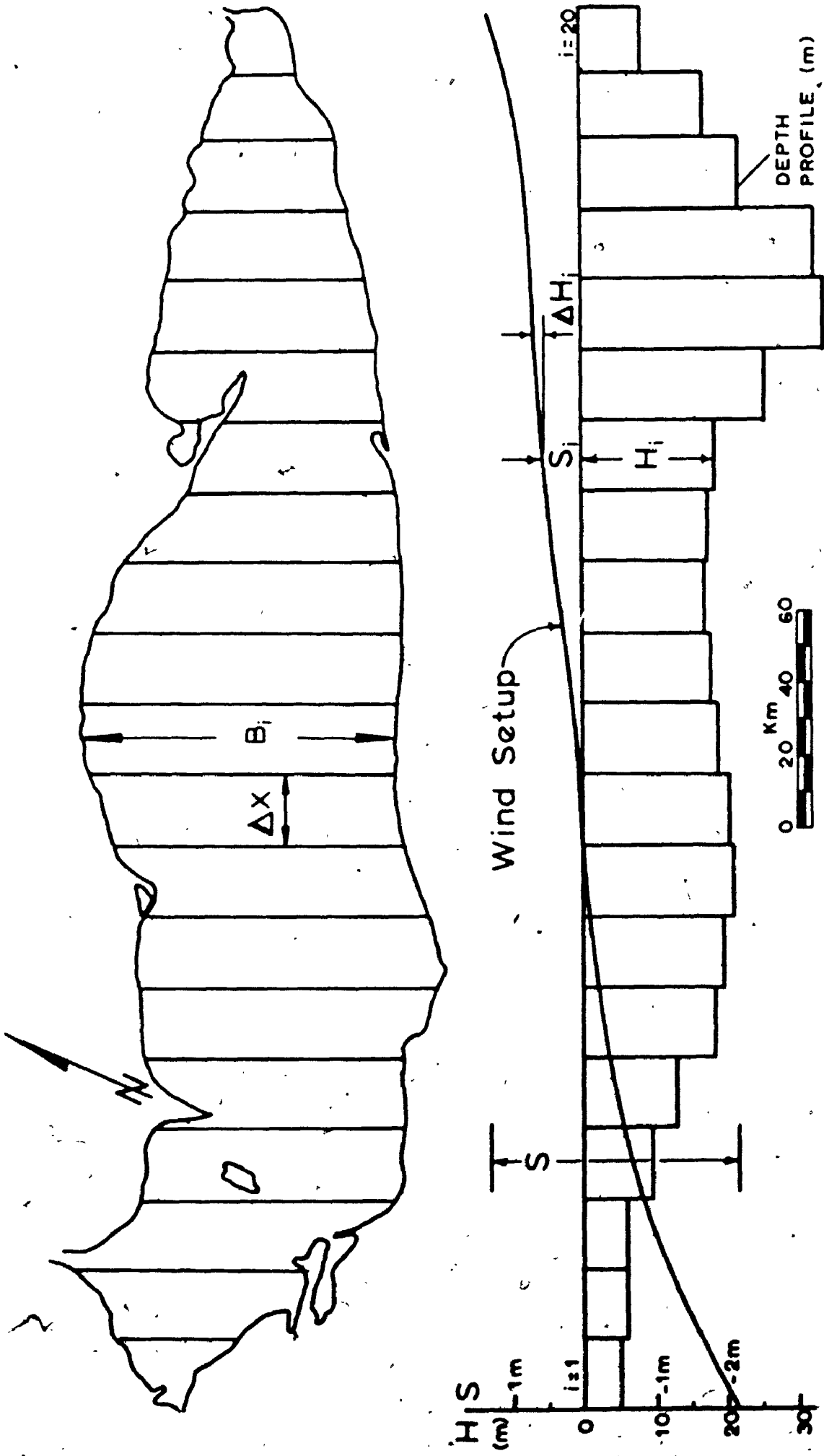


Fig. 3.24 Numerical Model for Wind Setup Calculations.

(negative setup). The volume balance is verified and if the error is too large, a second and subsequent approximation is done after changing the position of the nodal line in the direction which will minimize the error.

If the wind is blowing at an angle with the direction of the long axis of the lake, a two-step solution is sought by replacing U^2 by the dot product UU_x and UU_y where U_x and U_y are the components of the wind vector along the long axis (x) and the short axis (y) of Lake Erie. Along the y-axis, computations were made using Δy instead of Δx as the width of each section. The setup at any point (x,y) on the surface of the lake is the sum of the setup in each direction

$$\Delta h_{(x,y)} = \Delta h_{(x)} + \Delta h_{(y)} \quad \text{Eq. 3.3.13}$$

In this study, the wind setup was calculated for NE, E, SE, S, SW, and W winds with standard wind velocity U_{10} of 20, 30, 40 and 50 miles per hour (or 9.0, 13.5, 18.0 and 22.5 meters per second). The numerical solution was first applied to the long axis of the lake and up to five iterations were used to locate accurately the nodal line. Nine transversal sections of unit width were drawn in the y-direction, each of them divided into ten intervals Δy in order to get a better picture of the setup in that direction.

Contours of equal setup along and across the lake were plotted separately and added graphically (Eq. 3.3.13) to yield maps of setup for the entire Lake Erie.

3.3.3 Results of wind setup calculations.

The results of wind setup calculations are plotted on contour maps for different wind velocities and directions. Winds in opposite directions (NE-SW, E-W, etc.) yield an identical contour map but with opposite signs for contours, and this holds true in the range of wind velocities analysed here. Figures 3.25 to 3.30 illustrate the results for winds coming from the S, SW, and W directions for velocities of 40 and 50 miles per hour.

The frequency of winds capable of producing setups similar to those illustrated can be estimated using the method outlined in section 3.1.4. The regression lines for S, SW, and W winds are plotted on Figure 3.31. The probabilities $P(>U)$ that a given velocity U in meters per second will be equalled or exceeded is given in percent; for example, the probability that the wind will blow from the SW at 50 miles per hour (22.4 m/s) is 0.012% or roughly one hour per year. These curves were prepared from the wind data recorded at Clear Creek between 1956 and 1960.

In the study area, only winds from the S, SW and W directions will produce a positive setup thereby playing a detrimental role on erosion rates. The maximum rise in lake level due to wind setup to be expected will occur in the eastern section of the study area, east of Port Burwell where it can reach one meter. This rise doesnot include storm waves that can be estimated by the method outlined

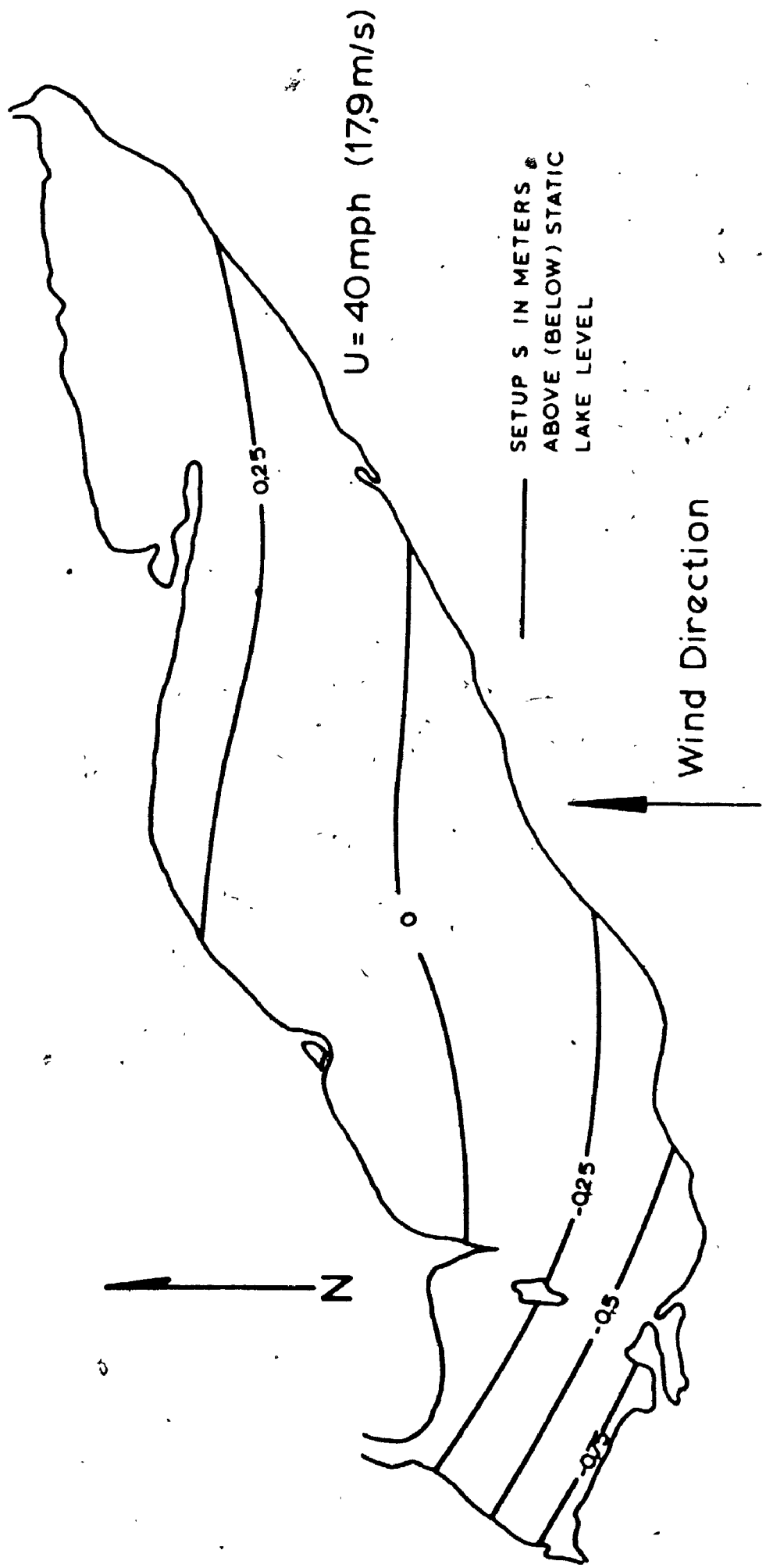


Fig. 3.25 Storm Setup Contours for S Wind (U=40mph)

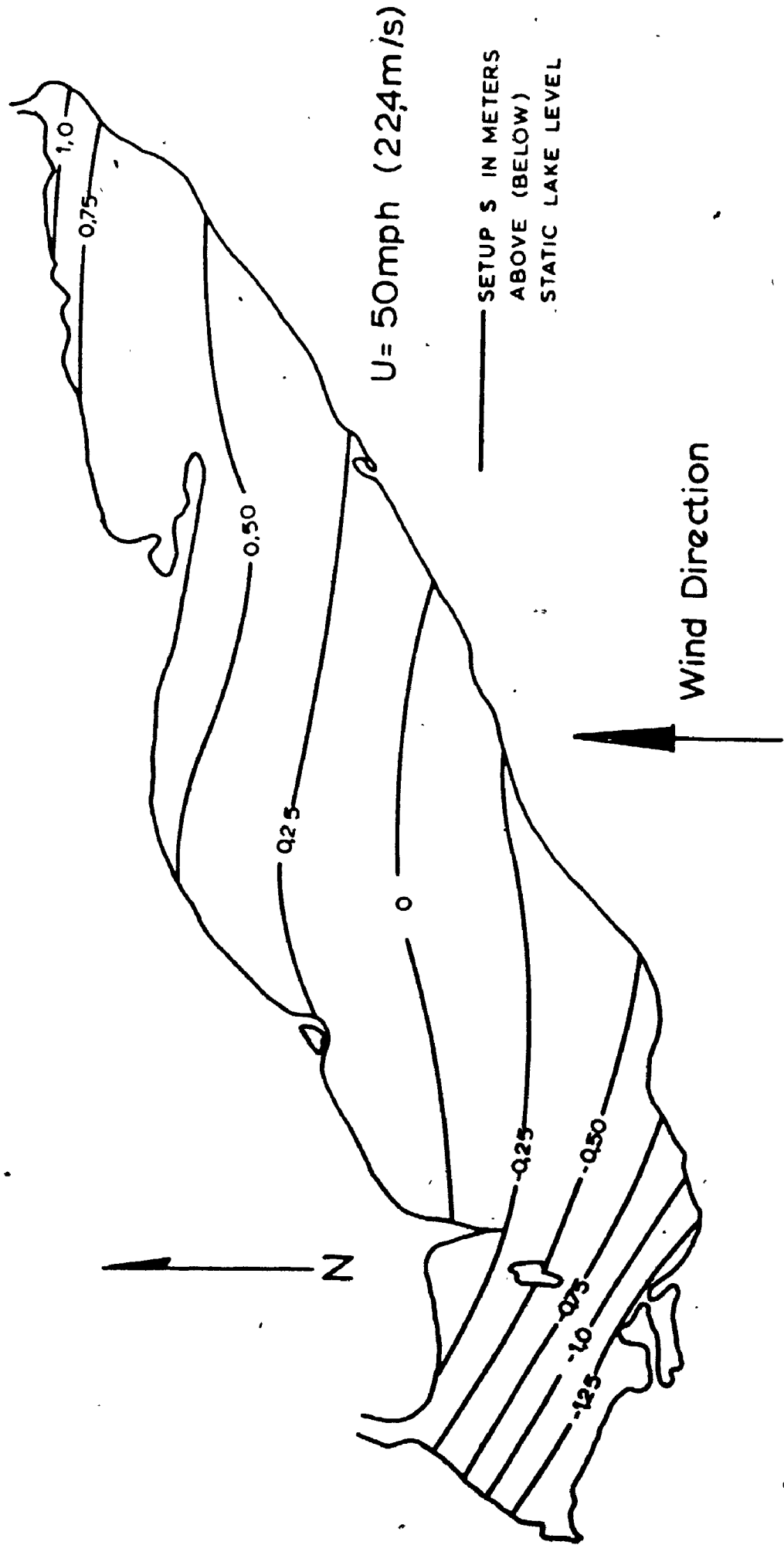


Fig. 3.26 Storm Setup Contours for S Wind, U=50mph (22.4m/s)

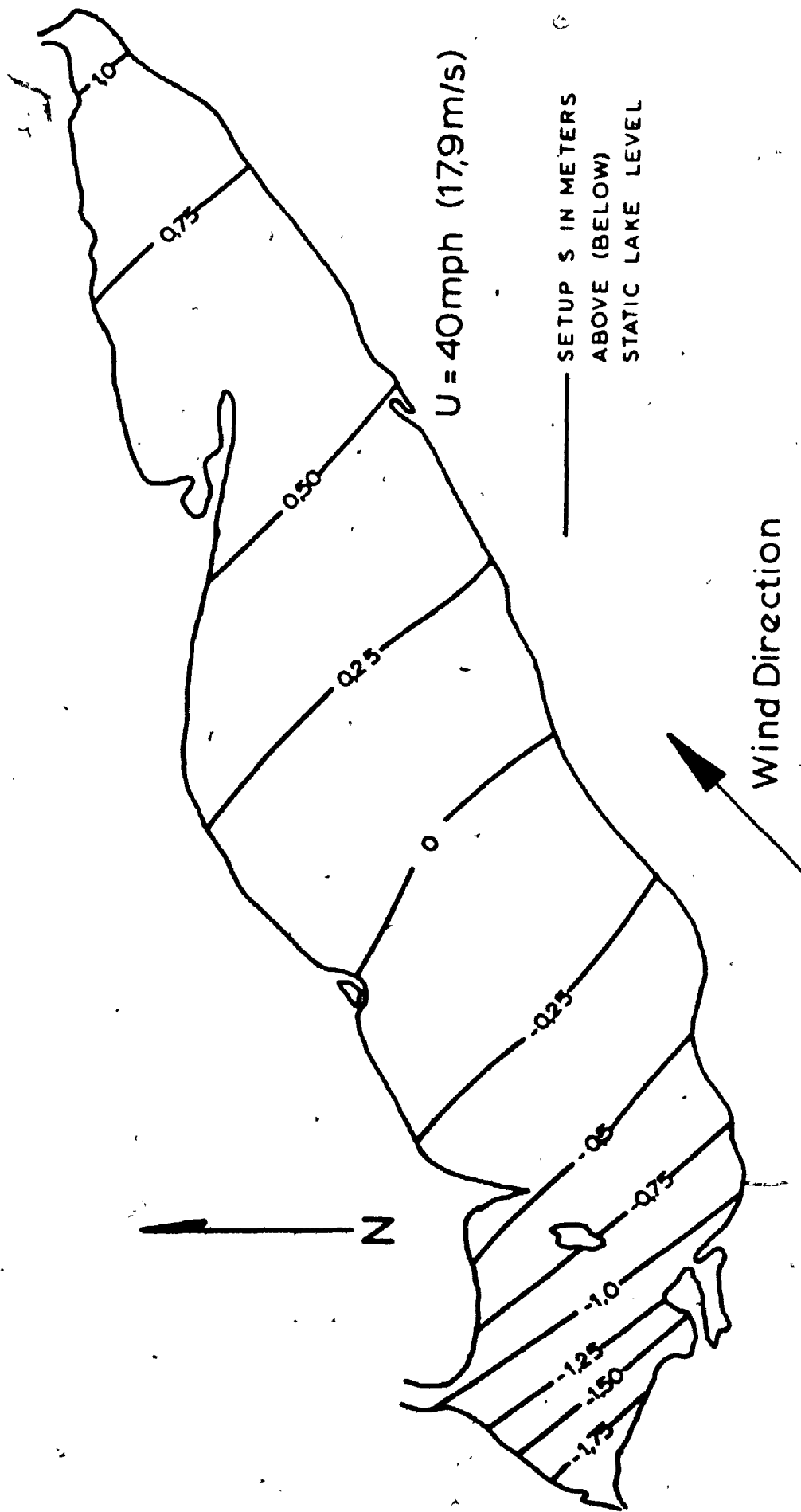


Fig. 3.27 Storm Setup Contours for SW Wind, U=40mph (17,9m/s)

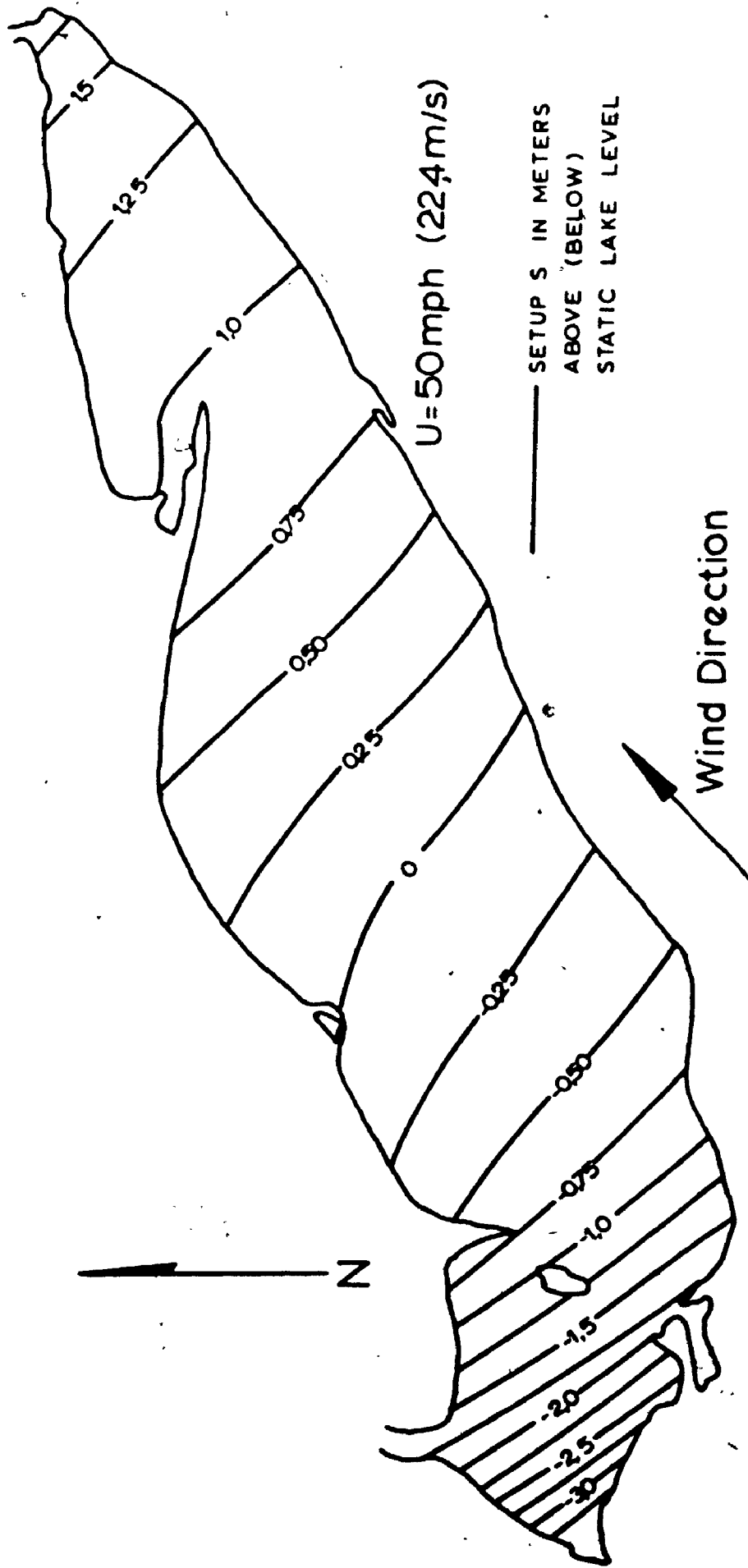


Fig. 328 Storm Setup Contours for SW Wind, $U=50$ mph (22.4 m/s)

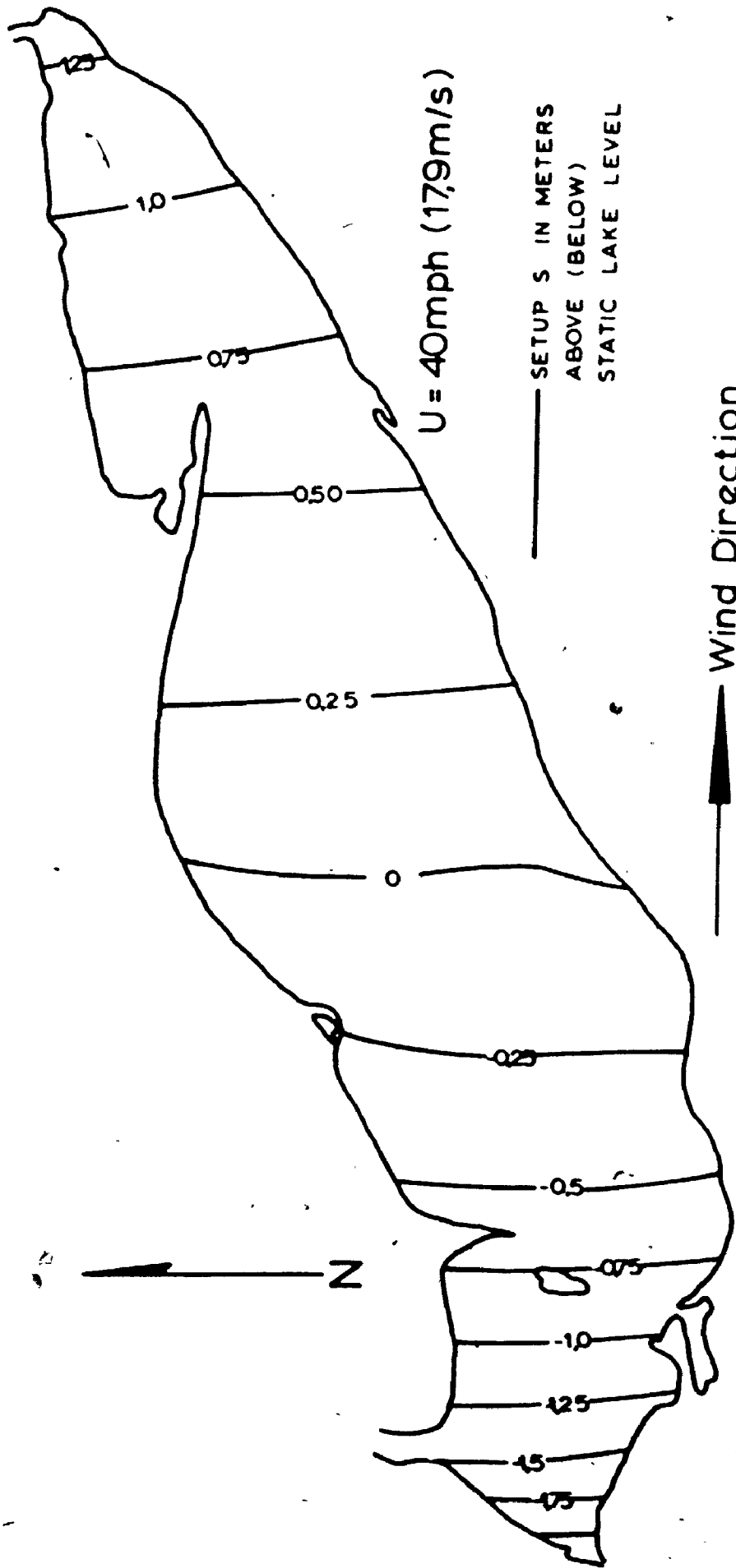


Fig. 3.29 Storm Setup Contours for W Wind, $U = 40 \text{ mph (17.9 m/s)}$ ⁹⁰

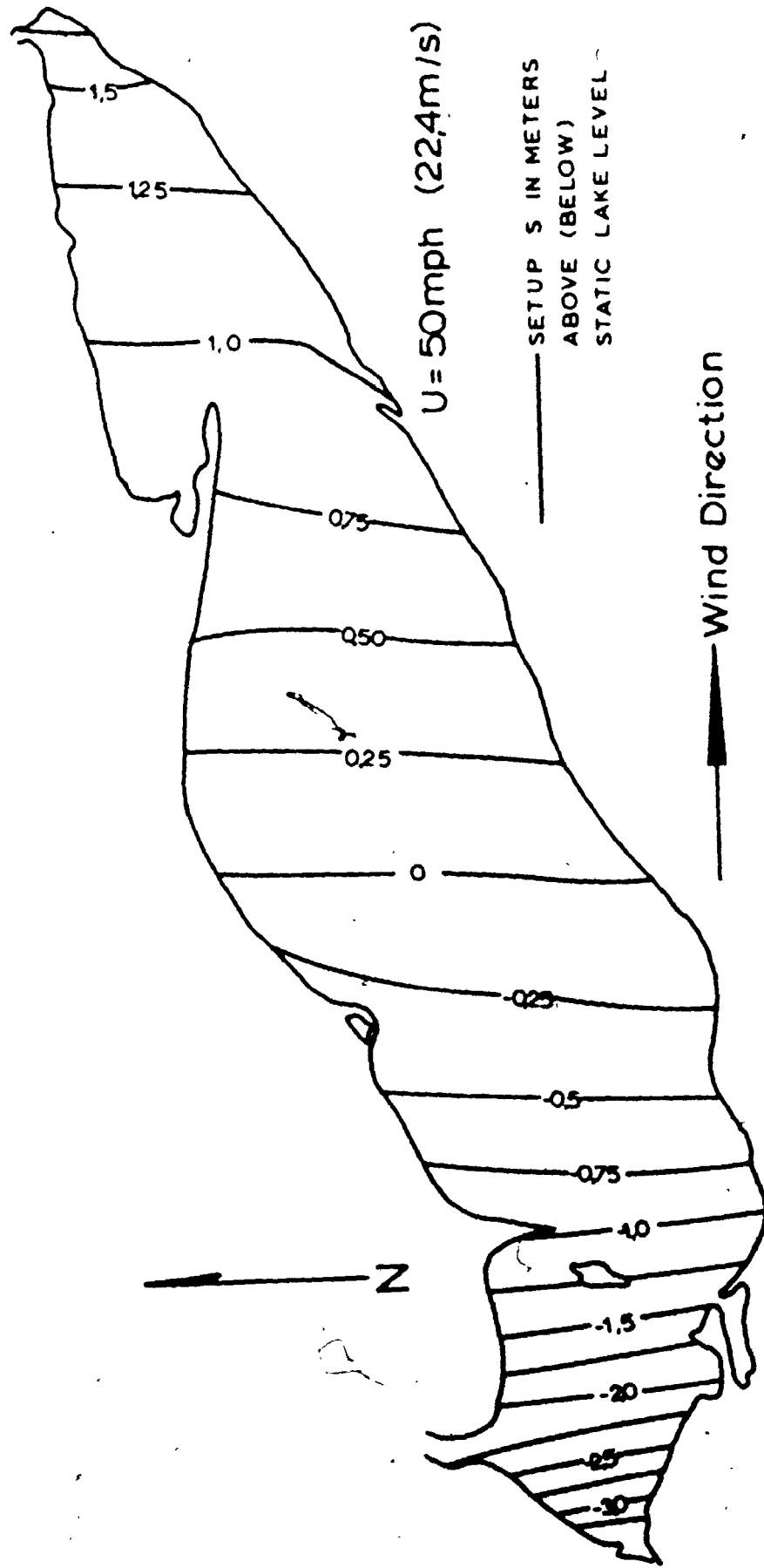


Fig. 3.30 Storm Setup Contours for W Wind, U=50mph (22.4m/s) ⁹¹

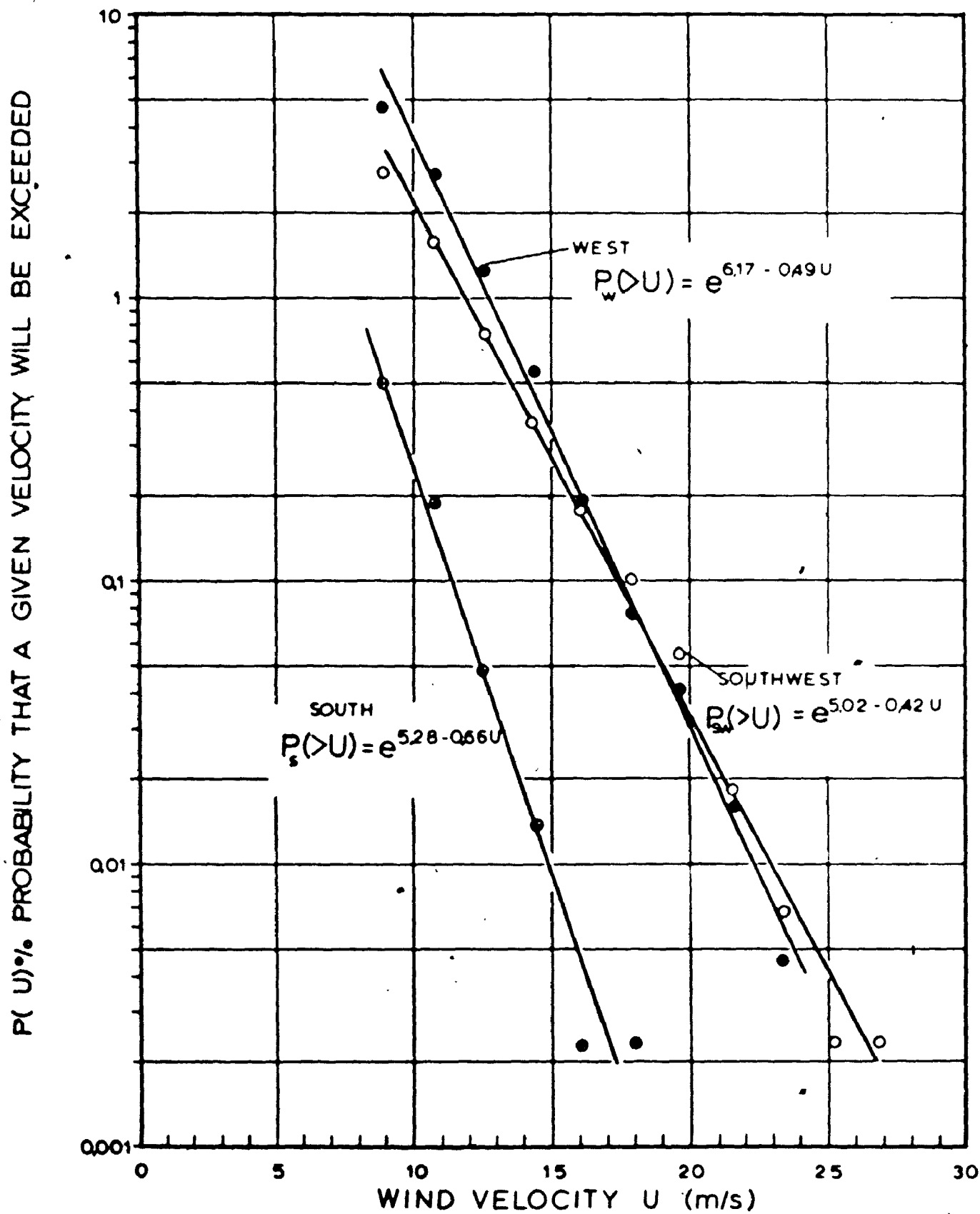


Fig. 3.31 Frequency of Strong Winds, S, SW, and W.

in section 3.2. Storms from the NE, E, and SE have a tendency to depress the water level in the central basin and therefore attenuate the adverse effects of the storm waves they generate.

Calculated setups are comparable to the setups observed at Fort Stanley. Table 3.8 shows the monthly maximum setup registered between 1965 and 1969; in this table the setup is understood as the difference between the instantaneous high level registered in any month with the mean water level at the time it happened; this mean water level is taken as the average of the levels on the three-day period centered on the day the maximum instantaneous high level was registered. The data for this table was compiled from the Marine Sciences Branch publications on daily lake levels. For instance, the setup of 0.50 meter in November 1965 and of 0.54 meter in July 1969 correspond to the setup predicted for S or SW winds of 50 miles per hour (22.5 m/s).

Wave action and storm setup depend in their effects on lake levels; up to this point, constant average lake level was used for calculations and it is easy to picture worst conditions occurring when a storm from the southwest happens in a period when lake levels are high; the immediate effects will be that beaches protecting the toe of the bluffs vanish under water and that the waves spend considerable amount of their energy directly on the in-situ material. The next section studies those variations in lake levels.

Table 3.8

Maximum Monthly Lake Setup
Observed at Fort Stanley
(1965 - 1969)

	1965		1966		1967		1968		1969	
	Day	Setup (m)	Day	Setup (m)	Day	Setup (m)	Day	Setup (m)	Day	Setup (m)
January	26	0,38	3	0,23	17	0,23	5	0,1-	25	0,25
February	13	0,23	11	0,25	16	0,46	17	0,16	3	0,16
March	13	0,27	24	0,19	21	0,13	23	0,26	21	0,20
April	12	0,27	1	0,21	18	0,24	24	0,32	21	0,20
May	17	0,18	18	0,18	2	0,21	19	0,17	9	0,40
June	29	0,15	14	0,19	29	0,13	12	0,1-	27	0,23
July	7	0,16	10	0,24	3	0,08	24	0,26	4	0,54
August	28	0,27	16	0,21	4	0,09	17	0,32	16	0,20
September	1	0,24	4	0,16	21	0,20	1	0,23	5	0,09
October	1	0,19	16	0,29	27	0,37	3	0,17	16	0,25
November	27	0,50	29	0,30	11	0,23	18	0,31	19	0,32
December	13	0,20	29	0,26	12	0,35	23	0,44	8	0,22

3.4 Lake Erie levels.

Previous discussions on wave action and storm setup were referred to a constant elevation of the lake surface. Much of the erosive power of waves and setup are in fact dependent on lake levels; during periods of low water, storm setup in the study area is virtually without effect and waves will be eroding offshore of the beach; when levels are high, both processes will be considerably more effective due to overtopping of the narrow beaches protecting the base of the cliffs. This section looks at Lake Erie levels since glacial times and in more detail at the water level fluctuations in the last century.

3.4.1 Lake levels since last glaciation.

The history of the last phases of Lake Erie formation has been investigated for a long time by observations of former beaches of an ancestral lake (Leverett and Taylor 1915). More recently (Hough 1958, 1963, 1966; Chapman and Futnam 1966, Prest 1969, Dreimanis 1969) several details have been added to this history. From the last high stage of Lake Erie (Lake Maumee III) at 238 meters above sea level some 14,000 years before present, lake levels have fallen continuously to a very low stage referred to as the Early Lake Erie at 140 meters, about 12,500 years B.P. During that interval, numerous glacial lakes existed in the Erie

basin following fluctuations in the ice retreat (figure 3.32).

The level of Early Lake Erie rose rapidly during the period between 12,500 and 10,500 years B.P. and more slowly in the subsequent 2000 years. Lake Erie as it is known now seems to have maintained a more or less constant elevation of about 174 meters for the last 8000 years (Frest 1969). This gradual rise in levels from Early Lake Erie to the present lake could account for the formation of a wave cut platform in the central basin along the north shore (Lewis 1966) by wave erosion.

For the purpose of this study, annual variations of lake levels about a long-term mean value are more significant to explain erosion rates. Daily measurements of lake levels have been performed on Lake Erie for more than a hundred years at different locations on the American and Canadian littoral. The records at Fort Dover, Ontario, extend back to 1860 and continuous monitoring at Fort Stanley for the past 60 years. Modern recorders are damped for short period fluctuations due to waves but can register seiches and setups caused by atmospheric disturbances.

3.4.2 Statistics on Lake Erie Levels.

Environment Canada publishes daily averages of Great Lakes levels at several gauging stations (Marine Sciences Branch 1972); these publications also give mean annual levels, monthly means and instantaneous high and low water marks for the period of record. Some of the extreme

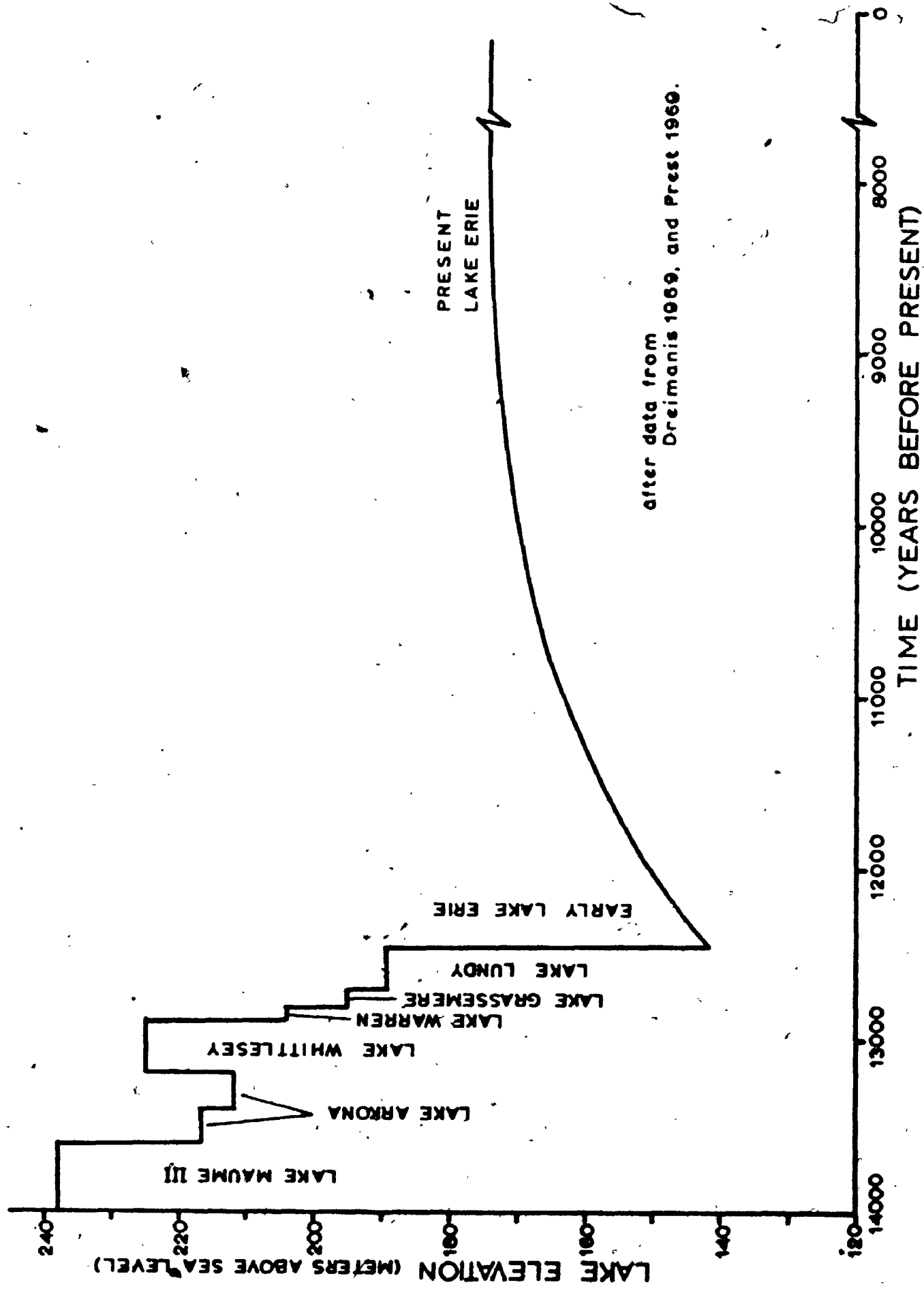


Fig. 332. Lake Erie Levels since Last Glacial Stage.

values and long-term means are summarized in Table 3.9.

Lake levels records form a continuous curve with time; this type of data is usually referred to as a time series. Many statistical models exist permitting the analysis of time-series in order to extract useful parameters: the method of moving averages, harmonic analysis, regression, probability models, etc.

It is first essential to recognize the principal elements of time-series that are grouped in four main types. A first component of the series is the long-term or secular movements (trends) such as those described in section 3.4.1 on post-glacial lake levels, and variations due to isostatic uplift in the Great Lakes area (Kites 1973). Other long-term effects are caused by permanent changes in the storage of a lake due to the withdrawal of water from a canal or diversions into the lake. These jumps in the time series are illustrated in Figure 3.33 showing the hydrograph of Lake Erie between 1860 and 1971. The Chicago diversion, since 1900, for the Chicago Sanitary and Ship Canal contributes to a decrease of 0,04 meter in Lake Erie elevation. The modern Welland ship canal, completed in 1932, contributes to a lowering of 0,12 metre. The LongLake Diversion in 1939 and the Ogoki Diversion in 1943 bring additional water to Lake Superior and their combined effect is to rise Lake Erie levels by 0,07 meter. The net difference between early records and present ones is then a lowering of 0,09 meter (Kirshner 1968). These changes are important for the flow characteristics and the storage

Table 3.9
 Extreme Lake Levels
 Recorded at Fort Stanley
 (1910-1970)
 in meters

	High		Low	
Annual	174,45	1952	173,27	1934
Monthly	174,68	May 1952	173,12	Feb. 1936
Daily	174,73	May 28 1952	173,05	Jan. 19 1936
Instantaneous	175,12	July 4 1969	172,81	Mar. 17 1935

Lake Erie datum: 173.31 m.

Maximum amplitude of fluctuations

Annual	1,18 m
Monthly	1,56 m
Daily	1,68 m
Instantaneous	2,31 m

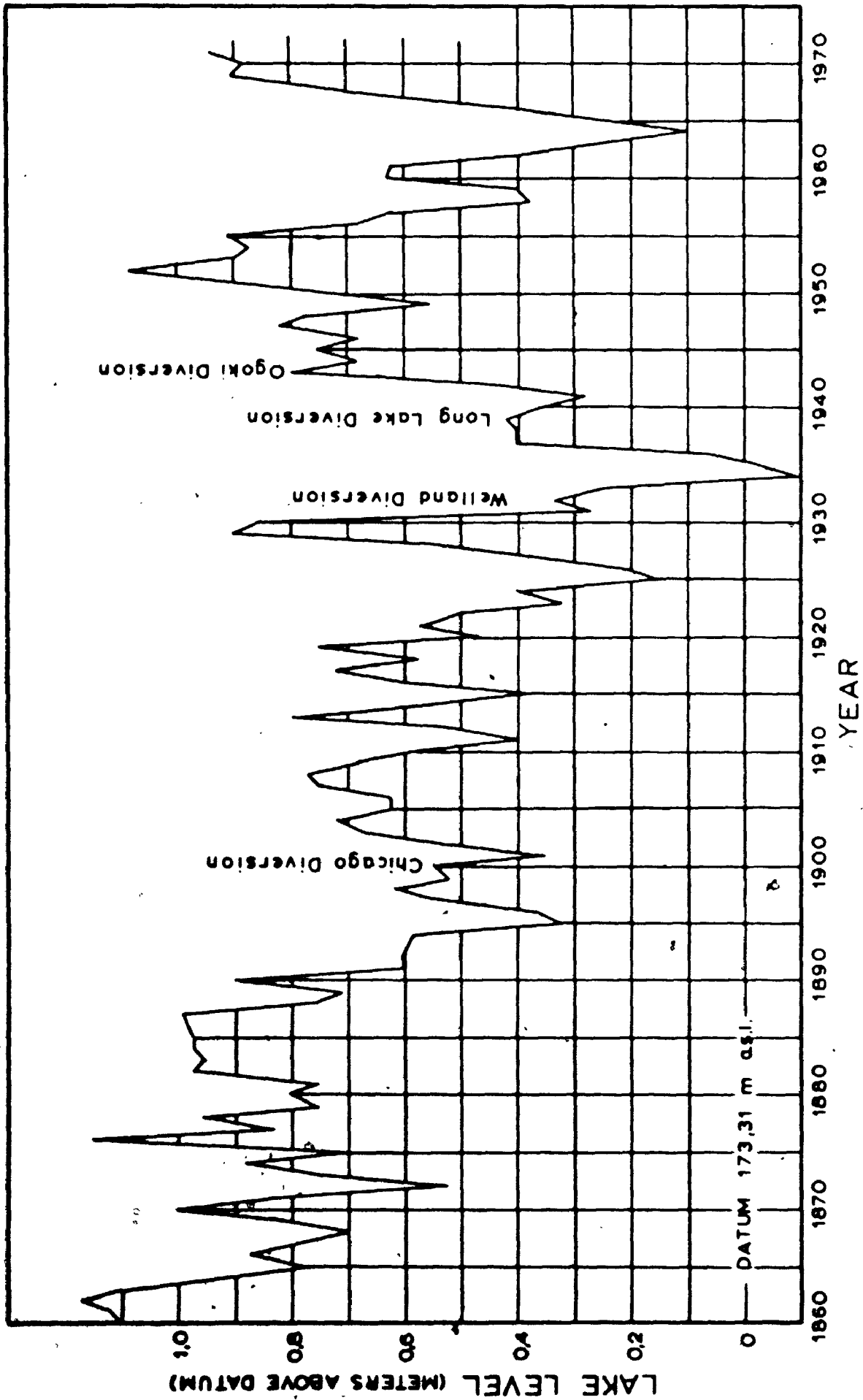


Fig. 333 Hydrograph of Lake Erie, 1860-1971.

capacity of lake Erie but have a minor influence on erosion.

Seasonal fluctuations in lake levels are a second component of the time-series. The annual hydrograph of Lake Erie for 1969 is shown on Figure 3.34 along with monthly extremes and means. The annual high occurs usually from May to July; the mean amplitude of seasonal variations is 0.38 meter based on monthly averages; this value is much less than the variations between years or between months in different years (Table 3.9). The shape of the hydrograph minimizes the effect of storm waves which have their greatest amplitude in November and December when levels are low.

Random or stochastic movements are also present in the series and can account for a large proportion of the variability observed (up to 50% according to Kites, 1973). The series is marked by irregular events caused by variation in climate (storms, precipitation, drought), changes in recording technique, relocation of gauging stations, human and instrumental errors.

One component will be investigated in more detail here: the cyclical movements extending over many years or decades are the most susceptible of influencing long- and short-term erosion rates. The search for long-term periodicities (excluding seasonal variations) can be done in several ways, two methods being described here.

Trends or cycles may be shown by using the technique of moving averages (Spiegel 1961). Given a set of data Y_1, Y_2, \dots the moving average of order N is defined

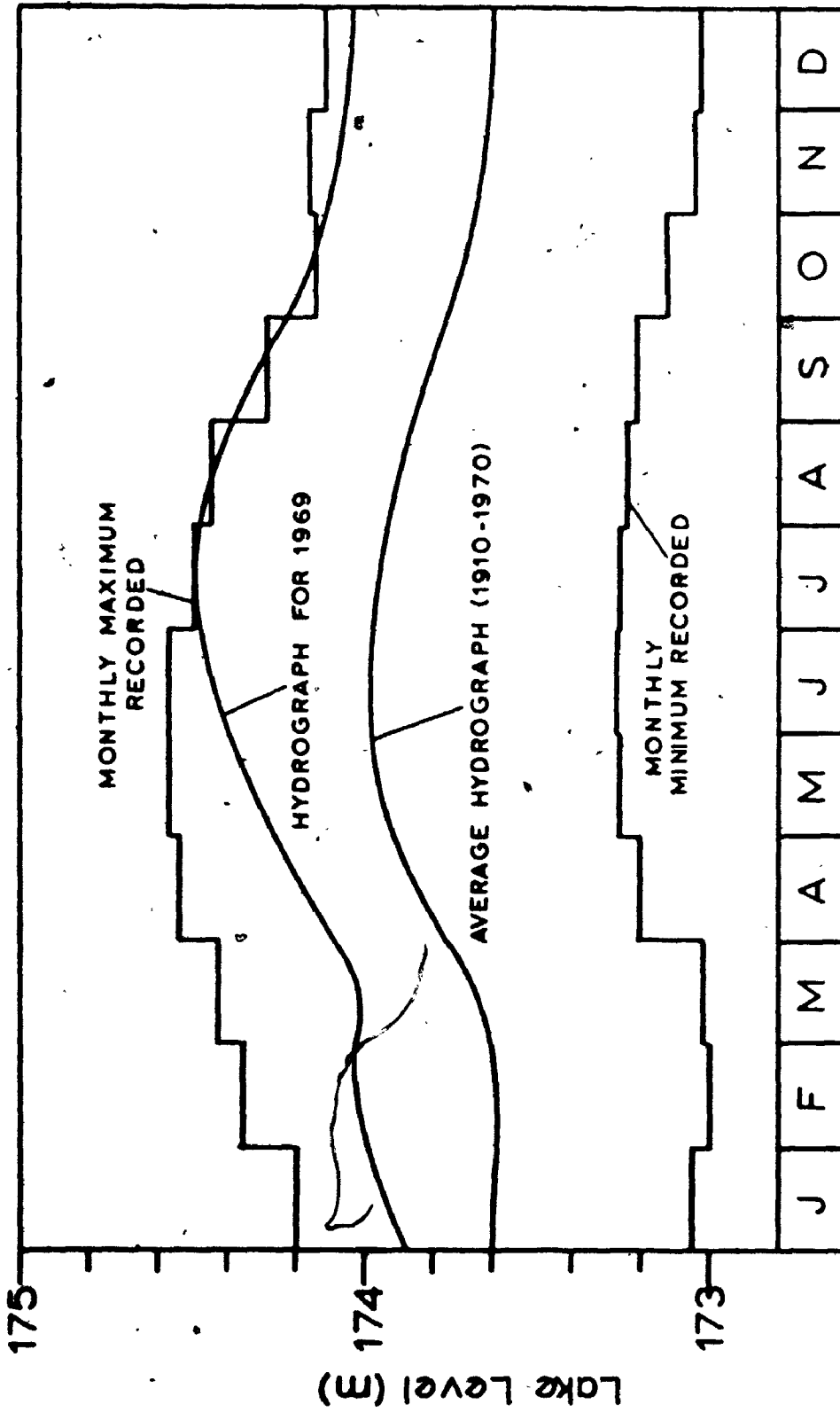


Fig. 334 Annual Hydrograph of Lake Erie.

by the sequence of arithmetic means

$$\frac{Y_1 + Y_2 + \dots + Y_n}{N}, \frac{Y_2 + Y_3 + \dots + Y_{n+1}}{N}$$

This new series is the N-year moving average of the data. By this process, the series is smoothed and much of the variability is eliminated. The 5-year moving average of Lake Erie annual means was calculated and is plotted on Figure 3.35 with the raw data. Typical cycles have different length as for instance 24 years between 1929 and 1953 and 20 years between 1953 and 1973 but also smaller cycles of 3 to 10 years appear in the series.

The search for periodicities can be done also by harmonic analysis that simulates a time-series by a trigonometric series. The complete series is the sum of sinusoidal curves of different amplitude and wave length. To simplify the problem and reduce the number of terms, harmonic analysis was done on 5-year averages of lake levels. The period of records from 1860 to 1970 was used for the analysis.

Generally the trigonometric series will have the form (Scheid 1968)

$$h(x) = \frac{1}{L} a_0 + \left(\sum_{k=1}^{L-1} \frac{a_k \cos \frac{\pi k x}{L} + b_k \sin \frac{\pi k x}{L}}{L} \right) + \frac{1}{L} a_L \cos \pi x$$

$$\text{where } a_j = \frac{1}{L} \sum_{x=0}^{2L-1} h(x) \cos \frac{\pi j x}{L} \quad j=0, 1, \dots, L$$

$$\text{and } b_j = \frac{1}{L} \sum_{x=0}^{2L-1} h(x) \sin \frac{\pi j x}{L} \quad j=1, 2, \dots, L-1$$

In this equation, $h(x)$ is the 5-year average lake level at the periods $x=0,1,\dots$ defined in Table 3.10, in meters above datum (173,31 meters above sea level). $(N + 1)$ is the number of such periods and L is defined as $\frac{N + 1}{2}$.

The complete solution of the series is given by finding the value of the coefficients a_j and b_j (Table 3.11). In this model, the term $(\frac{1}{2}a_0)$ represent the mean lake level over the period of study. The addition of the terms with coefficients a_1 and b_1 represents the first harmonic with a periodicity of 110 years; the addition of the terms in a_2 and b_2 gives the second harmonic of period equal to $110/2$ or 55 years and so on.

The amount of variability explained by each pair (a_j, b_j) of coefficients has been calculated in terms of the percent variance away from the mean explained by each pair; this permits an estimate of which cycles seem to represent more adequately the long-term fluctuations of lake levels. From Table 3.12 it can be seen that 84% of the variance away from the mean is explained by the superposition of the 110-year cycle, the 37-year cycle and the 22-year cycle (see also Figure 3.35).

This model however does not give any insight on the physical or random processes responsible for lake level fluctuations, since such a series exists for any type of data. Also it is very hazardous to extrapolate the model outside the period of observation even for a few years. For these reasons it is advisable to use also a probability model that can be used more directly and where extrapolation

Table 3.10
 Parameters Used for
 Harmonic Analysis

X	Time Interval	5-Year Average Level, $h(x)$ meters above datum
0	1860-1864	1,092
1	1865-1869	0,786
2	1870-1874	0,796
3	1875-1879	0,876
4	1880-1884	0,888
5	1885-1889	0,878
6	1890-1894	0,654
7	1895-1899	0,476
8	1900-1904	0,562
9	1905-1909	0,688
10	1910-1914	0,572
11	1915-1919	0,602
12	1920-1924	0,452
13	1925-1929	0,436
14	1930-1934	0,320
15	1935-1939	0,250
16	1940-1944	0,512
17	1945-1949	0,714
18	1950-1954	0,890
19	1955-1959	0,598
20	1960-1964	0,402
$N=21=2L-1$	1965-1969	0,576

Table 3.11

Coefficients a_j and b_j
for Harmonic Analysis

a_j	b_j
$a_0 = 1,274$	
$a_1 = 0,161$	$b_1 = 0,122$
$a_2 = 0,00382$	$b_2 = 0,00445$
$a_3 = -,0904$	$b_3 = 0,0752$
$a_4 = 0,0788$	$b_4 = 0,0356$
$a_5 = 0,126$	$b_5 = 0,0133$
$a_6 = 0,0732$	$b_6 = -0,00827$
$a_7 = 0,0328$	$b_7 = -0,0254$
$a_8 = 0,0475$	$b_8 = -0,0125$
$a_9 = 0,0035$	$b_9 = 0,00227$
$a_{10} = 0,0420$	$b_{10} = 0,0186$
$a_{11} = 0,0236$	

Table 3.12

Variance Explained
By The Harmonic Model

Coefficients	Periodicity (years)	% Variance Explained
a_1, b_1	110	48,4
a_2, b_2	55	0,0
a_3, b_3	36,7	16,3
a_4, b_4	27,5	8,0
a_5, b_5	22,0	19,3
a_6, b_6	18,3	0,0
a_7, b_7	15,7	2,1
a_8, b_8	13,8	3,0
a_9, b_9	12,2	0,0
a_{10}, b_{10}	11,0	2,5
a_{11}	10,0	0,4

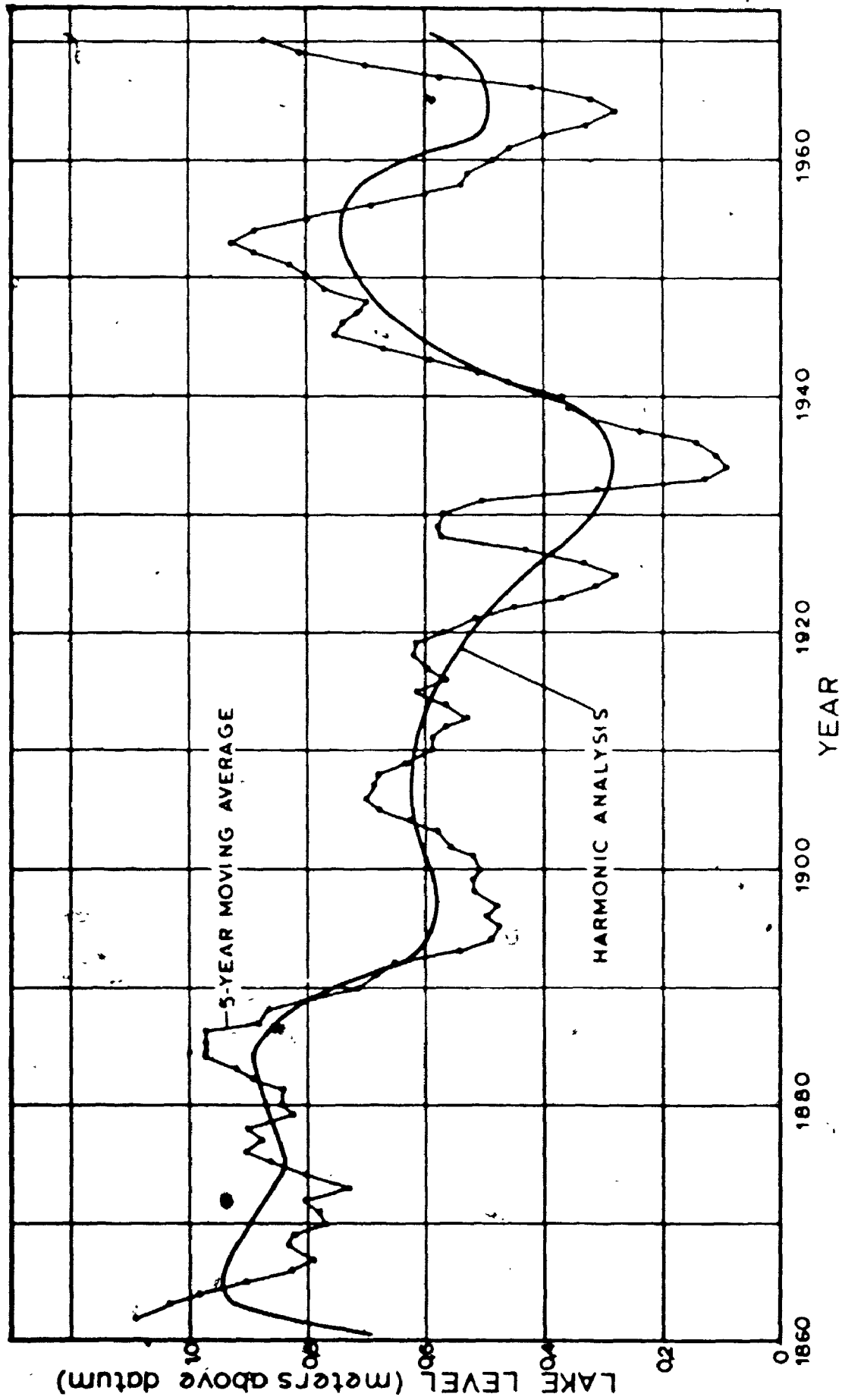


Fig. 335 Models for Long-Term Fluctuations in Lake Levels.

is permitted within certain limits.

A statistical model used in hydrology to estimate flood probability and return period (Hazen 1930, Wilson 1969) is also applicable to lakes (Saville 1953). Using the annual average levels, the probability F of a certain stage being reached or exceeded is (in percent)

$$F = \frac{100}{T}$$

where T is the return period in years of a given flood stage. T is calculated in the following way (Saville 1953, Wilson 1969)

$$T = \frac{n+1}{m}$$

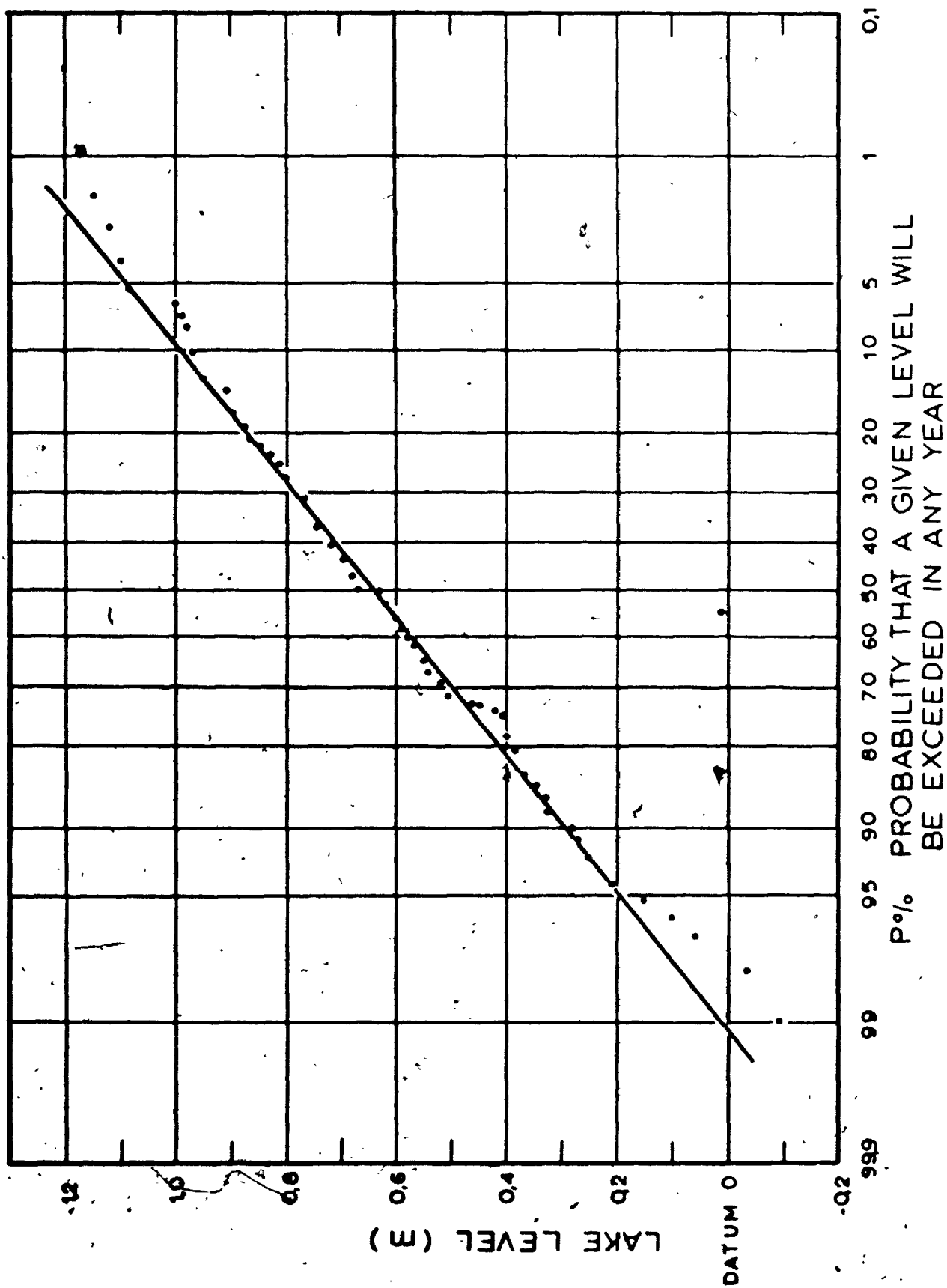
where 'n' is the number of years of record and 'm' is the number of times during the period on record that a given stage was reached or exceeded. These points are plotted on probability paper and the straight line relationship indicates a nearly normal distribution; discrepancies occur at both ends of the curve so that extrapolation is not warranted for extreme cases (Figure 3.36).

Prediction of lake levels even with a good mathematical model is conditioned by large random components that account for 50% of the total variance, the other half being described by long-term cyclical movements, the trend over that period being considered as negligible.

3.4.3 Effects of Lake Levels on Erosion.

Lake levels at any time will determine to a large

Fig. 336 Probability Model for Lake Levels.



extent the short-term erosion rates and also will contribute to subaqueous erosion in periods of low water.

The profile of the nearshore and beaches controls the way by which wave energy will be spent. Low gradient profiles force waves to break at a relatively large distance offshore; coarse material on beaches will absorb most of the wave energy reaching the shoreline after breaking of the wave. Soundings made by the Department of Public Works (DPW 1969) give a good picture of the nearshore and beach area through 33 profiles of lake bottom in the study area. Further discussions on the effects of lake levels on erosion will refer to those sections.

A typical bottom profile near Fort Talbot is illustrated on Figure 3.37. The overall gradient at 500 meters away from the shoreline is usually 1%, but near water edge it steepens to 3-4%. Table 3.13 gives a resume of the bottom configurations at 33 sections in the study area.

Fluctuations of lake levels will affect first the position of the shoreline. Due to steeper gradients near the shoreline, these fluctuations will not change the position of the water mark by more than 10 to 20 meters between the highest and lowest monthly averages. More important is the level of erosion: maximum wave energy is wasted in the breakers zone; since the position of the breakers zone is related to the depth of water, among other things (Figure 3.14 and Table 3.5) a wave of given height, length and period will break close or far from the bluffs depending on lake level. Figure 3.37 shows the position of the breakers

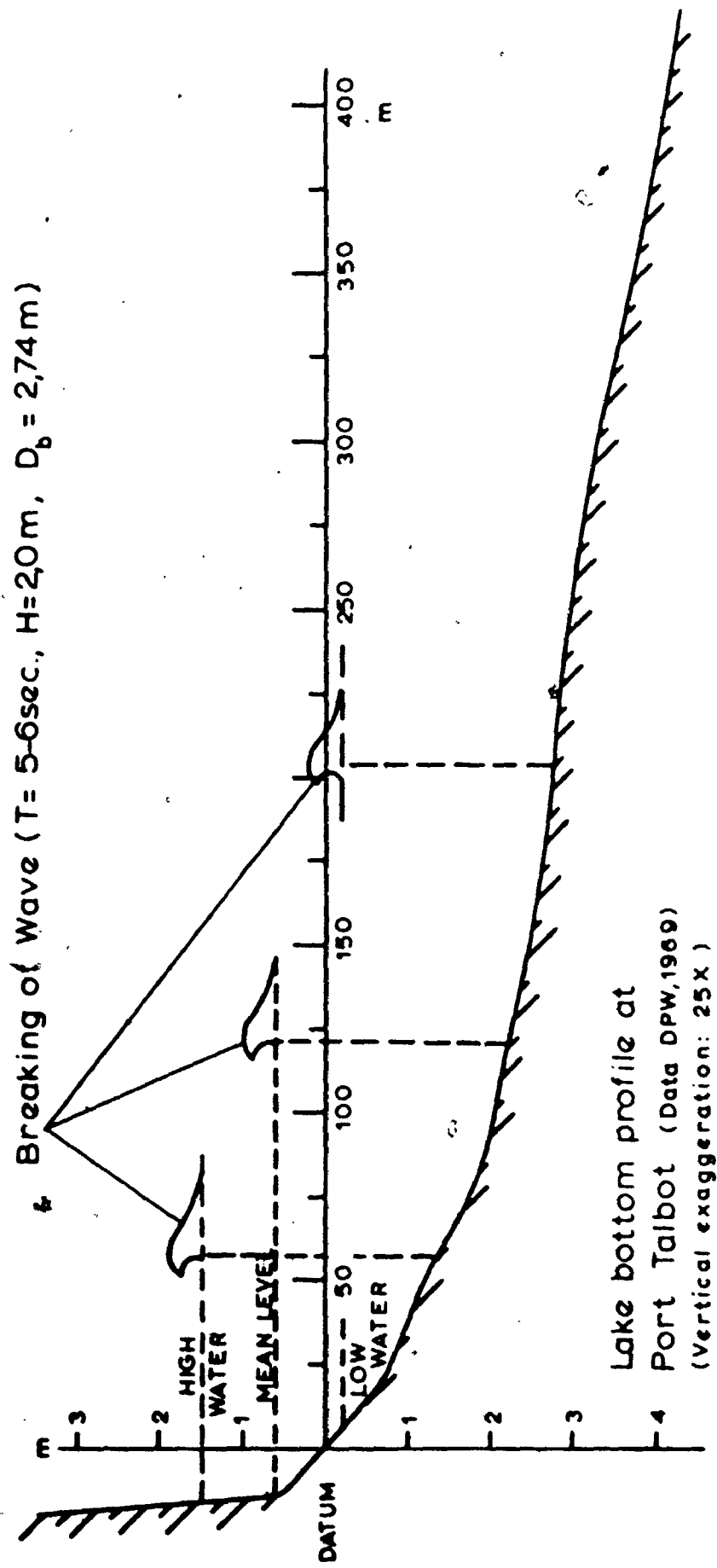


Fig. 3.37 Influence of Lake Level on the Location of the Breakers Zone

Table 3.13

Lake Bottom Profiles
(average of 33 sections)

Distance from shoreline (meters)	Depth (m)	Gradient %
-5	-0,43 ± 0,2	8,6 (0 to 30)
0	0	5,5 (0 to 8)
10	0,55 ± 0,5	3,1 (-2 to 9)
20	0,86 ± 0,5	2,0 (-3 to 4)
40	1,27 ± 0,5	1,2 (-2 to 5)
60	1,50 ± 0,5	2,5 (-1 to 3)
80	2,00 ± 0,5	1,2 (-1 to 4)
100	2,25 ± 0,5	0,6 (-1 to 4)
150	2,53 ± 0,5	0,9 (0 to 2)
200	3,00 ± 0,5	0,8 (0 to 2)
250	3,42 ± 0,5	0,7 (0 to 1)
300	3,77 ± 0,6	0,7 (0 to 2)
350	4,10 ± 0,7	0,8 (0 to 2)
400	4,48 ± 0,8	0,8 (0 to 2)
450	4,90 ± 1,0	0,8 (0 to 2)

Data from DPW, 1969.

for the average lake level (173,95 meters above sea level) for extreme high monthly level and for lowest monthly level calculated for a wave train having a period of 5 to 6 seconds and a height of 2,0 meters. The distance between the position of breakers for the two extreme levels is 150 meters. Therefore the location of the zone where maximum energy is spent varies considerably with lake level. One may add also that during storms, wind setup will further raise the level of the lake and consequently the wave will break still closer to the shoreline.

The second major effect will be in the swash zone; during periods of low water, waves lose most of their energy before reaching the bluffs because of the longer runup distance on the beach and therefore little is left for toe erosion. When lake is high, the beach is either completely submerged or washed away by longshore currents so that a great deal of work is done by impact at the base of the bluffs.

The periodical alternance of high and low stages produces changes in level of erosion and is a reason why erosion is still very active in the study area. Otherwise one might expect that at constant lake level a certain equilibrium would be reached for a certain gradient of the shoreline and the position of the bluff line. But erosion under water is still active (Lewis 1966). Therefore if bluff erosion is retarded or decreases during periods of low water, subaqueous erosion is at a maximum and cuts deeper into the offshore platform; in this way the severity of

of wave action during the next high stage of the lake is increased and bluff erosion starts a new cycle (Hough 1958).

3.5 Erosion Rates and Wave Action.

Comparison of long-term erosion rates with wave energy can be done by plotting erosion rates against the corresponding total wave energy at breaking (E_{fb}). Regression by least squares was attempted and the following empirical relationship was found (Figure 3.38)

$$E_r = 0,28 + 0,96 E_{fb}$$

where E_r is the erosion rate in meters per year averaged over 3 kilometers and E_{fb} is in kilowatts per meter of shoreline per year. The correlation coefficient, r , is 0,71 and is significant at the 99% level.

The amount of erosion that can be explained by wave action alone can be computed indirectly. Assuming that if wave action is nil there will be no erosion, the variance between observed erosion rates and zero erosion is computed by summing the squares of erosion rates at all points along the shoreline. Similarly the variance can be calculated by using erosion rates predicted from the regression line above. By comparing the total variance of the system due to all causes with the variance explained by wave action, it is found that wave energy can account for 75% of the total variance. The remaining 25% has to be explained by different factors such as the type of soil materials, the geometry of the bluffs, the presence of

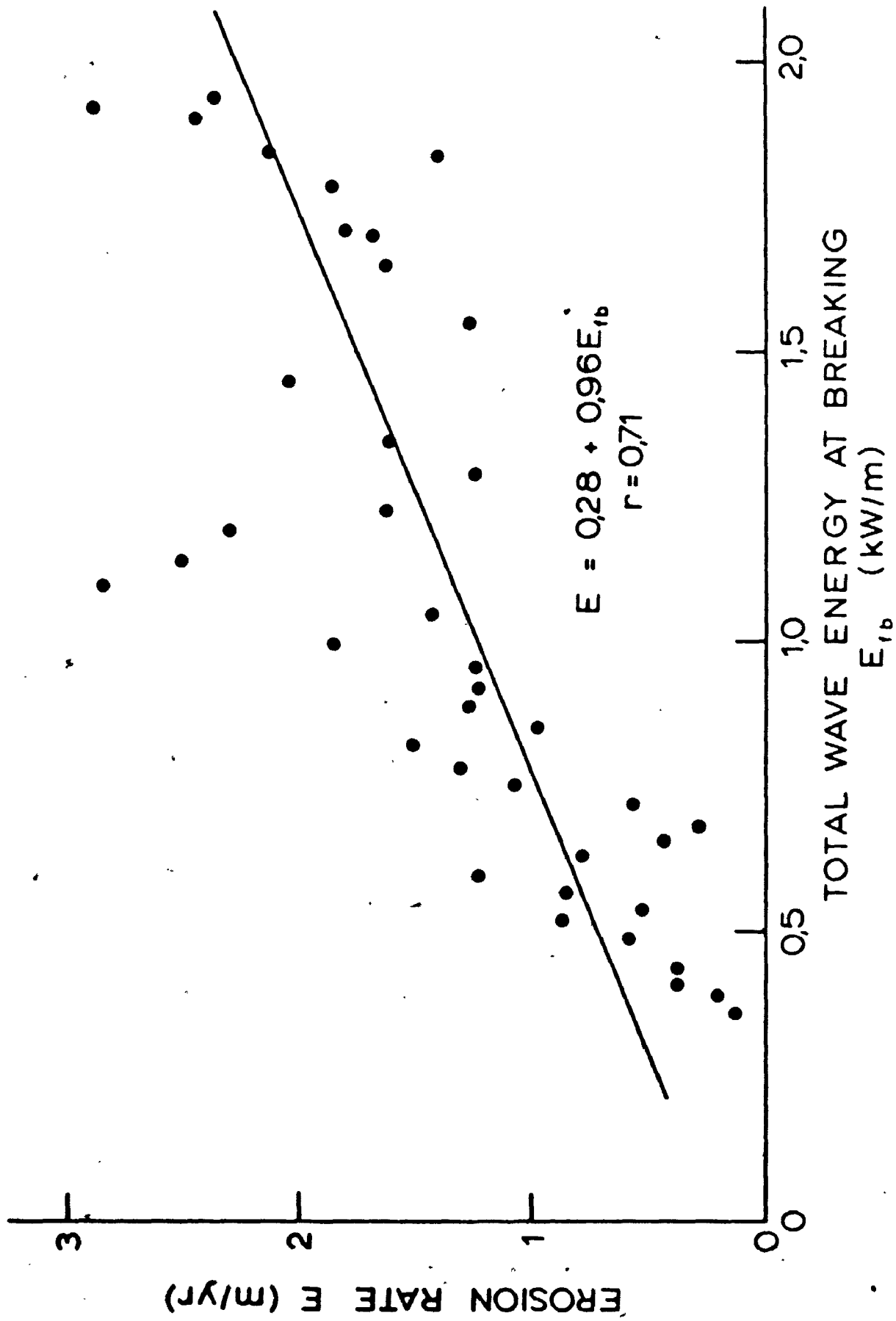


Fig. 3.38 Relationship between Wave Energy and Erosion Rate ¹⁶

protective structures, groundwater action, etc.

The effects of storm setup and lake levels on long-term erosion rates cannot be estimated but it is assumed that over a long interval of time they distribute more or less evenly and their effect is assimilated to wave action. Under short-term measurements however these parameters have to be recorded and corrections applied to evaluate long-term rates of erosion.

The variations in erosion rates along short sections of the shoreline are controlled in last resort by local geology and bluff morphology since wave conditions do not vary that much within a short distance. Also, human action may increase or decrease erosion rates locally: protective structures, drainage leading to gully formation, dredging and mining of beach material for road and concrete aggregates.

In the next chapter, details will be presented concerning variations in geology along the study area and also mechanisms of erosion by drying and wetting of soil materials that have been physically weathered.

CHAPTER 4

GEOLOGICAL MATERIALS AND PROCESSES

This chapter will briefly review the geological parameters that have some relevance in the study of erosion along the north shore of Lake Erie. In a first part, the materials and geological history of the area will be investigated including bedrock geology and topography and in more details the Pleistocene materials, their history, and their stratigraphy. In a second part, geological processes leading to or promoting erosion will be studied; these include the process of shrinkage and swelling caused by alternance of dry and wet cycles leading to the complete destruction of the structure of the soils making the bluffs. The degradation of slopes by physical weathering will lead to instability problems which will be discussed in Chapter 5 from an engineering point of view.

4.1 Bedrock Geology.

Most of southwestern Ontario is covered by thick glacial and lacustrine sediments, several hundred of meters thick in some areas. Bedrock geology is known by studies in rare quarries or outcrops and more extensively from cores recovered from oil exploration.

The bedrock geology in the study area has been investigated mainly by Caley (1941, 1943) and Sanford (1958,

1962, 1968). The platform-type sediments that cover the area were influenced by three major structural features: 1) the Algonquin Arch, forming a backbone of Precambrian rocks trending NE-SW across the southwestern Ontario peninsula; 2) the Michigan Basin forming an oval depression to the west and northwest and finally 3) the Appalachian Basin to the south and southeast. The relative thickness of Palaeozoic rocks, their facies and trends were controlled mainly by these three large scale features.

Rocks outcropping below glacial deposits are from Middle to Late Devonian age. They strike usually NW-SE and dip very gently to the southwest. The nomenclature for the various formations varies depending on the author consulted. More recent publications (Sanford 1968, Poole, Sanford and Williams 1970, Ferrigno 1971) recognize four major formations directly underlying the study area: the Dundee limestone, the Marcellus shale, and the Hamilton shale from the Middle Devonian and the Kettle Point Formation of Early Upper Devonian age. (Figure 4.1)

The Dundee Formation underlies most of southwestern Ontario but outcrops only in the eastern part of the study area, east of Port Burwell, under Long Point and Long Point Bay. It consists of tan-colored coarse grain calcarenite grading upward into aphanitic limestone; some brown chert is found in the margin of the basin. Near the eastern part of Lake Erie, the lower clastic limestone grades into dark argillaceous and cherty limestones of the Onondaga Formation. It reaches thicknesses of 50 meters beneath

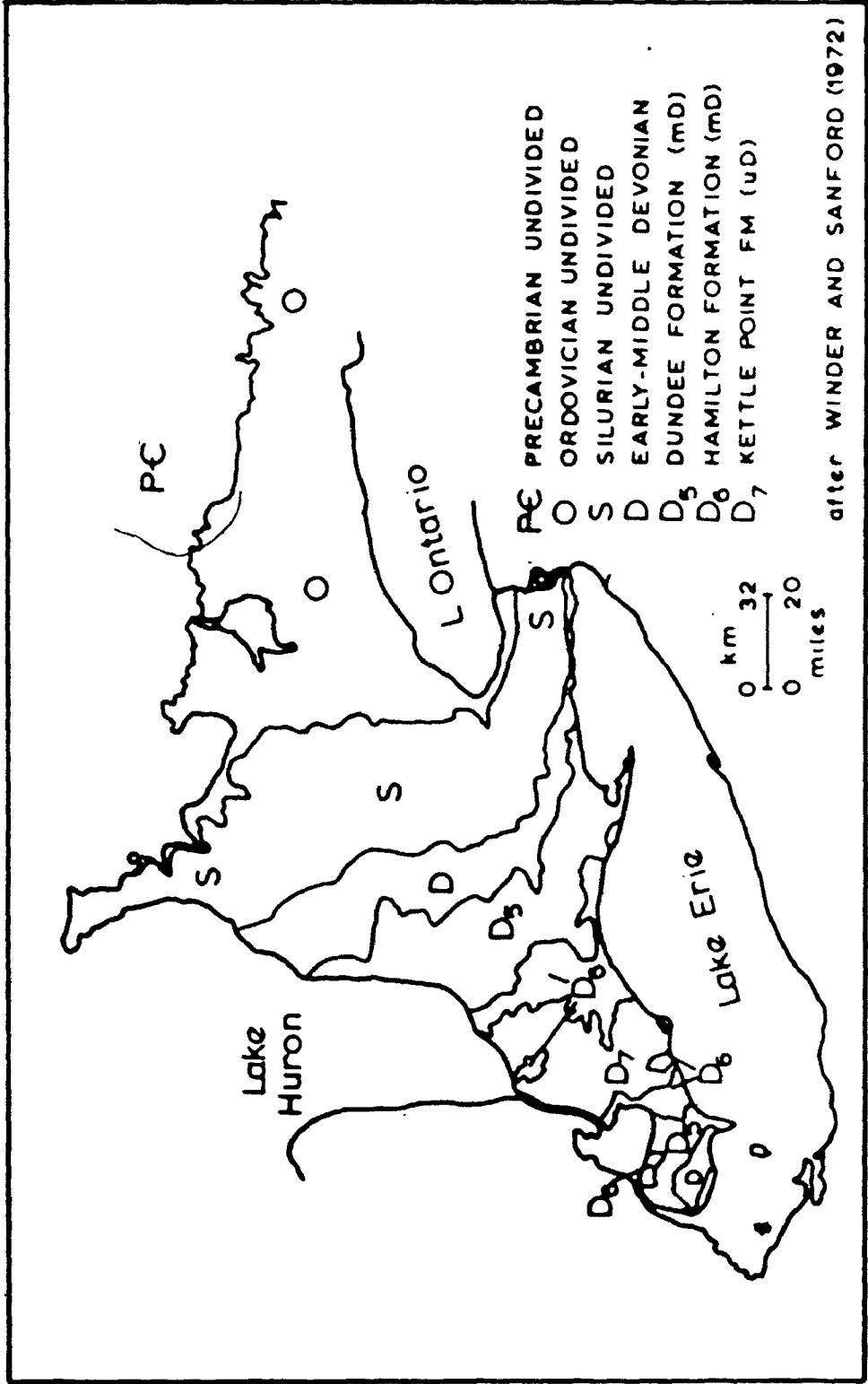


Fig. 4.1 Bedrock Geology, Southwestern Ontario.

central Lake Erie. This formation was previously called Norfolk Formation (Caley 1941, 1943) and Delaware Formation (Sanford 1958, 1962).

The Marcellus Formation overlies the Lunde limestone by gradational contact. This black bituminous shale is not exposed in Ontario but is present under Lake Erie in the central and eastern basin and also below glacial deposits in parts of Norfolk and Elgin Counties near Fort Burwell and Fort Bruce.

The Hamilton group occurs in a narrow band near the western extremity of Elgin County and follows Lake Erie shoreline between Plum Point and Fort Stanley. This group is composed mainly of grey shales and argillaceous limestones.

During the Upper or Late Devonian, the Kettle Point Formation was deposited consisting mainly of black bituminous shale with interbeds of grey-green silty shale. This formation thickens in a southeast direction reaching a maximum depth of 300 meters beneath the south shore of Lake Erie. These shales outcrop over a 50-km band centered on Rondeau sand spit.

Bedrock geology is more or less uniform in the study area consisting mainly of shales and limestones. Its chief importance in this study is in controlling the amount of clasts and boulders that were ripped by moving glaciers. Pebble lithology is then a good tool to differentiate the origin of different till layers. The amount of coarse particles derived from bedrock is also important

because this material is released by erosion of the bluffs and is the main source of coarse particles for the alimentation of beaches protecting the bluffs against further erosion by waves.

4.2 Bedrock topography

Information from oil and water wells permits one to establish the bedrock topography in the study area (Caley and Sanford 1952, Sanford 1953, 1954, Sibul 1969); the adjacent area under Lake Erie was studied by sub-bottom reflection survey (Wall 1968) in an effort to estimate sediments thickness (Figure 4.2).

From these maps it is seen that glacial and lacustrine sediments are very thick all over the study area. The average depth of bedrock below lake level is 55 meters; the highest rock elevation occurs beneath Plum Point (Dreimanis, Terasmae and McKenzie 1966) where limestone is found at 25 meters below lake level. On the other hand the bedrock dips to more than 90 meters below the surface in the vicinity of Long Point (Sanford 1954). In the central area between Port Stanley and Port Burwell where maximum erosion rates occur the bedrock elevation is more or less uniform at 60 meters below lake level.

Bedrock configuration may have had some influence on the attitude of some basal tills deposited in contact with bedrock; for instance, outcrops of Early Wisconsin tills near Plum Point show the role of bedrock topography in

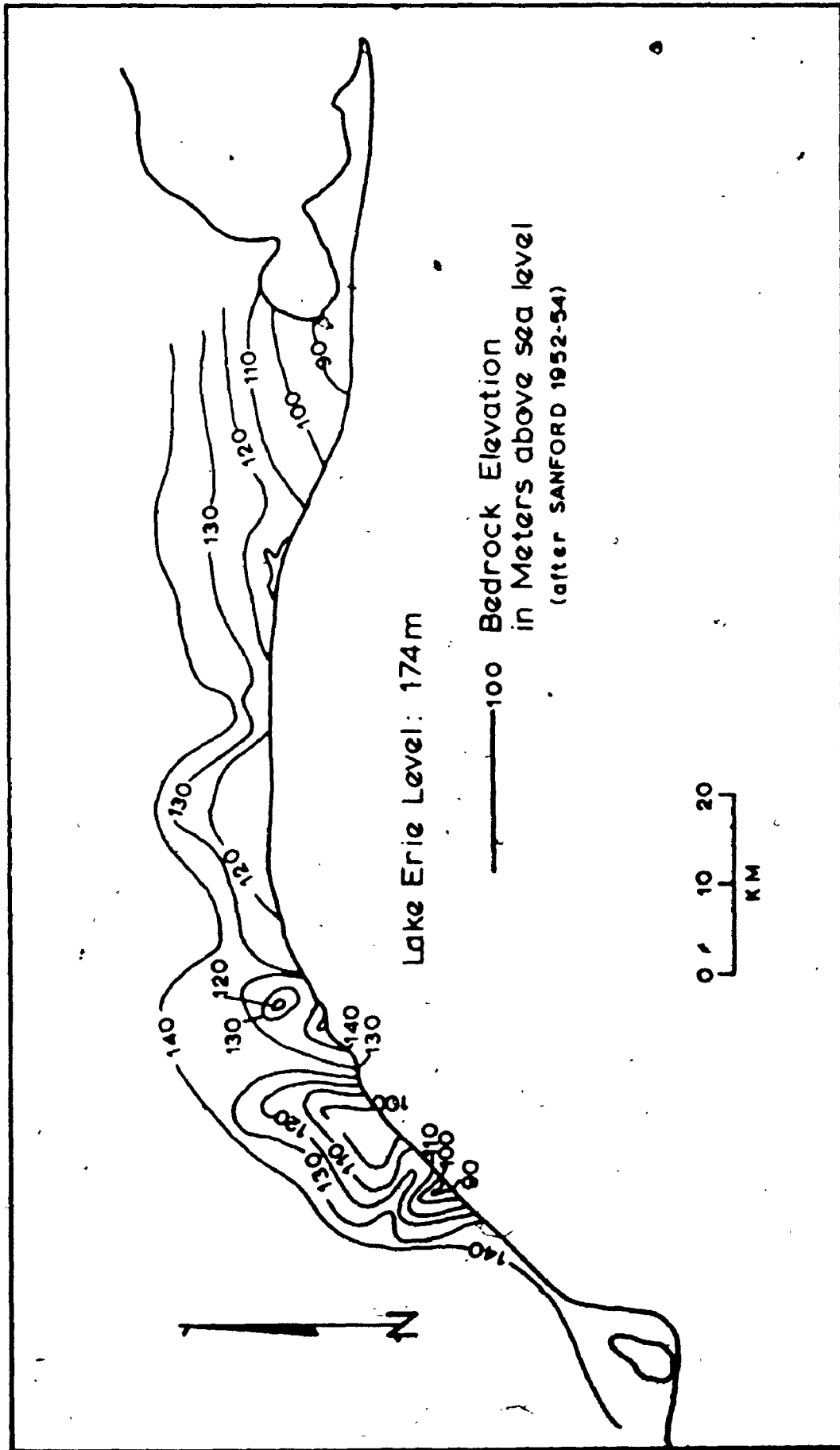


Fig. 4.2 Bedrock Contours, North Shore of Lake Erie.

controlling the stratigraphy locally since a hill in bedrock corresponds to upwarping of overlying till sheets.

For slope stability analysis it is often important to know the depth factor D , defined as the ratio of the total thickness of soil over the height of the slope (Taylor 1948). This value D is nowhere smaller than 2,0 (near Plum Point) and reaches values as high as 10,0 near Long Point. The average value (for mean bluff height of 28 meters and depth to bedrock of 55 meters below lake) is 3,0 and is close to 2,5 in the section between Port Stanley and Port Bruce where many slope failures are observed.

4.3 Pleistocene Geology.

This section reviews the main steps of the glacial history in southwestern Ontario and also describes the main physiographic regions in the study area; finally it gives more details on the different units that compose the bluffs and on some of their properties. Lastly a short discussion on recent sediments in Lake Erie gives some insight on the nature of the erosion processes acting in the last thousands of years.

4.3.1 Glacial History.

East central North America has been covered with continental glaciers at different times in the last million years. Four distinct glaciations are usually recognized and

named after their southernmost extension in the United States (Flint 1971). The Nebraskan glaciation is the earliest recognized but is covered everywhere by sediments from later glacial periods. Then followed the Kansan glaciation after the warm Aftonian Interglacial. After the Yarmouth Interglacial, the Illinoian glaciation once more covered Ontario and the northern states; only remnant of that glaciation in south Ontario is the York Till in the Toronto area (Coleman 1941, Karrow 1967). A subsequent warm interval, the Sangamon Interglacial, is responsible for the Don Formation overlying the York Till in the Toronto area.

In southwestern Ontario, all glacial materials can be attributed to the Wisconsin glaciation which prevailed in the last 100,000 years. Since it represents the bulk of Pleistocene deposits in Ontario, the Wisconsin was subdivided into three parts (Dreimanis 1960): the Early Wisconsin to about 53,000 years (Dreimanis 1970), the Mid-Wisconsin to about 23,000 years and the Late or Main Wisconsin to 10,000 years before present, when glaciers definitely left the area (Table 4.1).

During the Wisconsin glaciation, several intervals of warmer weather occurred in which ice retreated. The section at Plum Point, in the western part of the study area shows the sequence of events since the Bradville drift was deposited in Early Wisconsin (Dreimanis 1957, 1958, Dreimanis, Terasmae and McKenzie 1966, Quigley and Dreimanis 1972, Karrow and Dreimanis 1972). In Middle Wisconsin, from 53,000 years B.P., the climate changed during the Port Talbot Interstadial

Table 4.1

Time- and Rock-Stratigraphic Names
of the Wisconsin Stage in
the Erie Basin
(Dreimanis and Karrow 1972)

	Years B.P.	Time-Stratigraphic Units	Rock-Stratigraphic Units
	13.800	Fort Bruce Stadial	Fort Stanley Drift
	14.800	Erie Interstadial	Walahide Formation
Late	15.600	Nissouri Stadial	Catfish Creek Drift
	23.000	Plum Point Interst.	Wallacetown Formation
Middle	33.000	Cherrytree Stadial	Southwold Drift
	37.000	Port Talbot Interst.	Tyrconnell Formation
	53.000	Guildwood Stadial	Bradtville Drift
Early	63.000	St. Pierre Interst.	
	68.000	Nicolet Stadial	

(Tyrconnell Formation), and an other glacial period occurred during the Cherrytree Stadial (37.000 to 33.000 years B.P.). The Middle Wisconsin period was closed by the long Plum Point Interstadial from 33.000 to 23.000 years ago.

For most of the study area the interesting phase of the last glaciation is the Main or Late Wisconsin during which more than 90% of the materials exposed along the bluffs were deposited. From 23.000 years B.P. a major readvance of the ice covered Lakes Ontario, Erie and Huron (the Missouri Stadial) depositing the coarse textured Catfish Creek drift which is exposed inland along valley floors and in limited sections between Fort Talbot and Plum Point (Dreimanis 1969). Then the glaciers retreated to the extreme eastern portion of Lake Erie (Erie Interstadial, 15.600-14.800 B.P.); subsequent readvances of the ice cover were observed over most of the Erie basin (Port Bruce Stadial) and the fine-textured Fort Stanley drift incorporating material from the Erie Interstadial deposits was plastered in thick layers all over the north shore of the lake.

From about 13.800 years B.P. deglaciation occurred with minor readvances. During this last stage, various glacial lakes (section 3.4.1) existed for short time intervals and large quantities of sand, silt, and clay were deposited (Dreimanis 1969, 1970, 1971).

4.3.2 Physiography.

Surficial deposits along the shoreline of Lake

Erie can be classified into four main groups: sand spits, at Erieau and Long Point, clay plains, sand plains and terminal moraines (Chapman and Putnam 1951, 1966).

The two spits at either end of the study area are not strictly part of this study; they were formed by accumulation of sand on the crest of moraines submerged in Lake Erie and dating from the last retreat of the Erie Lobe (Woods 1951, Lewis 1966). The material was transported mainly by longshore currents acting on sand eroded from the bluffs.

Clay plains occupy several sections near the shoreline; between Morpeth and Erieau, a thin layer of stratified clay covers the till thickening towards the west. An other plain reaches Lake Erie near Plum Point and Port Talbot and extends inland north of Port Stanley and Port Bruce; these deposits are usually thin and sometimes let the till outcrop. A minor extension of that plain occurs along the lake west of Port Burwell.

Very wide sand plains extend over the clayey sediments in most of the study area. In the western half of the area a sand plain covers a wide stretch of shoreline between Patrick Point and Orford Township; its thickness is in the order of two meters. More extensive is the Norfolk sand plain overlying most of the area between the western limits of Port Stanley to the east near Long Point. The sand derives probably from deltas in Lake Whittlesey and Warren and was carried by Grand River. The thickness of this sand varies from a few meters to a depth of more than 30 meters east of Clear Creek; between Port Bruce and Port Stanley they reach commonly 10 to 15 meters.

Terminal moraines formed by subsequent readvances of the Erie Lobe are not important features along the shoreline.

The interest of this classification of surficial deposits is that they control the drainage characteristics of the land immediately in contact with the shoreline. Groundwater flow and its influence on the stability of the bluffs and also the type of slope failure are just two parameters that are controlled by the type of surficial deposits (see Chapter 5).

4.3.5 Stratigraphy Along the North Shore.

Many details on the succession of the different formations along the north shore of Lake Erie are due to the work of Dreimanis and his co-workers (Dreimanis 1957, 1958, 1961, 1966, 1969, 1970, 1971, Dreimanis and Reavely 1953, Dreimanis, Teresmae and McKenzie, 1966, Dreimanis and Karrow 1965, 1972, Quigley and Dreimanis 1972). Most of this work concerns the area between Plum Point and Port Bruce where erosion rates are very high. Outside this area, much less has been published and most of the interpretation is from air photographs, short field trips and some exploratory boreholes.

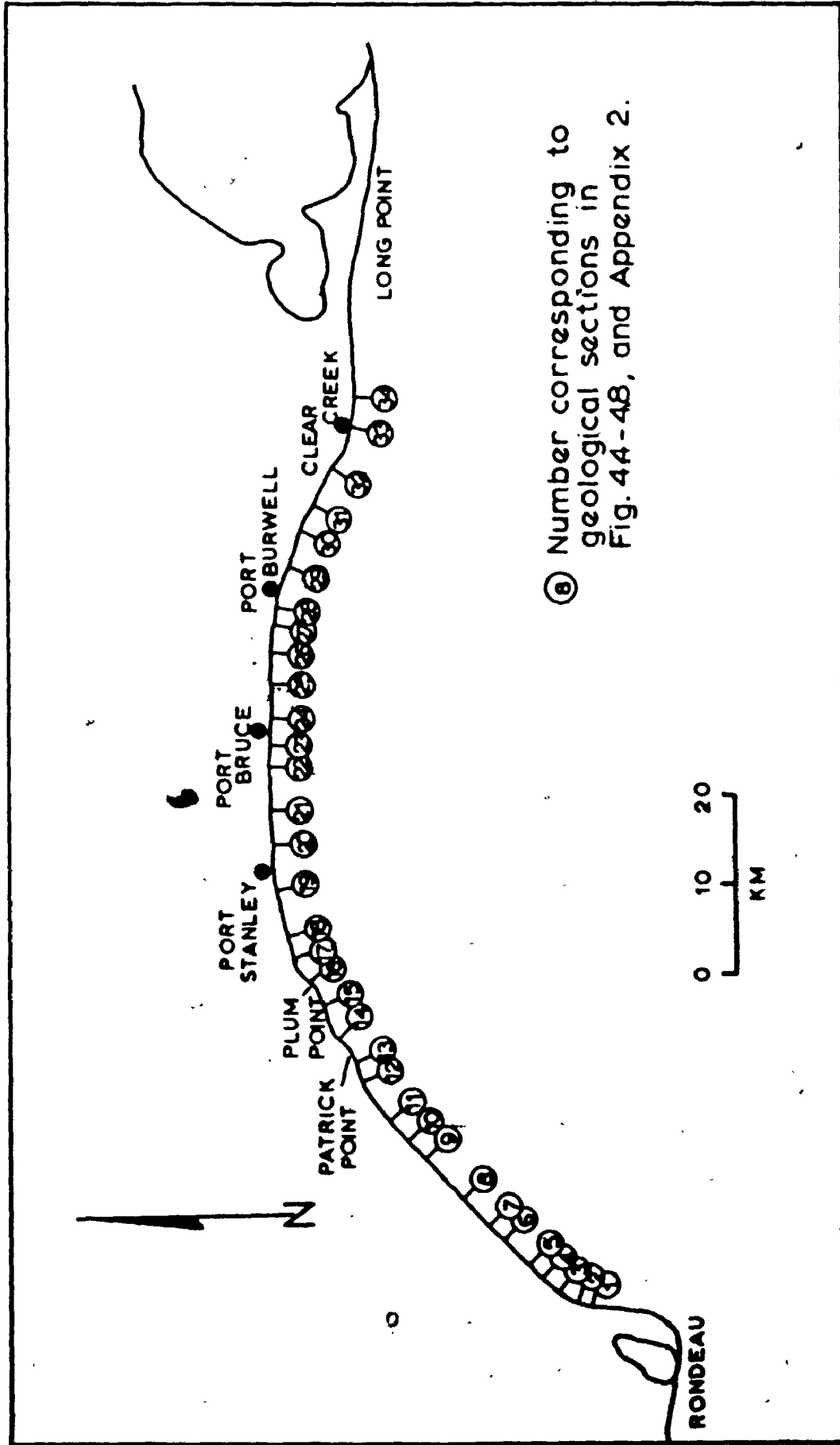
Except for minor occurrences of Middle Wisconsin material at lake level between Port Talbot and Plum Point all soil units in the study area belong to the Late or Main Wisconsin. Of the Main Wisconsin deposits, the Catfish Creek

drift is exposed in very limited areas near Flum Point and the bulk of materials date from the last glacial readvances that brought the Port Stanley Drift over the whole area with intervals of lacustrine sedimentation. Upper units are generally sands or silts deposited in post-glacial lakes.

Figures 4.3 to 4.8 illustrate in more details the variation in stratigraphy along the north shore at 34 locations. The description and references for these sections are given in Appendix II. Basically there are few types of materials: two till units, the Catfish Creek and the Port Stanley, and several lacustrine and fluvio-glacial deposits (stratified silt and clay between tills, deltaic sand, etc.).

Catfish Creek till (section 13 on Figure 4.5 and section 15 on Figure 4.6) forms massive gray layers containing a large proportion of sand and granules (25-28%) and a relatively small amount of clay-size minerals (12-25%) (Terasmae, Karrow, and Dreimanis 1972). It outcrops occasionally over 5 or 6 kilometers in the area between Patrick Point and Port Talbot.

The Port Stanley till is a grey-brown till with a very fine texture. It is very widespread over the whole study area and forms the principal material involved in the erosion process and in stability analysis. It is often difficult to distinguish basal till, waterlaid till and lacustrine material derived from it; usually the till is composed of reworked material of lacustrine origin and occasionally incorporates chunks of Catfish Creek till; inclusions in the form of clay pebbles, stringers of sand and silt are frequent.



⑧ Number corresponding to geological sections in Fig. 44-48, and Appendix 2.

Fig. 4.3 Index Map for the Geological Cross-sections.

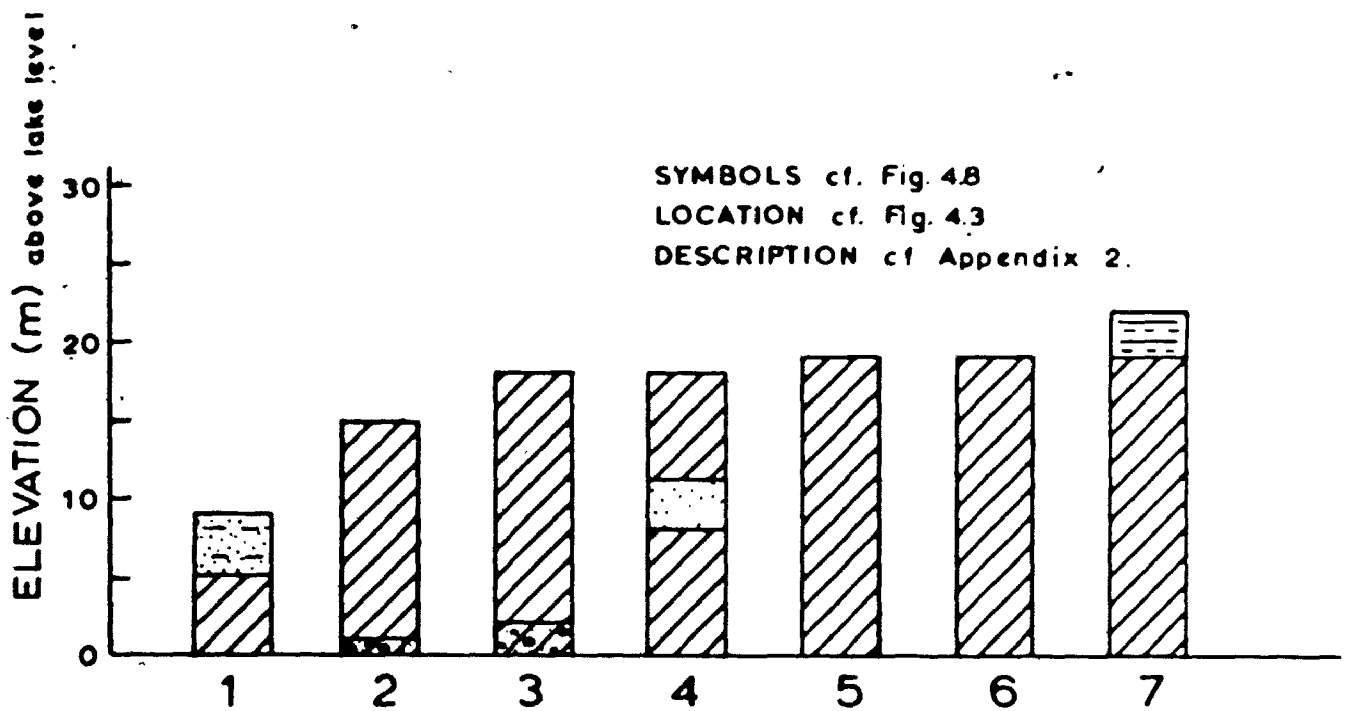


Fig. 4.4 Geological Sections 1 to 7.

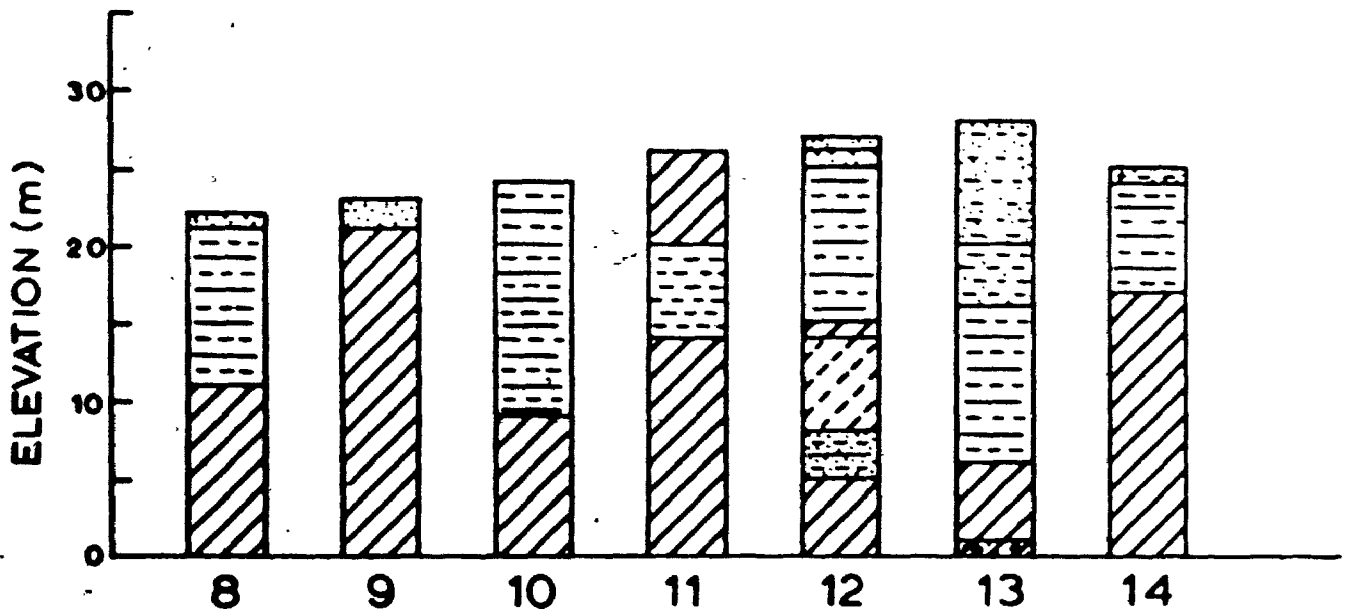


Fig. 4.5 Geological Sections 8 to 14.

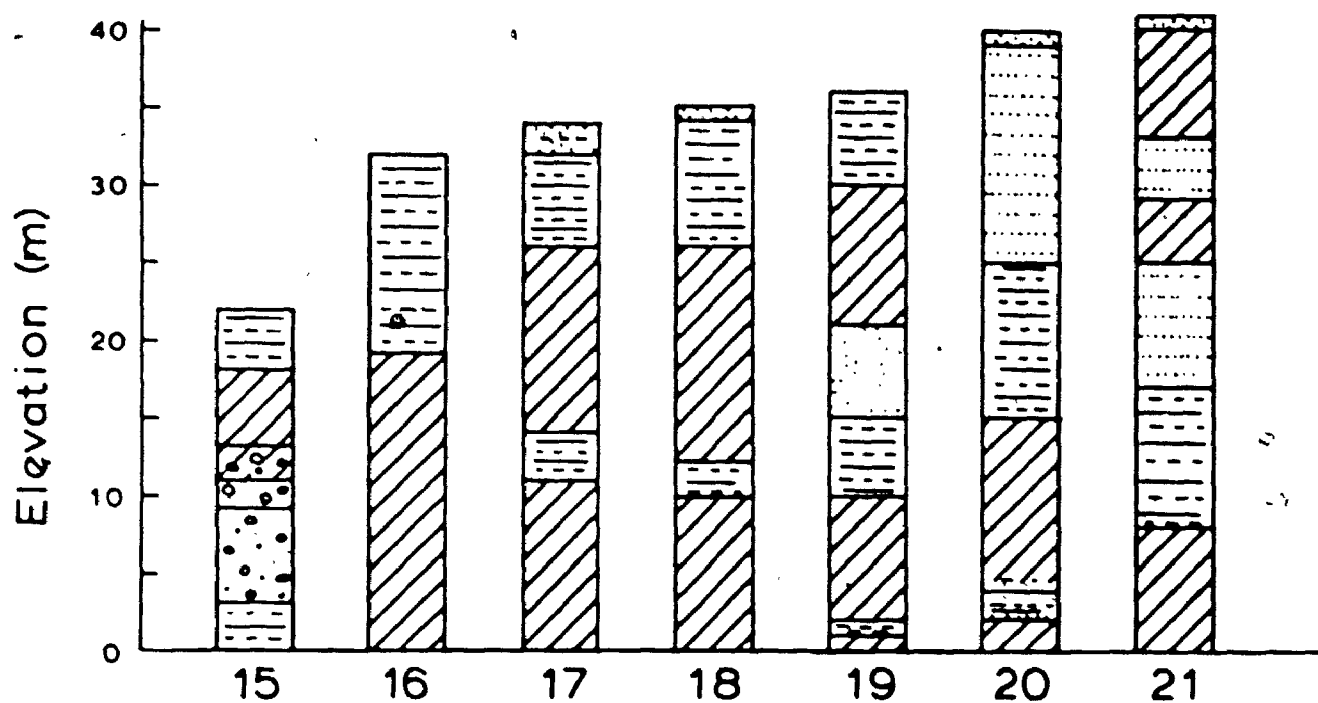


Fig. 4.6 Geological Sections 15 to 21.

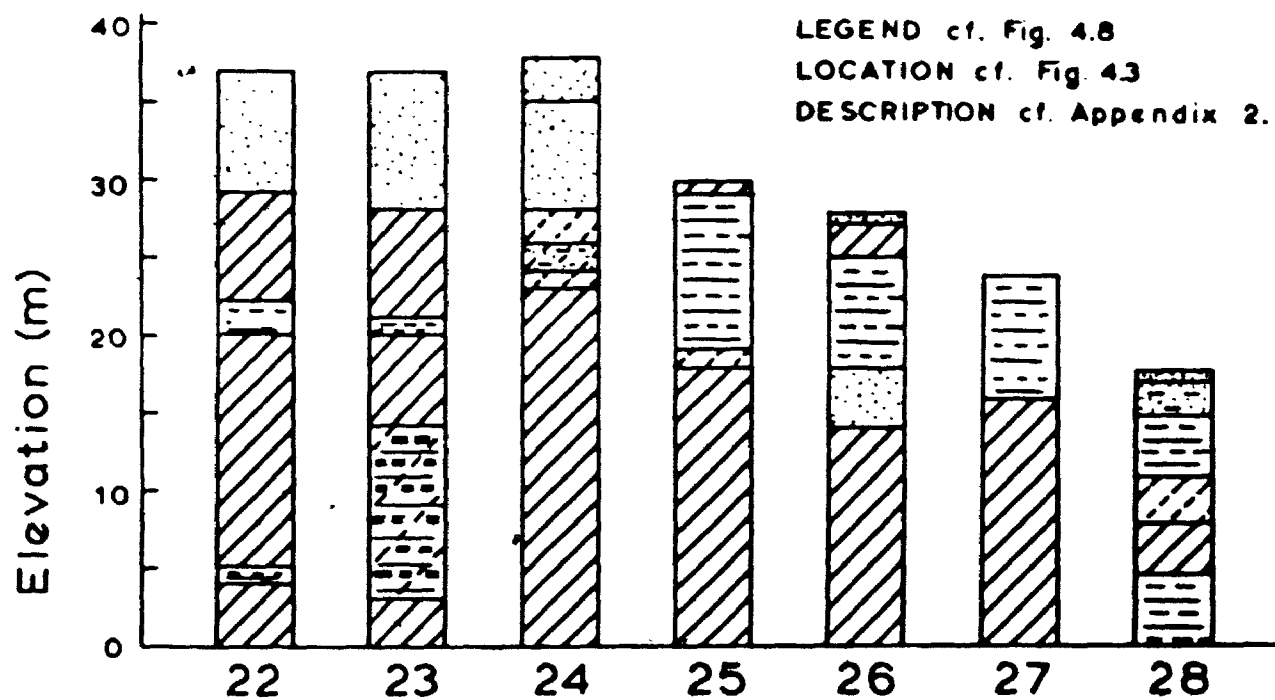


Fig. 4.7 Geological Sections 22 to 28.

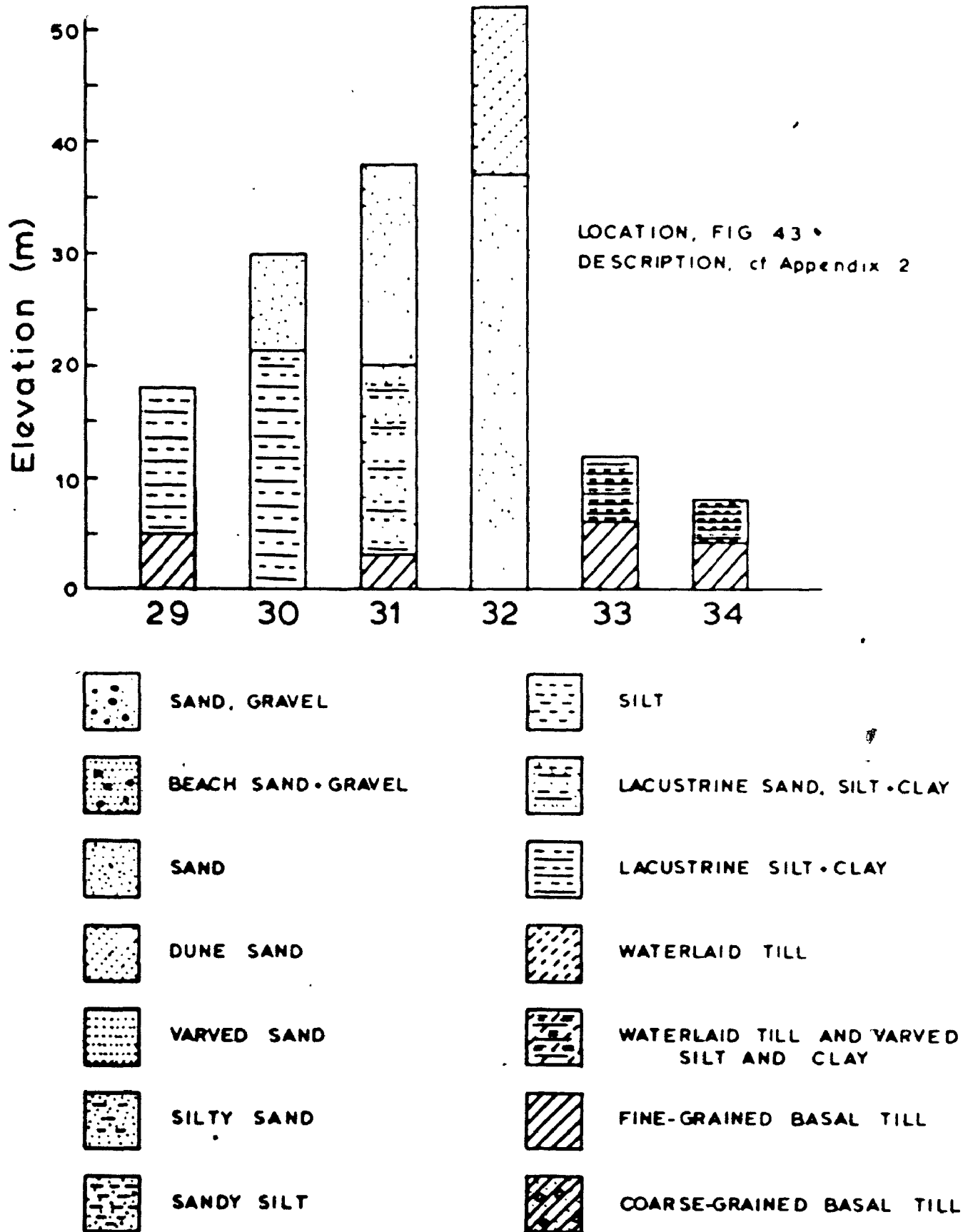


Fig. 4.8 Geological Sections 29 to 34.

For these reasons it is often more simple to designate the whole formation by the term 'Port Stanley Drift'. The basal till units are more gritty or pebbly, containing up to 10% coarse particles (Dreimanis and Reavely 1953) randomly distributed in the clayey silt matrix; when doing standard penetration tests (ch. 5) the basal till usually has a resistance greater than 50 blows per foot. Waterlaid till can be recognized by the occurrence of occasional clay pebbles and also by the segregation of coarse particles in thin layers; its penetration resistance using the standard test is usually from 30 to 50 blows per foot. On the average, the till has the following composition: sand and gravel 5-15%, silt (2-60 microns) 45-60%, and clay (less than 2 microns) 35-55%.

The glacio-lacustrine clayey silt associated with the Port Stanley drift is commonly varved but those varves are often indistinct in samples taken with a split spoon and in sections along the bluffs it is not unusual to see them contorted and reworked by subsequent readvances of the ice sheet. Lacustrine material is very poor in coarse particles (less than 5%) the bulk of the sediments being silt (50-63%) and clay (33-46%) in the vicinity of Port Burwell. Usually they have a much smaller resistance to penetration (15-30 blows per foot) due to the scarcity of sand and pebbles. Other properties (water content, Atterberg limits, specific gravity, unit weight) do not vary very much in the different varieties of Port Stanley Drift (Chapter 5).

Sand units often cap the sequence of glacial deposits (section 4.3.2) and are very important locally; near

Sand Hill in Houghton Township sand forms the entire section of 30 meters (Figure 4.8, section 32) and at the pumping station east of Port Stanley there is up to 16 meters of varved sands on the top of the section (Figure 4.6, section 20). Minor sand and silty sand layers exist also in some areas between till sheets (Figure 4.4, section 4, Figure 4.6 sections 19, 20, 21). The importance of sandy layers is threefold: it supplies material for beaches, it is responsible for increased erosion rates whenever it occurs in the zone subjected to wave action, and finally because of its permeability it discharges groundwater in large quantities enough to influence the stability of underlying jointed and fissured clay tills (Chapter 5).

4.3.4 Beach-Forming Materials.

The coarse fraction of tills has a special interest since it supplies large parts of the materials found on the narrow beaches at the toe of the bluffs. The pebble lithology of the Port Stanley Drift indicates a predominance of carbonates (limestone and dolomite) and shale, with minor amounts of chert, igneous and metamorphic fragments (Dreimanis and Reavely 1953, Dreimanis 1961).

The lag gravel left after transportation of finer fractions (sand, silt and clay) is rapidly abraded and worn away by wave action in the swash zone. A study of gravel composition along the beach at Port Burwell demonstrates this point. The 3.5-kilometer beach, built in a crescent shape

behind the jetty at Fort Burwell is mainly composed of sand but the western end is still rich in particles of gravel size. This gravel is continuously fed to the beach by long-shore currents bringing material that lies at the toe of the bluffs and also new particles derived from the cliff by erosion.

An analysis of the composition of the gravel (in the range of 5 to 25 mm) with distance of travel along the beach shows that the shale fraction, which is abundant in intact till is completely absent after 1.0 to 1.5 kilometers of travel along the beach. In the same distance the proportion in percent of limestone and dolomite is reduced from 51 to 39% while the relative amount of harder rocks (chert, sandstone, igneous and metamorphic) increases. A triangular diagram Figure 4.9 shows that evolution by comparing the relative percentages of limestone plus dolomite with sandstone plus chert and igneous plus metamorphic rocks at different distances along the beach. Shale is not included in the graph since it is absent in most samples.

Therefore, even if coarse particles in the bluffs can form protective beaches, wave action will rapidly break them to finer sand and silt fractions. For all practical purposes it can be assumed that only sand can form stable beaches, shingle beaches being rare (Port Bruce is an example) and ephemeral.

4.3.5 Bottom Sediments of Lake Erie.

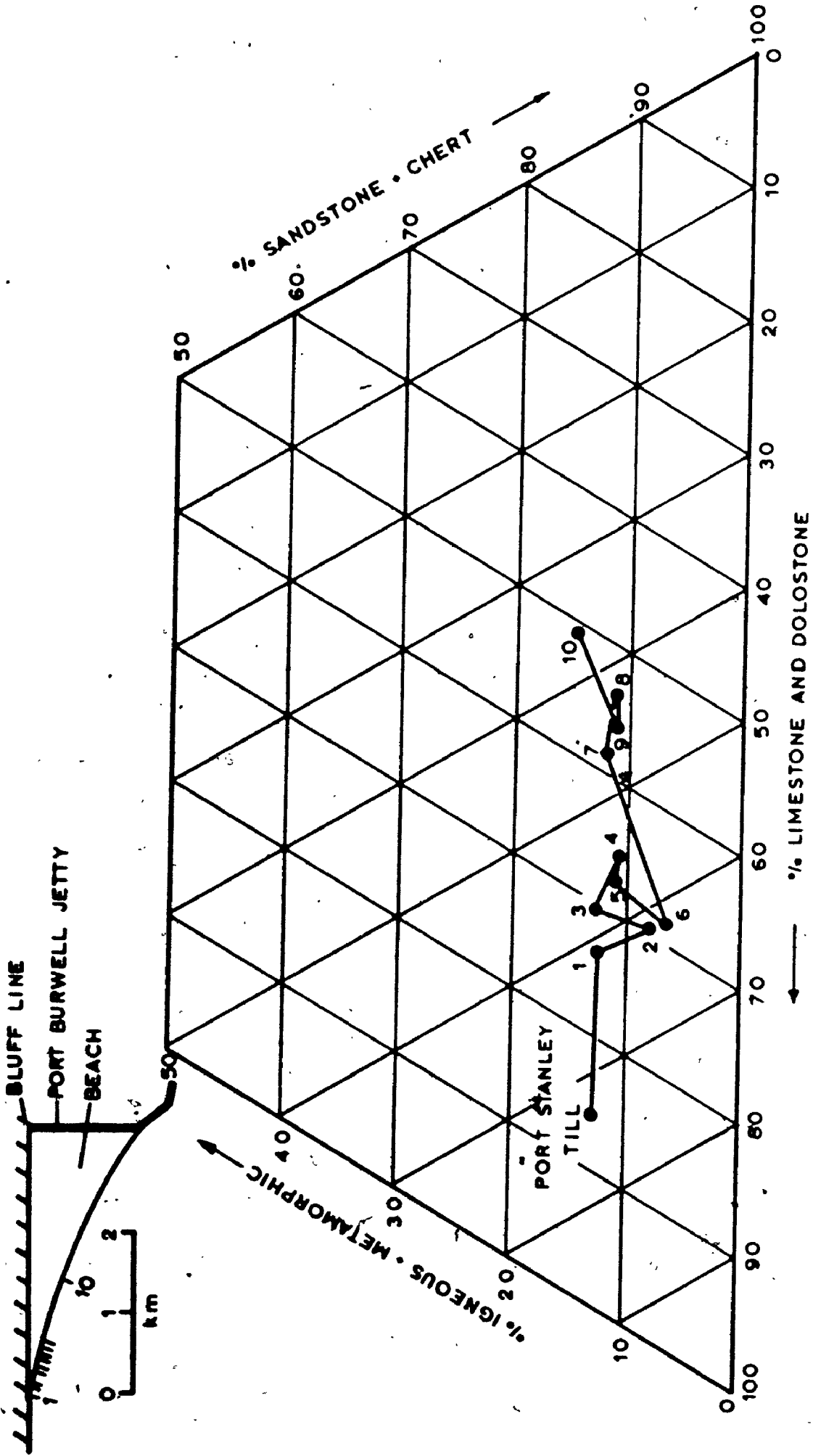


Fig. 4.9 Pebble Lithology on the Beach at Port Burwell, Ont.

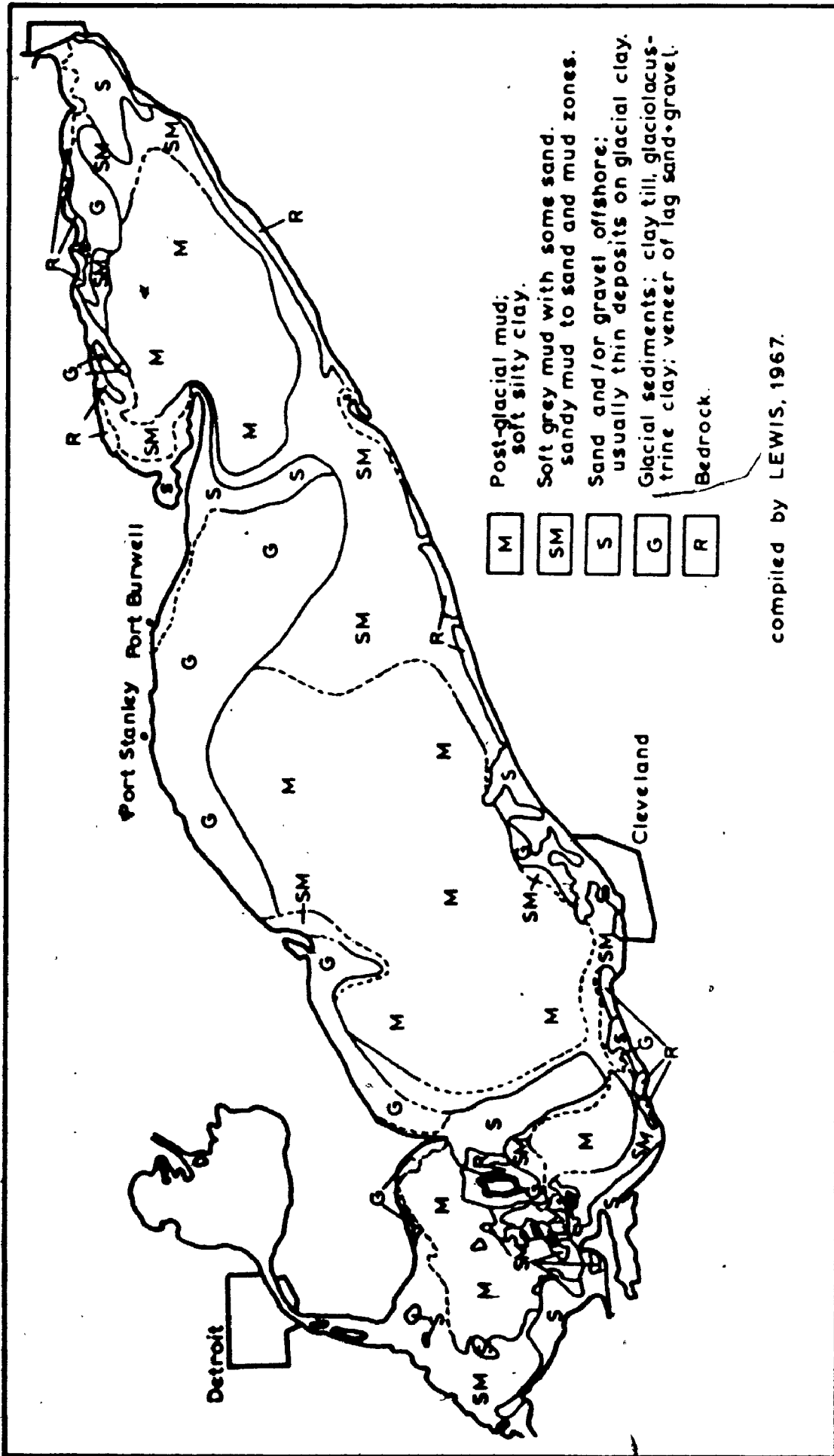
Lake Erie is divided in three distinct sedimentation basins: the eastern basin extends from Buffalo to the line joining Long Point and Erie Fa., the central basin extends to the ridge south of Point Pelée, and the western basin to the extremity of the lake.

The central basin has a maximum width of 92 km offshore of Port Talbot and a maximum depth of only 24 meters. The bedrock controlling the morphology of the lake lies at several tens of meters below lake bottom (Morgan 1964, Wall 1968).

Pleistocene deposits in the central basin are of many types: first, three ridges of till have been recognized (Long Point-Erie, Erieau-Cleveland, Pointe Pelée-Lorrain) which are the expression of end moraines produced during the retreat of the last ice lobe (Lewis 1966); stiff laminated clays of lacustrine origin coat these ridges and fill their depressions and shoulders.

Sediments of glacial origin in the central portion reach depths of 40-45 meters and are mainly fine-textured tills (14% sand, 39% silt, 47% clay) and glacio-lacustrine clays (78% finer than 4 microns, Lewis 1966). These deposits compare well with Port Stanley Drift exposed on the north shore.

Recent sediments cover the glacial materials with a thin veneer of sand and gravel near shore and with thicker deposits of silt and clay in the central portion. Figure 4.10 shows the distribution of those sediments as compiled by Lewis 1966. This distribution gives good indication of the mechanisms of erosion below lake level and the pattern



compiled by LEWIS, 1967.

Fig. 4.10 Distribution of Lake Erie Bottom Sediments.

of sediment transport.

Rippled fine sand was observed on the shoulders of the Long Point-Erie ridge at depths of 20 meters indicating that lake bottom is affected by surface waves and currents, (Hough 1958, Lewis 1966). An area of deep sand extends along the shoreline east of Port Burwell where there is abundant source material (Norfolk sand plain).

The greatest part of the study area is bordered by a zone of thin patchy sand deposits, rippled and rarely exceeding 30 cm thickness. This thin veneer is often cut by large windows showing till and lacustrine silty clay. The surface is littered with large particles of limestone, chert, shale, or granite representing a lag concentrate; this illustrates well the active erosion of glacial till in waters 5 to 10 meters deep (Hough 1958, Lewis 1966).

These observations and the study of lake bottom morphology on the north slope suggest that this is an erosion surface and that erosion is still active when storms occur at the surface or when lake levels are lowered. This is in good agreement with the conclusions of section 3.4.3 on the effects of lake level fluctuations on erosion rates.

4.4 Physical Weathering of Tills.

This section investigates the mechanisms of erosion of glacial materials. Much work has been done already by sedimentologists and engineers on the resistance of cohesive soils to erosion by flowing water; however, their work is

mainly concerned with soils fully saturated and submerged. Natural bluffs on the other hand are subjected to weathering through cycles of drying and wetting ; this process is responsible for the formation of cracks and fissures in fine-grained soils. A first section will study the shrinkage properties of tills, the next one will investigate the behavior of dried samples upon wetting and finally these results will be compared with field observations.

4.4.1 Drying and Shrinkage.

Let us assume that a saturated sample of silty clay is allowed to dry; moisture is drawn from the specimen by evaporation at a rate that depends on the relative humidity of ambient air; a gradient of vapor pressure is created at the interface between air and water at the surface. When solid particles come in contact due to compression of the sample by capillary forces, the resistance to further shrinkage will be met by an increase in the curvature of the interface air-water and air migrates in the soil until an equilibrium is reached between vapor pressure in the pores and curvature of the interface (DeJong and Warkentin, 1965, Terzaghi and Peck 1967).

In the field, this process is acting along the free surface of a bare slope and along joints created by drying. Therefore drying gives strength to a clayey soil but at the same time makes it more vulnerable to slaking and erosion because of increased permeability along fissures.

Four stages of drying are usually recognized (Tempany 1917, Haines 1923, Stirk 1954): 1) structural shrinkage involves drying or draining of a few large pores or fissures without much change in the volume of soil; 2) normal shrinkage occurs when the decrease in volume of the soil is equal to the change in water content; this is the main stage of soil compression and no drying is observed at the surface; 3) in the residual stage, air enters the sample and solid particles come in contact causing a change in sample volume smaller than the change in moisture; 4) when capillary forces become smaller than intergranular forces, shrinkage stops but the moisture content continues to decrease (Figure 4.11).

4.4.2 Drying and Shrinkage of Till.

In order to study shrinkage properties of till, two blocks were obtained from Port Bruce (Geography Station) and Port Talbot. Their properties are summarized in table 4.2; natural water content is an important variable and the blocks were taken near lake level where drying is minimal; the water content of the blocks compare with similar samples taken from boreholes.

Specimens were trimmed to a disc shape (diameter of 4.4 cm and thickness of 1.15 cm) and allowed to dry at room temperature of $22 \pm 2^\circ\text{C}$ and relative humidity of 45%. Samples were supported by a holder to allow free circulation of air on all faces, and partly confined under a glass jar to reduce the rate of drying. At regular time intervals the

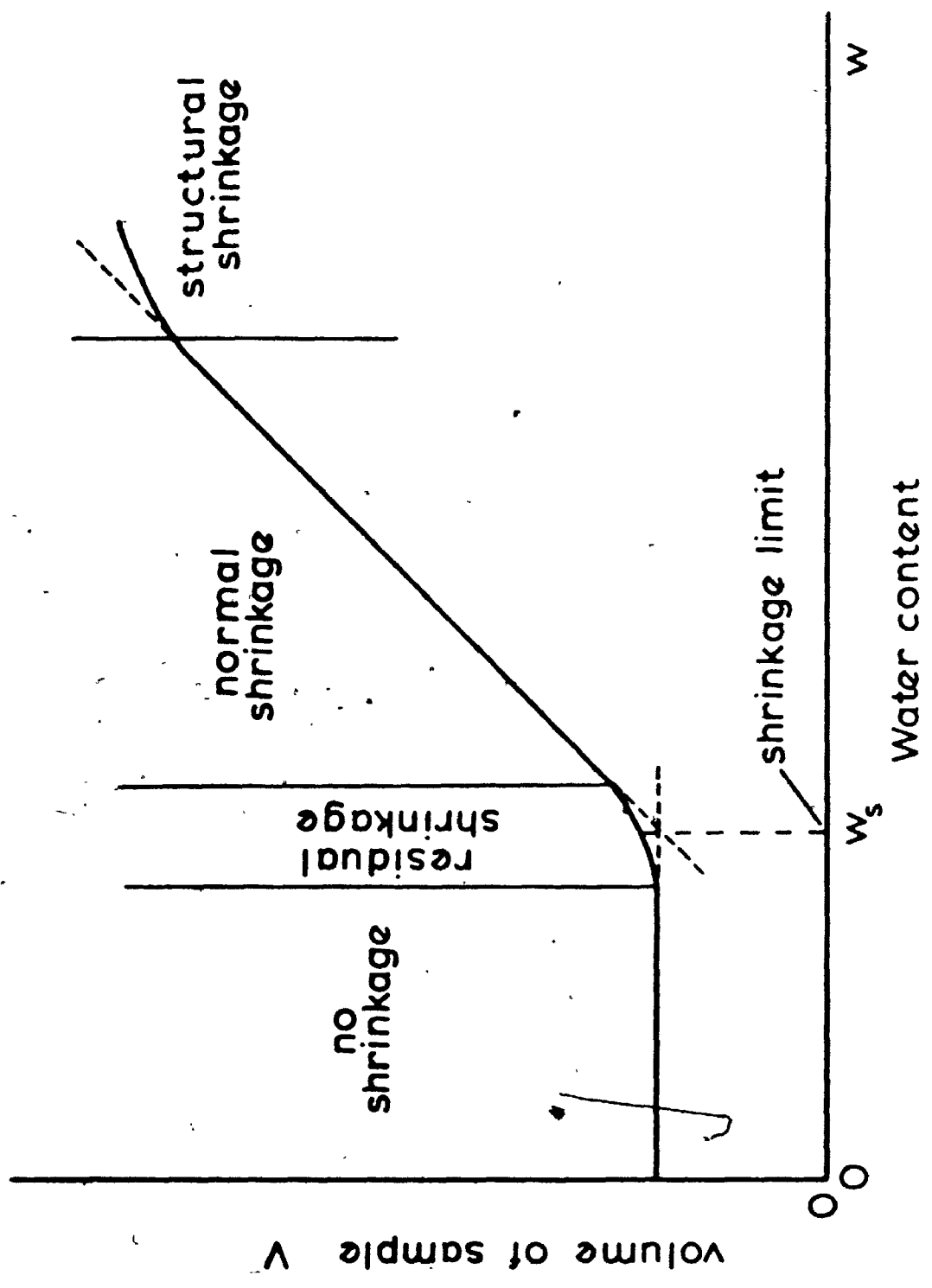


Fig. 4.11 Stages of Shrinkage Drying.

Table 4.2

Index Properties of Glacial Till

	Port Stanley Till (Geography Station)	Port Stanley Till (Port Talbot)
Sample elevation	Lake level	Lake level
Water content %	20	19
Plastic limit %	19	17
Liquid limit %	32	33
Sand %	5	7
Silt %	55	48
Clay %	40	45
Unit weight KN/m^3	21.5	21.2
Specific gravity	2.80	2.79

sample was weighed to 0,0001 grams and its dimensions along two mutually perpendicular diameters were measured with calipers to the nearest 0,025 mm. The amount of linear shrinkage is reported as a percentage of the air-dried dimensions and equivalent moisture content is calculated from the moisture content of an identical sample determined at the beginning of the test.

Figure 4.12 gives the shrinkage curves for two intact blocks of Fort Stanley till; three stages of shrinkage are easily recognized and the shrinkage limit, w_s , is defined by the water content at which normal shrinkage stops (Warkentin and Bozozuk 1962); in both cases w_s is 15.7%.

Similar tests for the determination of the shrinkage limit were done using the standard technique (Lambe 1951). There are slight discrepancies in w_s determined by the two tests and this is mainly due to the fact that the standard technique is done usually on remolded soils (specimen is prepared from dry soil mixed to a slurry with water and then dried). This second technique being more rapid it was used in most cases for the determination of shrinkage limit.

Estimates of the amount of volumetric and linear shrinkage are easily obtained if we assume that all shrinkage is normal and isotropic and that the in-situ soil is fully saturated. A range of values of linear shrinkage for till samples dried at room temperature is from 2 to 4% depending on the original water content and unit weight of the samples. These values will be compared with joint spacing and frequency in the field.

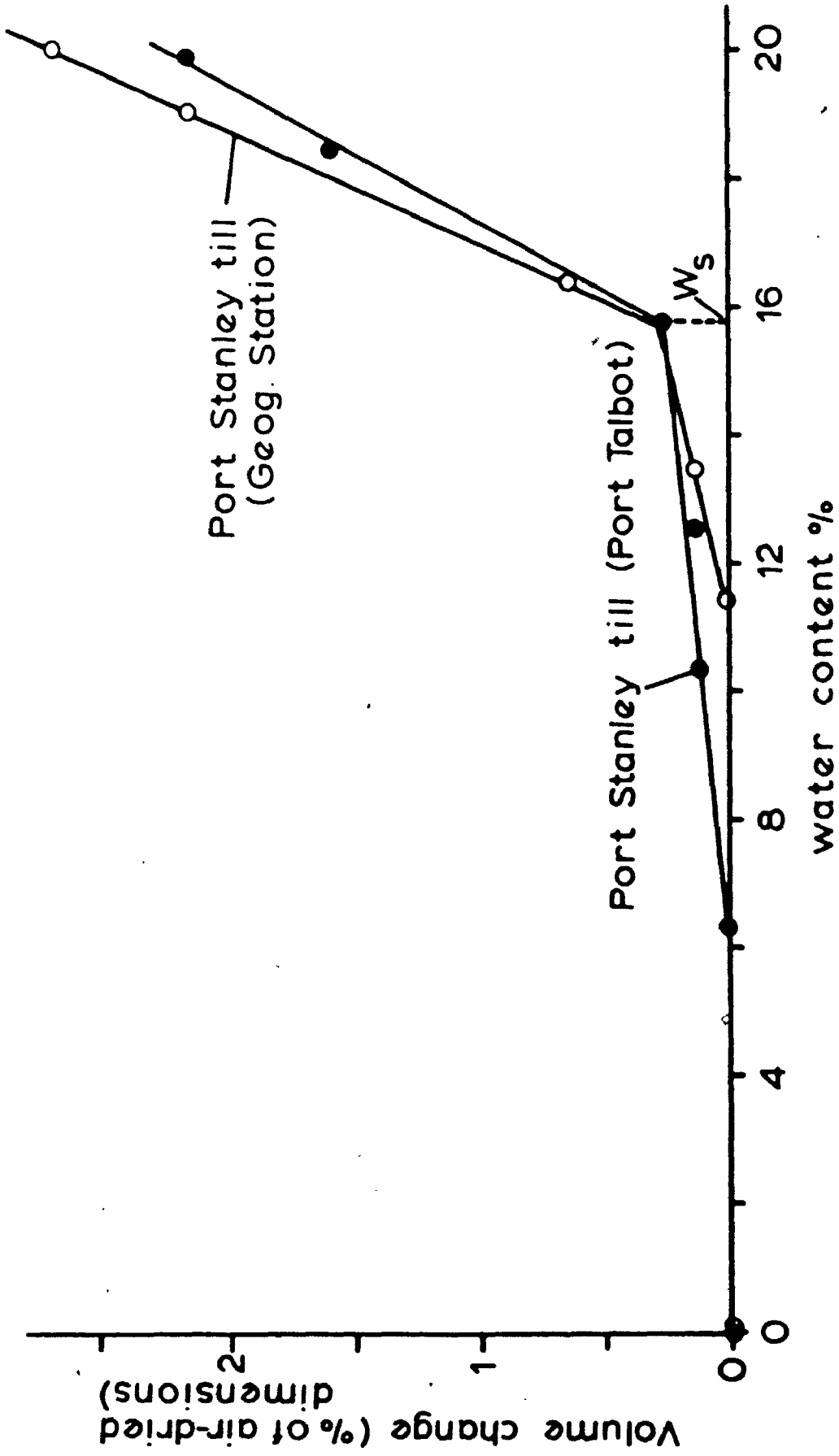


Fig. 4.12 Shrinkage Curves for Port Stanley Till.

4.4.3 Structural Changes During Shrinkage.

The formation of minute cracks and fissures was observed during the drying of laboratory specimens; this is due to uneven shrinkage of the outer parts of the sample while the center is still moist. These discontinuities are more readily observed when the rate of drying is fast since drying involves the permeability of the soil; if the rate of evaporation is out of balance with the permeability of the sample stress concentration occurs and local failure is produced by tension.

More commonly these defects are observed at the boundaries of small pebbles which do not shrink when the clay coating them does. The presence of these discontinuities plays an important role in the stability of the material when submerged in water. Next section investigates slaking of dry till samples and its importance in the process of slope degradation and erosion.

4.5 Swelling and Slaking of Clay Silt Tills.

Erosion of clay silt tills is done by water either in the form of wave action or runoff on the surface of the slopes. The action of water on air-dried samples can induce swelling and cause an increase of volume by water absorption without significant changes in the structure of the soil or it can cause slaking or desintegration of the soil structure by rapid wetting. This last process is more important for

erosion studies since it divides a coherent soil into minute particles that have a very low resistance to erosion by water.

4.5.1 Swelling and Slaking Mechanisms.

Experiments by Warkentin and Bozozuk (1962) give a procedure to study the cyclic drying and wetting of silty clays. The drying stage is done by the method described earlier (section 4.4.2) to prevent formation of cracks or fissures; the wetting stage was done by exposing the dry samples to an atmosphere of high relative humidity followed by absorption of water on a filter paper and finally by complete immersion in water. By this procedure, swelling occurs without structural breakdown of the soil structure.

On the other hand slaking occurs if the sample is wetted rapidly by immersion, preventing the trapped air in the soil from escaping. This is usually achieved by flood wetting of unsaturated samples below their shrinkage limit (Williams, Greenland, Lindstrom and Quirk 1966). During the drying process, compressive forces due to capillarity induce shear failure with resultant cracking if there are discontinuities of fabric or variable capillary potential in the material. These fissures disrupt the fabric and facilitate rapid entry of water when rewetting occurs.

Upon wetting two factors cause slaking: adsorption of water on clay minerals especially if these minerals are expansive, and the compression of air inside the sample under the force of penetration of water in the capillaries.


This last process is evidenced by the fact that most clays do not slake when wetted under vacuum (Yoder 1936).

Slaking tests on undisturbed Fort Stanley till were performed to verify the above hypotheses. When air-dried samples were slowly wetted using the technique of Warkentin and Bozozuk (1962) the moisture content went up to the natural moisture content of 20% without desintegration of the samples; samples showing hairline cracks and fissures before the test had a slightly higher water content (22-23%) after wetting.

Another series of tests was done by rapidly wetting dried samples by partial immersion in water leaving a free surface for air escape; within 10-15 minutes all samples (discs of 5cm diameter by 0.5 cm thickness) were completely desintegrated by slaking and the water content was in the range of 39-43%, which is double the natural field water content.

Finally another series of samples were completely flooded by immersion; for comparison, samples of till at natural moisture content were immersed at the same time. Within less than 5 minutes, the air-dried samples had completely crumbled but the saturated samples were still intact after many days. Air bubbles were observed along small fissures and the escape of air was usually accompanied by flaking and spalling of the samples.

In the field, cycles of drying and wetting would then lead to the destruction of the soil structure and the formation of a soil aggregate made of debris from slaking.



The sorption of water and the size reduction of these aggregates will be discussed now.

4.5.2 Sorption of water by Soil Aggregates.

Water-sorption on soil aggregates is made of two factors: adsorption at the surface of minerals and absorption in the voids between particles. Adsorption is more or less a constant for a given soil if enough water is supplied to the sample and enough time is allowed for all particles to reach an equilibrium. Absorption on the other hand is function of the size of the different particles forming the aggregate and also on the number of discontinuities present in a given volume of soil.

Sorption tests were made on dry till fractions of different sizes. A known amount of dry till of a uniform size is allowed to take water by capillarity through a filter paper resting on a porous stone. The quantity of water taken by the aggregate is determined by measurement of the water content at the end of the test (White and Fichler 1959).

The different sizes of aggregate used had diameters between -2 and $0,25 \phi$, $0,25$ to $1,25 \phi$, $1,25$ to $2,00 \phi$, $2,00$ to $3,75 \phi$, and smaller than $3,75 \phi$ units. The average water content for each test after 15 minutes of sorption is given in Figure 4.13. The increase in water content merely reflects the greater amount of pore space in the soil aggregate but it also gives clues to the behavior of material that has been through many wet-dry cycles. For instance the liquidity

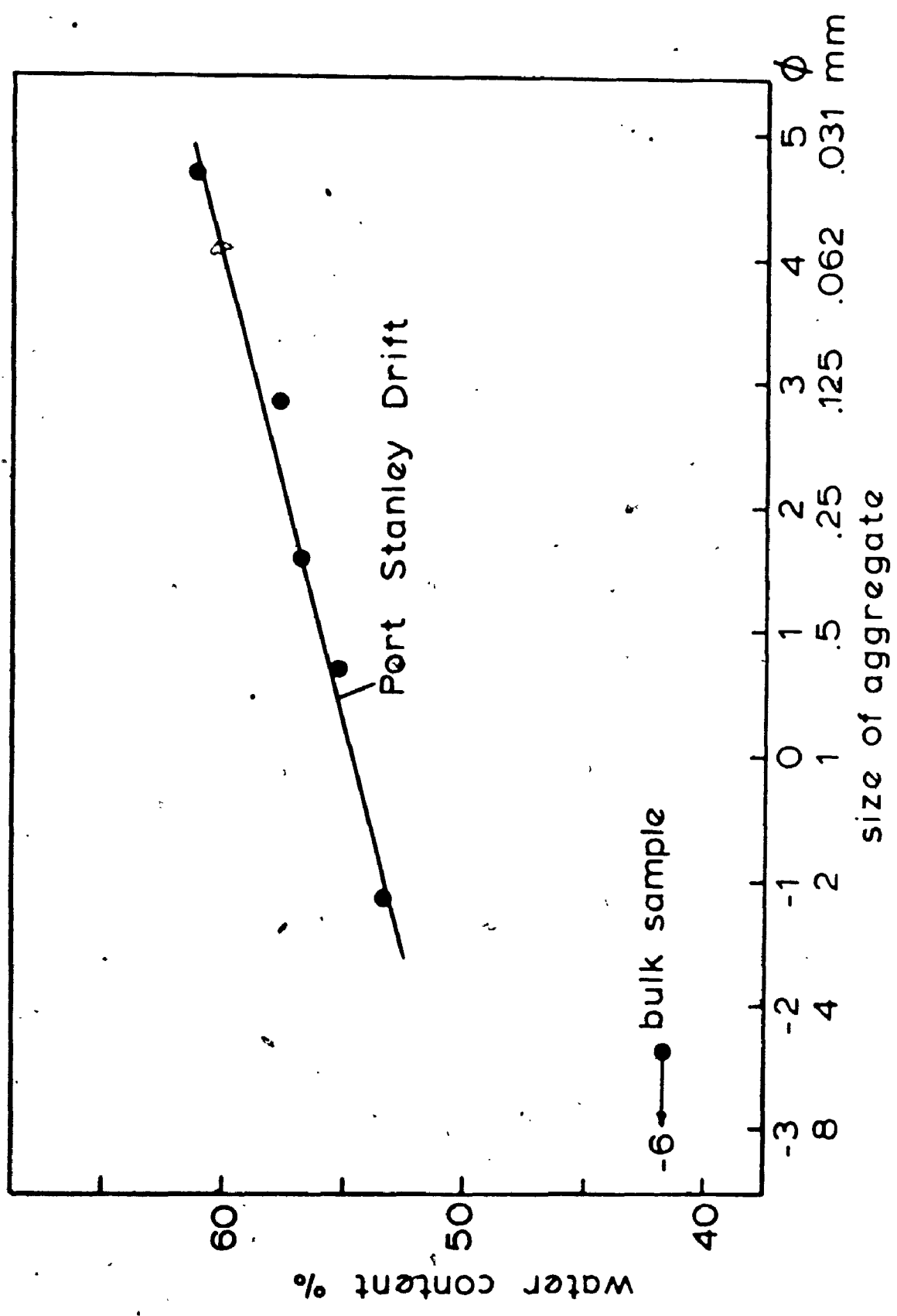


Fig. 4.13 Water Sorption on Dry Soil Aggregate.

index of weathered material that is completely soaked (by rain or wave splash) will be in the order^{of} of 2,0 or 3,0 (FL is 18% and FI is 15%) and consequently its shear strength will reach very low values; such material is involved in mudslides on slopes as flat as 15° (Chapter 5).

It remains to be known if till will breakdown in smaller aggregates that show such drastic increase in water content. The next section looks at the effects of repeated cycles of drying and wetting on the soil stability.

4.5.3 Size Reduction Due to Dry-wet Cycles.

Slaking of undisturbed dry till samples results in the breakdown of the original soil into smaller aggregates of different sizes. A measure of the amount of slaking is given by wet-sieving analysis (Yoder 1936). A till sample is slaked by immersion and then sieved under water on a nest of sieves by gently raising and lowering the sieves by 2.5 cm thirty times; the amount of material retained on each sieve is dried and weighed. The part that is retained is referred to as the water-stable aggregates using the terminology of soil scientists (Yoder 1936, Bryan 1969).

The size of water-stable aggregates is a parameter much in use in soil science to measure the stability of the soil structure and its erodibility (Bryan 1969). Erodiability for instance has been correlated with the percentage of aggregate greater than 0,5 mm. In this study five cycles of drying and wetting were done and Figure 4.14 shows the

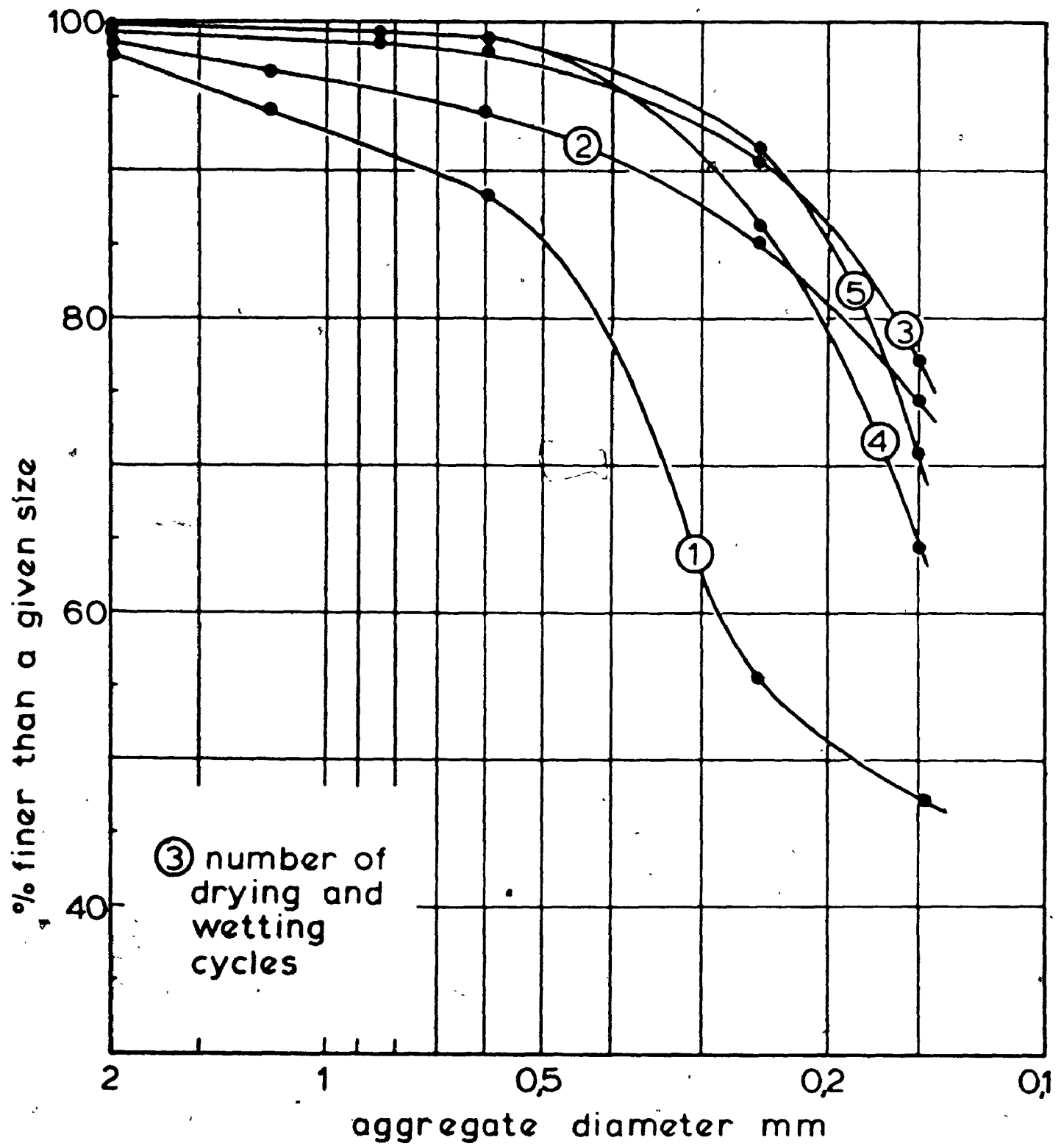


Fig. 4.14 Aggregate Size Reduction upon Drying and Wetting Cycles.

distribution of water-stable aggregate (WSA). Corresponding to the different cycles it gives a percentage of WSA greater than 0,5 mm of 1) 14,6, 2) 7,3, 3) 2,8, 4) 2,0, 5) 1,7%. Therefore there is a general decrease in stability or increase in erodibility with an increasing number of wet-dry cycles. Most of the damage to soil structure is done when fresh till is first exposed to drying.

Slaking then decreases the cohesion of a soil by creating numerous failure surfaces along which water enters the soil. Since the amount of water that is absorbed by the soil is function of the grain size of the aggregate (previous section) the mechanical properties of weathered material would be altered irreversibly.

An index of change in soil properties can be found by measuring the plastic and liquid limit after each cycle (Cornell 1951). A slight decrease in the liquid limit was observed (from 33,2 to 31,2%) but no definite change occurred in the plastic limit (Figure 4.15). No major change in the mineralogy seems to occur as a result of air-drying, only the soil fabric is affected.

4.5.4 Erosion Tests.

The resistance of soils to erosion by water is function of many factors (Soderblom 1963, Dos Santos and Castro 1965, Grissinger 1966, Yamamoto and Anderson 1967, Bryan 1968). Grain size and moisture content at the time of erosion seems to be the most important. Following the classical

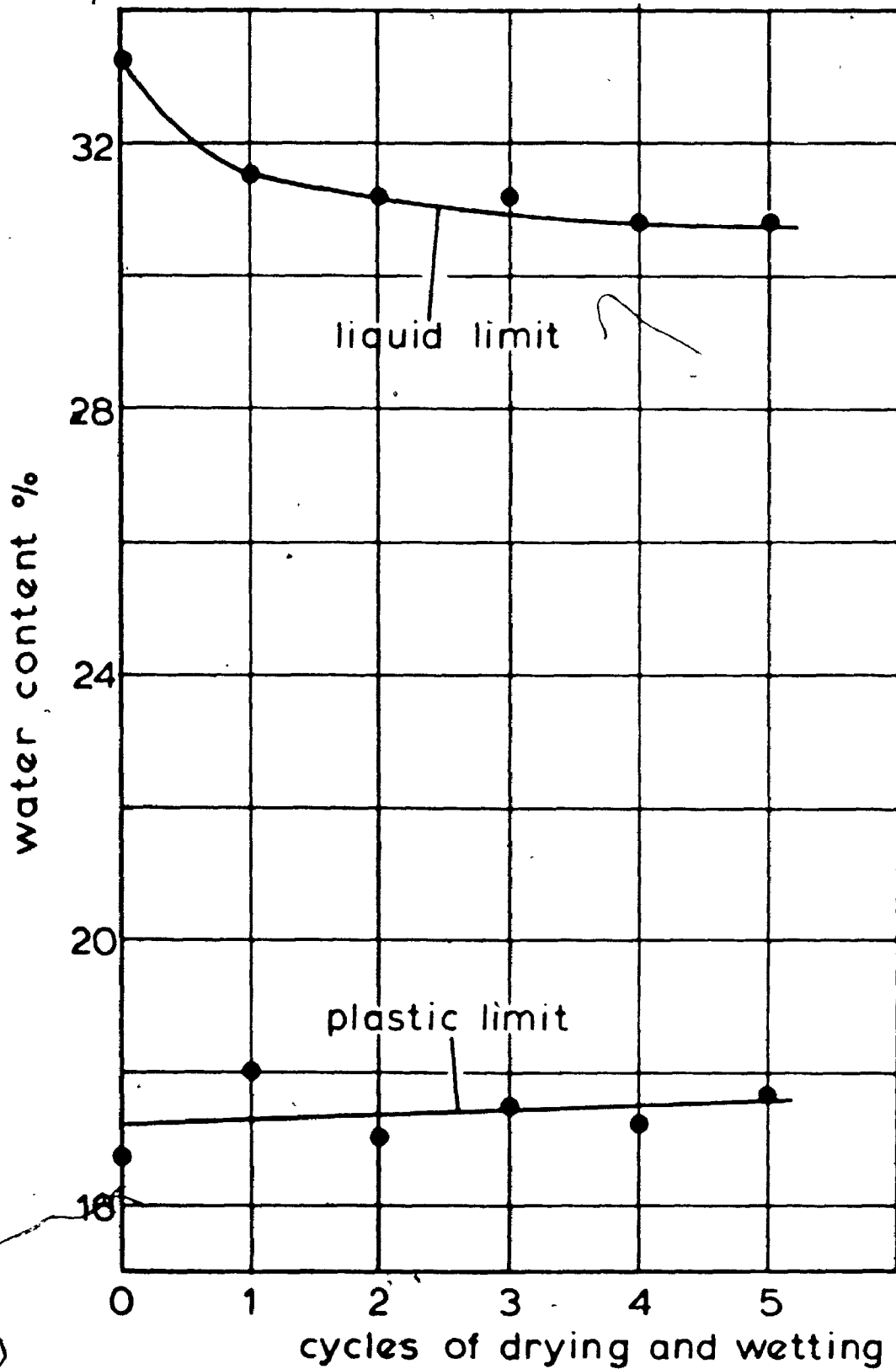


Fig. 4.15 Changes in Atterberg Limits with Dry-Wet Cycles.

studies of Hjulström (1935) fine sand and silt offers the smallest resistance to erosion by flowing water, while saturated intact clay and large particles in the gravel size offers the greatest resistance to erosion. Cohesive soils are resistant but their water content at the time of testing is also critical (Grissinger 1966).

A simple test to measure resistance to erosion by impact is described by Soderblom (1963). Sample at a known moisture content is subjected to erosion by dropping water from a burette 15 cm above the surface of the sample; 100 ml of water was released drop by drop on the till and the debris carried by the water were gathered in a glass container; at the end of the test the weight of eroded soil was calculated and expressed in grams per 100 grams of dry soil. The range of moisture content used goes from 20% (natural water content) down to about 10%.

The results are shown in Table 4.3 and Figure 4.16. The till samples have their greatest resistance to erosion when near their shrinkage limit as the soil is still saturated and the particles in close contact (water content of 14-16%). At lower water contents air enters the sample and minute cracks may develop inside the sample; a very large increase in erosion is observed because of slaking of the soil. Therefore the fact that clay resists well to erosion seems valid only when it is completely saturated. At water content higher than 20% one could expect increased erosion as was found by Grissinger (1966) for molded samples; only natural undisturbed samples were tested in this study.

Table 4.3

Influence of water Content on
the Amount of Soil Eroded

Water Content %	Eroded Soil (g/100g of dry clay)
19,5	0,16
16,7	0,18
16,6	0,02
14,8	0,03
14,6	0,04
14,0	0,01
12,7	1,39
12,2	11,52
11,7	21,68
11,0	19,60
9,4	34,96

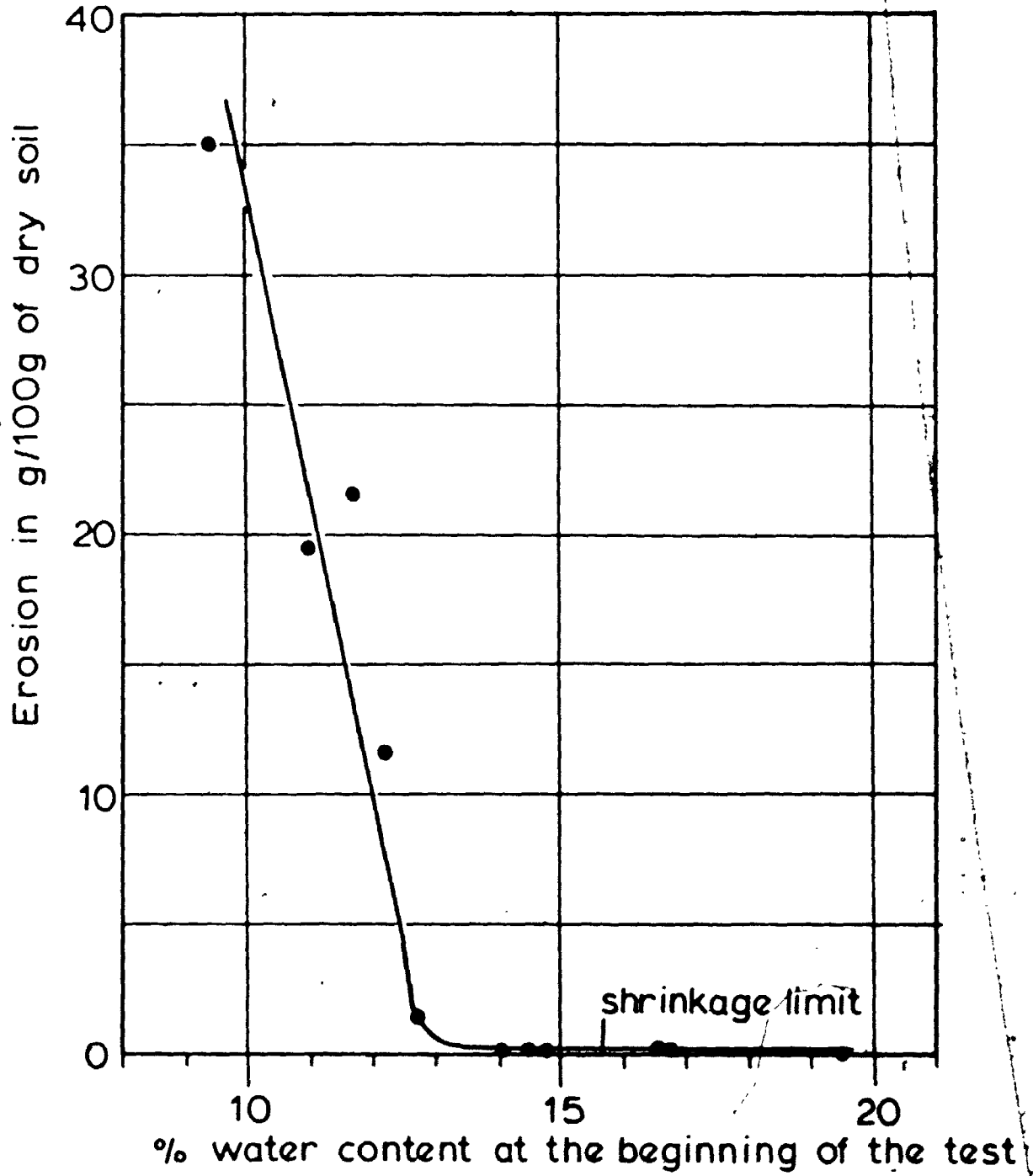


Fig. 4.16 Erosion Tests on Port Stanley Till.

In the laboratory it was found that till samples are destroyed by cycles of drying and wetting due to slaking by water entry in the soil. Physically weathered soils form fine aggregates that have different mechanical properties and that are very susceptible to erosion. In the next section, field evidence will be given to show that this mechanism is valid and that it can account for the rapid erosion rates observed along the north shore of Lake Erie.

4.6 Field Weathering.

Drying and wetting cycles are frequent along the shore of Lake Erie and the fact that the bluffs are not covered with vegetation in most areas suggests that slaking may be effective in breaking down the soil structure and causing rapid erosion of the silt and clay tills.

July temperatures in the study area have a mean of 21°C and an average maximum of 27°C (Phillips and McCulloch 1972). Temperature at the soil surface is in fact higher; experiments on bare soils (Baver, Gardner, and Gardner 1972) show that the soil temperature at the surface may be higher than air temperature by 10°C. This is far in excess of the laboratory temperature of 22°C at which the shrinkage tests were run. Because of the good exposure of the north shore bluffs to sun rays, it is expected that soils would dry and shrink to a sizable depth. At Port Burwell, on a slope of 23°, the surficial layer was dry to a depth of 1 to 2 meters during summer. Where the bluffs are nearly vertical near the toe of

slopes, evidence of drying and shrinkage exists to a distance of about one meter.

4.6.1 Joints and Fissures.

The consequence of drying and shrinking is the formation of discontinuities in the soil mass; two types of discontinuities were observed: systematic joints related to desiccation and non-systematic joints in the form of fissures cracks or fractures.

Systematic joints are best observed near lake level in areas where undercutting by waves left a nearly vertical cliff. The spacing between joints is commonly in the order of 15 cm to 1 meter and the opening or aperture of the joints varies from less than 0,5 to 5 cm. These joints strike perpendicular to the shoreline and are vertical or subvertical. For this reason it is concluded that they are caused by desiccation and are not related to internal structures in the till. In good exposures, the same joint can be traced vertically to a height of 20-25 meters; commonly the upper slope has weathered away and is covered with debris. The depth of the joints in the bluffs cannot be ascertained beyond one meter or so where the water content reach the same value as the intact material taken from boreholes further back in the slope; at natural moisture content, around 20%, the material is above its shrinkage limit and therefore no shrinkage joints occur.

The ratio of joint opening to joint spacing varies

from 3.3% to 5.0%, which is in good agreement with the predictions from shrinkage tests where the linear shrinkage was estimated at 2 to 4%. Widening of some joints by wave action may be responsible for higher ratios.

Non-systematic joints in the form of cracks and fissures have no preferential orientation; small fissures are often observed around pebbles and are caused by differential shrinkage. Large scale joints showing conchoidal fracture and plumose structure are observed at the boundaries of large till blocks that have fallen; they are related to tensile failure when soil falls occurred caused by wave undercutting. Several other fissures are observed in the till when pockets of different material (sand stringers, incorporated blocks of lacustrine material) are present; differential shrinkage seems to be the cause for these discontinuities.

The significance of joints and fissures is evident in explaining the mechanisms of erosion or the stability of slopes. The presence of dry fissured soil at lake level allows the entry of water under dynamic and hydrostatic pressure every time waves beat the toe of the cliff; this process will result in the formation of a notch or reentrant wall which diminishes considerably the stability of the soil mass above it. The presence of long vertical desiccation joints favors the circulation of groundwater from overlying sandy layers especially in areas where the thickness of the sand is important. Between Port Stanley and Port Bruce, and east of Port Burwell surficial sand reach several meters and supply an abundant quantity of water year round. Such a

geological setting is important in explaining high rates of erosion in those localities.

4.6.2 wetting and slaking.

The presence of loose soil debris on gentle slopes gives evidence to the active degradation processes occurring along the bluffs. Slaking of dried material is produced whenever the supply of water is large enough to completely saturate the surficial soil layers. This water is coming from many sources: on gentle slopes in the upper part of the bluffs rainfall and groundwater seepage are the main contributors; in the lower part of the bluffs where the slope angle is almost vertical, wave splashing will control wetting and slaking.

The condition for slaking as described in section 4.5 is that dry soil be allowed to become rapidly saturated under an excess of water. In the case of rainfall, these conditions will be met when the intensity of rainfall is equal or exceeds the rate of infiltration of water in the soil. At the beginning of rainfall, the rate of infiltration is very high due to the suction head existing in the dry material; however when the surface layer becomes saturated over a few centimeters, the gradient at the surface becomes so low that infiltration rate reaches a value approaching a constant which is proportional to the saturated hydraulic conductivity of the soil (Childs 1969). This reduction in the rate of infiltration is accelerated by the

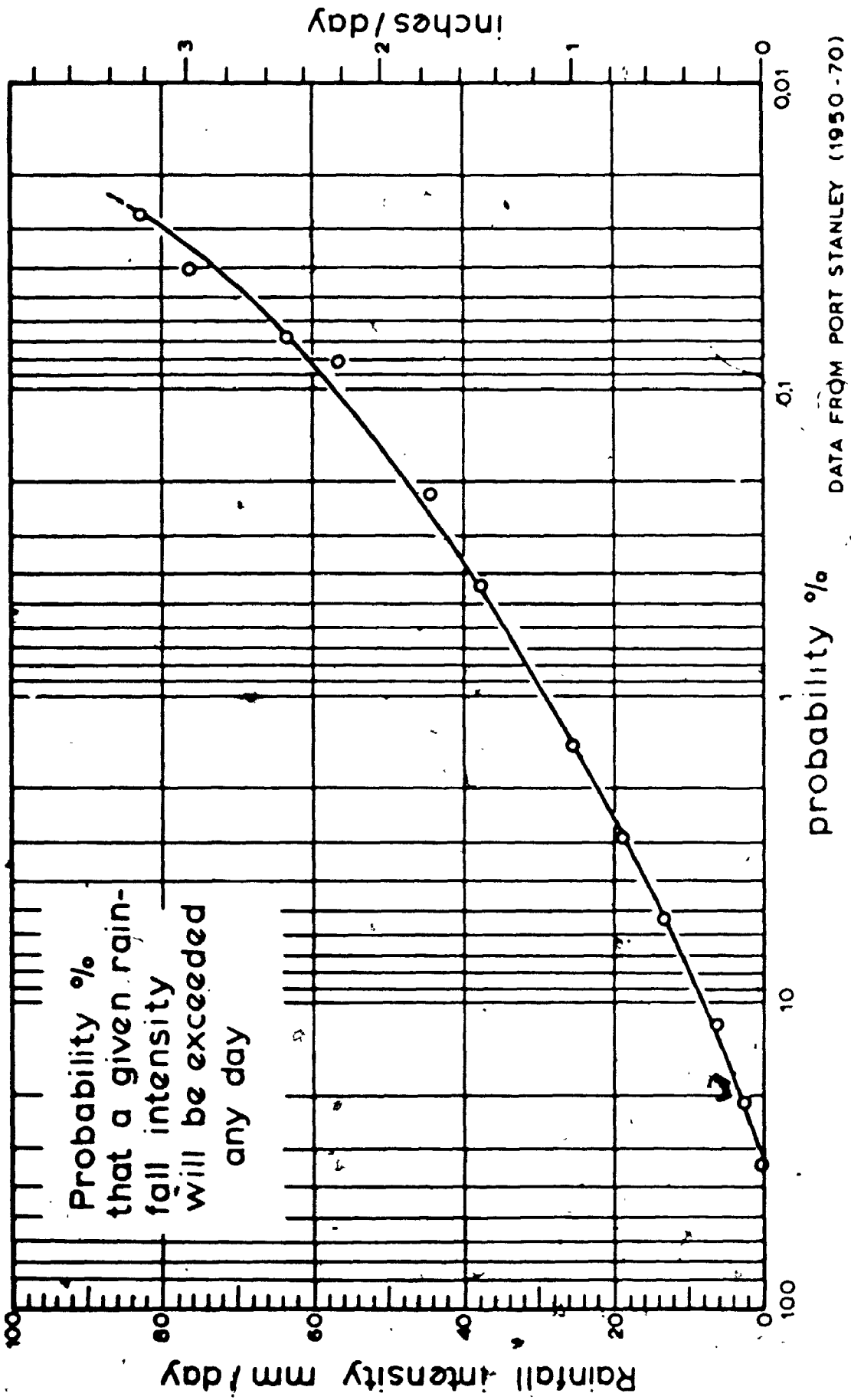


Fig. 4.17 Probability of Rainfall Intensity at Port Stanley, Ont.

swelling of clays upon hydration. Assuming that precipitation of 10mm of rain is sufficient to saturate the surface of dry soil over 2 or 3cm, the excess rain will be retained near the surface and active slaking will be initiated. A look at the precipitation records for the study area permits one to evaluate the frequency of occurrence of such conditions. The precipitation data for the years 1951-1970 at St. Thomas and Port Stanley was analysed to find the probability distribution of rainfall intensity. Figure 4.17 shows the probability, P , in percent, that a given rainfall intensity, R , will be equalled or exceeded on any day of the year. Precipitation exceeding 10mm/day is expected to occur 7.5% of the time, or approximately one day per month.

Extreme conditions of precipitation are also important for erosion studies. For instance, rainfall of 144 mm in 6 hours west of Toronto on August 16, 1969, and of 29 mm in 5 minutes at St. Thomas on September 1, 1954 illustrate the extreme conditions that can occur in the study area (Philips and McCulloch 1972). Data on rainfall intensity-duration-frequency is presented in Table 4.4 and Figure 4.18, representing conditions over the Great Lakes basin (Bruce 1968). The return period in years for a rainfall of a given intensity and duration can be estimated from those curves. Here again, conditions for slaking occur fairly often over short periods of time and may help to explain the rate of slope degradation that is observed.

Slaking induced by groundwater seepage is much less important because of the low rate of water table fluctuation.

a cliff at inclinations of 70° to 90° with some cases of overhanging. This near vertical face may develop over a height of several meters to more than 10 meters; the surface of the cliff is extensively jointed by desiccation and remains dry most of the time. After a storm, the height of wetting can be evaluated by looking at the effects: till washed away sand injected in the joints, wet surface, etc. The slope angle near the toe in areas where sand composes the totality of the bluffs height is more gentle (27° at Sand Hill); if the toe is protected by a wide beach, the slope angle approaches the residual angle of internal friction for the soils composing the slope (23° at Fort Burwell) and the soil at the toe is essentially made of debris of slides and falls resting on a blanket of beach sand and gravel. In localities where sand and silt outcrop at lake level (east and west of Fort Stanley), huge blocks of till from landslides normally conceal the toe of the bluffs.

The upper slope offers more variety in shape and profile. Soil type, seepage and slippage are the factors that determine its form and also vegetation to a certain degree. The edge of the bluff is generally abrupt and subvertical for a few meters due to the effect of the root mat giving additional cohesion to the soils. Treed areas in sand and silt cause a good size cliff whereas areas in clay covered with shrubs and weeds do not influence the geometry of the bluff much. There is a large occurrence of small slips on the brow of the cliff; they encroach usually a meter or so and form slices several meters long. Most are

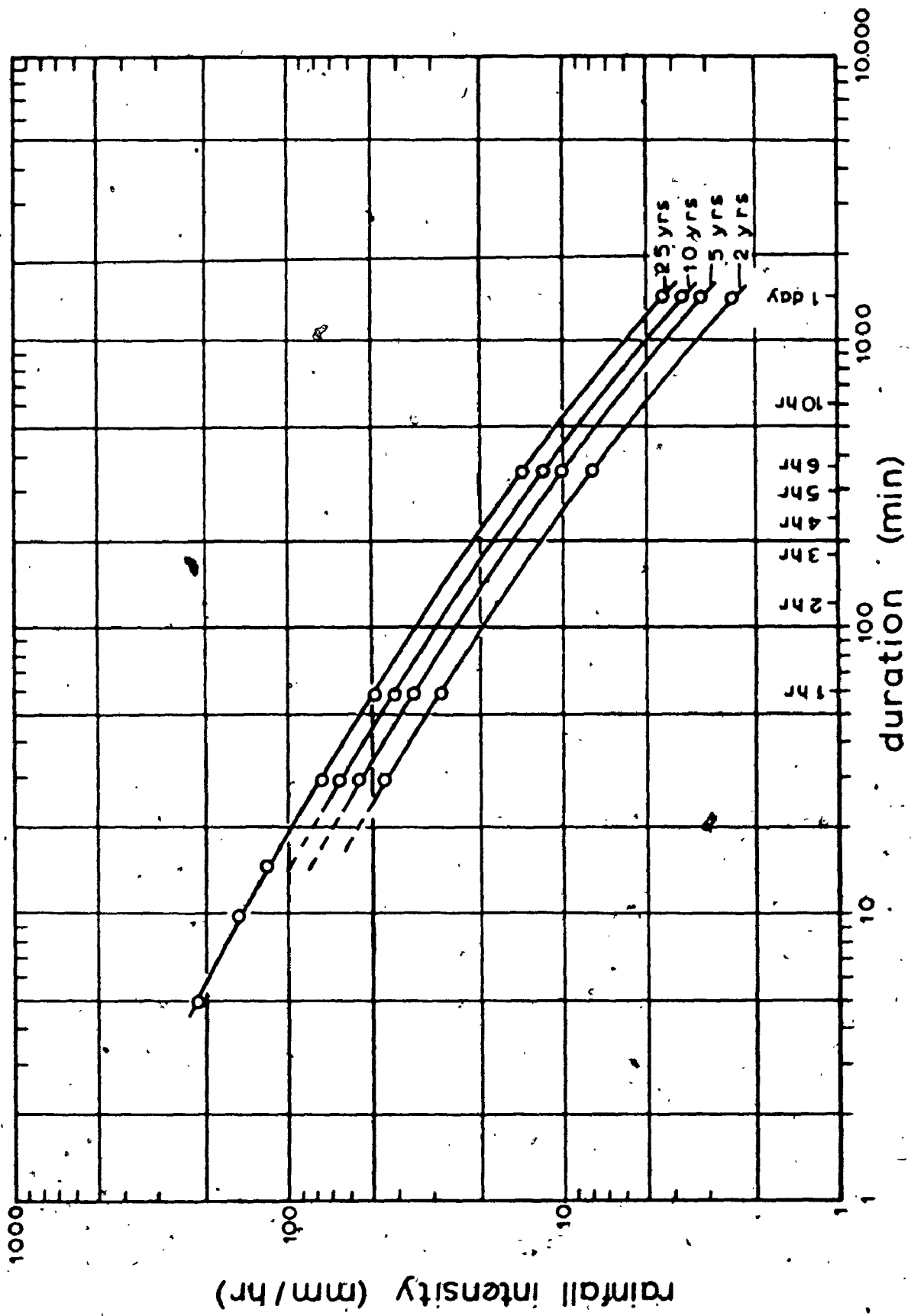


Fig. 4.18 Rainfall Intensity-Duration-Frequency, Great Lakes. 67

tuation. When the water table is rising the movement is slow enough to allow the escape of entrapped air in the unsaturated zone; in this way the clay till will swell to its original water content without slaking (section 4.5). If numerous fissures exist near the water table, softening occurs and water content is observed to go up to 35-45% in the zone of annual groundwater table fluctuations. Slaking may occur with more intensity at the springline or contact between water bearing sands and clay silt till, east of Port Stanley for instance.

Erosion near the toe is more complex. Slaking will be an important factor every time the dry surface is wetted but also by abrasion by coarse particles in water and the effect of shock by waves forcing a rapid retreat of the vertical cliff. The frequency of wetting periods may be estimated by studying a histogram of wave heights (Figure 3.18) and their seasonal distribution (Figure 3.19). The height of bluffs that will be affected is about twice the wave height at breaking, if the cliff is situated on the shoreline (Muir Wood 1969). As seen previously (section 3.4.3) lake level is critical in deciding if wave erosion will affect or not the toe of the bluffs. While degradation by weathering occurs all the time, toe erosion is intermittent and follows cycles of high and low stages in lake level (Seibel 1973). This observation will be of great importance in studying slope stability in relation with toe erosion (next chapter).

CHAPTER 5

MASS MOVEMENTS AND STABILITY ANALYSIS

This chapter describes in more detail the topography, slope morphology and types of mass movements that result from wave erosion and degradation by weathering. Laboratory and field work on the hydraulic and mechanical properties of the materials will be discussed in order to present a physical basis for slope stability analysis.

5.1 Description of Lake Erie North Shore.

The description of the bluffs forming the greater part of the study area was done by the study of air photographs taken in 1963-1964 and several field trips between 1970 and 1972. This section gives the general topography of the area, the typical slope morphology and discusses the types of mass movements occurring in the area with some indications on the relative importance of geology, rates of erosion and materials properties on the stability of the various profiles.

5.1.1 General Topography.

A look at the central north shore of Lake Erie shows the shoreline as a broad arc of circle running smoothly

from Rondeau spit in the west to Long Point in the east. Two small irregularities occur at Patrick Point and Plum Point where coarse tills (Catfish Creek and older formations) outcrop in those locations.

Three main streams enter the lake along the study area: Kettle creek at Port Stanley, Catfish Creek at Port Bruce, and Big Otter Creek at Port Burwell. They occupy valleys in glacial sediments and because of their low gradients, they are usually sluggish and bring little coarse material into the lake to modify the pattern of erosion.

The height of the bluffs is more or less uniform in that area. At the western extremity, near Rondeau, the bluffs increase rapidly from 10 meters to 20 meters near the township line between Howard and Orford. A slow rise to 27 meters occurs in the next section as far as the line between Aldborough and Dunwich. With minor fluctuations the bluffs rise to 36m immediately west of Port Stanley. Between Port Stanley and Port Bruce, the height reaches 40 meters near the pumping station and decrease slightly towards Port Bruce. East of that village, a continuous decline in height brings the bluffs at 23 meters near Port Burwell. East of Port Burwell the bluffs rise again to about 30 meters and decrease to 10 meter east of Clear Creek; in this last section, local high points occur at Houghton (42 meters) and Sand Hill (52 meters) due to the formation of sand dunes on the top of the bluffs.

The mean height over the study area is 26 meters. Comparison was attempted between average erosion rates over

four-kilometer intervals and average height of the slopes over the same distance; the correlation coefficient, R, was calculated as 0,65 at the 1% level. This correlation is less good than the one found between erosion rates and wave energy and may be fortuitous since the higher elevations also correspond to areas where sand accumulation at the surface is thicker. The method does not allow differentiation between the influence of the geology and the influence of gravity (height) and slope instability.

5.1.2 Morphology of the Slopes.

The geometry of the bluffs is conditioned essentially by geology and rates of erosion. Among important factors contributing to shape the slopes are the type of material, the type of slope failure, groundwater action and wave action. In this discussion the bluffs are divided in three portions: the toe, reaching up to about one third of the total height, the upper slope, extending down to less than 10 meters, and the median slope.

The toe, being affected mostly by wave action and lake level, will show a very different morphology in periods of low water and high water. When levels are low (1960-65) the toe is flat with an average angle of 40° (DFW 1969). This slope results from accumulation of debris at lake level and general flattening due to degradation by weathering and shallow sliding. During periods of high lake levels as in 1950-54 and from 1969-73, the toe area is truncated and forms

a cliff at inclinations of 70° to 90° with some cases of overhanging. This near vertical face may develop over a height of several meters to more than 10 meters; the surface of the cliff is extensively jointed by dessication and remains dry most of the time. After a storm, the height of wetting can be evaluated by looking at the effects: till washed away sand injected in the joints, wet surface, etc. The slope angle near the toe in areas where sand composes the totality of the bluffs height is more gentle (27° at Sand Hill); if the toe is protected by a wide beach, the slope angle approaches the residual angle of internal friction for the soils composing the slope (23° at Fort Burwell) and the soil at the toe is essentially made of debris of slides and falls resting on a blanket of beach sand and gravel. In localities where sand and silt outcrop at lake level (east and west of Fort Stanley), huge blocks of till from landslides normally conceal the toe of the bluffs.

The upper slope offers more variety in shape and profile. Soil type, seepage and slippage are the factors that determine its form and also vegetation to a certain degree. The edge of the bluff is generally abrupt and subvertical for a few meters due to the effect of the root mat giving additional cohesion to the soils. Treed areas in sand and silt cause a good size cliff whereas areas in clay covered with shrubs and weeds do not influence the geometry of the bluff much. There is a large occurrence of small slips on the brow of the cliff; they encroach usually a meter or so and form slices several meters long. Most are

associated with groundwater seepage and piping when a pervious horizon covers a more impervious layer. These shallow slips do not develop deeper than the base of the seepage face.

Several gullies cut through the surficial materials and many are caused by human interference: drainage ditches and tiles, septic tanks; Barnum Gully, 3 km west of Fort Bruce owes its origin to farm drainage (Wood 1951).

The median slope is more gentle ($15-35^\circ$) and is covered with debris coming from the upper slope and by material loosened by physical weathering and shallow slides. The surface is normally convex and wrinkled by vertical cracks parallel to the shoreline; the presence of these open fissures is due to intermittent movement of the surficial soil layer logged with water coming from seepage and rainfall.

A typical slope can be subdivided in three sections affected by slips (upper slope), slides and weathering (median slope) and wave action (toe). The type of mass movement characteristic of each section of the bluffs will be described next.

5.1.3 Mass Movements.

Mass movements occur along the bluffs as a means of restoring equilibrium after severe wave erosion has occurred at the toe of the slope. A complex nomenclature exists in the literature for the classification of mass movements (Sharpe 1938, Hutchinson 1968, Skempton and Hutchinson 1969,

Muir Wood 1972). Generally coastal landslides can be classified in three main types: falls of blocks subjected to rapid basal erosion, rotational slides occurring by back tilting of a mass of soil along a curved failure surface, and translational slides where movement of the material is along a planar failure plane with intense remolding of the soil involved (mudslides, mudflows, infinite slope failure, spreading failure in sand).

Falls are common occurrence in tills near the toe in periods of high water levels. Due to wave undercutting and formation of long dessication joints, prisms of soil weighing more than 500 tons are dissected in the bluff face. Stress concentration at the base of the prism and softening due to wave action provoke tensile stresses that lead to failure. Conchoidal fracture and plumose structure are often observed on the sides of failed blocks showing the mode of failure (Sharpe 1938, Hutchinson 1971). Failure surfaces at the toe cannot be observed because of the accumulation of debris. The action of groundwater and infiltration from heavy rainfall is also critical in the stability of these vertical slopes. This type of failure is by far the most common in the study area and the removal of this material at the toe lead to stress increase at this point and eventually may lead to a larger landslide. Soil falls are usually observed in fresh excavations (Bazett, Adams and Katyas 1961) a situation which is similar to a cliff being rapidly eroded.

Translational slides are characterized by a well-

defined sliding plane and by intense remolding of the material involved in the slide. In the study area the most common varieties are spreading failure in sand and mudslides.

Spreading failures occur in deep sand layers capping the bluffs east of Fort Burwell, and also to a lesser degree east of Fort Stanley. They are caused by excessive seepage at the contact between the sand and the till or lacustrine clayey silt below it. They are observed only where the sand is deeper than about 10 meters and where groundwater flow is important. The dimensions of six such slides are summarized in Table 5.1. The back slopes are steep and the sand is wet making the equilibrium very precarious. The cone of debris formed by such slides is ephemeral; on two air photographs taken in 1963 and 1964 one such cone completely disappeared washed by waves when the levels were the lowest in the last 20 years. The spreading failure stops when the perimeter of the slide area is long enough to provide dissipation of pore water pressure along the seepage surface. Underlying ledges of till or clayey silt do not seem to be affected by failure in the sand except through groundwater infiltration in fissures.

Mudslides are characterized by a more or less well-defined sliding plane rather than a failure plane. The slides are always superficial not reaching deeper than a few meters and involving essentially debris due to the weathering of in-situ soils or to shallow rotational slides on the brow of the bluff. The movement is intermittent and is function of the water content of the material; at high

Table 5.1

Dimensions of Spreading Slides
in Sand

Length L (m)	Encroachment E (m)	L/E	Location* (km)
150	32	4.7	11.0
72	40	1.8	11.2
48	24	2.0	11.0
73	64	1.2	12.5
96	121	0.8	12.8
72	24	3.0	13.0
85 ave.	51 ave.	2.3 ave	

L: length of the slide along the edge of the bluff (meters)

E: encroachment inland (meters)

The thickness of the sand layer is about 10 meters.

* The location is measured in kilometers from the east boundary of Houghton Township.

water contents (40-60%) they are more fluid and reach velocities exceeding 10 meters per day and are more truly mudflows (Muir Wood 1972). These slides occur mainly on flatter slopes where groundwater seepage and rainfall can accumulate (Hutchinson 1970).

Several varieties of mudslides are recognized in the study area: slides involving debris mainly, slides of weathered in-situ material, and mudflows. Along slopes made of two or more distinct soil units with contrasting properties tabular slides occur incorporating debris from the upper slope; most of these slides are observed in the middle part of the slope at low gradients. Best examples are seen in areas where an aquifer is present on the top of the section; seepage at the contact between sand and till or lacustrine silt and clay is important in controlling the amount and rate of movement of the slide. Typical examples exist at the Geography Station, west of Port Bruce, and south of Morpeth at the western end of the study area (Figure 5.1). The average angle in the median part of the bluffs is only 15-20° and during periods of heavy rainfall movement occurs (40 cm in the first week of November 1971) and mud puddles are present in several spots. The depth of debris does not exceed two meters at that location (less than one meter at Morpeth).

An other type of mudslide occurs when in-situ material has been weathered by dessication, water infiltration and also frost action. This occurs on slopes that are already flattened and where toe erosion is prevented. This

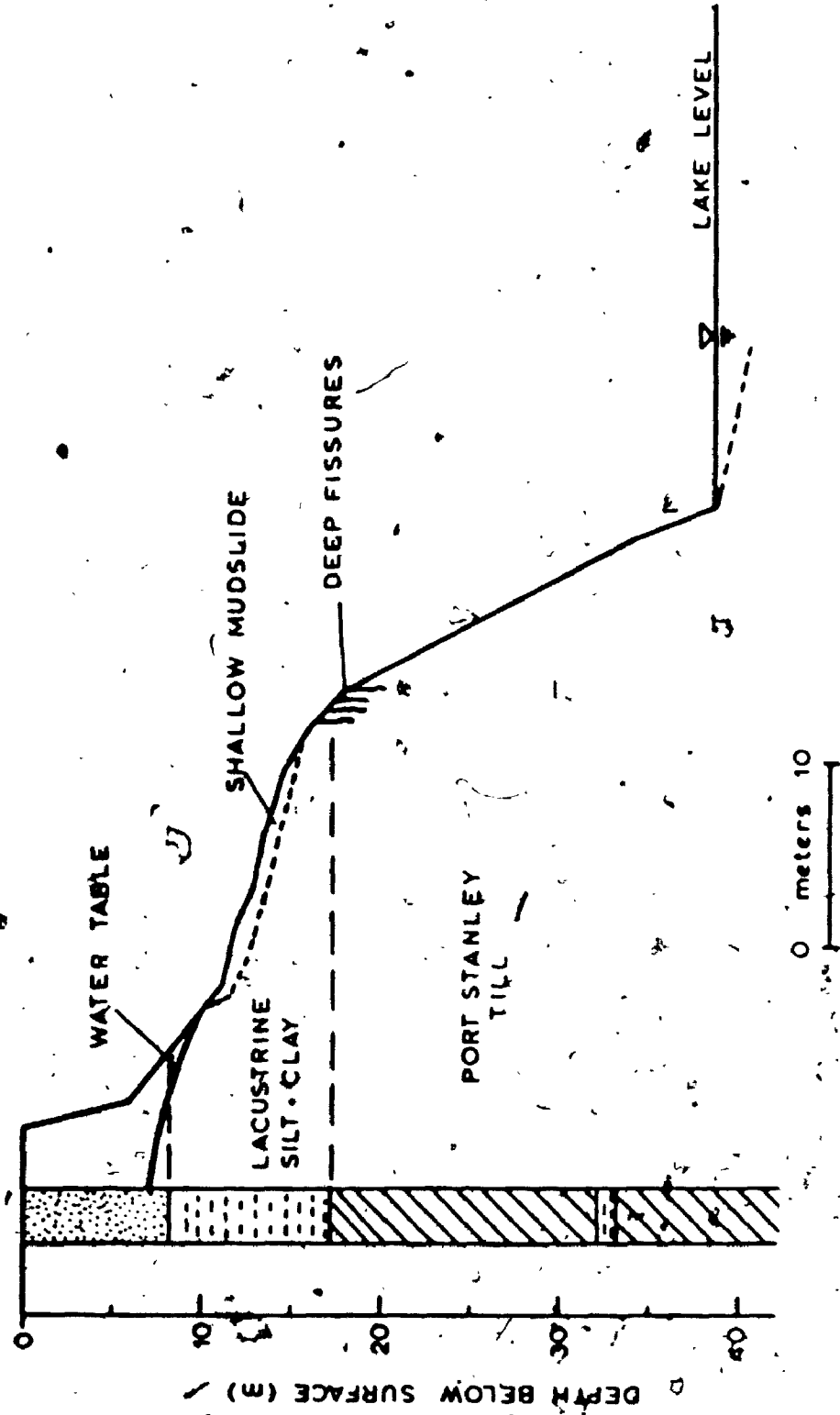


Fig. 51 Shallow Mudslide, Port Bruce (Geography Station)

using standard techniques (Terzaghi and Peck 1967). These penetration tests will be used later to give a crude estimate of undrained shear strength.

Borehole logs are reported on Figures 5.4 to 5.7 along with penetration resistance and water content. The names for the different units of glacio-lacustrine sediments are given from visual observations and also reflect the penetration resistance of the different units. Lacustrine clays and silts are homogeneous with very few coarse particles or are often banded or layered; the penetration resistance from the standard penetration test varies from 15 to 30 blows per foot; waterlaid till often resembles lacustrine deposits but has a greater resistance (30-50 blows per foot) and contains frequent brownish clay pebbles and coarser particles segregated in fine linear bands. basal till is gritty with occasional angular pebbles and no visible structure such as laminations; penetration resistance commonly exceeds 45 blows per foot. Based on penetration resistance alone, all glacial materials would be classified as stiff to hard clay and silt.

5.2.2 Groundwater Investigations.

Groundwater flow is an important variable in stability analysis and the groundwater pressure distribution along a potential failure plane may be critical. Several piezometers were installed at various depths to measure pore-water pressure, variations in groundwater levels, to estimate

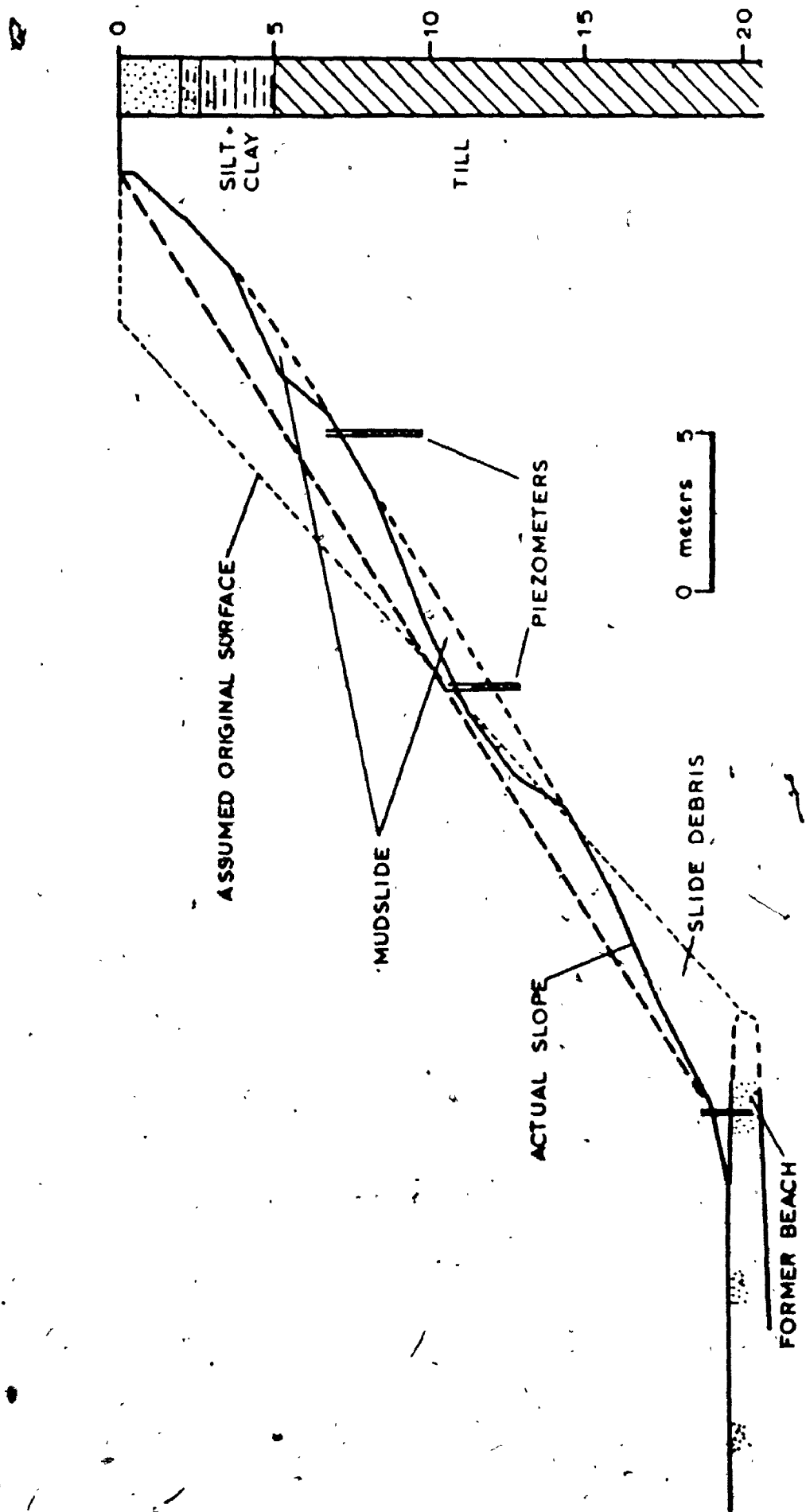


Fig. 5.2 Shallow Slides on Stabilized Slope, Port Burwell.

type is observed west of Port Burwell in lacustrine clays and silts where dessication extends to a depth of two meters and wide open vertical fissures parallel to the slope are filled with water in late fall and spring. The water content may reach 42% whereas in the in-situ material it rarely exceeds 25%. The slide occurs after bulging at the base and the material flows rapidly downslope and forms a small fan overlying beach material (Figure 5.2).

Minor flows occur in the form of mud streams on steep slopes immediately after a large rainfall. weathered soil is sloughed down in small rills and gullies at a very high water content of 60 to 70% (Hutchinson 1970). They are important in the process of slope degradation but affect very slightly the stability of the bluffs.

Rotational slides are produced along a well-defined failure surface almost cylindrical in shape. To this type belong a great number of shallow slips occurring on the edge of the cliff and also several large slides involving the entire bluff. Usually the soil fails as a block but in several instances larger slides result in a mass of debris with blocks several meters across down to individual particles. In this case the failure surface may not be perfectly circular or else structures in the soil mass may exist (joints especially) that reduce the global cohesion of the failed mass.

Shallow slides are very common in the upper slope, most frequently within lacustrine materials. They vary in length from a few meters to more than ten meters.

Their encroachment rarely exceeds a few meters. Usually shallow slips terminate at the spring line on the top of the median part of the slope. Desiccation cracks and lateral expansion initiate the slides and groundwater seepage by softening of the clays or piping of the sands lead to failure. The debris of these slides accumulate on the median slope where further weathering degrades the material which is finally carried down by mudslides.

Large landslides are less frequent but more spectacular and more significant for engineering works along the north shore. A small area west of Clear Creek and most of the shoreline in Southwold and Yarmouth Townships experience these slides. The large rotational slides are all toe failures and erosion at the base is critical on the stability as will be seen later (section 5.4). The length, L , of the crown is commonly between 40 and 100 meters and the slide encroachment, E , on the edge of the cliff is from 5 to 20 meters; the ratio L/E of the length of the crown to the encroachment is from 5 to 8 as compared with the spreading failure in sand where that ratio is between 0,8 and 4,5. The ratio, L/H , of the length to the height of the bluff is between 0,8 and 2,5 whereas for shallow slides in the upper slope that ratio is between 0,1 and 0,3.

There is a strong association between high erosion rates and occurrence of large rotational slides; since wave energy is not at a maximum near Port Stanley high erosion rates seem to reflect the particular geological conditions that lead to failure. East of Port Stanley, a 2-meter thick

layer of varved sand and silt occurs near lake level; this material having a very low resistance to erosion, there is rapid undercutting at the base of the cliff. On the top of the section there is a 15-meter layer of varved sands supplying large amounts of groundwater for infiltration along the joints and softening of the soil mass. When failure occurs the sliding block is extensively remolded by shearing and fracturing and a promontory made of debris extends in the lake at distances up to 70 meters from the shoreline. The total slope angle after the slide is about 40° with a vertical backscarp.

Smaller rotational slides passing through the toe also occur in areas with similar geological setting, but only the lower part of the slope is involved (Figure 5.1). The presence of transverse cracks on the median part of the slope and oversteepening by wave erosion are the principal causes of failure (section 5.4).

The next sections will describe field work including borings and groundwater observations and laboratory investigations on the soils of the study area (Sections 5.2 and 5.3); stability analysis will be done in Section 5.4.

5.2 Field Investigations.

Several field trips to the study area have been made between 1970 and 1972 to examine the general geology and patterns of erosion; most of the results were already discussed in previous chapters. Four locations were

chosen for more extensive exploration to determine the in-situ properties of soils (geology, water content, penetration resistance) and to investigate the groundwater situations.

5.2.1 Exploratory Borings.

Referring to Figure 5.3, one site (4) immediately west of Fort Burwell was bored in 1970, and the following year augering was done at the U.W.O. Geography Station (3), west of Port Bruce, at the boundary between Southwold and Dunwich Townships (2), and east of the Aldborough-Dunwich township line (1), south of Wallacetown.

The borings were done by continuous flight auger with a diameter of 10 cm. At the Geography Station, hollow-stem augers were used (outside diameter 15 cm, inside diameter 7,5 cm) because of the caving of water-bearing sands in the upper 10 meters. Casing was not used during borings because of the scarcity of interbedded sand layers of high transmissibility. It seems, indeed, that many of the interbeds of granular material are not continuous over wide areas and that very little water drains from them. Wash boring was used in one instance, at the Geography Station, because the hollow-stem augers would not operate below 30 meters.

Sampling was done at five-foot intervals (1,5 m) with a split spoon because the pebbly nature of the till did not allow use of thin-wall samplers. Standard penetration tests were performed at the same intervals

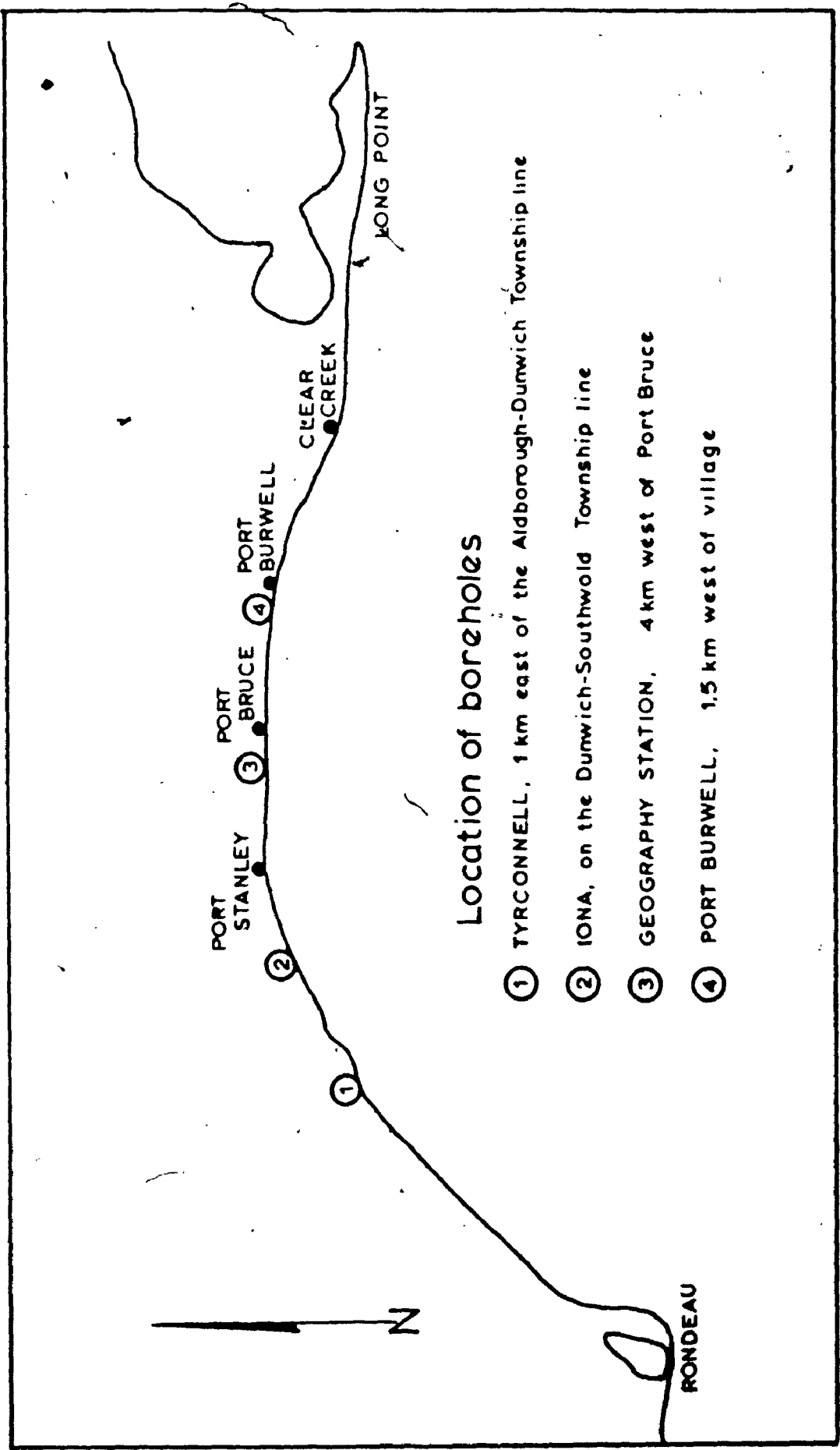


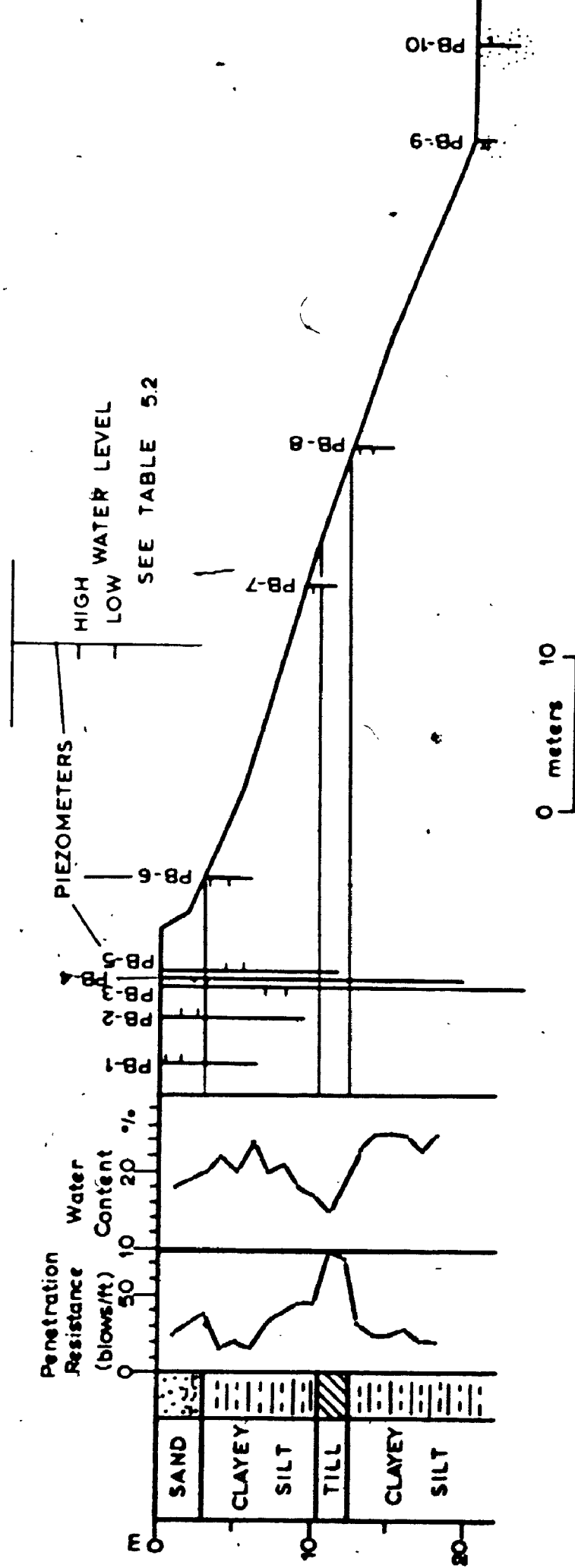
Fig. 5.3 Location of Exploration Boreholes.

using standard techniques (Terzaghi and Peck 1967). These penetration tests will be used later to give a crude estimate of undrained shear strength.

Borehole logs are reported on Figures 5.4 to 5.7 along with penetration resistance and water content. The names for the different units of glacio-lacustrine sediments are given from visual observations and also reflect the penetration resistance of the different units. Lacustrine clays and silts are homogeneous with very few coarse particles or are often banded or layered; the penetration resistance from the standard penetration test varies from 15 to 30 blows per foot; waterlaid till often resembles lacustrine deposits but has a greater resistance (30-50 blows per foot) and contains frequent brownish clay pebbles and coarser particles segregated in fine linear bands. Basal till is gritty with occasional angular pebbles and no visible structure such as laminations; penetration resistance commonly exceeds 45 blows per foot. Based on penetration resistance alone, all glacial materials would be classified as stiff to hard clay and silt.

5.2.2 Groundwater Investigations.

Groundwater flow is an important variable in stability analysis and the groundwater pressure distribution along a potential failure plane may be critical. Several piezometers were installed at various depths to measure pore-water pressure, variations in groundwater levels, to estimate



GEOLOGY, SEE APPENDIX 2

Fig. 5.4 Geology and Groundwater Conditions at Port Burwell.

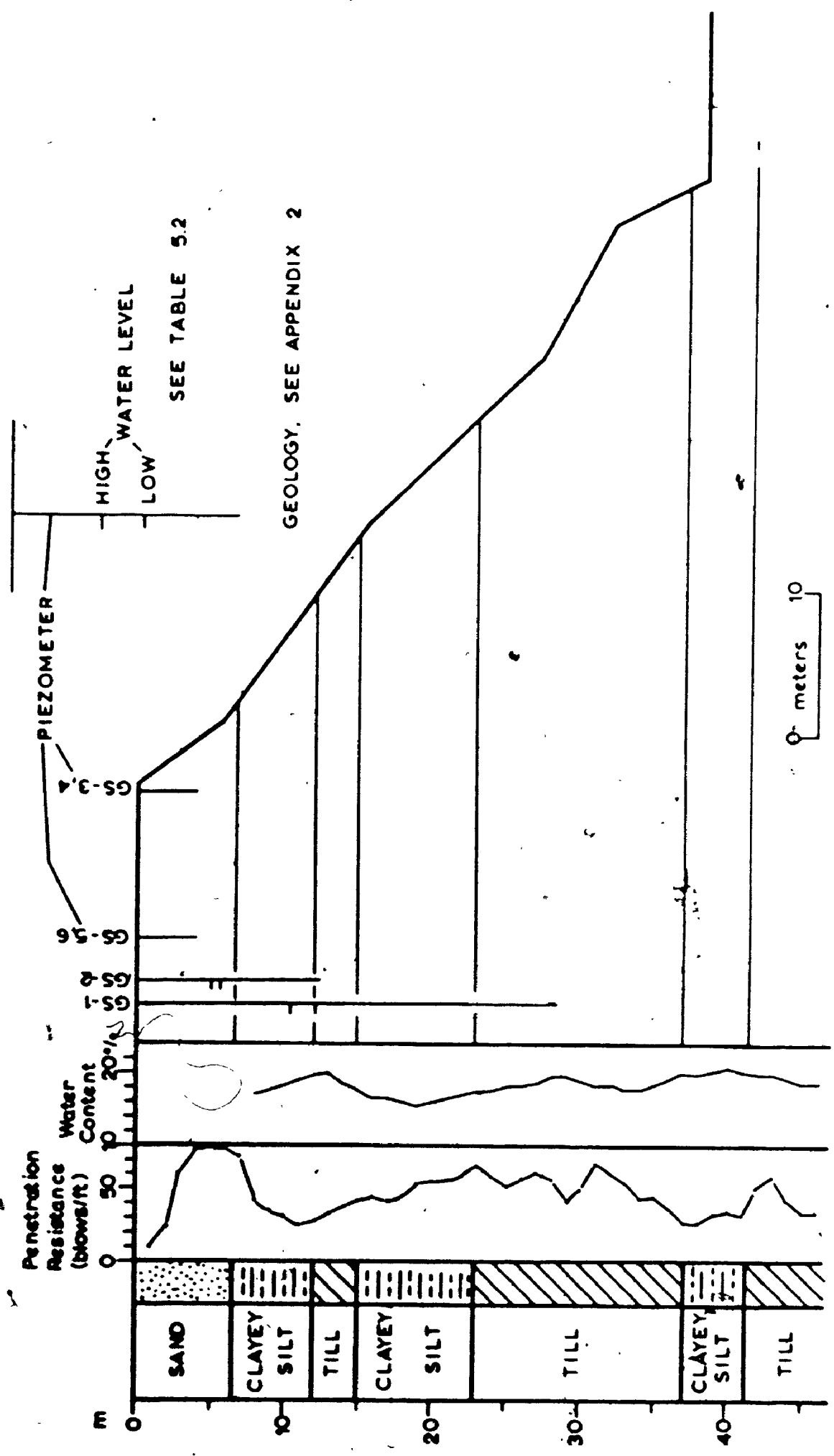


Fig. 5.5 Geology and Groundwater Conditions, Geography Station.

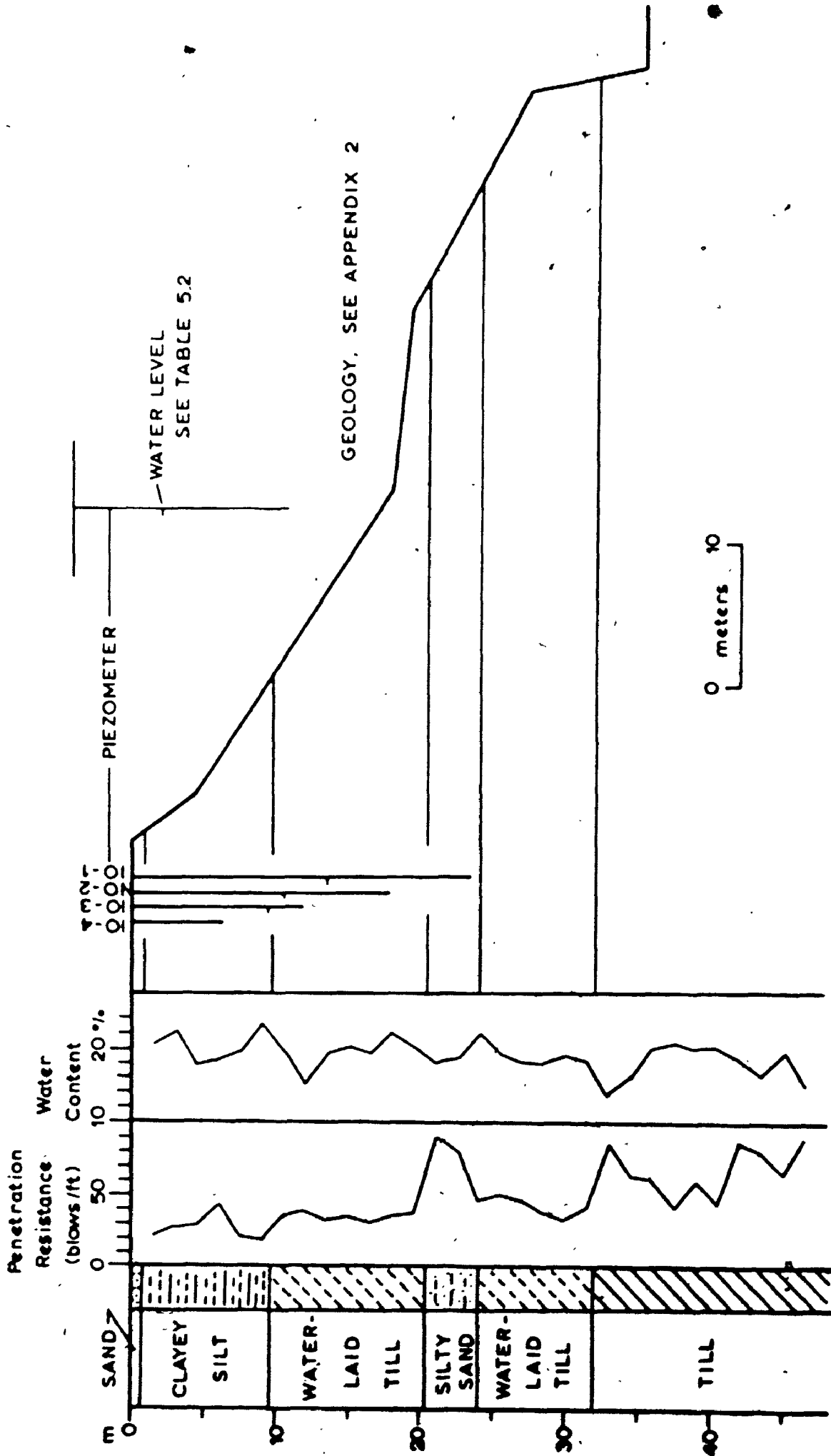
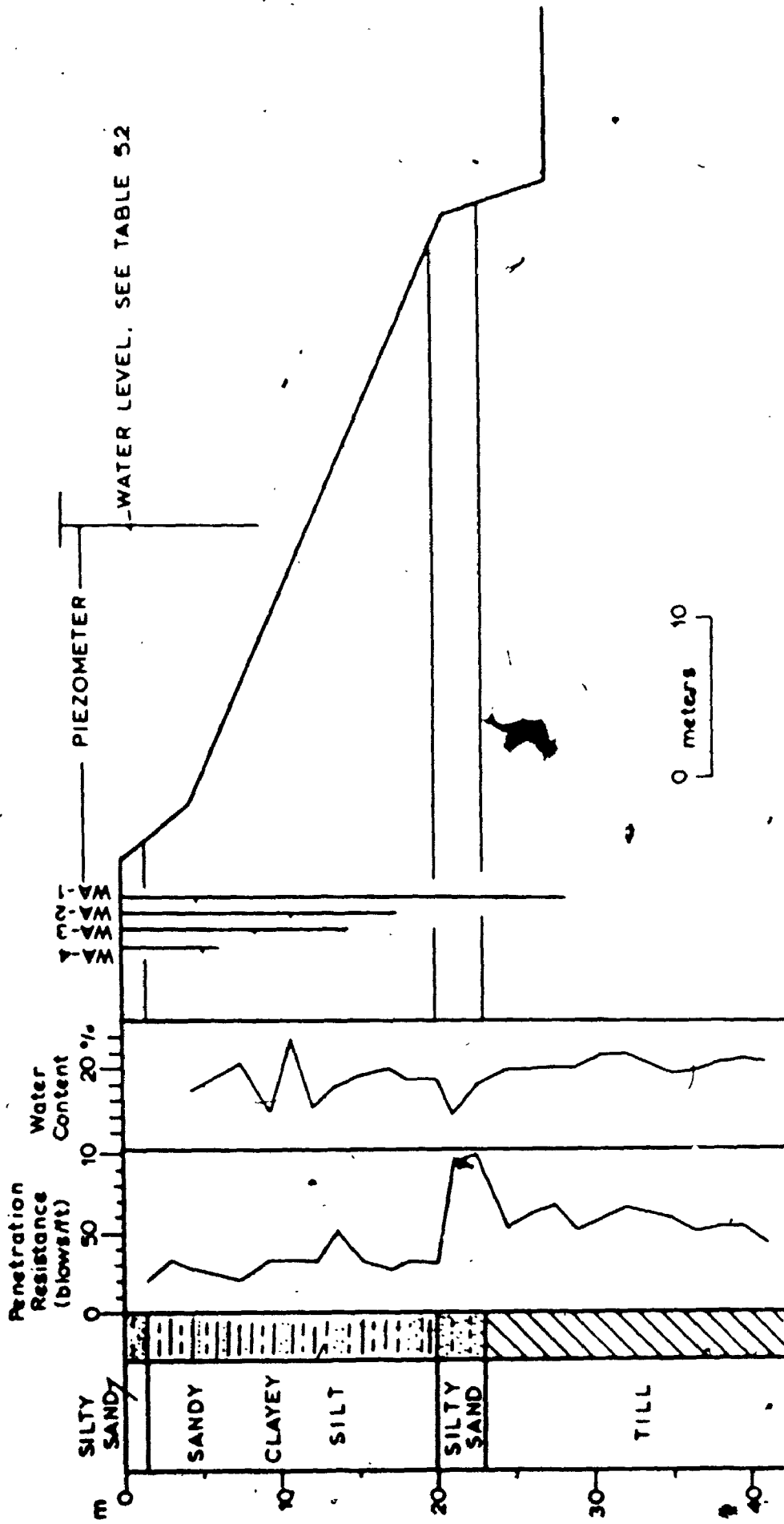


Fig. 5.6 Geology and Groundwater Conditions at Iona.



GEOLOGY, SEE APPENDIX 2

Fig. 5.7 Geology and Groundwater Conditions at Tyrconnell (Wallacetown).

the hydraulic conductivity of the different materials and also to help stating the main assumptions on groundwater flow patterns.

Settings to observe groundwater are of two types: piezometers measuring the water potential at a given point inside a mass of soil or rock, and observation wells which are merely recording the fluctuations of the water table.

The same instrument was used both as a piezometer and observation well: the 'Golder-type' piezometer which is a plastic tube with inside diameter of 9,5 mm (3/8 in.), perforated and surrounded by sand held in place with jute cloth. The piezometer is equipped with couplings permitting the insertion of plastic tubing that can be lowered to any depth. Water level is recorded by using a coaxial cable connected to a battery and a galvanometer: the contact between the two conductors forming the cable is made when the cable reaches water. Graduations permit localisation of water level at any depth within 5 mm.

Piezometers were installed in all boreholes and sealed in place with bentonite balls over one meter. The tip of the piezometer was surrounded by pea gravel over a height of 50 to 60 cm. The effective zone at which water potential is measured is then a cylinder having the approximate dimensions of 10 cm in diameter and less than one meter high. The bentonite was packed above the pea gravel using a tamping weight suspended to a long string.

Observation wells were augered by machine or by hand to shallow depths of less than 5 meters; the same type

of piezometer was used but no bentonite seal was placed, the hole being backfilled with sand. These shallow wells measure water table fluctuations with time.

Table 5.2 gives a list of observation wells and piezometers with their depth and ground elevation. Figures 5.4 to 5.7 gives the location of the piezometers along the slope and their extreme fluctuations during the period of observation.

5.2.3. Groundwater Fluctuations.

Groundwater level fluctuations were recorded intermittently at Fort Burwell and the Geography station. Generally fluctuations are small in magnitude with a maximum of 1.5 m in one piezometer. High and low water levels are illustrated in Figures 5.4 and 5.5 and the static water level at one time in other piezometers, Figure 5.6 and 5.7. Observation wells operated by the Ontario Water Resources Commission (Sibul 1969) north of Fort Burwell show the same trends; piezometers in till, sand and silt record sensibly the same annual or seasonal fluctuations over a three-year period. Low water occurs in July and August when evapotranspiration reaches a maximum and high levels occur in April and May when the snowmelt reaches the water table.

The importance of groundwater fluctuations is mainly because it controls groundwater seepage in surficial aquifers. Monitoring of a gentle slope at Fort Burwell shows that the water table fluctuation in the weathered material is in the order of one meter. Such variations bring

the water table near the surface in winter and spring saturating dried material and contributing to soil desintegration by slaking; mudslides on gentle slopes occur significantly in late fall and early spring when water levels are high. In other areas where sand is thick at the surface, increase in water levels results in increased seepage at the contact with the less pervious soils; groundwater discharge is soon absorbed along dessication joints lower in the slope and softening of clayey soils leads slowly to failure of the entire slope.

5.2.4 Hydraulic Conductivity.

In-situ determination of hydraulic conductivity was performed in most boreholes instrumented with piezometers. Due to the low transmissibility of the soils, pumping tests were not possible and injection tests were done. The injection test or slug test consists in introducing in the tubing a known amount of water and in observing the decay of water head with time. Two methods exist to analyse this type of test and gave comparable results in this study.

A first method (Hvorslev 1949) permits the calculation of hydraulic conductivity by injection in a piezometer sealed at one point below the surface of the soil (Figure 5.8); infiltration of water from such a setting is essentially horizontal. The soil is assumed to be saturated, incompressible, and the hydraulic conductivity is taken as isotropic. Permeability ratios even for varved clays tend

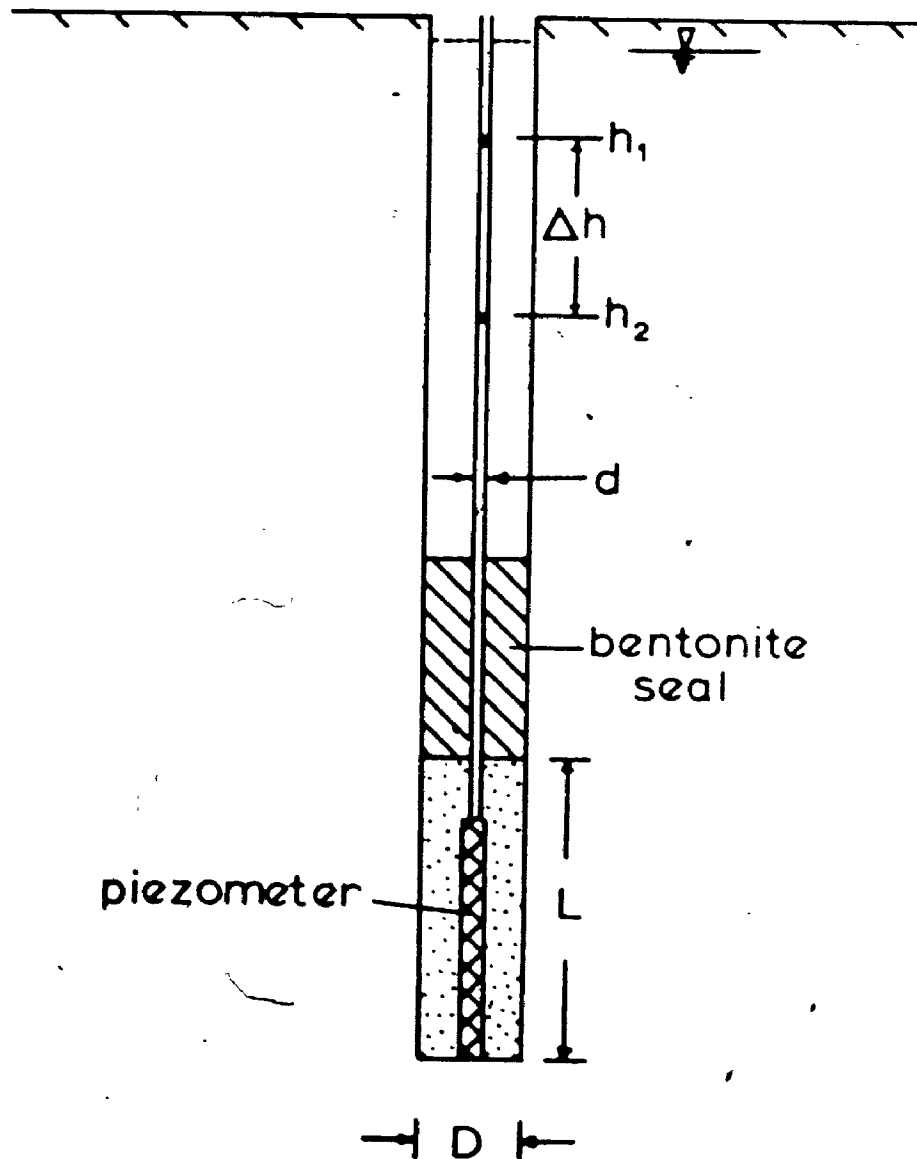


Fig. 5.8 Piezometer Installation.

Table 5.2

Piezometers and Observation Wells

Location	Elevation Surface (m)	Depth (m)	Hydraulic Conductivity (cm/sec)	Low Water Level in meters below surface	High Water Level in meters below surface	Static Level (m)
Port Burwell (Fig. 5.4)						
PB-1	195.34	6.10	$2.0 \cdot 10^{-7}$	1.37 (6-70)	0.41 (4-71)	-----
PB-2	195.47	9.15	$2.0 \cdot 10^{-7}$	2.39 (6-70)	1.34 (4-71)	-----
PB-3 *	195.36	23.55	$2.4 \cdot 10^{-7}$	8.04 (6-70)	6.98 (12-70)	-----
PB-4 *	195.62	19.40	$2.4 \cdot 10^{-8}$	3.01 (4-71)	2.12 (6-70)	-----
PB-5 *	195.68	11.35	$1.1 \cdot 10^{-7}$	5.30 (12-70)	4.14 (4-71)	-----
PB-6	192.93	2.93	-----	1.56 (8-70)	0.22 (12-70)	-----
PB-7	186.57	1.98	-----	1.00 (8-70)	0.51 (12-70)	-----
PB-8	183.79	2.75	-----	1.15 (8-70)	0.30 (12-70)	-----
PB-9	176.26	1.51	-----	0.71 (8-70)	0.38 (12-70)	-----
PB-10	176.72	2.80	-----	-----	-----	0.80 (8-70)
Geography Station (Fig. 5.5)						
GS-1 *	213.08	28.15	$3.1 \cdot 10^{-7}$	12.00 (8-72)	10.22 (10-71)	-----
GS-2 *	213.07	12.20	$5.2 \cdot 10^{-8}$	5.34 (8-72)	5.03 (4-72)	-----
GS-3	213.59	4.0	-----	Dry	Dry	-----
GS-4	213.39	4.0	-----	Dry	Dry	-----
GS-5	213.32	4.0	-----	Dry	Dry	-----
GS-6	213.59	4.0	-----	Dry	Dry	-----
GS-7	213.31	4.0	-----	Dry	3.66 (4-72)	-----
GS-8	213.48	4.0	-----	3.66 (8-72)	3.66 (4-72)	-----

Table 5.2 (Continued)

Location	Elevation Surface (m)	Depth (m)	Hydraulic Conductivity (cm/sec)	Low Water Level in meters below surface	High Water Level in meters below surface	Static Level (m)
GS-9	213,37	4,0	-----	3,07 (8-72)	2,83 (4-72)	---
GS-10	213,52	4,0	-----	2,97 (8-72)	2,68 (4-72)	---
GS-11	213,40	4,0	-----	2,85 (8-72)	2,59 (4-72)	---
GS-12	213,57	4,0	-----	2,68 (8-72)	2,42 (4-72)	---
GS-13	213,39	4,0	-----	2,76 (8-72)	2,58 (4-72)	---
GS-14	213,60	4,0	-----	2,71 (8-72)	2,44 (4-72)	---
GS-15	213,45	4,0	-----	2,68 (8-72)	2,45 (4-72)	---
GS-16	213,68	4,0	-----	2,64 (8-72)	2,39 (4-72)	---
Iona (Fig. 5.6)						
IO-1 *	207,34	23,55	$6,0 \cdot 10^{-8}$	----	----	13,60 (9-71)
IO-2 *	207,50	17,85	$2,6 \cdot 10^{-8}$	----	----	10,22 "
IO-3 *	207,58	11,42	$5,6 \cdot 10^{-8}$	----	----	8,75 "
IO-4 *	207,55	6,18	-----	----	----	Dry
Wallacetown (Fig. 5.7)						
WA-1 *	202,81	28,30	$1,8 \cdot 10^{-8}$	----	----	4,85 (9-71)
WA-2 *	202,72	17,40	$3,0 \cdot 10^{-8}$	----	----	10,85 "
WA-3 *	202,68	11,24	$2,3 \cdot 10^{-7}$	----	----	8,59 "
WA-4 *	202,74	6,11	$8,5 \cdot 10^{-6}$	----	----	5,12 "

* Indicates a piezometer sealed in place.

to be low, more so for tills which do not show preferential directions of flow (Chan and Kenney 1973, Kenney and Chan 1973).

During a small interval of time, dt , after the test has started, the water level in the tubing drops by a quantity $(-dh)$ and the volume of water released in the soil through the piezometer is q :

$$q = -\frac{\pi d^2}{4} \cdot \frac{dh}{dt}$$

where d is the diameter of the tubing. The volume of water entering the ground is expressed by

$$q = khF$$

where k is the hydraulic conductivity, h is the head of water at any time t , and F is a shape factor depending on the geometry of the hole, the size and type of piezometer and the influence of the bentonite seal.

Since q leaving the tubing is equal to q entering the soil, then

$$-\frac{\pi d^2}{4} \cdot \frac{dh}{dt} = khF$$

or

$$k \cdot dt = -\frac{\pi d^2}{4F} \cdot \frac{dh}{h}$$

By integrating this last equation over a time interval from t_1 to t_2 the hydraulic conductivity can be easily calculated as:

$$k = \frac{\pi d^2}{4F} \frac{\ln(h_1/h_2)}{(t_2 - t_1)}$$

The factor F for the setting illustrated on Figure 5.8 is given as being (Hvorslev 1949):

$$F = 2\pi L / \ln(2L/D)$$

where L is the length of the borehole through which filtration occurs and D is the diameter of the borehole; therefore

$$k = \frac{d^2 \cdot \ln(2L/D)}{8 \cdot L \cdot (t_2 - t_1)} \cdot \ln \frac{h_1}{h_2}$$

This expression for k is valid without much error if the permeability ratio k horizontal over k vertical is less than 10.

In practice a known amount of water was poured in the tubing and several readings of head of water versus time elapsed were taken. By working on pairs of such readings the hydraulic conductivity was calculated using the above equation. The values of k are given in Table 5.2 in centimeters per second. One restriction to this method is that at high values of hydraulic gradient, at the beginning of the test, hydraulic conductivity is no longer linear with head of water. To avoid that problem, the value of k should be determined for small gradients, or in other words when the head of water is little different of the head of water existing in nearby soil. An other alternative is to use non-equilibrium equations which take into account the storage coefficient of the soil which is a measure of its compressibility and porosity.

Such a method (Cooper, Bredehoeft, and Papadopoulos 1967) exists that describe the response of a well to an instantaneous change in water head. An exact solution to this problem has been developed and a set of type curves computed from this solution permits the determination of the

transmissibility of the formation.

These curves relate the ratio h/h_0 to the values of the permeability factor Tt/R_c^2 for the different values of a . The head at any time after injection is h and h_0 is the head immediately after injection; T is the transmissibility (hydraulic conductivity times the thickness of the aquifer), t is the time interval since injection started, and R_c the radius of the tubing. The parameter ' a ' is defined as

$$a = S \cdot (R_s^2 / R_c^2)$$

where R_s is the radius of the borehole and S is the storage coefficient, or the volume of water per unit area that is taken by the aquifer for a unit decline in head per unit area.

Type curves for three different values of ' a ' are plotted on Figure 5.9 (data from Cooper et al. 1967). Transmissibility is found by plotting on a separate graph the ratio h/h_0 versus time for a given test and trying to match this curve with one of the type curves (Figure 5.10); a matching point is found with coordinates of t and Tt/R_c^2 for a given value of ' a '. The example illustrated on Figure 5.10 is from Piezometer GS-1; the hydraulic conductivity is found by dividing the value of T by the thickness of soil L intercepted by the piezometer (Figure 5.8). Using this method, the value of k is $3.5 \cdot 10^{-7}$ cm/sec which is about 10% higher than the value found by Hvorslev's method; this difference is less than the accuracy with which the borehole diameter or the length of the pervious section are known.

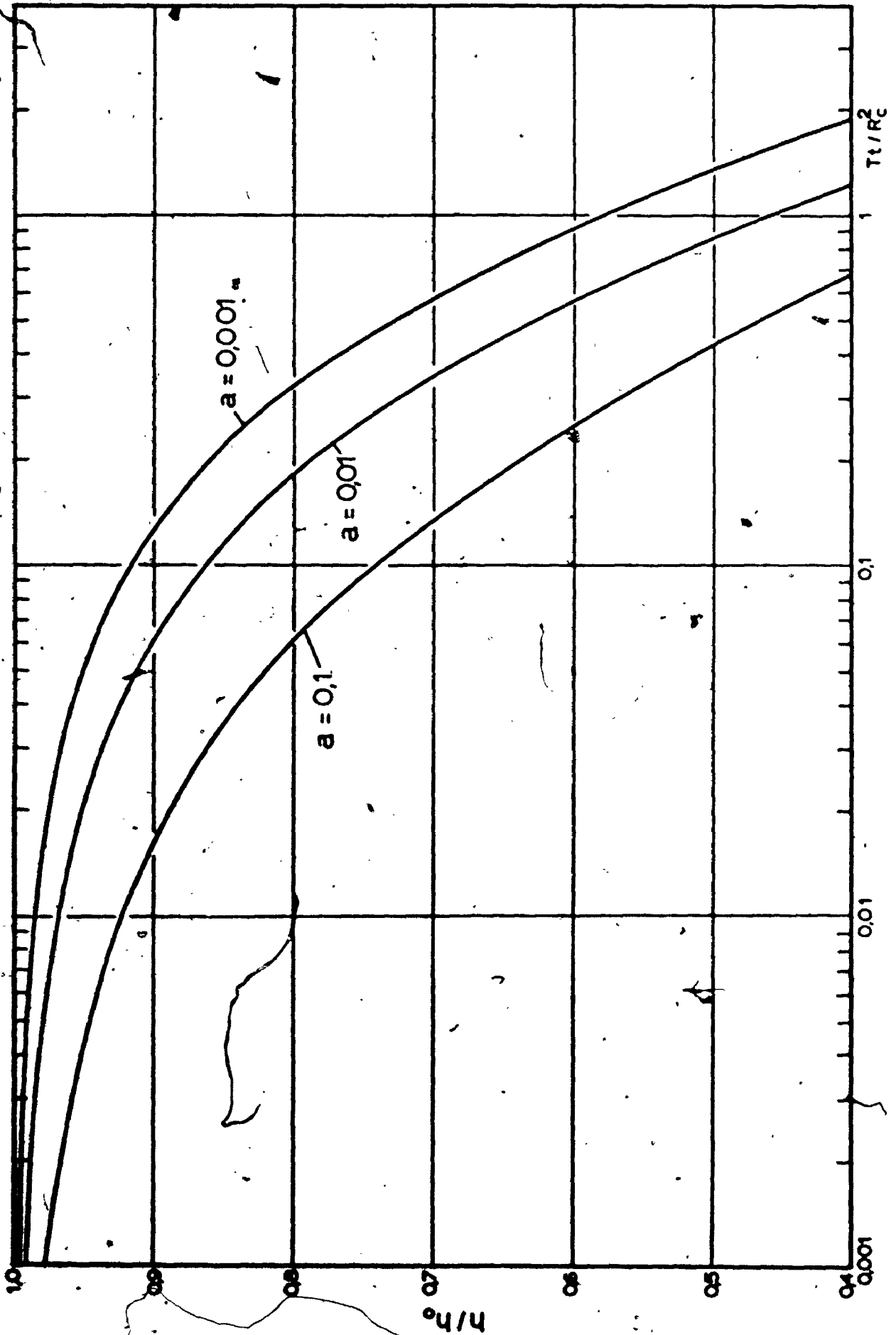


Fig. 5.9 Type Curves to Determine Transmissibility T.

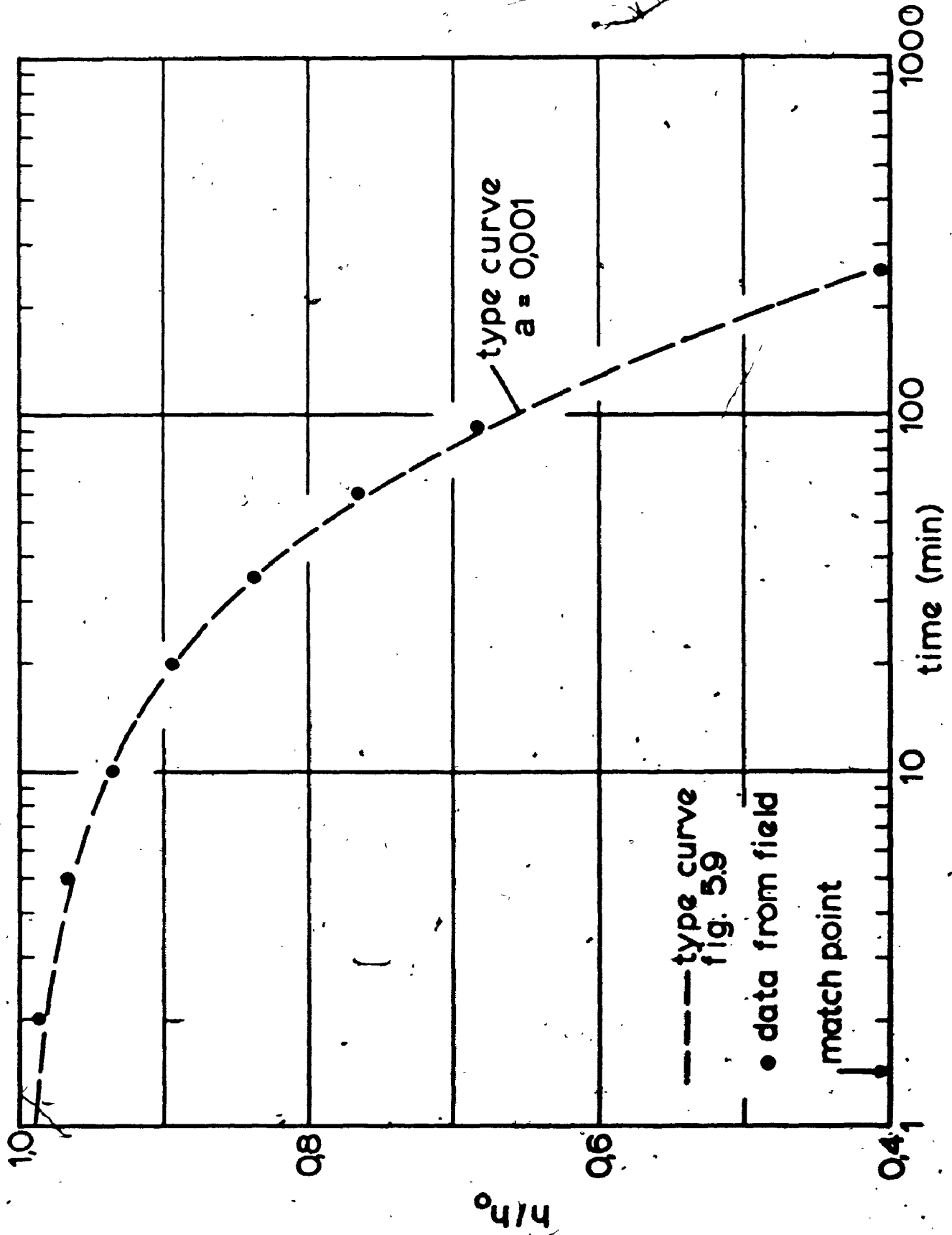


Fig. 5.10 Injection Test in Piezometer GS-1, Port Bruce.

5.2.5 Discussion of the Results.

Measurements of hydraulic conductivity on the field fall in the range of 10^{-6} to 10^{-8} cm/sec which is very low but normal for clayey-silty soils. Directional variations of permeability could not be measured and it is assumed that it is isotropic for basal tills and waterlaid tills; lacustrine silt and clay, provided that they do not include continuous sand layers can be considered slightly anisotropic with permeability ratios below 5 as was observed in varved sediments at New Liskeard (Kenney and Chan 1973), and the fact that most analyses of lacustrine material in the study area contain very little sand (Section 5.3).

The direction of groundwater flow can be inferred from piezometer readings, permeability measurements and from geological and morphological observations. Figure 5.11 illustrates the flow net for an idealized situation; this net is based on calculations using finite differences (relaxation method) by assuming that Darcy's law is valid at low gradients (Verruijt 1970). Assuming isotropic hydraulic conductivity both in sand and till, and a water divide far away from the slope it is possible to draw flow lines and equipotential lines for the boundary conditions specified on the problem. This model represents fairly well the situation at the Geography station and near the pumping station east of Port Stanley. Based on this model it is possible to evaluate the order of magnitude of groundwater discharge. For a slope height of 30 meters, hydraulic

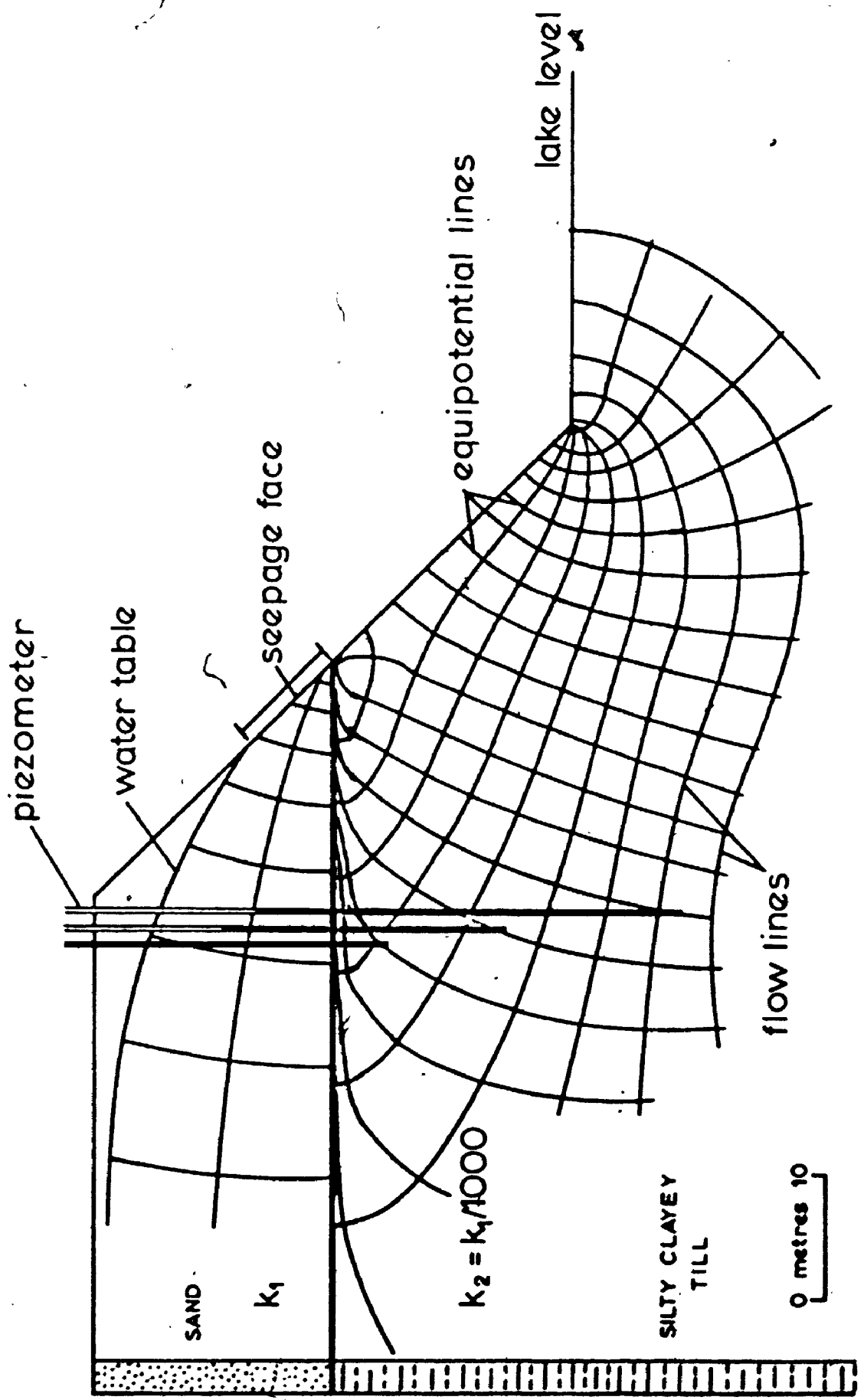


Fig. 5.11 Groundwater Flow Model, Port Bruce Vicinity:

conductivity of 10^{-4} cm/sec for sand and 10^{-7} cm/sec for till the quantity of seepage in the sand is in the order of a few hundred liters per day per meter of outcrop; in the till outflow is negligible being in the order of one liter per day per meter of shoreline.

Observations in piezometers installed at four sites show that generally the head diminishes with depth of the piezometer tip below the ground surface; this is normal considering that Lake Erie acts as a natural discharge area for groundwater. Actual heads are distributed as illustrated on Figure 5.11 which leads to think that this idealized flow system may correspond to reality.

The seepage face at the base of sand is a common observation along the bluffs and this is expected in view of the contrast in permeability between sand and till (3 to 4 orders of magnitude). The flow of groundwater in till is in general parallel to the slope and the presence of desiccation cracks will accentuate that tendency already predicted by the model in Figure 5.11. This groundwater flow model will be used in stability analysis (Section 5.4).

5.3 Laboratory Investigations.

Simple identification tests were performed on the glacial materials of the study area. Natural water content Atterberg limits, specific gravity, grain size analysis and mineralogy were used to classify the different soils in order to get some feeling for their mechanical properties.

Shear strength was also investigated using a direct shear box.

5.3.1 Natural Water Content.

Natural water content was determined on undisturbed samples coming from blocks and from remolded samples taken with a split-spoon in four test borings. All samples come from below the water table and are assumed to be fully saturated.

Water content varies within very narrow limits for all soil tested; for 6 blocks and 92 spoons samples taken between Fort Burwell and Wallacetown at depths up to 47 meters water content in tills and lacustrine silt and clay has a mean of 19.5% and a standard deviation of 2.2%; 90% of the samples are in the range of 16 to 23% and extremes are 14% in sandy horizons and 26% in lacustrine silt. There is no clear difference in moisture content between tills and associated glacio-lacustrine soils, but a tendency exists for coarser sediments (pebbly tills, sandy silt) to be lower. Weathered material, or material disturbed by drying and wetting cycles have water content ranging from 0 to 55%.

5.3.2 Atterberg Limits.

Liquid and plastic limits were performed on samples representing soils over the whole study area. Some of the tests were done on material that was previously air-dried but this does not seem to change the limits by a large amount (chapter 4.5).

As for water contents, Atterberg limits tend to cluster in a narrow band on the plasticity chart (Figure 5.12); this suggests similarity in mineralogy and geological provenance. The 'green' clay at Port Talbot (Quigley and Dreimanis 1972) is not included since it represents a soil horizon developed under conditions very different than those presently existing. From the plasticity chart most sediments are classified as low-plasticity inorganic silts and clays. The liquid limits are in the range of 26 to 35% and the plastic limits from 17 to 19%.

5.3.3 Specific Gravity.

Specific gravity was measured for 20 samples and the values range from 2.74 to 2.84. These are slightly above average for clay minerals given as 2.70 by Terzaghi and Peck (1967). This suggests a low proportion of lighter minerals such as quartz (2.66) and a relatively large amount of carbonates (dolomite, 2.87) and heavier clay minerals (muscovite 2.8-2.9, chlorite 2.6-3.0), as confirmed later.

5.3.4 Grain Size Analysis.

Several grain size analyses were performed on tills and lacustrine materials. The results from forty samples over the study area show a large proportion of silt and clay both in tills and associated sediments. The clay content varies between 30 and 60% and is usually between 35 and 45%.

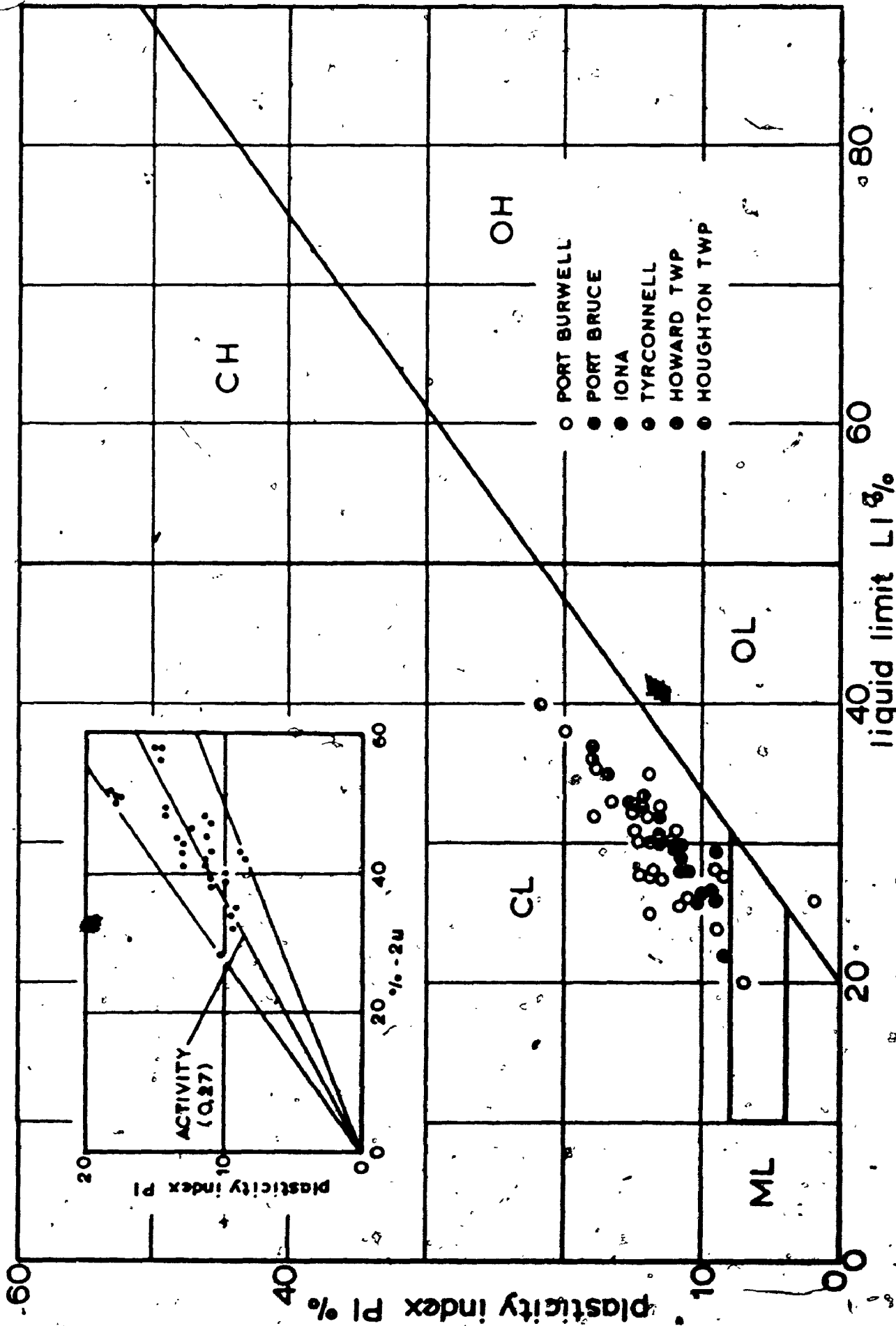


Fig. 512 Plasticity and Activity of Glacial Sediments.

Silt content (2-60 microns) varies from 30 to 65% and is typically between 45 and 60%. Sand and coarser fractions are present in very small amount in the till (less than 20%) and rarely exceeds 10%; lacustrine clayey silts contain less than 5% sand.

Typical cumulative curves are illustrated in Figure 5.13; the curves are usually covering a large numbers of sizes and extend down to rock flour; the slope of the curves for lacustrine material can be compared with the corresponding curves for till from which they were derived.

The results of all analyses are plotted on a ternary diagram (Figure 5.14) permitting comparison with other published data on the same area (Wood 1951, Dreimanis and Reavely 1953, Dreimanis 1960, Lewis 1966, Terasmae, Karrow and Dreimanis 1972). Some variations occur in the results since the first three authors use 5 microns for the boundary between silt and clay, while Lewis (1966) puts it at 4 microns. The upper boundary for silt is put at 50 microns in several papers as compared with the engineering usage of 60 microns (MIT scale). The contour line on Figure 5.14 encloses material belonging to the 'upper till' or Fort Stanley Drift (Dreimanis and Reavely 1953).

5.3.5 Mineralogy.

Published studies on till mineralogy deal mainly with the coarse fraction, carbonates and heavy minerals (Dreimanis and Reavely 1953, Dreimanis 1960, Terasmae, Karrow

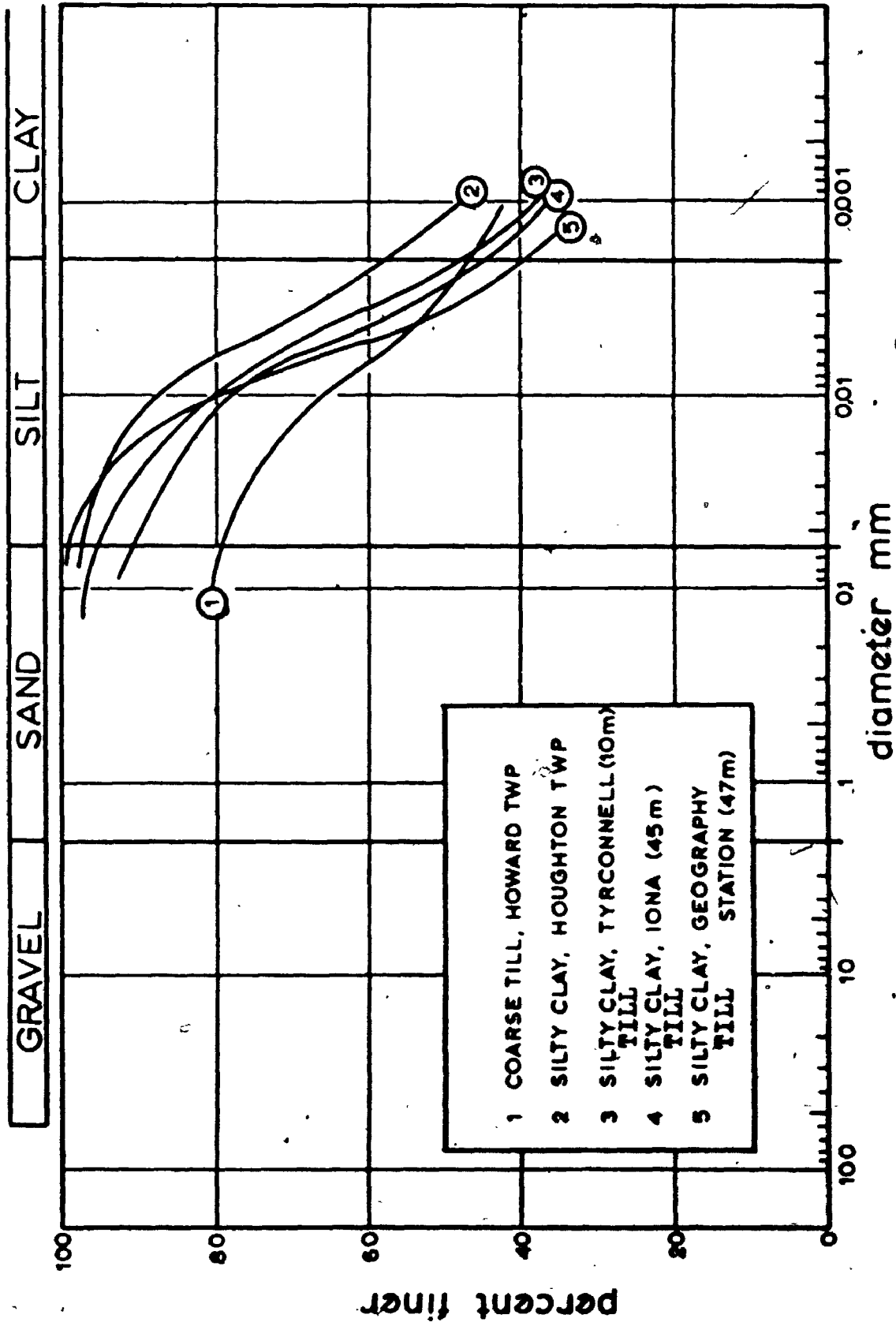


Fig. 5.13 Typical Grain Size Curves for Glacial Sediments.

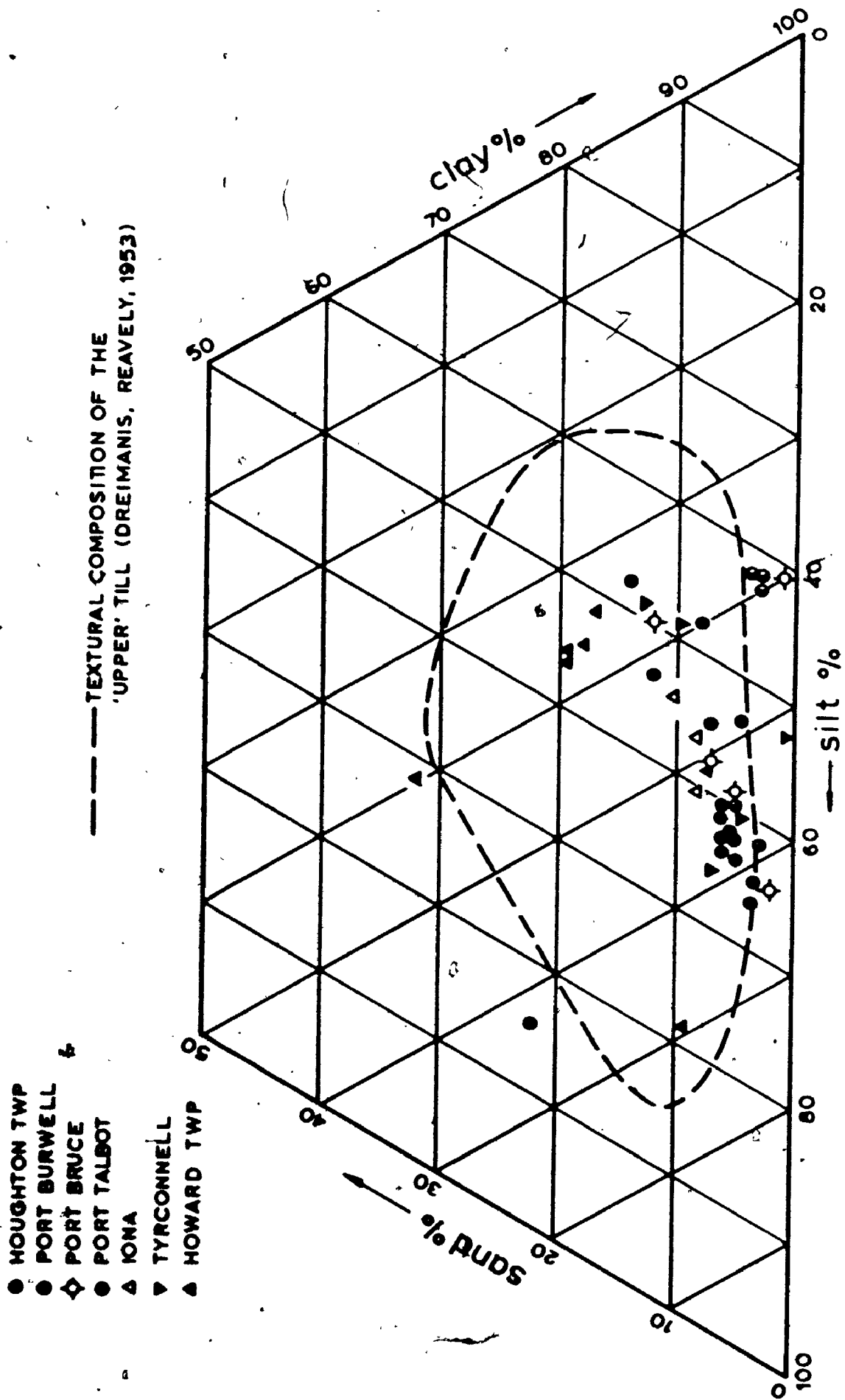


Fig. 5.14 Granulometry of Glacial Materials.

and Dreimanis 1972). The coarse fraction representing usually less than 10% of any sample is mainly composed of silica sand and local rock fragments in the granule to pebble size: limestone, dolomite, chert, shale, etc. From a soil mechanics point of view silt and clay are more important in determining the behavior of the soils.

Carbonates in silt and clay fractions make 30 to 35% of the minerals present (Dreimanis 1960, Quigley and Dreimanis 1972). The bulk of silt size is made of quartz with minor amounts of feldspar and heavy minerals. In the clay size (finer than two microns) apart from carbonates and minor amounts of quartz, the common clay minerals are illite and chlorite.

An X-ray analysis was performed on one sample of Port Stanley Till coming from the bluffs at Fort Talbot, near lake level. The clay fraction was separated by dispersion of the sample in distilled water and sedimentation; samples for X-rays were given a preferred orientation by sedimentation on a porous stone and high-speed centrifugation. Air-dried and glycolated samples were analysed.

Figure 5.15 shows typical X-ray trace of a clay sample. Illite is characterized by a very strong peak near 10 \AA and chlorite by a strong peak at 7.1 \AA and a smaller one at 14.2 \AA . A slight shoulder on the left side of the illite peak suggests that some interlayering of illite with minor amounts of smectite probably occurs (Grim 1968); however smectite peaks would not be individualised if its proportion is less than 10%. The potassium content (as K_2O) in

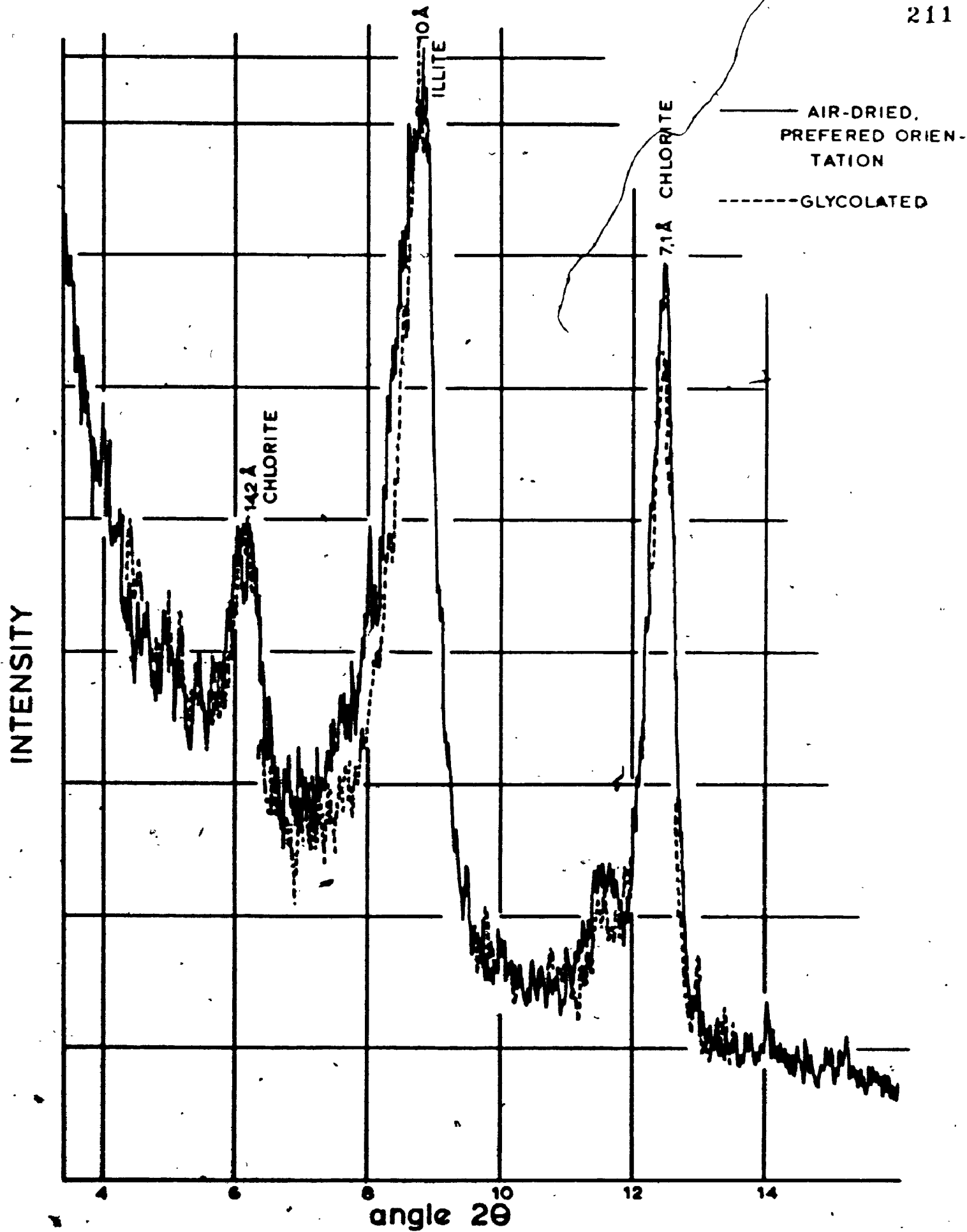


Fig. 5.15 X-Ray Trace, Port Stanley Drift (-2u).

the clay fraction is 4,7% suggesting a large proportion of illite (50-80%) if all that potassium is assigned to illite. Glycolation of the sample reduces slightly the strength of the 7,1 peak of chlorite and gives a better resolution for the 10,0 peak of illite; the presence of smectite cannot be ascertained and the only indication of its presence is the reduction of background noise at 12-13 Å that may have been caused by the presence of swelling minerals in the dry state. Quigley (1972) and Quigley and Dreimanis (1972) give similar results for lower tills in the same area.

There is no evidence of chemical weathering of the clays along the slopes due to the rapid erosion rates causing new material to be exposed continuously. Some alteration along fissures is observed near the surface but does not seem to be relevant in the present study.

5.3.6 Summary of identification tests.

Table 5.3 gives a summary of the tests already described and some other derived soil parameters such as unit weight (in kN/m^3), activity (Skempton 1953), and liquidity index. The unit weight varies from 19,8 to 22,8 kN/m^3 and this range is normal for compact glacial tills (Terzaghi and Peck 1967). The activity of the soils is low with an average value of 0,28 as compared with London Clay (0,95) or pure illite (0,90) (Skempton 1953). The liquidity index LI which is the ratio of the difference between the natural water content and the plastic limit over the plasticity index

Table 5.3
Index Soil Properties

	Number of Samples	Average	Range of Values
Natural Water Content %	98	19,5	14-26
Atterberg Limits	55		
Liquid Limit (LL) %		30	20-40
Plastic Limit (PL) %		18	17-19
Plasticity Index (PI) %		12	7-22
Liquidity Index (LI)		0,24	-0,20-0,80
Activity (Ac)		0,28	0,28-0,36
Unit Weight (kN/m ³)		21,0	19-23
Specific Gravity (G)	20	2,77	2,74-2,84
Void Ratio (e)		0,54	0,38-0,74
Porosity (n)		0,35	0,28-0,42
Percent Finer than 2 microns	52	43%	33-59%

ranges from -0,2 to 0,8 with an average value of 0,24.

In his discussion of landslides, Terzaghi (1936) classifies the clays in three main groups: soft intact, stiff intact, and stiff fissured; the difference between soft and stiff is based on the liquidity index, the clay being soft if LI is greater than 0,5 and stiff if LI is near 0. According to Skempton and Hutchinson (1969) most tills are compact and belong to the group of stiff intact clays; fissured clay tills are uncommon except where they have been disturbed by later ice readvances.

5.3.7 Shear Strength.

Determination of shear strength proved a difficult problem for many reasons. The size of the study area prevented an extensive program of sampling and testing and laboratory work was carried only on a few representative samples of the materials forming the bluffs. Some difficulties are inherent to the geological conditions such as non homogeneity of material, presence of large particles, distortion of lacustrine sediments by overriding till, and so on. The problem of sampling was important also; from boreholes only badly disturbed split-spoon samples were obtained since it was impossible to drive thin wall samplers due to the stiffness of till and the presence of coarse particles. Digging for block samples proved a dangerous operation in this period of high lake levels when no access was provided to the lower slopes.

The purpose was then to get a logical estimate of strength based on penetration tests (undrained strength) and direct shear test in the lab. A crude relationship given by Terzaghi and Peck (1967) allows the estimation of undrained shear strength for clays; for instance undrained strength is between 100 and 200 kN/m^2 for stiff soils (15 to 30 blows per foot) and larger than 200 kN/m^2 for hard soils (more than 30 blows per foot). All soils encountered had a resistance higher than 20 blows per foot which corresponds to shear strength greater than about 150 kN/m^2 (3000 psf).

Drained shear strength was measured with a direct shear box. Quigley and Tutt (1968) investigated the tills at the Geography Station using this method. Undisturbed samples from Fort Burwell and Fort Talbot were tested at low rates of shearing (0,0073 to 0,037 mm/mm) to allow dissipation of pore pressure. The dimensions of the samples were 6 by 6 by 1,5 cm and the test procedure follows standard method (Lambe 1951).

The block sample at Fort Talbot was first tested at its natural moisture content (18-19%) and typical stress-strain curves are shown on figure 5.16. The failure envelope is illustrated on Figure 5.17; the parameters c_d and ϕ_d are respectively 23 kN/m^2 and $24,5^\circ$. Since the material near the surface is subjected to cycles of drying and wetting, those conditions were simulated in the shear box by drying a sample and subsequently allowing it to get soaked by water. An other series of tests involved making samples out of

powder (of the same block) and soaking it in the shear box. The samples were allowed to consolidate and then sheared under drained conditions. This drastic treatment does not affect the shear strength parameters too much; there is a decrease in cohesion from 23 to 8 kN/m^2 but the friction angle increases slightly to 26° (Figure 5.17).

Lacustrine clayey silt from Port Burwell was tested at low normal stresses (below 100 kN/m^2) since most slides in that area occur on flatter slopes and involve only surficial materials. This curve is plotted also for comparison on Figure 5.17. The drained shear strength parameters are c_d of 0 kN/m^2 and ϕ_d of 33° . The results of these tests including those of Quigley and Tutt (1968) for the Geography Station are summarized in Table 5.4.

The friction angle for sand was estimated from standard penetration tests (Teng 1962). For the sand at the Geography Station and at Port Burwell, the penetration resistance varies between 20 and 50 blows per foot which classifies this soil as a medium to dense sand with a ϕ angle of 33 to 37° .

The shear strength data is far from exhaustive but it compares well with data on similar soils in the literature (Wu 1966, Terzaghi and Peck 1967, Lambe and Whitman 1969) based on different soils with similar index properties or origin. Generally the cohesion intercept c_d varies between 5 and 25 kN/m^2 for stiff glacial clays and friction angle varies between 25 and 33° depending on the plasticity index or the activity ratio. For the study area

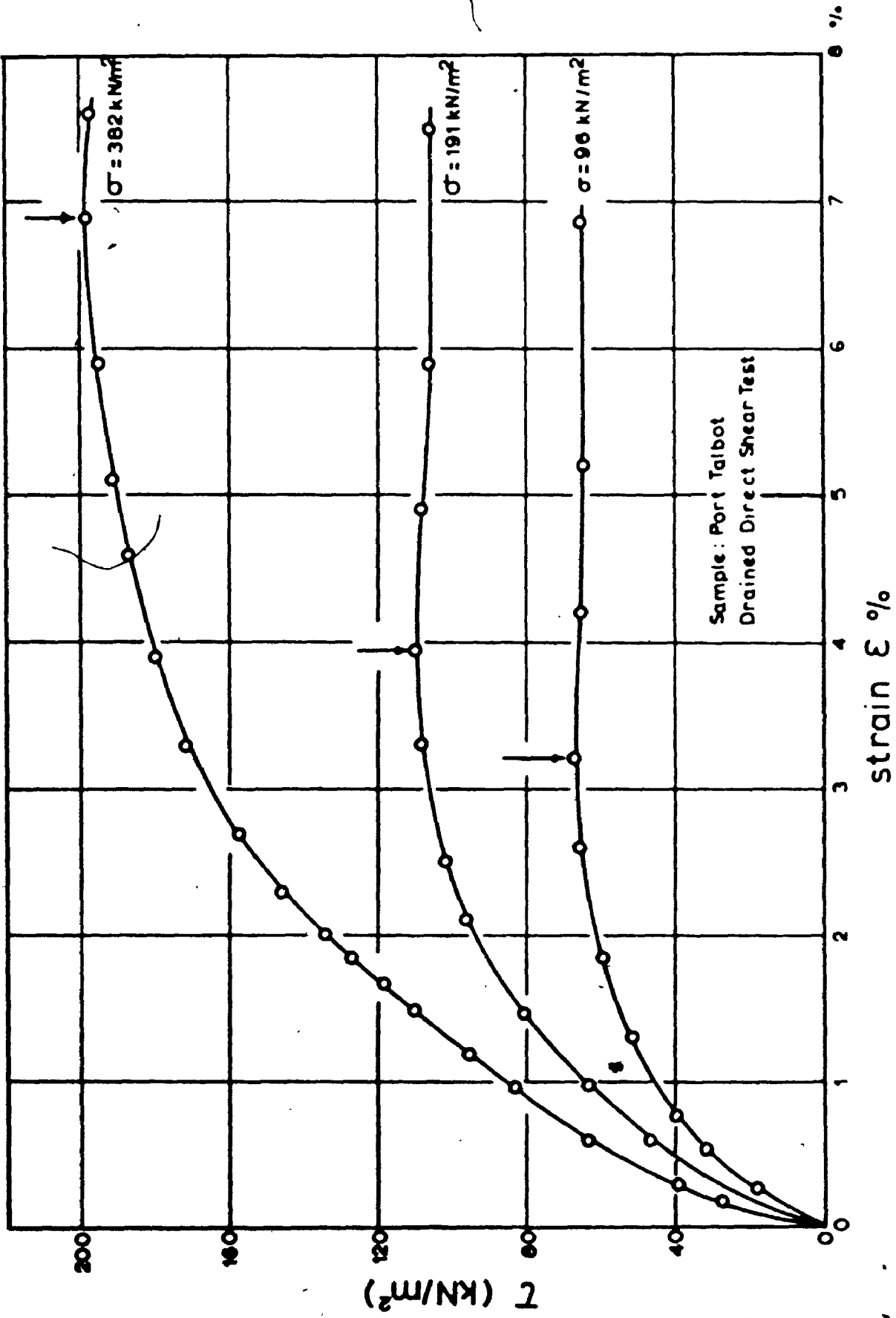


Fig. 5.16 Typical Stress-Strain Curves, Port Stanley Drift.

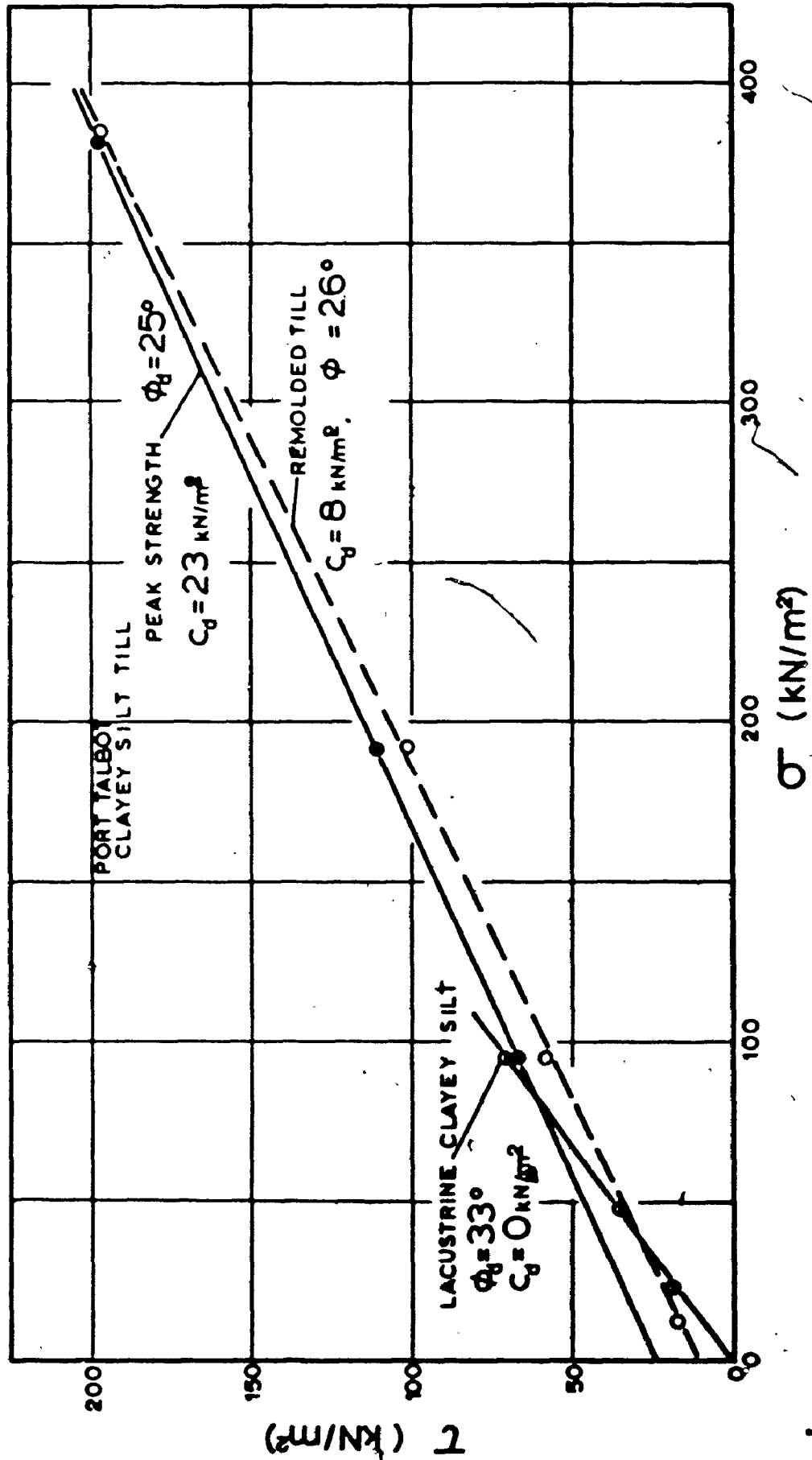


Fig. 5.17 Shear Strength Parameters, Glacial Materials.

Table 5.4

Drained Shear Strength Parameters

Location	Depth (m)	Water Content %	c_d kN/m ²	ϕ_d	Notes:
Fort Burwell	8	26	6,0	33°	Lacustrine
Fort Talbot	Lake level	19	23,0	24,5°	Fort Stanley Till
"	"	18-20	8,0	26,3°	Remolded by drying and slaking
Geography Station*	8	18	33,5	26°	Fort Stanley Till
"	23	19	13,4	28°	"
"	Lake level	21	16,7	28°	"

* Data from Quigley and Tutt, 1968.

the tests results may not warrant wide extrapolation, but because of similarities in water content, Atterberg limits, grain size, mineralogy, and geological provenance of these soils it is assumed that the properties in Table 5.4 are representative of the order of values that may be expected.

The data on shear strength will be used to assess the relative stability of a slope of changing geometry caused by erosion and degradation.

5.4 Stability of Lake Erie Bluffs.

Long-term slope stability of the bluffs is difficult to analyse because the slopes are in constant evolution due to the combined effect of toe erosion and weathering. The discussion on stability will first review some of the factors that control slope stability and after see some examples of stability analysis for a variety of local conditions.

5.4.1 Preliminary Considerations.

The stability of natural slopes is usually considered as a long-term problem. However, the bluffs are not maintaining a constant geometry with time; toe erosion is often high enough to lead to short-term slope failure in the form of falls or shallow slips; weathering also contributes to flatten slopes and in this way tends to increase the long-term factor of safety. Therefore the type of failure and the method of stability analysis is dependent on the relationship that exist between rates of erosion and rates of slope

degradation by weathering (Hutchinson 1967, 1971).

If weathering is in balance with erosion rates the amount of debris released from the bluffs by shallow slips, mudslides and falls is removed by wave action and never unweathered material is eroded directly. This situation is quite rare along the study area and may develop only during a long period of low lake levels. If erosion rates are greater than weathering, there is steepening of the toe of the slope and attack of 'in situ' (unweathered) material, leading to instability in the form of shallow failures (soil falls, shallow toe failures) or deeper rotational failures. If erosion is nil, as is the case behind the wide beaches at Fort Stanley, Port Bruce and Fort Burwell, degradation by weathering will usually cause shallow mudslides that reduce slope angles to their ultimate angle of stability against sliding. Examples of the last two situations will be given in the next section on slope stability analysis.

5.4.2 Softening and Progressive Failure.

Other factors that may influence the long-term stability of the bluffs are softening of the clay silt till and progressive failure. It was shown earlier (Sections 4.5 and 4.6) how cycles of drying and wetting affect the properties of till, especially their water content and resistance to erosion. The zone of weathered material at the surface of the slope receives annually large amounts of water in the form of rainfall, groundwater seepage and wave splashing.

Softening occurs also subsequent to unloading by excavation, erosion or after a slide (Terzaghi 1936, Skempton and Hutchinson 1969); however this last mechanism has a minor effect in the study area since water contents determined in deep boreholes far from the slope are consistent with those determined from block samples in the toe area. Most of the softening then seems to occur in the surficial materials at depths less than a few meters; during the wet season, water content near the surface rises to 35-45% as compared with 18-22% for 'in situ' materials. In softened clays, ϕ_0 may remain sensibly constant if the clay is not sheared, but the value of c_d will tend to zero (Skempton and Hutchinson 1969) as was shown in the direct shear tests on remolded materials.

Progressive failure occurs when some points in the soil mass are stressed beyond their peak strength; after failure of that small element stresses are transferred to adjacent elements as the failure zone progresses in the soil mass (Terzaghi and Peck 1967, Bjerrum 1967). Necessary conditions for progressive failure have been outlined by Lo (1972): 1) the material should have a strain-softening post-peak stress-strain relationship, and 2) non-uniform stresses and strains should exist so that the peak strength is exceeded at some points in the soil leading to redistribution of stresses. The second condition is easily met by the stresses developed from the geometry of the problem; the first condition may be evaluated by considering the brittleness index of the soil (Bishop 1967). This index is defined as the ratio of the difference between peak strength

and residual strength over the peak strength; this ratio is zero for non-brittle, plastic soils, and approaches one for very sensitive soils. Based on the data from Quigley and Tutt (1968) the brittleness ratio varies between 0,10 and 0,38 which means that the till does not lose much shear strength after it has reached its peak value. The problem becomes more complex if the time dimension is added. Because the geometry of the bluffs changes rapidly due to toe erosion and degradation by weathering, stress redistribution occurs continuously without necessarily working on a well-defined failure zone. Toe steepening would logically lead to progressive failure but it remains to be known if erosion rates are faster than the rate of shearing induced by progressive failure.

5.4.3 Methods of Stability Analysis.

The parameters used for stability analysis were discussed previously and are summarized here. The slope geometry was determined by surveying with a transit and inclined stadia; points on the top of each section were established by precise levelling from known elevation bench marks. The sections south of Iona and south of Wallacetown are taken from the report on erosion by the Department of Public Works (DPW 1969) and were surveyed in 1964-65. Groundwater flow is assumed to be parallel to the slope of the ground for all shallow failure analysis; this is based on observations of piezometers and wells at several localities as discussed

in section 5.2. In areas where sand forms a deep layer near the surface, the flow net is assumed to be of the shape of the net illustrated in Figure 5.11, with adjustments for location of groundwater table in the surficial sand. In general the analysis is performed for high groundwater levels with water table at the surface along the slope.

Soil properties as summarized in Tables 5.3 and 5.4 are assumed to be typical of the glacial materials in the area. The cohesion intercept is taken as zero and the friction angle remains constant for weathered material. It is interesting to note that the strength properties of weathered soils are similar to the ultimate or residual strength parameters for the same soils (Quigley and Tutt 1968); there is an important loss of cohesion without much reduction in frictional properties for soils of low plasticity and low clay content (Skempton 1964).

The stability analyses were done by using Bishop's simplified method of slices where the forces acting on the side of any slice are assumed to have a zero resultant in the vertical direction (Bishop 1955). The factor of safety, F , is defined as

$$F = \frac{\sum_{i=1}^n (c_d \cdot x_i + (w_i - u_i) \cdot x_i \tan \phi_d) (1 / \cos \theta_i (1 + \tan \theta_i \cdot \tan \beta))}{\sum_{i=1}^n w_i \cdot \sin \theta_i}$$

where (Figure 5.18) x_i is the width of each slice in meters, c_d is the drained cohesion intercept (kN/m^2), w_i is the weight of each slice (kN), u_i is the pore-water pressure at the base

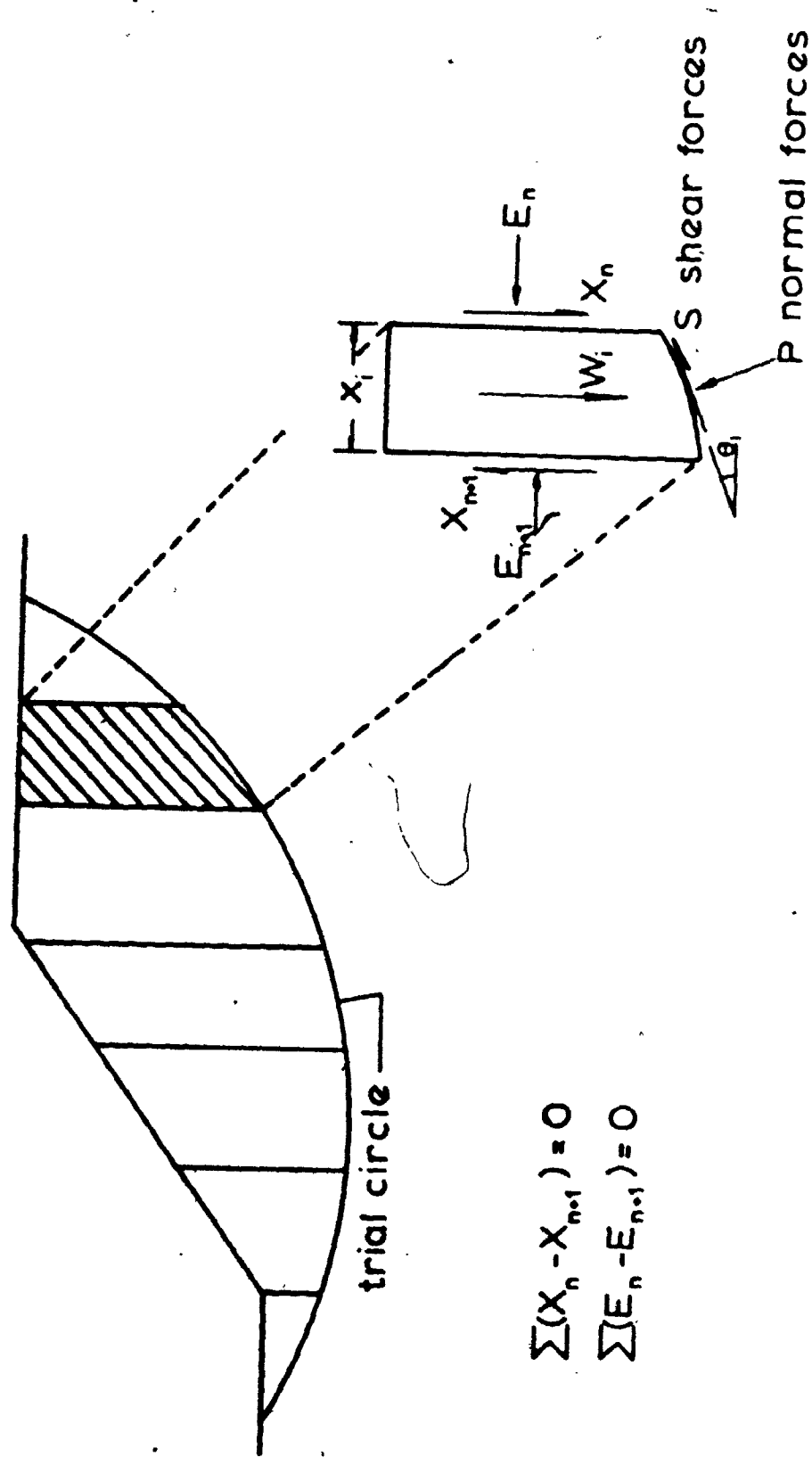


Fig. 5.18 Forces in the Slices Method (Bishop, 1955).

of each slice (kN/m^2), ϕ_d is the drained friction angle, and θ_i is the angle between the tangent to the base of each slice and the horizontal.

Since the factor of safety appears on both side of the equation, the solution is found by trial and error method by first assuming a value for F and calculating the factor of safety. Several circles were calculated at each of the locations in an effort to find the most critical failure plane.

Short-term stability analysis was done by using a much simplified expression for the factor of safety, always using the slice method; the $\phi=0$ analysis assumes that all the resistance to sliding is provided by the undrained shear strength, S_u , mobilized along the failure surface. Therefore

$$F = \frac{\sum S_u \cdot dl_i}{\sum W_i \cdot \sin \theta_i}$$

where dl_i is the length of each slice along the failure plane. Due to uncertainties in the value of S_u the factor of safety is calculated for estimated values of $S_u = 150 \text{ kN/m}^2$ (3100 psf) and 200 kN/m^2 (4200 psf) which are on the conservative side.

The stability of mudslides can be estimated by assuming that failure occurs on an infinite slope and that the failure surface is more or less planar. Since this type of slide develops in deeply weathered and disturbed materials, it is assumed that cohesion is zero and only friction forces are operative. It was also observed that those slides occur principally in periods of high water table and for stability analysis it is supposed that the water table is at the

surface. The classical analysis of this problem (Taylor 1948) gives the following expression as the condition for static equilibrium

$$\tan i = \frac{\gamma_b}{\gamma_t} \tan \phi_d$$

where i is the angle of the slope, γ_b the buoyant unit weight and γ_t the total (saturated) unit weight of the soil.

The results of stability analyses on several sections where geotechnical information exists (boreholes, piezometers, etc.) are discussed in the next section.

5.4.4 Results of Stability Analysis.

Four different sites were investigated for long- and short-term stability: the sections at Fort Burwell, Port Bruce, Iona, and Wallacetown were described earlier in Figures 5.3 to 5.7 and the groundwater conditions and soil properties were studied in deep boreholes at each location.

The conditions at Wallacetown are shown on Figure 5.7 and 5.19; in general the slopes are gentle at 25-30° except for a wave-cut cliff near the toe which is almost vertical for a height of 5 to 10 meters, as observed during a period of high lake level (1969-72); surveys in 1964-65 (DPW 1969) do not show the presence of a cliff at that location indicating that the rate of erosion has been between 1.0 and 2.0 meters per year during that interval of time. Toe circles show a factor of safety between 0.79 and 1.1 over long-term conditions and factors of safety greater than

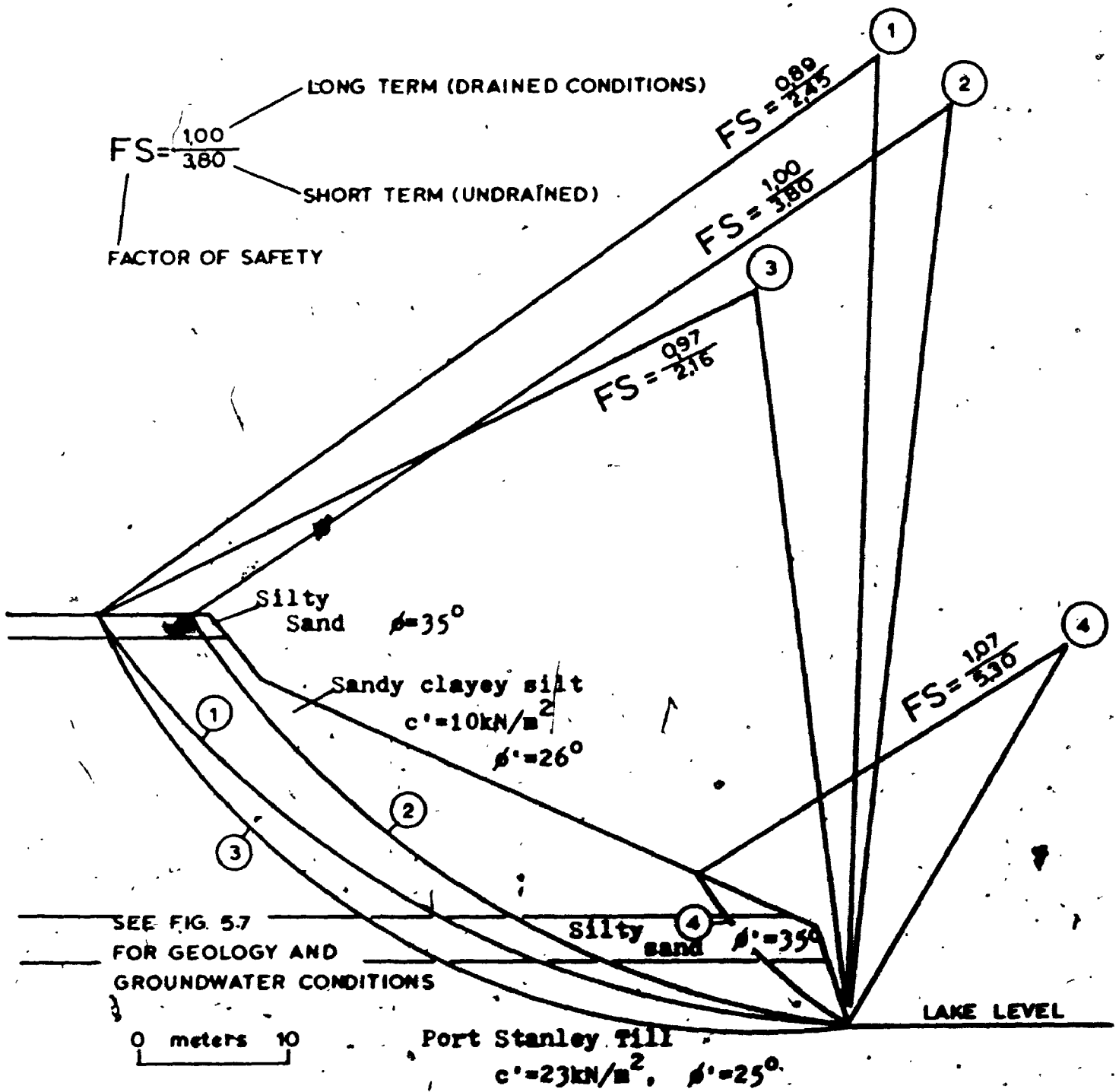


Fig. 5.19 Stability Conditions at Wallacetown (Tyrconnell).

2,0 for short-term conditions. No rotational slides are observed in that area since the long-term erosion rates are on the average 0,50 meter per year. It is thought that the weathering processes are acting fast enough to induce flattening of the slope before long-term shear strength is fully mobilized. The most common types of mass movements observed are shallow mudslides in the median part of the bluff and soil falls in the toe area during periods of high lake levels.

At Iona the bluffs are higher (36 meters) but the geometry is very similar to the slopes at Wallacetown (Figures 5,6 and 5.20). Long-term erosion rates are in the range of 1,0 meter per year, and a cliff of about 10 meters has developed at the base in the last few years. The long-term factor of safety is from 0,94 to 1,2 and the short-term factor is greater than 2,0. Several shallow failures occur near the the edge of the bluffs but none seems to reach the toe of the slope; this is probably due to the presence of a sandy-silt layer at about 22 meters below surface. The shallow slips contribute to the rapid flattening of the slope and supply much debris that protects the toe of the bluff against more severe erosion. Aided by surficial weathering, these minor slips contribute to the equilibrium that exists between rates of erosion and rates of weathering.

The section west of Port Bruce (Geography Station) is quite typical of the slopes between Fort Stanley and Port Bruce. Usually a thick layer of sand is present at the top of the section so that groundwater flow nets will have the

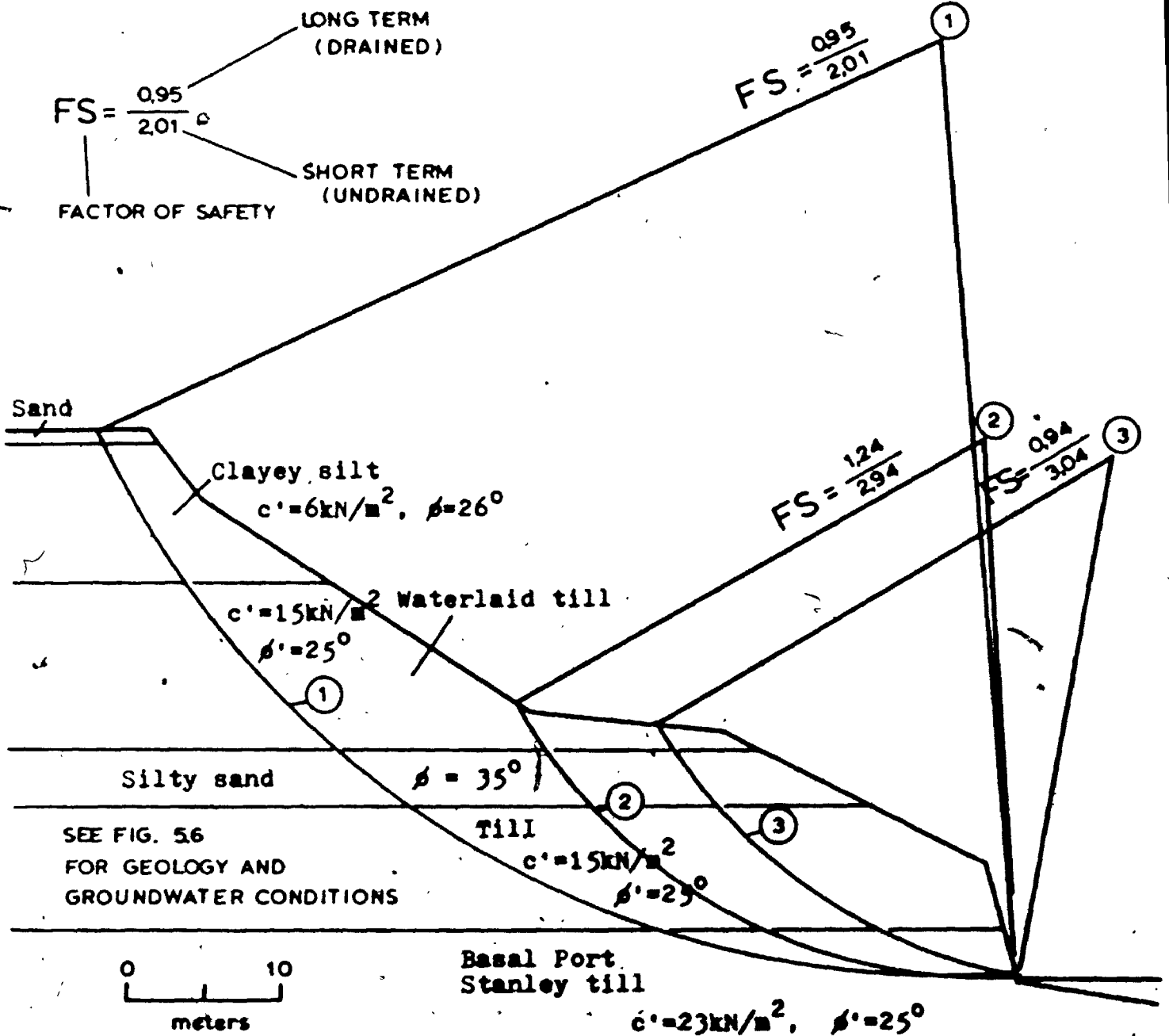


Fig. 5.20 Stability Conditions at Iona.

same shape as the one illustrated on Figure 5.11. The stability calculations were done for two different slope geometry: the first section, Figure 5.21, represents the slope during a period of low lake levels as surveyed by the Department of Public Works (DPW 1969). The factor of safety over the long-term is between 0.80 and 0.90 for several sections intersecting the toe. In fact several slope failures occur in this portion of the shoreline, the best ones being just east of Fort Stanley in the vicinity of the new pumping station. The steeper failure circles and the shallower are more critical. The short-term factor of safety is usually above 1.3 for the trial circles.

A second section at the Geography Station represents the conditions after several years of high lake levels and severe toe erosion at rates higher than 2.0 meters per year as compared with long-term average of 1.4 to 1.6 m/y in the vicinity of the Geography Station. The geometry of the slope is different in two ways: at the toe the slope is much steeper with an overall angle on 65° and a near vertical cliff at the base; in the upper slope there are many instances of shallow failures near the edge of the bluff that extend to mid-height near the contact between sand and till (section 5.1). Due to increased steepness the factor of safety for long-term stability are in the range of 0.75 to 0.80. This decrease in factors of safety can be attributed to base erosion modifying the geometry of the slope. This process is observable everywhere as the result of fluctuations in lake levels with consequent changes in erosion rates.

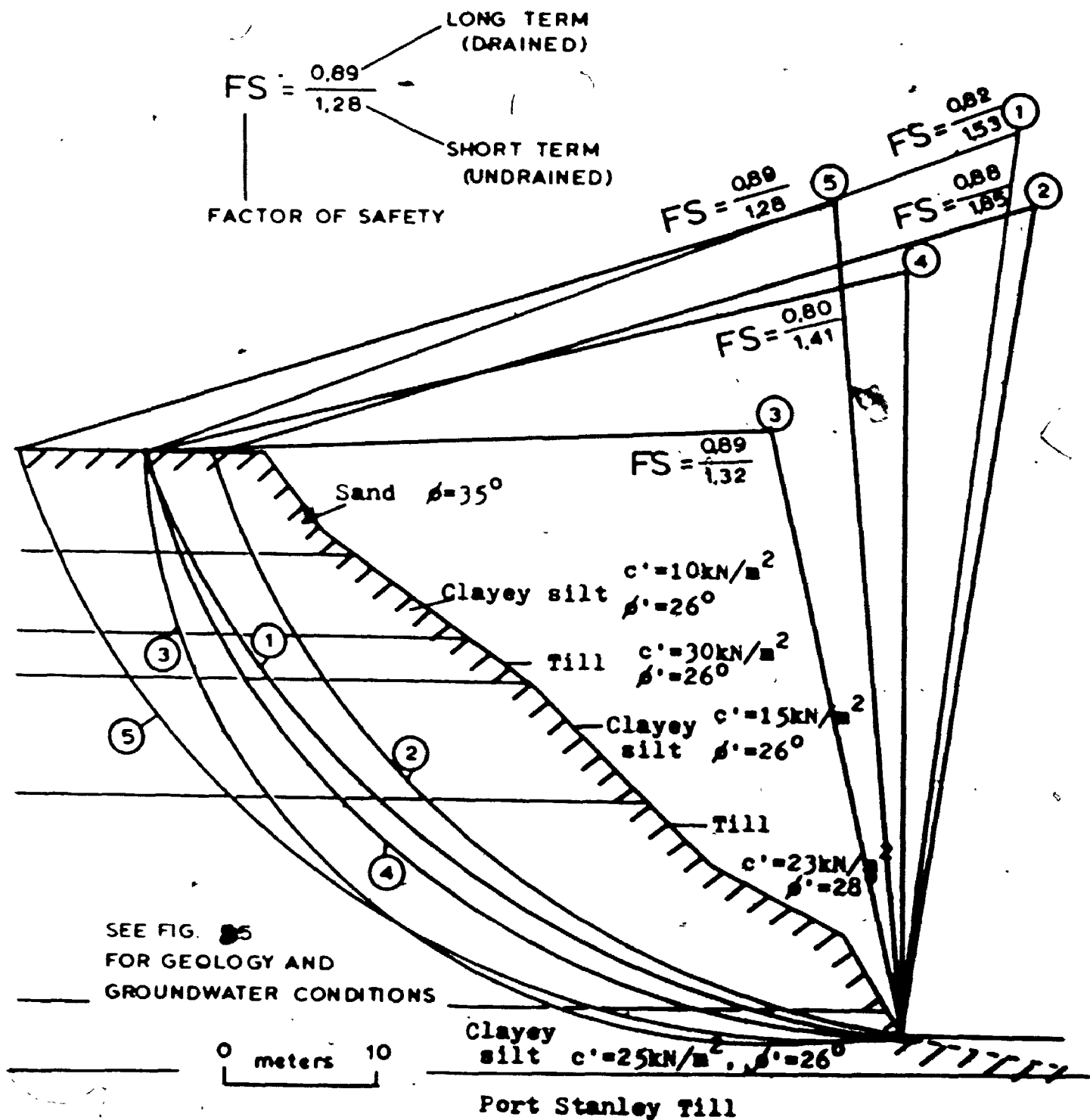


Fig. 5.21 Stability Conditions at the Geography Station (low lake level).

$$FS = \frac{0.77}{2.31}$$

LONG TERM (DRAINED)
SHORT TERM (UNDRAINED)
FACTOR OF SAFETY

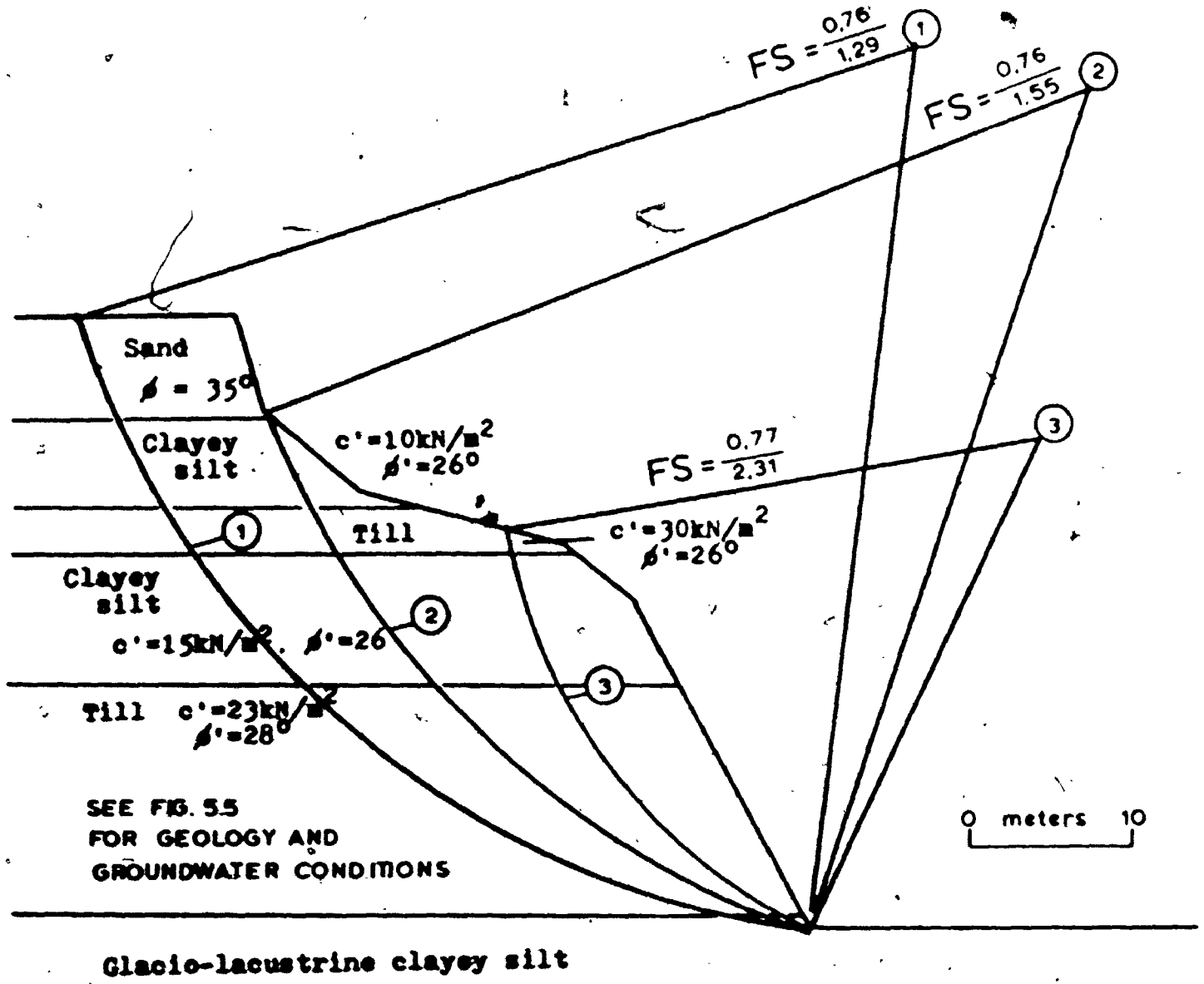


Fig. 5.22 Stability Conditions at the Geography Station. (high lake level).

The occurrence of numerous failures between Fort Stanley and Fort Bruce is a good illustration of the fact that weathering and flattening of the slopes are not in equilibrium with the forces of erosion. Rapid desintegration of the 'in situ' material by landsliding is then a probable cause for the anomalously high rates of erosion observed in that area. The presence of aquifer sand on the top of the bluffs also decreases stability by supplying water that infiltrates through dessication cracks and induce softening of the mass. Inspection of slide debris suggests that the rate of movement of the soil mass during sliding was very rapid and caused the complete desintegration of the sliding block.

The last section at Fort Burwell represents a stabilized slope; the toe of the slope is protected by a wide accretion beach and the action of waves at the toe of the slope has not been felt since the beginning of the twentieth century. The base of the slope has developed a system of underdrainage since the original beach was covered with debris coming from the weathering of the upper slope. A small cliff (1 meter) is still present on the top of the section sustained by the root mat. The most common type of mass movement is shallow mudslides moving intermittently with seasons when slaked material is completely saturated by rising water table. These movements however seem to have stopped on that slope as evidenced by vegetation and the presence of adult trees. The drained factor of safety against sliding is 1.5. Since the slope angle is only 22° this probably represents the residual angle of friction for

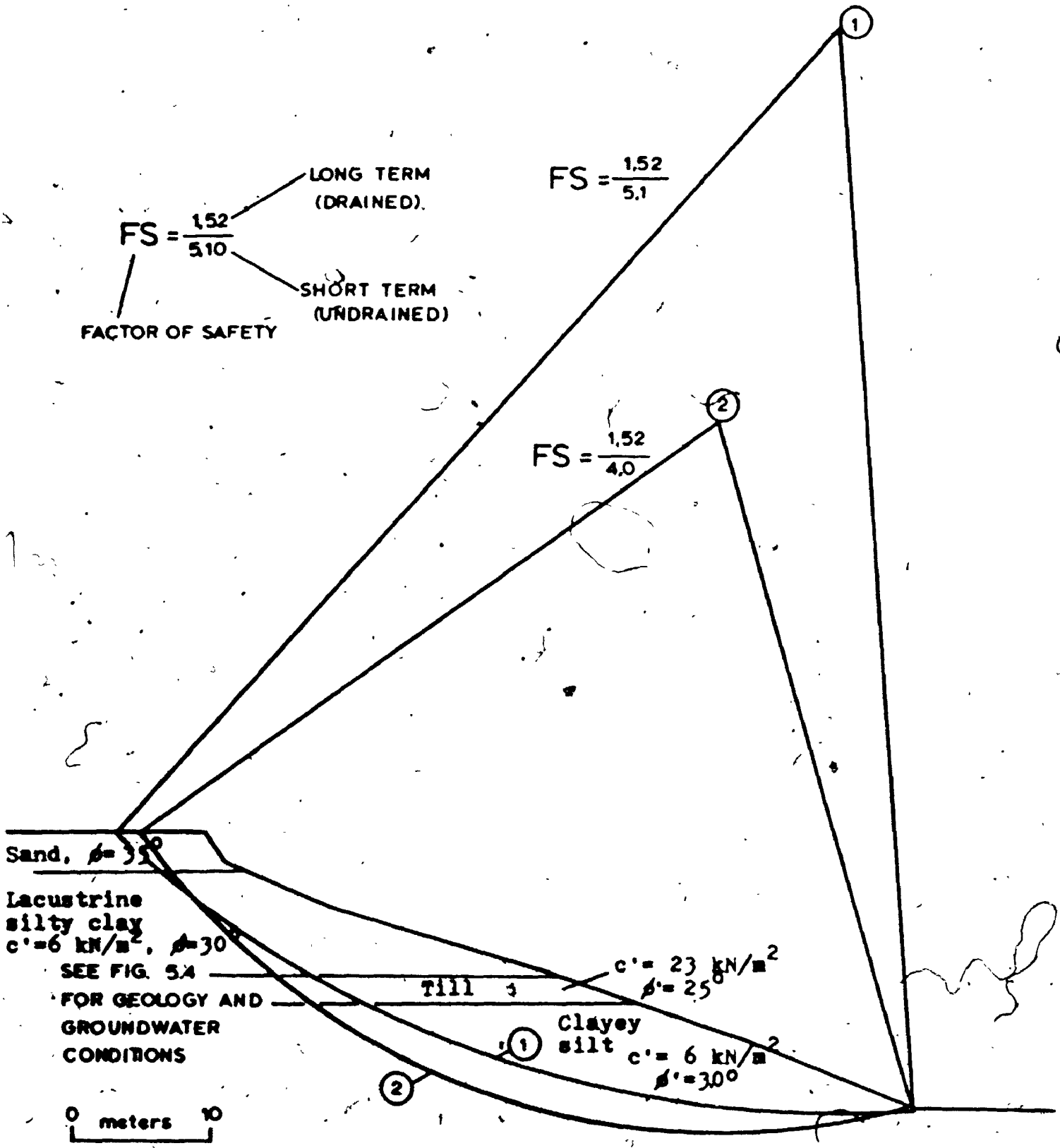


Fig. 5.23 Stability Conditions, Port Burwell.

10. Since the geometry of the slopes keeps changing in response to erosion and weathering, stability analysis will be representative of one instant in time. Factors of safety are continuously decreasing until failure occurs; if the toe of the slope is stabilized, weathering will flatten the bluffs and consequently factors of safety will increase more and more with time.

As mentioned in the introduction, erosion is a complex problem involving processes such as wave action, storm setup, lake level fluctuations, drying and wetting of the materials, freezing and thawing, and also it involves materials that have a certain composition, stratigraphy, resistance to erosion or resistance to shear. Several other factors that were neglected in this study may also have some importance: interference of man, vegetation, earthquakes, freezing of the lake surface, movement of drift along the shoreline, profile of the lake bottom near the shore, etc. For these reasons it is not possible at this time to have a deterministic model that permits a prediction of erosion rates if one knows only some meteorological parameters or some properties of the soils or the geometry of the bluffs.

The model presented here is a statistical relationship between the most important of these factors (wave action) and long-term erosion rates. Better knowledge of the mechanics of erosion could improve on that model.

If the rate of degradation is slow, the stability may be assessed by classical methods as discussed above, but on the contrary if rates of degradation are high, the flattening of the slope through a series of minor events (falls, mudslides, erosion by runoff) may cope with the stability problem and prevent long-term slope failure along a deeper sliding plane.

Because of the preceding factors, it is not surprising to note that major slope failures by rotational sliding are not very common along the bluffs. In areas where erosion rates are low (less than 1 meter per year) it seems that the rate of weathering and degradation can help the slope to adjust to erosion and consequently no major failure occurs; in this case, if stabilisation at the base is afforded, no slope failure will occur with time as the slope angle is reduced before the long-term conditions are reached. In zones of strong erosion rates, the equilibrium is never achieved between erosion and weathering leading to major slope failures that tend to reestablish equilibrium. It is worth mentioning that zones of very active erosion correspond well to areas where surficial sands are thick or with areas where a layer of low resistance to erosion occurs at lake level (lacustrine sand and silt in the vicinity of Fort Stanley, and the sand layer extending to lake level at Sand Hill). The controls of areas subjected to sliding are then of two types: adverse groundwater conditions in areas capped by sand, and greater erosion rates in materials having a low resistance to the action of waves. At present, it is not possible to say which factor is more determinant for failure.

CHAPTER SIX
SUMMARY AND CONCLUSIONS

6.1 Summary.

Long-term erosion rates are estimated by comparison of early surveys of Lake Erie townships and recent air photographs of the same area. They represent the combined effect of active forces such as wave action, storm setup, and lake level fluctuations, as well as passive factors such as lithology, water content, slope angle, etc.

Wave energy and associated lake effects can explain in a large proportion (75%) erosion rates that are observed. The local geology will in the last instance control the rates of erosion because of the different resistance to erosion of the materials outcropping at lake level (sand and silt in the vicinity of Port Stanley and east of Port Burwell). Cyclic drying and wetting, because of the volume change it causes in fine-grained soils is the primary weathering factor bringing about slope flattening and degradation.

Bluff geometry and the occurrence of slides along the north shore represent an instantaneous picture of the state of equilibrium that exists between the different factors shaping the coastline: erosion, weathering, height, geology, groundwater conditions, strength of materials, etc. Since the bluffs are in constant evolution, every analysis

is valid only for the time at which that analysis is performed. Ultimate slope stability is achieved only a long time after the slope has been protected from waves at the toe and flattened through weathering.

6.2 Conclusions.

The more important conclusions of the research performed for this thesis are presented below in point form.

1. In general, erosion rates increase from West to East in the study area. The average rate is 1.30 meter per year with extreme values near zero in the western part (even negative values of erosion when accretion progresses near groynes and jetties) and reaching 3 meters per year near Port Stanley and east of Port Burwell. Several irregularities modify that trend; they are caused by changes in geology, height of bluffs, occurrence of landslides, construction of defence works, etc.
2. Erosion rates were calculated as an average over a long interval of time (approximately 150 years) to minimize the influence of rare events. Long-term rates represent a state of equilibrium between erosive forces and the resistance of the materials forming the coastline.

3. By comparison with rates calculated over shorter intervals of time and by analysis of long-term fluctuations in lake levels, the minimum period of observation required to give a good estimate of the average rate of erosion is 25 years.
4. Winds are indirectly an important cause of erosion in generating waves over the lake. Predominant winds are from the West and the South-West. This orientation with respect to the shoreline will favor more intense erosion in the eastern part of the study area in agreement with observed erosion rates.
5. Models of wave forecasting from meteorological data were used to obtain an estimate of the amount of wave energy available for erosion. The interest resides not in the absolute values but in the distribution of the computed wave energy along the shoreline. A good correlation was obtained between erosion rates and total wave energy. This model can explain as much as 75% of the erosion occurring along the north shore.
6. Storms setups and high lake levels increase erosion in the eastern part of the study area; flooding of protective beaches allows waves to reach the toe of the bluffs more easily. In periods of low lake levels, most of the energy is spent offshore and very little erosion occurs on the bluffs themselves. Long-term erosion rates take into account these two extreme cases. The five-year wind record includes typical

storms on Lake Erie and this period is long enough to be statistically meaningful when calculating wave energy.

7. Major discrepancies in erosion rates are caused by local variations in geology. Sand and silt outcropping at lake level usually correspond to areas of excessive erosion because of the lack of cohesion of these materials (east of Port Stanley and near Sand Hill are good examples). Clay and till in the area provide a good resistance in the saturated state.
8. Physical weathering in the form of drying and wetting causes a reduction in the cohesion of fine-grained material through shrinkage and swelling. This process of slaking is responsible for the loss of resistance to erosion of fine-grained soils when allowed to soak in water after drying at a water content lower than their shrinkage limit. Slaking is also responsible for the degradation and flattening of slopes in areas not subjected to wave erosion.
9. The shallow landslides observed in the study area can be explained mainly by oversteepening of the bluffs. Locally, the soil properties will have some influence on the type of failure but also local stratigraphy and groundwater conditions. The combination of fast erosion rates at the toe and thick sand layers at the surface (seepage problem) are critical when weathering and degradation on the slopes proceed at a slower pace than erosion.

10. Since the geometry of the slopes keeps changing in response to erosion and weathering, stability analysis will be representative of one instant in time. Factors of safety are continuously decreasing until failure occurs; if the toe of the slope is stabilized, weathering will flatten the bluffs and consequently factors of safety will increase more and more with time.

As mentioned in the introduction, erosion is a complex problem involving processes such as wave action, storm setup, lake level fluctuations, drying and wetting of the materials, freezing and thawing, and also it involves materials that have a certain composition, stratigraphy, resistance to erosion or resistance to shear. Several other factors that were neglected in this study may also have some importance: interference of man, vegetation, earthquakes, freezing of the lake surface, movement of drift along the shoreline, profile of the lake bottom near the shore, etc. For these reasons it is not possible at this time to have a deterministic model that permits a prediction of erosion rates if one knows only some meteorological parameters or some properties of the soils or the geometry of the bluffs.

The model presented here is a statistical relationship between the most important of these factors (wave action) and long-term erosion rates. Better knowledge of the mechanics of erosion could improve on that model.

6.3 Suggestions for Future work.

Several problems related to shoreline erosion are still to be resolved. Two of them are of special interest for all Great Lakes problems: the generation of waves on lakes and the transfer of energy from waves to shoreline, and secondly the evolution of slope stability with time and with changing geometry of the bluffs.

Wave generation is still calculated with empirical models based on studies performed usually for seas or oceans. For any important project, instruments should be installed that measure the wave spectrum along with relevant meteorological parameters. At different distances from the shoreline it would then be possible to study how the total energy is being spent between the breaking point of waves and the bluffs. Concomitantly studies on the influence of beaches and defence works on the distribution of erosion should be made possible in the bluff area.

Since slope stability is dependant on erosion rates that shape the lower part of the bluffs, and that some soil properties are time dependant, more research is needed to discriminate between the failures caused by softening of the soils from the ones caused by oversteepening. For that purpose, more testing is needed on the hard till, and also better field methods to assess the degree of fissuring of a mass of soil that is macroscopically jointed at the surface.

BIBLIOGRAPHY

- A.S.C.E., 1961. American Society of Civil engineers, Report of Task Committee on Wind Forces; Structural Division, Trans., vol. 126:1124-1198.
- Baver, D.J., Gardner, W.H., and Gardner, W.R., 1972. Soil Physics. 4th ed. New York, John Wiley and Sons. 498p.
- Bazett, D.J., Adams, J.L., and Matyas, E.L., 1961. An investigation of a slide in a test trench excavated in fissured sensitive clay. Proc. 5th Int. Conf. Soil Mech. and Found. Eng., Paris, 1:431-435.
- Bishop, A.W., 1955. The use of the slip circle in the stability analysis of slopes. Géotechnique 5:7-17.
- Bishop, A.W., 1967. Progressive failure, with special reference to the mechanism causing it. Proc. Geotech. Conf. (Oslo), 2:3-10.
- Bjerrum, L., 1967. Progressive failure of slopes of over-consolidated clays and clay shales. Proc. A.S.C.E., 93:1-49.
- Blunt, W.T., 1897. Effects of gales on Lake Erie. Report to U.S. Deep Waterways Comm., 155 p.
- Brebner, A., and Kennedy, R.J., 1962. Correlation of waves and shore winds, Lake Ontario. Proc. 5th Conf. Great Lakes Res., p.116-122.
- Bretschneider, C.L., 1954. Generation of wind waves over a shallow bottom. U.S. Army Corps of Engineers, Beach Erosion Board, Tech. Memo. No. 51.
- Bretschneider, C.L., 1956. Wave statistics for the Gulf of Mexico. U.S. Army Corps of Engineers, Beach Erosion Board, Tech. Memo. Nos. 86, 87, 88, 89.
- Bretschneider, C.L., 1958. Revisions in wave forecasting; deep and shallow water. Proc. ASCE, Waterways and Harbors Div., WW2, Paper 1568.
- Bretschneider, C.L., 1959. Wave variability and wave spectra for wind-generated gravity waves. U.S. Army Corps of Engineers, Beach Erosion Board, Tech. Memo. n. 118.
- Bretschneider, C.L., 1959. Engineering aspects of hurricane surge. Proc. Tech. Conf. Hurricanes, Miami, Am. Meteor. Society.

Bretschneider, C.L., 1963. Modification of wave spectra over continental shelf. Proc. 8th Conf. on Coastal Eng., Mexico City.

Bretschneider, C.L., 1966. Wave generation by wind, deep and shallow water. In Estuary and Coastline Hydrodynamics Ippen, ed. McGraw-Hill, p.133-197.

Bretschneider, C.L., 1967. Storm Surges. In Advances in Hydrosience. Academic Press, New York, Ven Te Chow, ed., vol.4:341-418.

Bretschneider, C.L., and Reid, R.O., 1953. Change in wave height due to bottom friction, percolation and refraction. 34th Ann. Meeting, AGU.

Bruce, J.F., 1968. Atlas of rainfall intensity-duration-frequency data for Canada. Climatological Studies No. 8, Dept. of Transport, Meteorol. Branch, 31pp.

Bryan, R.B., 1969. The development, use and efficiency of indices of soil erodibility. Geoderma 2:5-26.

Caley, J.F., 1941. Paleozoic geology of the brantford area, Ontario. G.S.C., Memoir 226, 176pp.

Caley, J.F., 1943. Paleozoic geology of the London area, Ontario. G.S.C., Memoir 237, 171pp.

Caley, J.F. and Sandford, B.V., 1952. Preliminary maps, Kent County, Ontario, showing drift thickness and bed-rock contours. G.S.C., Paper 52-4.

Chan, H.T., and Kenney, T.C. 1973. Laboratory investigation of permeability ratio of New Liskeard varved soils. Can. Geotech. J., 10:453-472.

Chapman, L.J., and Putnam, L.P., 1966. The Physiography of Southern Ontario. 2nd ed., Toronto, Un. of Toronto Press.

Chieruzzi, R., and Baker, R.P. 1958. A study of Lake Erie bluffs recession. Ohio State Univ. Eng. Expt. Sta. XXVII,6: 100pp.

Childs, E.C., 1969. The Physical Basis of Soil Water Phenomena. Wiley-Interscience. London, 493pp.

Christopher, J.E., 1959. An investigation of Lake Erie shore erosion between Fairport and the Pennsylvania state line. Unpub. Ph.D. Thesis, Ohio State Univ.

- Cole, A.L., 1967. An evaluation of wind analysis and wave hindcasting methods as applied to Great Lakes. Proc. 10th Conf. on Great Lakes RES., pp.186-196.
- Coleman, A.P., 1941. The last million years. A history of the Pleistocene in North America. Toronto, Univ. of Toronto Press, 216pp.
- Cooper, H.H., Bredehoeft, J.D., and Papadopoulos, I.S., 1967. Response of a finite-diameter well to an instantaneous charge of water. Water Resources Research 3:263-269.
- Cornell University, 1951. Final Report on soil solidification research. Ithaca, New York.
- Cuthbert, P.L., 1944. Clay minerals in Lake Erie sediments. American Mineralogist, 29:378-388.
- Earbyshire, J., 1957. Investigation into the generation of waves when the fetch is less than 100 miles. Quat. J. Royal Meteorol. Soc., 82:461-468.
- DeJong, E., and Warkentin, B.P., 1965. Shrinkage of soil samples with varying clay concentration. Can. Geotech. J., 2:16-22.
- Department of Public Works, 1969. Lake Erie shoreline inventory and land use. Prelim. Report to Int. Joint Comm., 111p.
- Dreimanis, A., 1957. Stratigraphy of the Wisconsin Glacial stage along the north-west shore of Lake Erie. Science, 126:166-168.
- Dreimanis, A., 1958. Wisconsin stratigraphy at Port Talbot on the north shore of Lake Erie, Ontario. Ohio J. Sci. 58:65-84.
- Dreimanis, A., 1960. Pre-classical Wisconsin in the eastern portion of the Great Lakes region, North America. Rept. 21st session, Int. Geol. Cong., Norden, part 4:108-126.
- Dreimanis, A., 1961. Tills of Southern Ontario. In Soils in Canada, Roy. Soc. Can. Publ. 3, R.P. Legget, ed., p.80-96.
- Dreimanis, A., 1966. Cross-sections along the north shore of Lake Erie; unpubl. rept. to the Dept. of Public Works, Lake Erie Task Force.
- Dreimanis, A., 1969. Late Pleistocene lakes in the Ontario and Erie basins. Proc. 12th Conf. Great Lakes Res. 170-180.

- Dreimanis, A., 1969. Surficial geology, Fort Stanley map area, Ontario. Geol. Surv. Can. Paper 69-1 Part A:190-1.
- Breimanis, A., 1970. Last ice-age deposits in the Fort Stanley area, Ontario. Geol. Surv. Can. Paper 70-1, Part A, pp.167-169.
- Dreimanis, A., 1971. Wisconsin stratigraphy, north shore of Lake Erie, Ontario. Geol. Surv. Can. Paper 71-1-A p.159-160.
- Dreimanis, A., and Reavely, G.H., 1953. Differentiation of the lower and the upper till along the north shore of Lake Erie. J. Sed. Petrol., 23:238-259.
- Dreimanis, A., Terasmae, J., and McKenzie, G.L., 1966. The Fort Talbot interstage of the Wisconsin glaciation. Can. J. Earth Sc., 3:305-325.
- DosSantos, M.P.P., and de Castro, E., 1965. Soil erosion in roads. International Conf. Soil Mech. Found. Eng., Montreal, 1:116-120.
- Ferrigno, K.F., 1971. Environmental influences on the distribution and abundance of conodonts from the Dundee Limestone, St. Mary's, Ontario. Can. J. Earth Sc., 8:378-386.
- Flint, R.F., 1971. Glacial and Quaternary Geology. New York, John Wiley and Sons, 892pp.
- Garriott, E.B., 1903. Storms of the Great Lakes. U.S. Weather Bureau, Bul. K, 9p.
- Grim, R.E., 1968. Clay Mineralogy. 2nd ed. New York, McGraw-Hill, 596p.
- Grissinger, E.H., 1966. Resistance of selected clay systems to erosion by water. Water Resources Res. 2:131-8.
- Haines, W.B., 1923. The volume changes associated with variations of water content in soil. J. Agr. Sci. 13:296-310.
- Hayford, J.P., 1922. Effects of winds and of barometric pressures on the Great Lakes. Carneg. Inst. of Washington, 133p.
- Hazen, A., 1930. Flood flow. New York. John Wiley and Sons.
- Hellström, B.M.O., 1941. Wind effects on lakes and rivers. Bull. No. 41, Inst. Hydraulics, Roy. Inst. Technol. Stockholm.

- Henry, A.J., 1902. Wind velocity and fluctuations of water level in Lake Erie. U.S. Weather Bureau, Bull. J. 22p.
- Hjulström, P., 1935. Studies on the morphological activities of streams as illustrated by the River Fyris. Univ. Uppsala, Geol. Inst., Bull. 25.
- Hough, J.L., 1958. Geology of the Great Lakes. Urbana, Univ. of Illinois Press.
- Hough, J.L., 1963. The prehistoric Great Lakes of North America. Am. Scientist, 51:84-109.
- Hough, J.L., 1966. Correlation of glacial lake stages in the Huron-Erie and Michigan basins. J. Geol. 74:62-77.
- Hunt, C.B., 1972. Geology of Soils. San Francisco, W.H. Freeman, 344 p.
- Hunt, I.A., 1958. Winds, wind setups and seiches on Lake Erie. U.S. Corps of Eng. Lake Survey, 36 p.
- Hutchinson, J.N., 1967. The free degradation of London Clay cliffs. Proc. of the Geotech. Conf., Oslo, 1:113-8.
- Hutchinson, J.N., 1968. Mass Movements. In Encyclopedia of Geomorphology, Fairbridge, ed., Reinhold Pub., 688-96.
- Hutchinson, J.N., 1970. A coastal mudflow on the London clay cliffs at Beltinge, North Kent. Géotechnique, 20:412-438.
- Hutchinson, J.N., 1971. Field and laboratory measurements of a fall in Upper Chalk cliffs at Joss Bay, Isle of Thanet. Roscoe Memor. Symp., Cambridge Un.
- Hutchinson, J.N., 1971. The response of London clay cliffs to differing rates of erosion. Paper submitted to IRPI Conf. on Natural Slopes Stability and Conservation, Naples.
- Hvorslev, M.J., 1949. Time-lag in the observation of ground-water levels and pressures. U.S. Army Waterways Exper. Sta., Vicksburg, Miss.
- International Joint Commission, 1969. Report to the International Joint Commission on the pollution of Lake Erie. vol. 2.
- Johnson, J.W., O'Brien, M.P., Isaacs, J.D., 1948. Graphical construction of wave refraction diagrams. U.S. Navy Hydrographic Office Publ. No. 605, 45 p.
- Karrow, P.P., 1967. Pleistocene Geology of the Scarborough area. Ont. Dept. Mines, Geol. Rept. no. 46.

- Kempt, A.W., 1971. Organic carbon and nitrogen in the surface sediments of Lakes Ontario, Erie, and Huron. *J.Sed. Petrol.* 41:537-48.
- Kenny, T.C., and Chan, H.T., 1973. Field investigation of permeability ratio of New Liskeard varved soil. *Can. Geotech. J.* 10:473-488.
- Keulegan, G.H., 1953. Hydrodynamic effects of gales on Lake Erie. *J. Res. Natl. Bureau Standards*, 50:99-109.
- Kindle, E.M., 1933. Erosion and sedimentation at Pointe-Pelé. *Ont. Dept. Mines 42nd Rept.*, 42(2):1-29.
- Kirschner, L.D., 1968. Effects of diversions on the Great Lakes. *Proc. Great Lakes Wat. Res. Conf.*, Toronto, 277-310.
- Kite, G., 1973. Crustal movements around the Great Lakes. Unpubl. Ph.D. thesis, Civil Eng. Un. of Ottawa.
- Lambe, T.W., 1951. Soil testing for engineers. John Wiley.
- Lambe, T.W., and Whitman, R.V., 1969. Soil Mechanics. New York, John Wiley, 533 p.
- Lauritzen, C.W., 1948. Apparent specific volume and shrinkage characteristics of soil materials. *Soil Sci.* 65:155-179.
- Leverett, F., and Taylor, F.B., 1915. The pleistocene of Indiana and Michigan and the history of the Great Lakes. *U.S. Geol. Surv. Mono.* 53.
- Lewis, C.P.M., 1966. Sedimentation studies of unconsolidated deposits in the Lake Erie basin. Unpub. Ph.D. Thesis, Univ. of Toronto.
- Lo, K.Y., 1972. An approach to the problem of progressive failure. *Can. Geotech. J.*, 9:407-429.
- Longuet-Higgins, M.S., 1952. On the statistical distribution of the height of sea waves. *J. of Marine Res.* vol. XI, no. 3.
- Marine Sciences Branch, 1970. Water Levels 1969, vol. 1, Inland. Dept. Energy, Mines & Res., Ottawa.
- Miller, W.C., 1967. Vignettes of Early St. Thomas. Sutherland Press, St. Thomas, Ont.
- Morgan, N.A., 1964. Geophysical studies of Lake Erie by shallow marine seismic methods. Unpubl. M.Sc. thesis, Un. of Toronto, 170 p.

- Muir-Wood, A.M., 1969. Coastal Hydraulics. London, Macmillan, 187 pp.
- Muir-Wood, A.M., 1972. Engineering aspects of coastal landslides. Inst. of Civ. Engrs., London, Paper 7421:257-76.
- Neumann, G., 1953. On ocean wave spectra and a new method of forecasting wind-generated sea. U.S. Army Corps of Eng. Beach Erosion Board, Tech. Memo. No. 43.
- Neville, A.M., and Kennedy, J.B., 1964. Basic statistical methods for engineers and scientists. International Textbook Co., Scranton, Pa. 325 p.
- Ontario Department of Lands and Forests, nodate. Unpublished "Reports and Field Notes". Microfilm Series, Toronto.
- Phillips, D.W., and McCulloch, J.A.W., 1972. The climate of the Great Lakes Basin. Climatological Studies no. 20, Environment Canada, Ottawa. 40p. + 57 charts.
- Fincus, H.J., 1959. Type features of the Ohio shoreline of Lake Erie. Proc. A.S.C.E., Rivers and Harbors Div. Paper 2297.
- Fincus, H.J., 1962. Recession of Great Lakes shorelines. in Great Lakes Basin, Am. Assoc. Advanc. Sci., Publ. 71 123-137.
- Platzman, G.W., 1963. Dynamical prediction of wind tides on Lake Erie. Am. Meteor. Soc., Monog. No. 26.
- Foole, W.H., Sanford, B.V., Williams, H. and Kelley, D.G., 1970. Geology of Eastern Canada. in Geology and Economic Minerals of Canada, Douglas, ed, Geol. Surv. Can. Econ. Geol. Reprt. 1, p.227-304.
- Frest, V.K., 1970. Quaternary Geology of Canada. in Geology and Economic Minerals of Canada, Douglas, ed., Geol. Surv. of Can. Econ. Geol. Rept. 1:675-764.
- Putnam, J.A., and Johnson, J.W., 1949. The dissipation of wave energy by bottom friction. Trans. Am. Geophys. Union, 31:674-74.
- Putz, R.R., 1952. Statistical distribution for ocean waves. Trans. Am. Geophys. Union, 33:5.
- Quigley, R.M., 1972. Clay mineralogy, Wisconsin deposits, southwestern Ontario. Int. Geol. Cong. A-42 Field Trip Symp. Civ. Eng. Rept. SM-2-72, Un. West. Ont. 10 p.
- Quigley, R.M., and Dreimanis, A., 1972. Weathered interstadial green clay at Port Talbot, Ont. Can. J. Earth Sc. 9:991-1000.

- Quigley, R.M., and Tutt, D.B., 1968. Stability- Lake Erie north shore bluffs. Proc. 11th Conf, Great Lakes 230-8.
- Richards, T.L., 1964. The Douglas Point project- an analysis of surface winds data. Dept. of Transport, Meteor. Branch, CIR.4092-TEC.534, Toronto.
- Sanford, B.V., 1953. Preliminary maps Elgin County and parts of Middlesex County, Ontario, showing drift thickness and bedrock contours. Geol. Surv. Can. Paper 53-6.
- Sanford, B.V., 1954. Preliminary maps of Norfolk County, Ontario, showing drift-thickness and bedrock contours. Geol. Surv. Can. Paper 53-31.
- Sanford, B.V., 1958. Geologic map of Southwestern Ontario. Map 1062A, Geol. Survey Canada.
- Sanford, B.V., 1962. Sources and occurrences of oil and gas in the sediments of Ontario. Proc. Geol. Assoc. Can. 14:71-82.
- Sanford, B.V., 1968. Devonian of Ontario and Michigan. Proc. Int. Devonian Symp. Calgary, 2:973-999.
- Saville, T., 1953. Wave and lake level Statistics for Lake Erie. U.S. Army Corps Engrs., Beach Eros. Board, Tech. Memo 37.
- Scheid, F., 1968. Numerical Analysis. New York, McGraw-Hill, 422 p.
- Seibel, E. 1973. Shore erosion in relation to lake level in Lake Michigan and Huron. Abstr. 16th Conf. on Great Lakes Res., Huron, Ohio, p. 58.
- Sharpe, C.P.S., 1938. Landslides and related phenomena. New York, Columbia University Press, 137 p.
- Sibul, O., 1955. Laboratory study of the generation of wind waves in shallow water. U.S. Army Corps Engrs. Beach Erosion Board, Tech. Memo., No. 22.
- Sibul, U., 1969. Water Resources of the Big Otter Creek drainage basin. Ontario Water Res. Comm, Wat. Res, Rep.1.
- Skempton, A.W., 1953. The colloidal activity of clay. Proc. 3rd Int. Conf. Soil Mech. and Found. Eng. 1:57.
- Skempton, A.W., 1964. Long-term stability of clay slopes. Géotechnique, 14:77-101.

- Skempton, A.E., and Hutchinson, J.N., 1969. Stability of natural slopes and embankments foundations. Proc. 7th Int. Conf. Soil Mech., Mexico. State-of-the-Art Vol., 291-340.
- Skempton, A.W., and Laroche, F., 1965. The Bradwell slip a short term failure in London clay. Geotechn. 15:221-42.
- Söderblom, R., 1963. Some laboratory experiments on the dispersion and erosion of clay materials. Int. Clay Conf. Stockholm. Macmillan, p. 277-84.
- Spiegel, M.R., 1961. Theory and problems on statistics. New York, Schaum Pub. Co. 359pp.
- Stirk, G.B., 1954. Some aspects of soil shrinkage and the effect of cracking upon water entry into the soil. Austral. J. Agr. Res., 5:279-91.
- Taylor, D.W., 1948. Fundamentals of Soil Mechanics. New York, John Wiley, 700pp.
- Tempany, H.A., 1917. The shrinkage of soils. J. Agr. Sci. 8:312-330.
- Teng, W.C., 1962. Foundation design. Prentice-Hall, 466p.
- Terasmae, J., Karrow, F.P., and Dreimanis, A., 1972. Quaternary stratigraphy and geomorphology of the Eastern Great Lakes region of Southern Ontario. Guidebook A42, 24th Int. Geol. Congress, Montreal, 75pp.
- Terzaghi, K., 1936. Stability of slopes of natural clay. Proc. First Int. Conf. on Soil Mech., 1:161-165.
- Terzaghi, K. and Peck, R.B., 1967. Soil Mechanics in Engineering Practice. John Wiley, New York.
- Thompson, D.W., 1966. Men and Meridians, vol I. Ottawa, Dept of Energy, Mines, and Resources.
- U.S. Army, Corps of Engineers, Beach Erosion Board, 1962. Waves in inland reservoirs. Tech. Memo. 132.
- U.S. Army Coastal Engineering Research Center, 1966. Shore protection, planning, and design. Tech. Rept. 4, 3rd ed.
- Verruijt, A., 1970. Theory of Groundwater Flow. London, Macmillan, 190pp.
- Wall, R.E., 1968. A sub-bottom reflection survey in the central basin of Lake Erie. Geol. Soc. Am. Bull. 79:91-106.

- Warkentin, B.F., and Bozozuk, M., 1961. Shrinking and swelling properties of two Canadian clays. Int. Conf. Soil Mech. Found. Eng., Paris, 1:851-55.
- Weiler, H.S., 1969. Prediction of vertical profiles of wind speed over a lake. Proc. 12th conf. Great Lakes Res. 492-503.
- White, W.A., and Fichler, E., 1959. Water-sorption characteristics of clay minerals. Illinois St. Geol. Surv. Cic. 266, 20pp.
- Williams, B.G., Greenland, D.J., Lindstrom, G.R., and Quirk, J.F., 1966. Techniques for the determination of the stability of soil aggregates. Soil Science 101:157-163.
- Wilson, E.M., 1969. Engineering Hydrology. London, Macmillan, 182pp.
- Wood, H.A.H., 1951. Erosion of the north shore of Lake Erie. Pointe-aux-Fins to Long Point. Unpubl. M.A. thesis, McMaster Univ., Hamilton, 210pp.
- Wu, T.H., 1966. Soil Mechanics. Boston, Allyn and Bacon, 431pp.
- Yamamoto, T., and Anderson, H.W., 1967. Erodibility indices for wildland soils of Oahu, Hawaii, as related to soil forming factors. Water Res. Research, 3:785-98.
- Yoder, R.E., 1936. A direct method of aggregate analysis of soils and a study of the physical nature of erosion losses. J. Am. Soc. Agron. 28:337-351.

ADDITIONAL REFERENCES:

- Brigham, R.J., 1971. Structural Geology of Southwestern Ontario and Southeastern Michigan. Mines and Northern Affairs, Petrol. Res. Section, Paper 71-2, 110p.
- Gale, J.E., 1971. Analysis of Bedrock Topography Mapping in Southwestern Ontario. Unpub. M.Sc. Thesis, Un. of Western Ontario, London, Ontario. 106p.
- Karrow, P.F., 1973. Bedrock Topography in Southwestern Ontario; a progress report. Geol. Assoc. Can. Proc. 25:67-77.

APPENDIX 1

Theory of Gravity Waves

This section shows the provenance of some of the equations used in Chapter 3 to compute wave energy. Most of the material is taken from Milne-Thompson (1968) "Theoretical Hydrodynamics" 5th ed., Macmillan, and from Muir-Wood, 1969.

A wave motion of the form

$$y = a \sin (mx + nt) \text{ or}$$

$$y = a \sin m(x + \frac{nt}{m})$$

is called a simple harmonic progressive wave of amplitude a . The speed of propagation of the wave is given by

$$C = n/m$$

Along the wave, the distance between two consecutive crests is the wave length L . Thus

$$L = 2\pi/m$$

Similarly the form of the wave is identical after a certain interval of time, which is the wave period T

$$T = 2\pi/n$$

It follows from the definition of C that

$$L = CT$$

Then the wave form becomes

$$y = a \sin 2\pi/L (x - Ct)$$

and if we use the height of the wave (from trough to crest) H

$$y = \frac{H}{2} \sin \frac{2\pi}{L} (x - Ct).$$

In deep water, where the height of the wave is negligible as compared to the depth of water, the water participating in the wave motion is subjected to a velocity potential ' ϕ ' such as

$$\frac{\partial^2 \phi}{\partial t^2} + g \frac{\partial \phi}{\partial y} = 0 \text{ where } y=0$$

A solution to that equation is given by the velocity potential

$$\phi = \frac{HC}{2} \frac{\cosh \frac{2\pi(y+d)}{L}}{\sinh \frac{2\pi d}{L}} \cos 2\pi \left(\frac{x}{L} - \frac{t}{T} \right)$$

where C is the speed of propagation of the wave and is

$$C^2 = \frac{gL}{2\pi} \tanh \frac{2\pi d}{L}$$

The components of this potential in the x and y direction respectively are given by

$$u = -\partial\phi/\partial x$$

and

$$v = -\partial\phi/\partial y$$

where u and v represent the oscillatory motions of the water molecules.

The energy is carried by the wave train at a velocity different from the speed of propagation of individual waves. The group velocity C_g for the case of waves of length L is given by

$$C_g = dn/dm = d(mc)/dm = C + mdC/dm$$

Since we know the value of C , the group velocity is given by

$$C_g = \frac{1}{2} C \left(1 + \frac{4\pi d}{\sinh \frac{4\pi d}{L}} \right) = n \cdot C$$

and when the value of $2d/L$ is large the group velocity tends toward the value of $\frac{1}{2} C$, or $n = \frac{1}{2}$.

The energy of a wave is derived from its deviation about a mean position (potential energy E_p) and from its movement in the oscillatory agitation of the water (kinetic energy E_k).

The kinetic energy per unit width of the wave is

$$E_k = \int_0^L \int_0^{-H} \rho g \frac{(u^2 + v^2)}{2} dx dy$$

which reduces to

$$E_k = \rho g \frac{H^2 L}{16}$$

Similarly the potential energy is

$$E_p = \int_0^L \rho g y^2 dx dy$$

which is solved as

$$E_p = \rho g \frac{H^2 L}{16}$$

Then the total energy of a single wave is the summation of kinetic and potential energy

$$E_t = \rho g \frac{H^2 L}{8}$$

And since that energy is moving with the group velocity the net forward energy will be given as

$$E_f = n \cdot E_t$$

APPENDIX 2
GEOLOGICAL SECTIONS

Section 1. Howard Twp. South of Morpeth.

Total height: 9m. (Dreimanis and Reavely, 1953)

5-9 m : fine sand, and clayey silt (sand 12%,
silt 66%, clay 22%).

0-5 m : till (sand and gravel 20%, silt 42%, clay 38%).

Section 2. Howard Twp. 1.6 km east of Morpeth.

Total height: 15 m. (Wood, 1951)

1-15 m : till (sand and gravel 18%, silt 34%,
clay 48%)

0-1 m : coarse till.

Section 3. Howard Twp. 3.2 km east of Section 1.

Total height: 18m. (Section 2/17; DFW, 1969)

2-18m : till (sand+gravel 18%, silt 37%, clay 45%).

0-2m : coarse till (sand+gravel 31%, silt 41%,
clay, 28%); brown red.

Section 4. Howard-Orford Twp. Line.

Total Height 18m. (Wood, 1951)

11-18m : till

8-11m : sand, little silt.

0-8 m : silty till (sand 8%, silt 51%, clay, 41%).

Section 5. South of Palmyra, Orford Twp. Long. 81°45.0'

Total height: 19 m. (Section 1/17, DFW, 1969; wood 1951)

0-19m. : upper till of section 1, 2, and 3.

Section 6. Longitude 81°43.2' w.

Total height: 19m.

0-19m. : till as in section 5.

Section 7. Orford Twp. Longitude 81°41,5'W.

Total height: 22m. (Wood, 1951)

19-22m Lacustrine silty clay

0-19m Till as in previous sections.

Section 8. Aldborough Twp. Longitude 81°39,3'W.

Total Height: 22m. (Dreimanis 1966)

21-22m Sand

11-21m Lacustrine silt and clay

0-11m Clay till

Section 9. Aldborough Twp. Fort Glasgow. Long, 81°36,5'W

Total height: 23 m. (Dreimanis 1966)

21-23 m Sand

0-21 m Till

Section 10. Aldborough Twp. Long. 81°34,7'W.

Total height 24 m. (Dreimanis 1966)

9-24 m Clay and silt

0-9 m Till

Section 11. Aldborough Twp. South of Eagle. Long. 81°33,1'W

Total height 26 m. (Dreimanis 1966)

20-26 m Till

14-20 m Silt

0-14 m Till

Section 12. Dunwich Twp. Long. 81°30,0'W

Total height: 27 m. Borehole for this project.

26-27 m Silty sand

15-26 m Lacustrine clayey silt

14-15 m Basal till

8-14 m Clayey silt till (waterlaid)

5-8 m Lacustrine sandy silt

0-5 m Fort Stanley till, extends at least 14 m below lake level.

Section 13. Dunwich Twp. Patrick Point.

81°27.9'W

Total height 28 m. (Dreimanis 1966)

20-28 m Silty sand

16-20 m Sandy silt

6-16 m Lacustrine clay

1- 6 m Fort Stanley till

0- 1 m Pebbly till (Catfish Creek)

Section 14. Dunwich Twp. West of Plum Point

81°26.3'W

Total height 25 m. (Dreimanis 1966)

24-25 m Silty sand

17-24 m Lacustrine silty clay

0-17 m Fort Stanley till.

Section 15. Dunwich Twp. West of Bradtville.

81°23.5'W

Total height 22m. (Quigley and Dreimanis 1972)

18-22 m Lake Maumee silt and clay

13-18 m Fort Stanley drift, clayey sit till, interbeds of lacustrine silty clay and water-laid till.

11-13 m Catfish Creek silty sand till

9-11 m Plum Point interstadial beach sand and gravel

3- 9 m Southwold drift gravel

0- 3 m Fort Talbot Interstadial glaciolacustrine silt clay,

Section 16. Dunwich Twp. Port Talbot.

81°21.1'W

Total height 32 m. (Terasmae, Karrow, Dreimanis, 1972)

19-32 m Lake Maumee III silt and clay

0-19m Fort Stanley till

Section 17. Boundary Southwold and Dunwich Twp. $81^{\circ}19.6'W$

Total height 34 m. (Borehole for this project)

- 32-34 m Silty sand
- 26-32 m Lacustrine silt and clay
- 14-26 m Fort Stanley till
- 11-14 m Lacustrine silt and clay
- 0-11 m Fort Stanley till

Section 18. Southwold Twp. South of Pingal. $81^{\circ}17.5'W$

Total height, 35 m. (Dreimanis 1966)

- 34-35 m Sand
- 26-34 m Lacustrine silt and clay
- 12-26 m Fort Stanley till
- 10-12 m Lacustrine silt and clay
- 0-10 m Fort Stanley till

Section 19. Southwold Twp. End of beach at Fort Stanley

Total height, 36 m. (Dreimanis 1966) $81^{\circ}15.0'W$

- 30-36 m Clay and silt
- 21-30 m Till
- 15-21 m Sand
- 10-15 m Lacustrine silt and clay
- 2-10 m Fort Stanley till
- 0-2 m Silt

Section 20. Yarmouth Twp. 4 km east of Fort Stanley.

Total Height, 40 m. (Terasmae, Karrow, Dreimanis, 1972)

- 39-40 m Aeolian sand
- 25-39 m Varved sand
- 15-25 m Lacustrine silt and clay

4-15 m Port Stanley till incorporating silt and sand at the base.

2- 4 m Varved fine sand, silt and clay

0- 2 m Basal silty clay till and waterlaid till.

Section 21. Yarmouth Twp. 8 km east of Port Stanley.

Total height, 41 m. (Dalrymple 1971) 81° 7.0'W

40-41 m Surficial soil and aeolian sand

33-40 m Till

29-33 m Varved sand

• 25-29 m Till

17-25 m Varved sand

8-17 m Lacustrine silt and clay

0-8 m Port Stanley Till.

Section 22. Yarmouth Twp. UWO Geography Station 81° 3.5'W

Total height, 37 m. (Borehole for this project)

29-37 m Sand

22-29 m Till

20-22 m Interbeds of silt, sand, and clay

5-20 m Till

4-5 m Silty clay

0-4 m Port Stanley till

Section 23. Malahide Twp. West of Port Bruce. 81° 1.5'W

Total height, 37 m. (Dreimanis 1966)

28-37 m Sand

21-28 m Port Stanley till

20-21 m Silt

14-20 m Port Stanley till

3-14 m Waterlaid + varved clay and silt

0- 3 m Port Stanley till

Section 24. Malahide Twp.

80°59.3'W

Total height 38 m. (Dreimanis 1966)

35-38 m Dune sand

28-35 m Sand

26-28 m Waterlaid till

24-26 m Till, sand and silt

23-24 m Waterlaid till

0-23 m Till

Section 25. Malahide Twp.

80°56.3'W

Total height 30 m. (Dreimanis 1966)

29-30 m Till

19-29 m Clay and silt

18-19 m Waterlaid till

0-18 m Port Stanley till

Section 26. Malahide Twp.

80°54'W

Total height, 28 m. (Dreimanis 1966)

27-28 m Sand

25-27 m Till

18-25 m Silt and clay

14-18 m Sand

0-14 m Till

Section 27. Bayham Twp. Eastern Boundary.

80°51.6'W

Total height, 24 m.

16-24 m Silt and clay

0-16 m Till

Section 28. Bayham Twp. Drilling site, Port Burwell.

Total height, 18 m.

80°50.2'W

17-18 m Fine to coarse sand
 15-17 m Sandy silt
 11-15 m Lacustrine clay and silt
 8-11 m Waterlaid till
 5- 8 m Fort Stanley till
 0-.5 m Lacustrine silt and clay.

Section 29. Bayham Twp.

80°46.7'W

Total height, 18 m.

5-18 m Lacustrine silt and clay
 0- 5 m Till

Section 30. Bayham Twp. West Boundary.

80°44'W

Total height, 30 m.

21-30 m Sand
 0-21 m Lacustrine silt and clay.

Section 31. Houghton Twp.

80°41.4'W

Total height, 38 m.

20-38 m Sand
 3-20 m Silty clay and sand
 0- 3 m Till

Section 32. Houghton Twp. Sand Hill Park

80°38.7'W

Total height, 52 m.

37-52 m Dune sand
 0-37 m Sand

Section 33. Houghton Twp. Clear Creek.

80°35.3'W

Total height, 12 m.

6-12 m Lacustrine silt and clay
 0- 6 m Till

Section 34. Houghton Twp. Eastern Boundary.

80°33.0'W

Total height, 8m.

4-8 m Lacustrine silt and clay

0-4 m Till.